

A Robot for Wrist Rehabilitation

by

Dustin Williams

B.S., Mechanical Engineering (1999)

University of California, Los Angeles

Submitted to the Department of Mechanical Engineering
in Partial Fulfillment of the Requirements for the Degree of
Master of Science in Mechanical Engineering

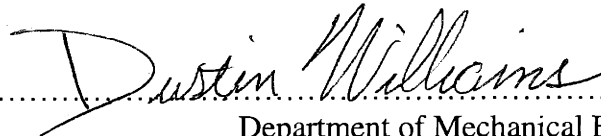
at the

MASSACHUSETTS INSTITUTE OF TECHNOLOGY

June 2001

© 2001 Massachusetts Institute of Technology
All rights reserved

Signature of Author.....



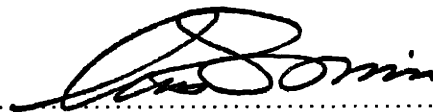
Department of Mechanical Engineering
Feb. 23, 2001

Certified by.....



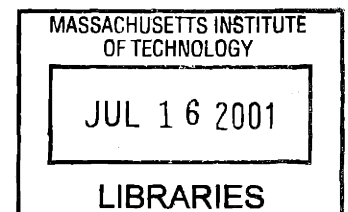
Neville Hogan
Professor of Mechanical Engineering
Professor of Brain and Cognitive Sciences
Thesis Supervisor

Accepted by.....



Ain A. Sonin
Chairman, Departmental Committee on Graduate Students

ARCHIVES



Handwritten scribble or signature at the bottom center of the page.

A ROBOT FOR WRIST REHABILITATION

by

DUSTIN WILLIAMS

Submitted to the Department of Mechanical Engineering
on February 23, 2001 in partial fulfillment of the
requirements for the Degree of Master of Science in
Mechanical Engineering

ABSTRACT

In 1991, a novel robot named Manus I was introduced as a testbed to study the potential of using robots to assist in and quantify the neuro-rehabilitation of motor skills. Using impedance control methods to drive a 2 d.o.f. planar robot, Manus I proved an excellent fit for the rehabilitation of the upper arm and shoulder. This was especially true in the case of rehabilitation after stroke. Several clinical trials showed that therapy with Manus reduced recovery time and improved long term recovery after stroke.

This successful testbed naturally led to the desire for additional hardware for the rehabilitation of other degrees of freedom. This thesis outlines the mechanical design of one of four new rehabilitation robots. Its focus is the mechanical design of a robot for wrist rehabilitation. The anthropometric background data, the design's functional requirements, the strategic design selection and the detailed design are presented.

Acknowledgements

It has been a great experience working in the Newman Lab and I have many people to thank. First of all I would like to thank Prof. Neville Hogan and Dr. Igo Krebs. Prof. Hogan has been an inspiration to work with. His intellectual abilities and especially his talent for teaching place him at the top of his field. I was often amazed at his ability to lead others and to clarify and simplify difficult engineering problems. Dr. Igo Krebs was very helpful with my many design and manufacturing questions. His creativity and experience with robot hardware had a large influence on the wrist robot's design.

Lori Humphrey was always willing to lend a hand or give a friendly smile. Jerry Palazzolo has a great talent for controls engineering; his help in 2.152 was greatly appreciated. Kris Jugenheimer is an excellent engineer and designer. She patiently taught me a great deal about Pro/E and design in general. Her sidekick, Rainuka Gupta, was always willing to lend an ear and brightened up many a boring day at the lab. Steve Buerger is an extremely talented engineer and helped me with many actuator questions. Brandon Rohrer, Sue Fasoli, James Celestino and Phil Tang each bring great resource to our research group. I'd also like to thank Fred Cote in the Edgerton Student Shop for patiently lending his machining expertise.

Lastly, I would like to thank my parents and brothers for their support and encouragement. Without their love and sound advice this opportunity would not have been possible.

Table of Contents

1. Introduction	17
1.1 Motivation.....	17
1.2 Current Capabilities.....	19
1.3 CPM Devices.....	21
1.4 Prior Wrist Device.....	23
1.5 A New Wrist Device.....	24
2. Anthropometry	25
2.1 Wrist, Hand, and Forearm Dimensions.....	26
2.2 Axes of Rotation and Ranges of Motion.....	30
2.3 Maximum Angular Speed, Acceleration and Power.....	34
2.4 Wrist and Forearm Inertias.....	34
2.5 Wrist and Forearm Strengths.....	35
3. Functional Requirements	37
3.1 Kinematics.....	37
3.1.1 Kinematic Variability.....	37
3.1.2 Ranges of Motion.....	38
3.2 Applied Forces.....	39
3.3 Required Output Torques.....	40
3.4 Endpoint Impedance.....	42
3.4.1 Endpoint Inertia.....	42

3.4.2 Endpoint Friction.....	43
3.5 Connectivity.....	43
3.6 Support.....	43
3.7 Ease of Use.....	44
3.8 Simplicity.....	45
3.9 Cost.....	45
3.10 Safety Requirements.....	45
3.11 Power Source.....	45
4. Kinematic Selection.....	47
4.1 A Model of the Human Wrist.....	47
4.2 Universal Joint for the Robot Kinematics.....	48
4.2.1 Connection to the Patient.....	48
4.3 Spherical Joint for Robot Kinematics.....	56
4.4 A Rotating Planar Mechanism.....	57
4.5 Compliant Kinematics.....	58
4.6 Mobility Conclusions.....	59
4.7 Locating the Kinematics with Respect to the Patient.....	59
4.8 A Mockup of the Kinematics.....	63
5. Actuator Transmission Selection.....	65
5.1 Options for Actuator Placement and Transmission.....	65
5.2 Transmission With All Actuators on the Ground.....	69
5.2.1 Hydraulic Transmission Using Flexible Lines.....	69
5.2.2 Arcing Sliders.....	73

5.3	Transmission with One Actuator on Ground and Two Actuators on Link Two.....	75
5.3.1	Differential Mechanism.....	75
5.3.1.1	Kinematics of the Differential.....	76
5.3.1.2	Torque Output.....	79
5.3.2	Actuating Pronation and Supination.....	81
5.4	Actuators on Each Successive Link.....	81
5.4.1	Torque Output.....	82
5.5	Transmission Conclusions.....	84
5.6	Actuator Options.....	85
5.6.1	DC Servomotors.....	85
5.6.1.1	Advantages and Disadvantages of Brushed Motors.....	87
5.6.1.2	Advantages and Disadvantages of Brushless Motors.....	87
5.6.2	ServoDisc Motors.....	88
5.6.3	Ultimag Rotary Actuators.....	89
5.7	Actuator Conclusions.....	91
5.8	Actuator Selection.....	92
6.	Sensor Selection.....	99
6.1	Position Sensors.....	100
6.1.1	Incremental Encoders.....	100
6.1.2	Absolute Encoders.....	101
6.1.3	Resolvers.....	102
6.2	Sensor Conclusions.....	103
6.3	Encoder Resolution.....	104

7. Hardware Overview	105
7.1 Connection to the Patient.....	106
7.2 Abduction/Adduction and Flexion/Extension Transmission.....	108
7.3 Pronation/Supination Transmission.....	116
7.4 Material Selection and Fabrication.....	120
8. Conclusions	123
8.1 Present Status.....	124
8.2 Future Work.....	124
Appendix A: Component List	125
Appendix B: Component Specifications	129
Appendix C: Detailed Drawings	153
Bibliography	205

List of Figures

1.1 Therapy with Manus I.....	19
1.2 A Vertical Extension for Manus.....	21
1.3 Smith and Nephew's Kinetic 8080.....	22
1.4 Orthologic's W2 Wrist.....	22
1.5 Prior Wrist Device.....	23
2.1 Wrist and Hand Dimensions.....	27
2.2 Wrist and Hand Dimensions While Griping a Handle.....	28
2.3 Forearm Dimensions.....	29
2.4 Flexion, Extension, Abduction and Adduction.....	31
2.5 Pronation and Supination.....	32
2.6 Bone References for Pronation and Supination.....	33
2.7 Average Strength Values for Men and Women.....	36
3.1 Applied Forces.....	39
3.2 Wrist Torqueing Device.....	41
3.3 Wrist Torqueing Device Applied to Each Wrist Degree of Freedom.....	41
4.1 Universal Joint.....	48
4.2 Incomplete Kinematics.....	49
4.3 Compliant Connection to Distal Forearm.....	50
4.4 Links and Joints.....	52

4.5a A Gimbal Solution.....	53
4.5b Equivalent Ball and Socket Joint Solution.....	54
4.6 Working Model Simulation.....	55
4.7 Spherical Joint for Robot Kinematics.....	56
4.8 Rotating Planar Mechanism Kinematics.....	57
4.9 Compliant Kinematics.....	58
4.10 Selected Kinematic Configuration.....	60
4.11 Kinematics for Abduction and Adduction Only.....	61
4.12 (Torque on Patient)/(Robot Input Torque) vs. Robot Angle θ	62
4.13a The Mockup in Flexion and Extension.....	63
4.13b The Mockup in Abduction and Adduction.....	64
4.13c The Mockup in Pronation and Supination.....	64
5.1 Candidate Links for Actuator Placement.....	66
5.2 All Actuators on the Ground.....	67
5.3 One Actuator on Ground and Two in Link 2.....	68
5.4 An Actuator on Links 1,2 and 3.....	68
5.5 Hydraulic Transmission Using A Flexible Line and Two Bellows.....	70
5.6 Antagonistic Bellows System.....	71
5.7 Coupled Input Bellows.....	72
5.8 Arcing Slider Transmission.....	73
5.9 Arcing Slider Mockup.....	74
5.10 Differential as A Geared Cardan Joint.....	76
5.11 Input Angles and Output Orientation of the Differential.....	77
5.12 Using the Differential to Actuate Abduction/Adduction and Flexion/Extension...	78
5.13a Torque Inputs to Gears A and B and Forces and Torque Output from Arm.....	80
5.13b Free Body Diagram of Spider Gear and Attached Arm.....	80
5.14 Actuators on Successive Links.....	81
5.15a Torque Inputs With Actuators on Each Successive Link.....	83

5.15b Resultant Torque Output to the Arm.....	83
5.16 Counterbalanced Actuators.....	85
5.17 Servodisc Actuator.....	88
5.18 Servodisc Advantages.....	89
5.19 Ultimag Rotary Actuators.....	90
5.20 Torque vs. Position for Ultimag Actuators.....	91
5.21 Added Inertial Impedance in Flexion/Extension and Abduction/Adduction.....	93
5.22 Frictional Impedance in Flexion/Extension and Abduction Adduction.....	95
5.23 Inertia Added in Pronation/Supination due only to the Flexion/Extension and Abduction/Adduction Motors.....	95
5.24 Frictional Impedance in Pronation and Supination.....	98
5.25 Increase in Inertial Impedance in Pronation and Supination.....	98
6.1 Incremental Encoder Output.....	101
6.2 Absolute Encoder Disk.....	102
6.3 Resolver Windings.....	102
6.4 Gurley R119 Encoders.....	103
7.1 Complete Wrist Device.....	105
7.2 Connection to the Patient.....	107
7.3 Transmission for Abduction/Adduction and Flexion/Extension.....	108
7.4a Simplified Model of Gear Train.....	111
7.4b Free Body Diagram of Each Gear.....	111
7.5 Transmission for Pronation/Supination.....	117
7.6 Static Analysis of Slide Rings.....	120



List of Tables

2.1 Wrist and Hand Dimensions.....	27
2.2 Wrist and Hand Dimensions While Gripping a Handle.....	28
2.3 Forearm Dimensions.....	29
2.4 Maximum Angular Speed, Acceleration and Power.....	34
2.5 Hand and Forearm Rotational Inertias and Masses.....	35
7.1 Gear Dimensions and Parameters.....	109
7.2 Resultant Forces on each Gear.....	112
7.3 Actual and Allowable Tangential Loads.....	113
7.4 Factors in the AGMA pitting stress equation.....	114
7.5 Actual and Allowable Loads for Pitting Resistance.....	115
7.6 Maximum Expected and Allowable Loads on Transmission Bearings.....	115
7.7 Actual and Allowable Tangential Load.....	118
7.8 Actual and Allowable Tangential Load for Pitting.....	119

Chapter 1

Introduction

1.1 Motivation

Stroke, or cerebrovascular accident (CVA), is one of the leading causes of adult disability in the United States. There are approximately four million Americans presently living with the effects of stroke and each year approximately 730,000 new strokes occur. Stroke can occur at almost any age but usually occurs in the elderly. Two thirds of strokes occur in individuals over the age of 65. In the next twenty five years, the number of people in this age range will approximately double in size as those now in their 40s and 50s, the “Baby Boom” generation, get older. Because of this, there will likely be an increase in the rate of stroke and an increase in the need for stroke therapy to help individuals recover and regain function they have lost.

The type of function lost or impaired after a stroke can vary greatly and is largely dependant on the section of the brain in which the stroke takes place. Stroke in the right hemisphere of the brain, most often affects visual perceptual abilities, short term memory and control movement of the left side of the body. Stroke in the left hemisphere of the brain usually affects speech interpretation and production, behavioral characteristics and

control of movement of the right side of the body. Finally a stroke in the brain stem can affect vital involuntary functions such as breathing rate, blood pressure and heartbeat [1].

The impairment that the Biomechanical control group is most interested in is the impairment of motor skills. The idea behind the current research is to use robots to help stroke victims recover their lost motor skills. Conventionally, this has been done with one to one interaction between a stroke victim and a physical therapist. The therapist typically asks the patient to produce certain movements, such as outstretching an arm or taking a small step. The patient then responds as best they can and if they are unable to complete the movement, the therapist will help them. These tasks are practiced repeatedly and the patient often regains part or all of their original ability. In this process, the improvement over previous sessions and the current skill of the patient are measured in a qualitative manner by the therapist. The therapist basically determines these abilities by “feel” and approximation. With these approximations, the therapist then qualitatively applies the required effort to help the patient complete the task.

By using robots, a quantitative means of providing therapy is available. With the current sensing technology we can precisely measure the positions, velocities, and accelerations of a patient. These measurements allow for a precise record of the patient improvement over time and an accurate assessment of their present state of progress in a given task. With today’s actuator technology we can, in addition, apply a well controlled, finely adjustable, and repeatable helping hand. Both of these technologies can help to speed and improve recovery. Precise measurement, in addition, allows for data extraction for non-therapeutic purposes. Scientific information can be gathered. The data collected

can be “mined” for patterns and relationships which can help lead to new insights into motor learning and human kinematics.

1.2 Current Capabilities

A two degree of freedom planar robot, Manus I, which has been in service for seven years and its successor, Manus II, which has been in service for three years have each demonstrated the effectiveness of robotic therapy. Figure 1.1 shows Manus I currently in use at the Burke Rehabilitation Hospital in White Plains, New York. This device exercises the upper arm and shoulder by moving the patient’s hand through planar



Figure 1.1 Therapy with Manus I

movements. The patient usually plays a “video game” which requests that he or she move from one point to another in the robot workspace. The video game gives the patient visual feedback about their current position and the location where they are required to be. To allow for interaction with the patient, the robots use a special type of control called impedance control. In Manus I and II’s case, this type of control creates an effective stiffness and damping at the robot endpoint. Basically, the robots act as if there were a “virtual spring” and a “virtual damper” between the current patient position and the position where they are required to be. The stiffness and damping can be adjusted by the attending therapist to vary the degree of assistance the robot provides.

The successes of these devices naturally led to the desire to actuate other degrees of freedom. Currently in the late stages of development is an additional module for Manus which will allow for vertical movements out of the present planar workspace. It is shown in figure 1.2 .

In addition to this device, three other new devices are currently under development. These include a robot for finger and thumb therapy, and a robot for walking therapy, and a robot for wrist therapy which is described in this thesis.

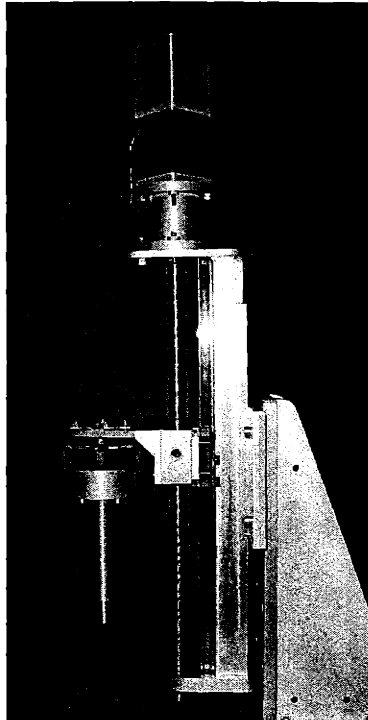


Figure 1.2 A Vertical Extension for Manus

1.3 CPM Devices

Presently there are a few commercially available devices for wrist therapy. Unlike the robots above, however, these devices are not meant to help patients relearn motor skill. They are meant to help in physiological recovery after surgery or injury. These devices are called CPM or continuous passive motion devices. By moving the wrist passively through its ranges of motion, for several hours at a time, these devices can increase blood flow, reduce swelling and reduce cartilage deterioration. A CPM device from Smith and Nephew called the Kinetic 8080 is shown in figure 1.3 and a device from Orthologic called the W2 Wrist is shown in figure 1.4 .

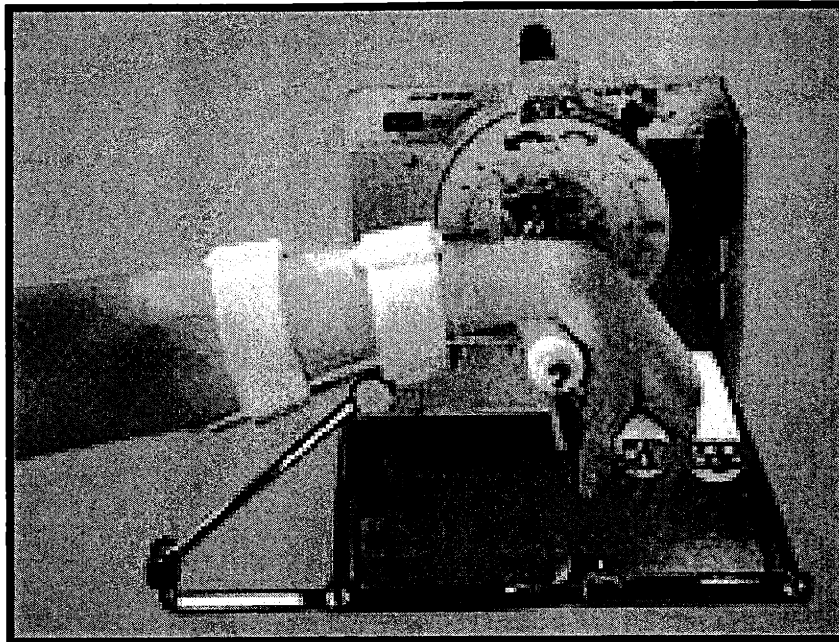


Figure 1.3 Smith and Nephew's Kinetic 8080

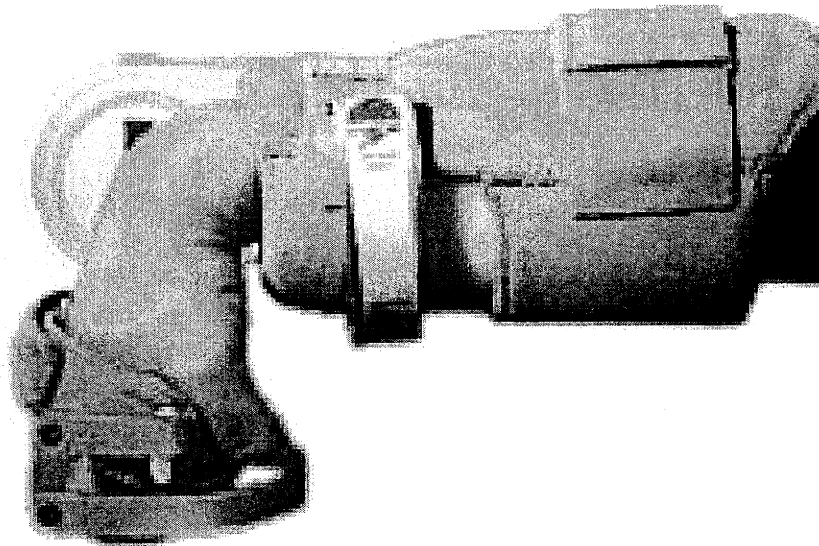


Figure 1.4 Orthologic's W2 Wrist

1.4 Prior Wrist Device

When Manus I was made, a three degree of freedom wrist device was also built to attach to its endpoint. The device is shown attached to Manus' last link in figure 1.5. This device was not put to use, however. This was mainly due to problems with patient access. It was found to be difficult to insert and remove the patient from the device. The patient's hand had to be fit through a small opening (the linkage loop shown at the bottom of figure 1.5) and then attached to the device.

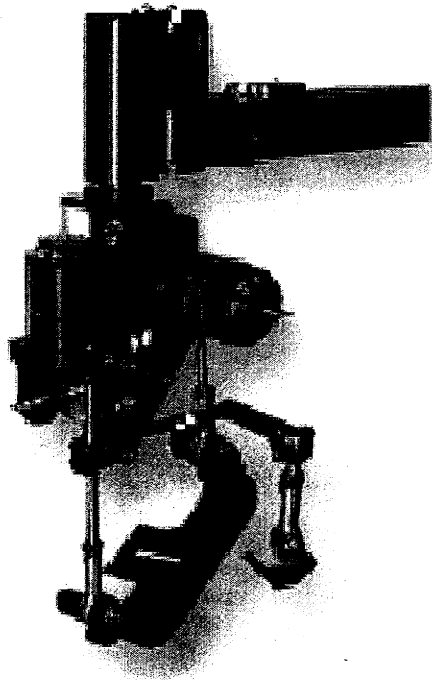


Figure 1.5 Prior Wrist Device

1.5 A New Wrist Device

A new wrist device has been designed and is in the process of being manufactured. This thesis outlines how the new device was developed. The background data, the conceptual development of the design and the detailed design are presented. A brief summary of each chapter of the thesis follows.

- Chapter 2 gives the anthropometric properties of the human wrist. Data on the dimensions of the wrist, hand, and forearm are given. The kinematic and dynamic properties of the wrist are also presented.
- Chapter 3 gives the functional requirements for the device. It explains what is expected of the device.
- Chapters 4 gives a model of the human wrist and explains how the model was used to determine the kinematics of the device. Interference with the patient is also reviewed.
- Chapter 5 describes the different transmissions and actuators considered. A transmission is selected followed by an actuator type. The optimum actuator brand and actuator size are then selected.
- Chapter 6 explains how the sensors were selected.
- Chapter 7 is an overview of the actual system hardware. Each major subsystem is reviewed. The machining processes and the material selection are also given.
- Chapter 8 gives the final conclusions.

Chapter 2

Anthropometry

Since the wrist robot will in some way connect to a person's hand and arm and will actuate the degrees of freedom of the wrist, it is essential that data about the hand, arm and wrist be gathered. In order to properly hold on to the patient, the appropriate dimensions of the hand and arm must be known. In order to actuate the hand and forearm it is essential that their kinematics and dynamics be determined.

Since several different patients will use the wrist device it will need to fit various hand and wrist sizes. The wrist device will need to adjust in some way to different patient dimensions. Also, the locations of the patient axes of rotation with respect to the robot will change. The locations of the axes will change from one patient to the next and from one session to the next.

The following data is taken from samples of unimpaired individuals. For the most part this data accurately represents the expected patient sizes. There is, however, a common stroke patient symptom called edema which will cause differences between the collected data and the patients. Edema is a swelling of the impaired limb. This difference effects mainly the circumference measurements of the wrist, palm and fingers. At the time of design, data on the increase in patient size was not available. It was approximated as at most a 20% increase in circumference.

2.1. Wrist, Hand and Forearm Dimensions

Except where noted, the data included in this section are taken from *The Measure of Man and Woman: Human Factors in Design* [2]. This book is an updated and more comprehensive version of the *HumanScale* books published in the 1970's and 1980's. The book is based on a large quantity of data accumulated for several years by the Henry Dreyfuss Associates. It is meant to give an accurate representation of 98% of the global adult population. Figure 2.1 shows various wrist and hand dimensions which are important for the design of the wrist robot. Table 2.1 gives their 1st, 50th and 99th percentile values. Figure 2.2 and Table 2.2 give dimensions of the wrist and hand when holding a cylindrical handle. These dimensions, as will be shown, are also important for the wrist robot's design.

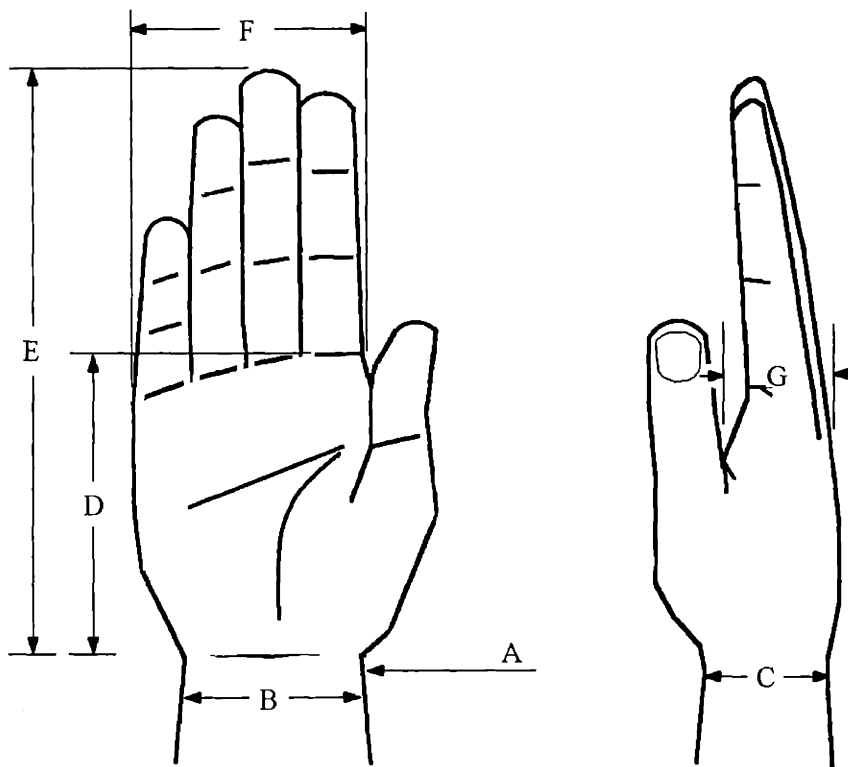


Figure 2.1 Wrist and Hand Dimensions

	1%ile	50%ile	99%ile
Male			
A – wrist circumference	6 in.	6.9 in.	7.8 in.
B – wrist breadth	2.3	2.7	3.0
C – wrist thickness	1.5	1.7	2.0
D – dorsum length	2.6	3.0	3.4
E – hand length	6.6	7.5	8.4
F – hand breadth	3.1	3.5	3.9
G – hand thickness	1.1	1.3	1.5
Female			
A – wrist circumference	5.3	5.9	6.6
B – wrist breadth	2.0	2.3	2.6
C – wrist thickness	1.2	1.5	1.7
D – dorsum length	2.5	2.9	3.3
E – hand length	6.0	6.9	7.8
F – hand breadth	2.7	3.0	3.3
G – hand thickness	0.93	1.09	1.25

Table 2.1 Wrist and Hand Dimensions

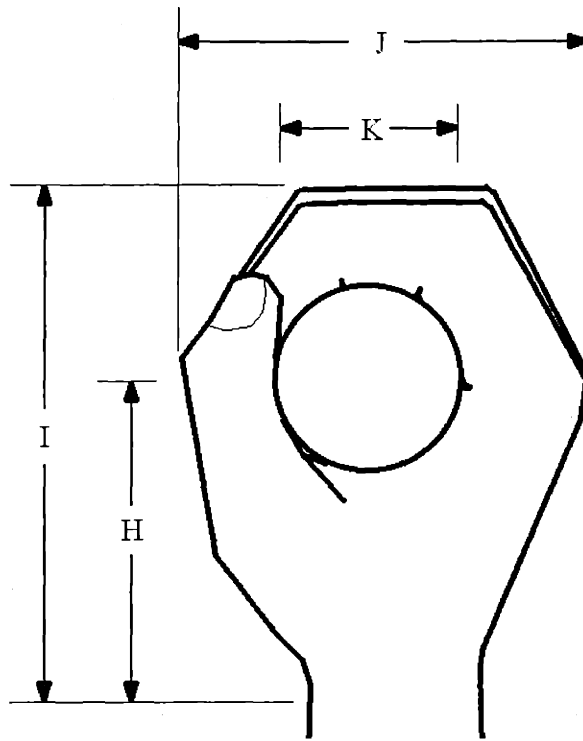


Figure 2.2 Wrist and Hand Dimensions while Gripping a Handle

	1%ile	50%ile	99%ile
Male			
H – distal wrist crease to handle center	2.6 in.	3.0 in.	3.4 in.
I – grip length	3.8	4.7	5.6
J – grip width	3.4	3.7	4.1
K – optimum handle diameter	1.25-1.5	1.25-1.5	1.25-1.5
Female			
H – distal wrist crease to handle center	2.5	2.9	3.3
I – grip length	3.8	4.3	4.8
J – grip width	3.0	3.3	3.6
K – optimum handle diameter	1.25-1.5	1.25-1.5	1.25-1.5

Table 2.2 Wrist and Hand Dimensions While Gripping a Handle

The dimensions of the patients forearm are also important as it will be necessary to support its weight and constrain its movements while the patient undergoes wrist therapy.

Figure 2.3 and table 2.3 give the useful dimensions.

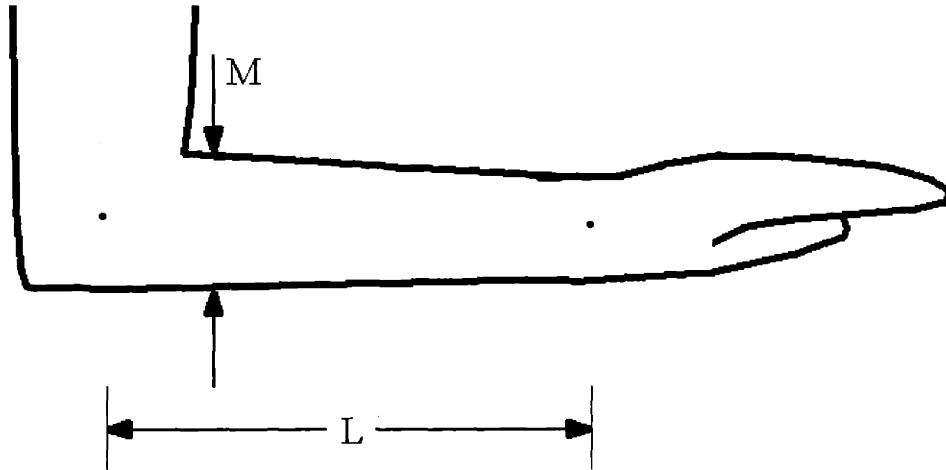


Figure 2.3 Forearm Dimensions

	1%ile	50%ile	99%ile
Male			
L – Forearm length (between elbow and wrist axes)	9.2 in.	10.1 in.	10.8 in.
	5%ile		95%ile
M – Upper forearm circumference [3]	2.4		3.2
	1%ile	50%ile	99%ile
Female			
L – Forearm length (between elbow and wrist axes)	8.3	9.2	9.7
	5%ile		95%ile
M – Upper forearm circumference [3]	2.4		3.2

Table 2.3 Forearm Dimensions

2.2. Axes of Rotation and Ranges of Motion

In order to actuate the human wrist it is important to have a good understanding of its kinematics. Using radiographic techniques it has been found that the wrist has two axes of rotation which can be located with respect to the carpal bones of the wrist. These axes are as shown in figure 2.4. Rotations about the first axis are called flexion and extension. Flexion occurs when the hand moves volarly (toward the palm) and extension occurs when the hand moves in the opposite direction or dorsally. This axis passes transversely through the head of the capitate bone. The capitate bone is the third in a series of four bones which make up the distal carpal row. Rotations about the second axis are called abduction and adduction. Adduction occurs with rotations of the hand toward the thumb and abduction occurs with rotation toward the last digit. The axis of abduction and adduction is an anteroposterior axis which passes through the head of the capitate slightly more distal to the axis of flexion extension [4].

For most movements, flexion is limited to about 70 degrees and extension 65 degrees. Adduction is normally limited to 30 degrees and abduction 15 degrees. These ranges of motion are shown in figure 2.4. Note, however that the ranges of motion are coupled. For instance, when the wrist is fully flexed or extended, abduction and adduction are not possible. When the wrist is abducted or adducted only a limited amount of flexion and extension can occur [5].

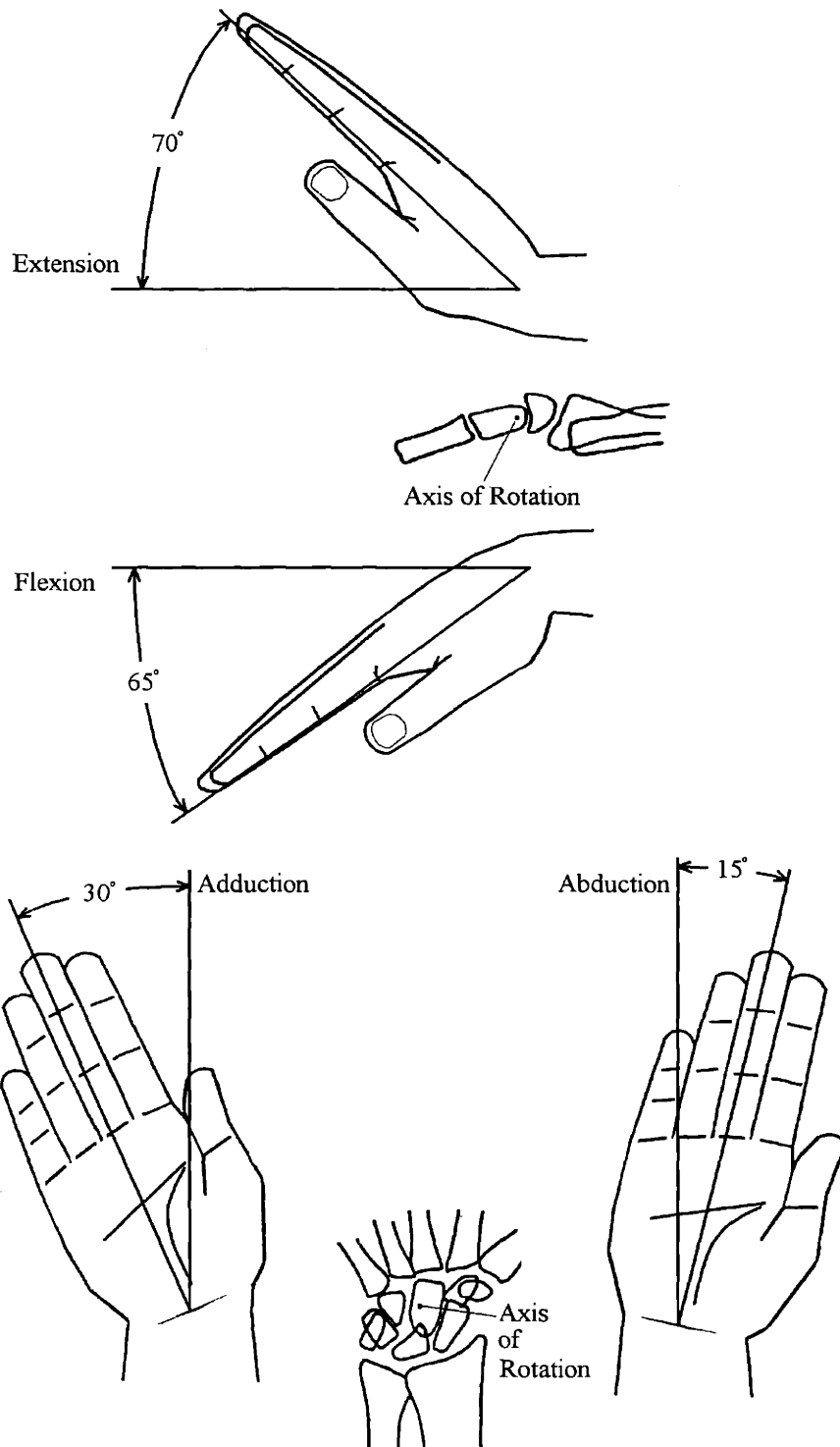


Figure 2.4 Flexion, Extension, Abduction and Adduction

In order to properly place the patient it may be helpful to find palpable anatomical markers which help to locate these axes of rotation. A study in reference [6] located them as follows:

“The axis of radioulnar deviation (abduction/adduction) was identified by drawing a line along the ulnar border of the third metacarpal upon which the mid point between the distal radius and the proximal end of the third metacarpal was marked. To identify location of the flexion/extension axis, this same point was extended ulnarly, perpendicular to the forearm bones until it reached the midpoint between the distal radius and the pisiform’s volar edge.”

The third rotation axis of interest for the design of the wrist robot is that which allows pronation and supination (see figure 2.5). The bone references for this axis can actually vary. Reference [4] explains:

“The axis of pronation and supination can vary depending about which finger the movement is occurring. It always passes through the center of the head of the radius, but at the level of the wrist it can pass through any point between the ulnar and radial styloid processes. Nevertheless, it will tend to lie in the medial half [on the ulnar side] of this region in most instances.”

The positions of the forearm bones in pronation and supination and the location of the radial head and the styloid processes are shown in figure 2.6 .

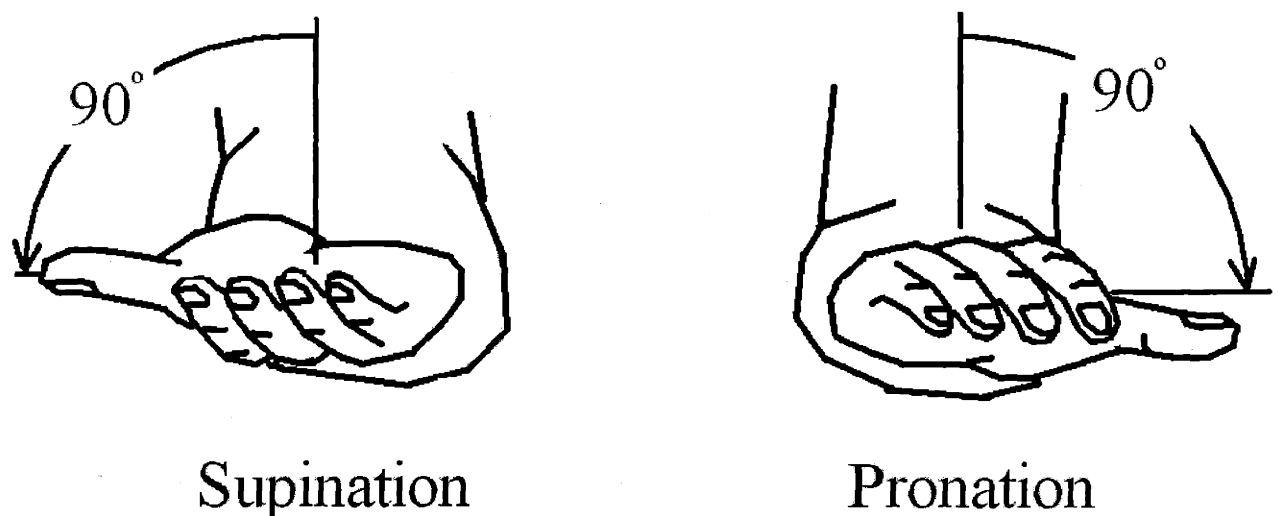


Figure 2.5 Pronation and Supination

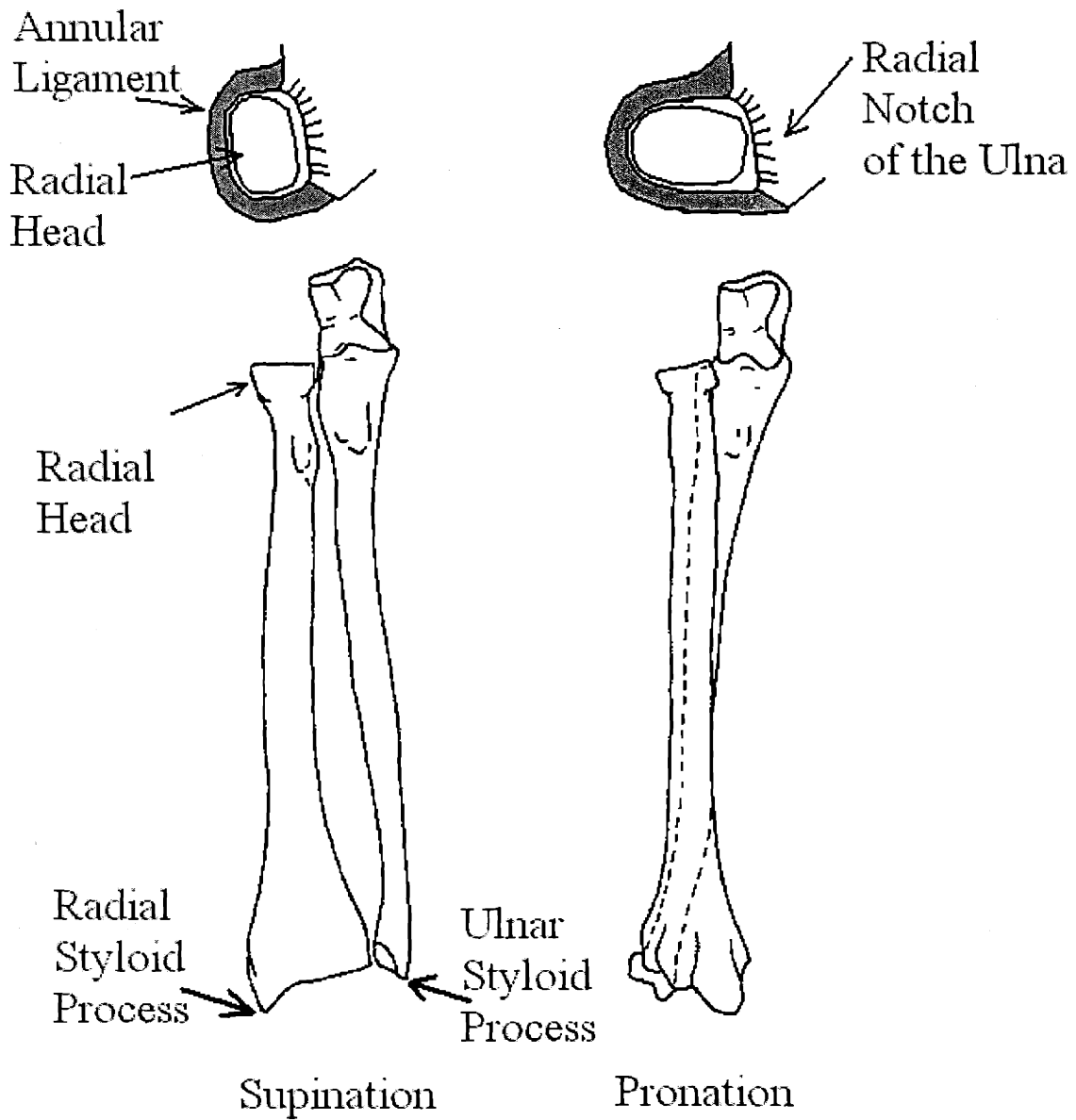


Figure 2.6 Bone References for Pronation and Supination (Adapted from [4])

The range of motion in pronation and supination is nearly 90 degrees in each direction (see figure 2.5) when there is no medial rotation of the humerus. When the humerus is allowed to rotate it then becomes possible to rotate the hand through almost 360 degrees [4].

2.3 Maximum Angular Speed, Acceleration and Power

The maximum angular speed, acceleration, and power for different arm movements are given in table 2.4. The angular velocity values were found to be useful for sensor selection.

Mode of motion	Maximum angular speed (rad/s)	Maximum angular acceleration (rad/s ²)	Power (W)
Bending in shoulder joint	7.0	70	200
Upper arm twist	10.0	120	200
Forearm bending	17.0	300	150
Forearm twist	15.0	200	120
Wrist bending	20.0	500	50
Wrist twist	15.0	450	40
Grip	15.0	350	40

Table 2.4 Maximum Angular Speed, Acceleration and Power [13].

2.4 Wrist and Forearm Inertias

An approximation of the hand and forearm rotational inertias about their respective axes, as will be shown, is important to the design of the wrist robot. *Anthropometric Relationships of Body and Body Segment Moments of Inertia* [7] gives the results of a stereophotometric approximation of the moments of inertia of various segments of the human body. The sample set used for the test was a number of US air force pilots. These values should of course give larger inertial values than that expected for the normal user of the wrist robot. However, of the little data available on body

segment moments of inertia it was the only source found with the detail required for the robot's design. Table 2.5 gives the relevant minimum, mean, and maximum inertial values from the sample. Mass values are also given. Note that all data is of the right hand and right forearm.

	Minimum	Mean	Maximum
Rotational Inertia about Flexion/Extension Axis (lb*in ²)	7.8	10.2	16.7
Rotational Inertia about Abduction/Adduction Axis (lb*in ²)	10.5	14.4	23.5
Rotational Inertia about Pronation/Supination Axis (lb*in ²)	3.7	5.9	12.5
Rotational Inertia about Pronation/Supination Axis (with hand flexed) (lb*in ²)	14.2	20.3	36.0
Mass of Hand (lb*in ²)	1	1.2	1.6
Mass of Hand and Forearm (lb)	3.5	4.6	6.9

Table 2.5 Hand and Forearm Rotational Inertias and Masses

2.5 Wrist and Forearm Strengths

Strength values in flexion/extension abduction/adduction and pronation/supination were not available for stroke rehabilitation patients. Strength measures for unimpaired individuals given in figure 2.7 were found to be useful, however.

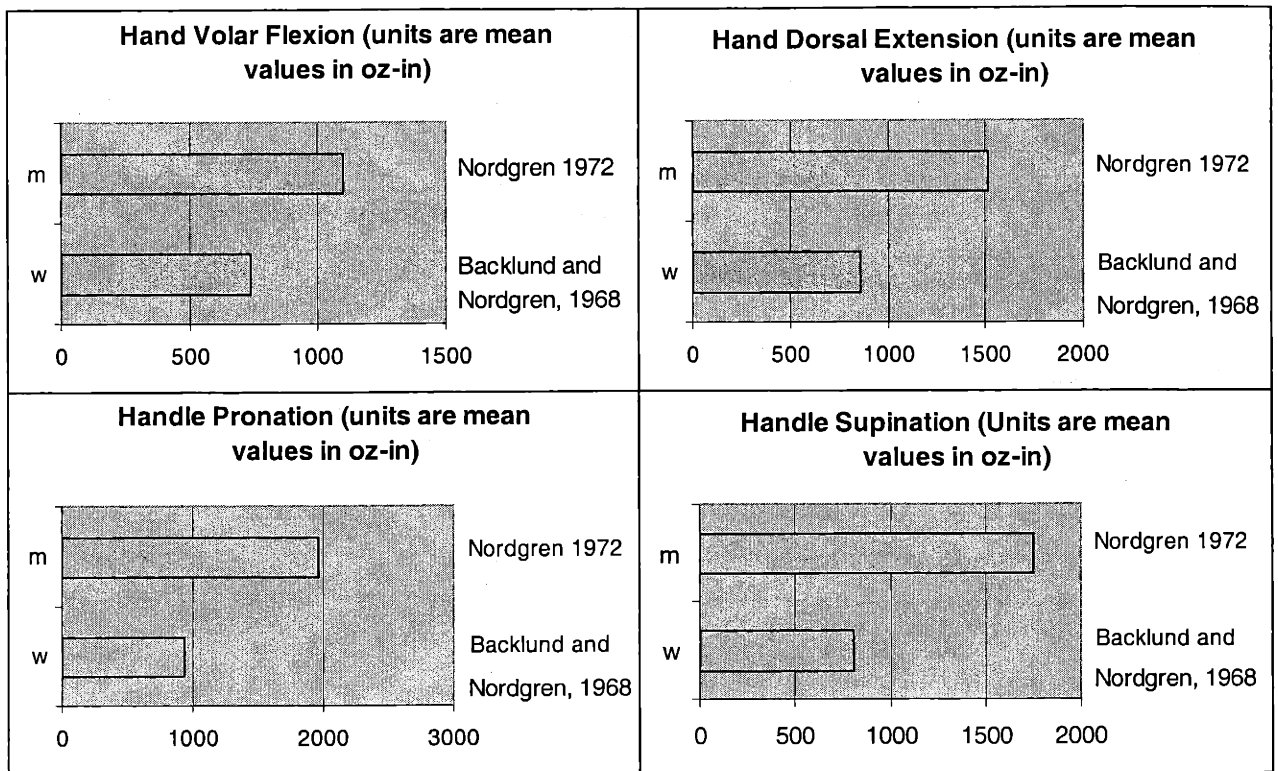


Figure 2.7 Average Strength Values for Men and Women [3]

Chapter 3

Functional Requirements

In order to evaluate new designs, compare candidate designs, and keep the goals of the project clear, a set of functional requirements was determined. These requirements were built around the fact that the robot needs to be simple, easy to use, and an effective therapy device. The robot must have a simple design and at the same time provide the function required of it. It also needs to be easy to use. The therapist needs to be able to easily add and remove the patient, start the therapy process and collect data about the patient recovery. The robot itself also needs to appropriately apply therapy. It must apply forces and torques to the patient which appropriately help them to move. At the same time, the hardware which provides these forces and torques must minimally impede the patients's motion.

3.1 Kinematics

3.1.1 Kinematic Variability

A first pass design of the robot kinematics might be a three degree of freedom robot with kinematics identical to the wrist. One might consider three revolute joints placed in

alignment with the patient axes and connected with rigid linkages. With this device directly connected to the patient, problems would arise. To prevent overconstraint¹ and inappropriate forces² in the robot/patient system it would be necessary to accurately align the robot and patient axes. Two factors make this alignment problematic. First of all, the large variability in patient sizes would necessitate several adjustment components for alignment of the axes and for repositioning connections to the patient. This would be quite time consuming for a therapist and difficult for the designer. Secondly, the most practical way to locate patient axes of rotation would be the use of external bone references. This again would be time consuming and could possibly be inaccurate enough to cause problems with over-constraint. It is necessary then that the robot kinematics allow for misalignment of the robot and patient axes. As will be explained in chapter 4 this can be achieved by using robot kinematics with more than three degrees of freedom.

3.1.2 Ranges of Motion

Another kinematic requirement of the device is that it have appropriate ranges of motion. The device should cover the ranges, used in everyday tasks, of a wrist with normal function. These are as follows: flexion - 70°, extension - 65°, adduction - 15°, abduction - 30°, pronation - 90°, supination 90°. In addition, the device should prevent over-rotation of the patient which could lead to injury.

¹The joints of the robot enforcing rotations about its own axes and the patient about their own axes.

²Such as shear forces to the patient's skin and compressive and tensile forces on the patients joints.

3.2 Applied Forces

If possible, forces applied by the robot to the patient should be perpendicular to the surface of the limb being actuated (See figure 3.1). Forces along the limb (or transverse to it) will introduce shear forces at the connections between the robot and patient. These forces can cause the robot component connected to the patient to shift or to slip with respect to the patient.

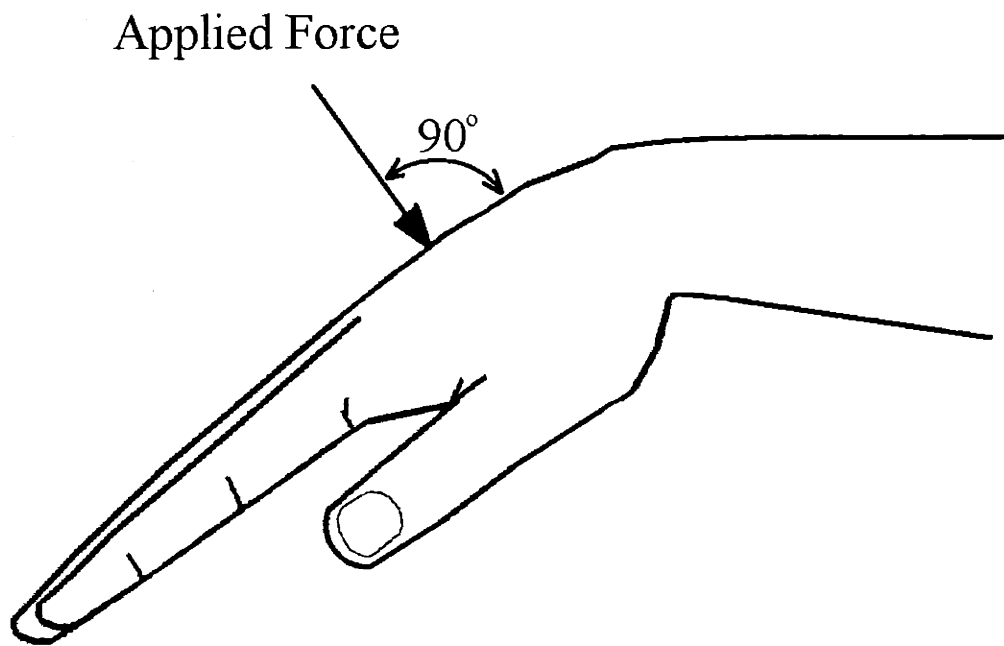


Figure 3.1 Applied Forces

3.3 Required Output Torques

The torque necessary to actuate the patient must be determined in order to size the wrist robot's actuators. The applied torques need lift to patient against gravity, accelerate the patient's inertia and overcome patient spasticity. Because data on the impedance due to spasticity was not available, and because an appropriate angular acceleration requirement was difficult to determine, the torque requirements for the wrist device were determined qualitatively.

By attaching a D.C. motor with a 6:1 reduction ratio to a handle, a simple wrist torquing device was made (See figure 3.2). Using this device, torques were applied to the three degrees of freedom of my own wrist (see figure 3.3) and to the wrist of an occupational therapist who works in the Biomechanical Control Group. After applying different torques to each degree of freedom of our wrists, it was qualitatively determined that 170 oz-in was appropriate for flexion/extension and abduction/adduction and that 240 oz-in was appropriate for pronation/supination. According to the therapist, these torques were sufficient to overcome patient spasticity, lift a patient against gravity and accelerate them [14].

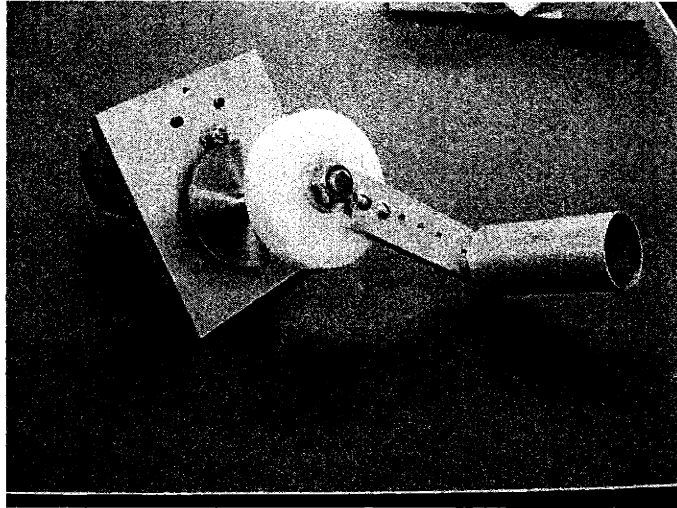


Figure 3.2 Wrist Torquing Device

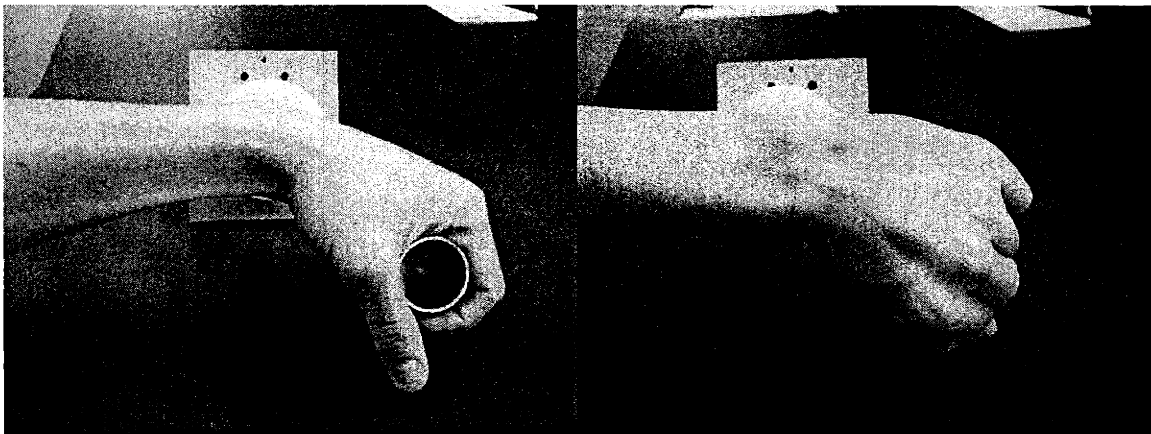


Figure 3.3 Wrist Torquing Device Applied to Each Degree of Freedom

3.4 Endpoint Impedance

The wrist robot will act as an active and a passive device. In the active mode, the robot is a *source* of power to the robot/patient system. The patient may also be a *source* of power. In the passive mode, only the patient *supplies* power to the system. A good design should, in the passive mode, have a low endpoint impedance. That is, when the patient attempts to backdrive the robot, the effective friction, inertia and stiffness that he feels should be low enough so that it is as if no robot or very little robot is connected to him.

The “backdrivability” of a given robot is a qualitative measure. To determine the maximum inertial and frictional impedances which still allow the wrist robot to be backdrivable, simple qualitative tests were used as will be explained.

3.4.1 Endpoint Inertia

By holding a mass at a distance from each axis of rotation of the wrist, additional inertia was added to each wrist degree of freedom. By varying the distance of the mass from the axis of rotation, the inertia about this axis was increased or decreased. This mass was moved sinusoidally in a horizontal plane in flexion/extension, abduction/adduction and pronation/supination. It was determined qualitatively whether or not the given added amount of inertia due to the mass would be backdrivable. With this simple test, the maximum backdrivable amount of inertia in abduction/adduction and flexion/extension was about 10-15 lb*in². Table 2.5 shows that this is about 1-1.5 times the inertia of an average hand in flexion/extension and abduction/adduction. The maximum “backdrivable” amount of inertia in pronation/supination also found to be about 10-15

$lb \cdot in^2$. Table 2.5 shows that this is approximately 2 times the inertia in pronation/supination.

3.4.2 Endpoint Friction

Using a setup which created torsional friction and a force transducer to measure this friction, it was qualitatively determined that the maximum friction added to each patient axis should be less than 30 oz-in.

3.5 Connectivity

The connections to the patient should be modular. This will allow for changes in the way the robot connects to the patient. In connecting to the hand, for instance, one module might allow the hand to be open for functional tasks. A second module might close a patient's hand around a handle for the initial stages of therapy where it is often difficult and painful to open the hand. Each of these connections to the patient should be somewhat compliant to keep the patient comfortable. They should also be rigid enough to actuate the patient.

Prior experience with therapeutic robots has shown that connections sized using the mean anthropometric data and with a reasonable amount of simple adjustability, are appropriate for the vast majority of patients. However, in the extreme cases (very large and very small patients), it is preferable to use separate modules which fit the patient

more appropriately instead using excessive amounts of adjustability with a connection piece which is clearly too small or too large for the patient.

If possible, the robot itself should be modular. That is, it should be capable of stand alone operation for exercises requiring wrist isolation. It should also interface, if possible, with Manus and/or the hand and finger device for exercises involving the shoulder, upper arm and fingers. The complexity of the combination of such devices does have the potential to be quite high, however. The degree of freedom of such a robot would range from 5 to 14 degrees of freedom. If such a combination is unreasonable at this time, robot modularity will be left for future designers.

3.6 Support

The robot structure should be capable of supporting the entire range of expected patient hand and forearm weights. The effect on system performance (especially friction) should be minimal.

3.7 Ease of Use

One of the most important aspects of the design is that it be simple to connect and disconnect the patient and robot. Addition and removal should take the therapist no longer than 2 minutes. Typical therapy sessions last from 45 minutes to an hour and setup times over five minutes begin to significantly cut into therapy time.

3.8 Simplicity

It is very important to keep the design as simple as is possible. The design should meet its functional requirements with the simplest possible components. Such components usually contain fewer moving parts and thus have a lower probability for failure. They also tend to cost less and are easier to manufacture. Cost and manufacturability also make redesign more feasible.

3.9 Cost

It is preferable to keep the cost low. Function should'nt be sacrificed to cost, however.

3.10 Safety Requirements

In the event that the patient must be quickly removed from the machine, there should be a simple mechanical method for removal. In this case and in cases where it has been determined that angular accelerations or torques are unusually high, the supervising control system should shutdown power to the actuators and in some way dissipate dynamic energy.

3.11 Power Source

Since electrical power is the most convenient source available, power inputs for the actuators should be either electrical or be easily obtained from an electrical source.

Chapter 4

Kinematic Selection

4.1 A Model of the Human Wrist

Figure 4.1 depicts the essential kinematics of a universal or cardan joint. It consists of two perpendicular revolute joints whose axes are orthogonal to one another. They are often configured in a cross shaped member as shown in figure 4.1. This type of joint is frequently used to transfer rotary motion between two shafts whose axes pass through same point and can rotate with respect to one another (axes A and D in figure 4.1). When used in this way, the universal joint has kinematics which are very similar to those of the human wrist. Rotations about axis A correspond to pronation and supination and rotations about axes B and C correspond to abduction/adduction and flexion/extension respectively. There are some minor differences, as can be seen in section 2.2, between the positions and orientations of axes of the human wrist and those of the universal joint. However, for the following analysis, the universal joint provides a sufficiently competent model of the human wrist.

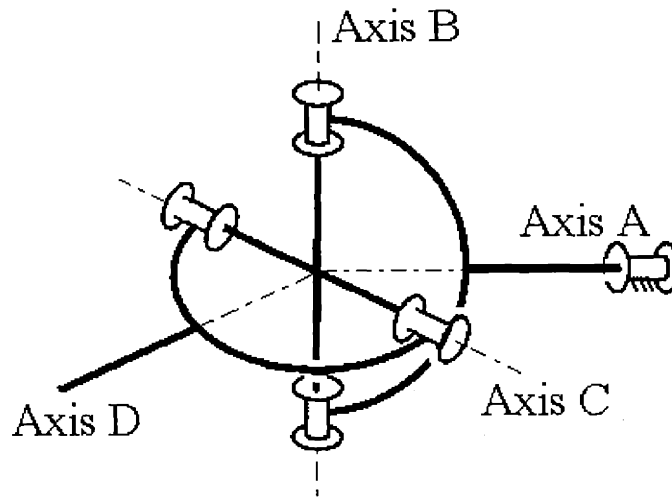


Figure 4.1 Universal Joint

4.2 Universal Joint for Robot Kinematics

The similarity between the universal joint and the kinematics of the human wrist suggests that a universal joint is a feasible option for the robot kinematics. The question then is how to connect a universal joint to the patient while insuring that the kinematic and dynamic functional requirements of sections 3.1 and 3.2 are met.

4.2.1 Connection to the Patient

Figure 4.2 shows a universal joint representing the patient kinematics and along side it another universal joint representing the robot.

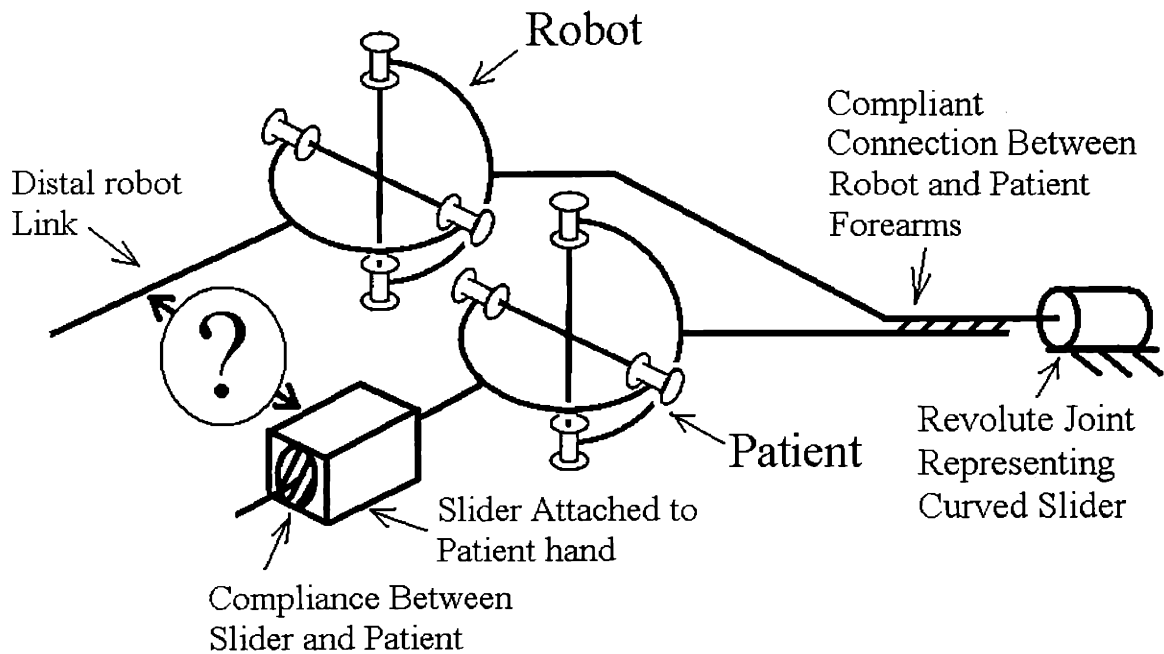


Figure 4.2 Incomplete Kinematics

As explained in section 3.2, it is important that forces applied to the patient be perpendicular to the surface of the limb of which they are actuating. In order to fulfill this requirement, a prismatic type joint can be placed in a proximal/distal orientation down and along the limb of the patient. This method was deemed the most feasible for the application of forces producing flexion/extension and abduction/adduction of the patient's hand. Figure 4.2 shows a slider connected to the patient's hand for this purpose. A compliant element is shown between the slider and the patient to represent the compliance of the patient's skin and tissue.

A simple compliant connection was found to be sufficient for the connection between the robot and patient forearms. This connection is shown in figure 4.3. The curved slider shown allows the patient to rotate about an axis within his or her forearm.

For simplicity figure 4.2 represents the curved slider with a revolute joint. The compliance due to the connection and to the patient's skin are also shown in figure 4.2. The connection was found not to overconstrain pronation/supination rotations of the forearm and to apply perpendicular forces to the forearm when the slider was twisted about its axis. The perpendicularity of the forces prevented the connection from slipping up or down the forearm.

As shown in figure 4.2 the components between the slider and the distal link of the robot's universal joint still need to be found. A clue as to what these components should be was found by looking at the mobility of the robot/patient mechanism in figure 4.2. Because we want three joint angles (either of the robot or of the patient) to determine the positions and orientations of each of the links in the mechanism, we need to ensure

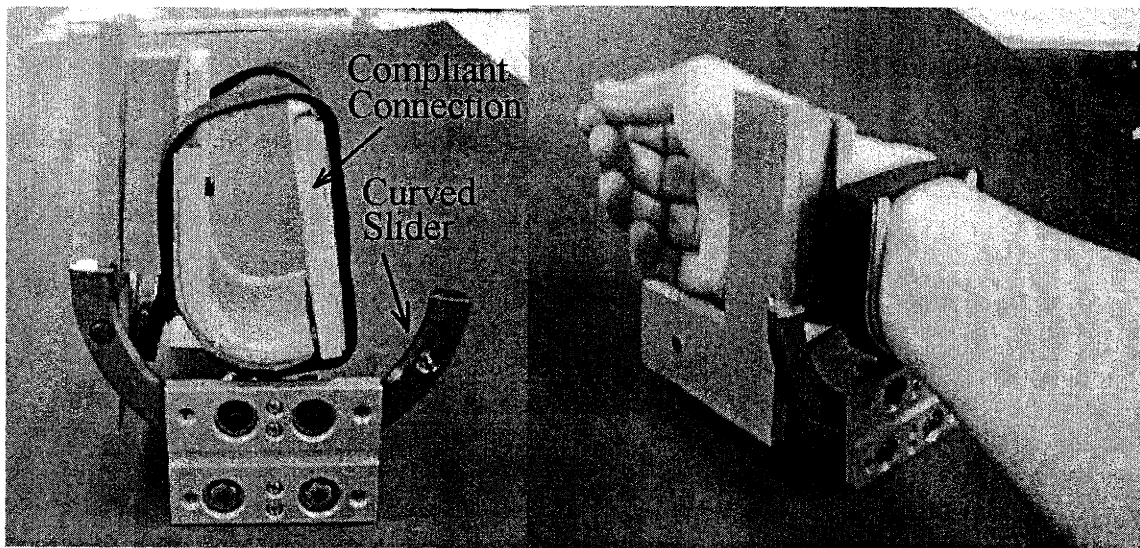


Figure 4.3 Compliant Connection to Distal Forearm

that it has a mobility of three. To do this we can use the mobility equation. It is as follows:

$$M = 6(n - j - 1) + \sum_{i=1}^j f_i \quad (1)$$

where M is the mobility of a given mechanism, n and j are the number of links and joints respectively, and f_i is the degree of freedom of the i th joint. As shown in figure 4.4, the system presently has 7 links and 6 joints each with 1 degree of freedom⁶. With a mobility of $M=3$, and b the number of new joints to be added and a the number of new links to be added, the mobility equation becomes:

$$3 = 6((7 + a) - (6 + b) - 1) + 6 + \sum_{i_n=1}^b f_{i_n} \quad (2)$$

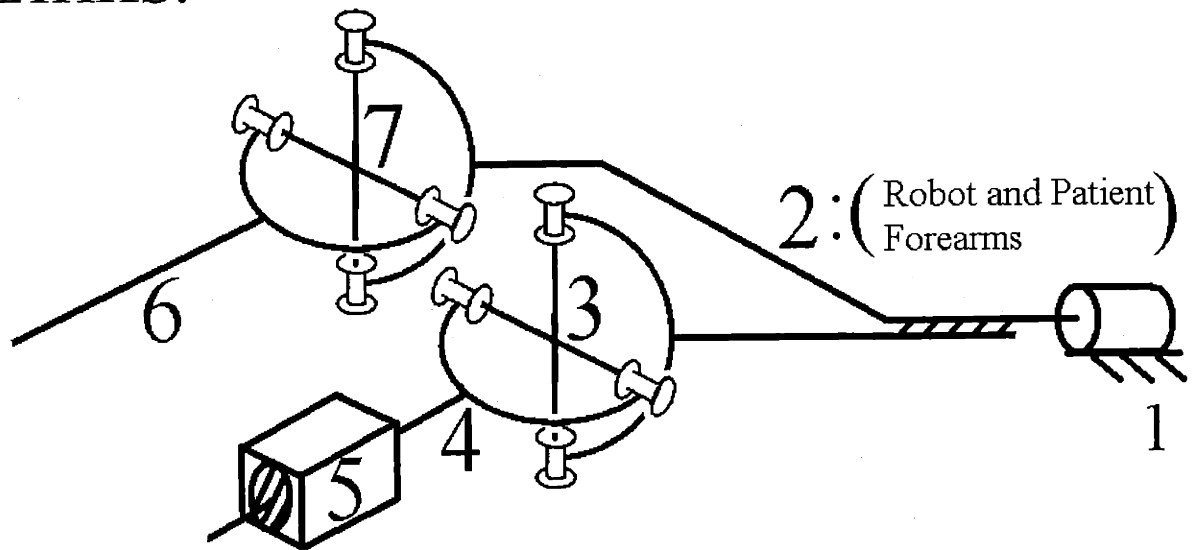
The last term is the sum of the degrees of freedom of each new joint i_n . In order to find a solution to this equation, we can simplify the equation by assuming that each new joint will have only one degree of freedom. This gives:

$$6a = 5b - 3 \quad (3)$$

This equation of course allows only integer solutions. It shows that b must be odd in order that 5b be odd to combine with the odd number 3 to form an even number 6a. We can see that $b=1$ is not a solution because it gives a non-integer value, $1/3$, for a. With $b=3$, however, we find that $a=2$ which gives a solution. We could also start with $a=0$ and

⁶ Note that the compliant connections between the patient and slider and between the patient forearm and the robot forearm are joints with six degrees of freedom. However, as can be seen in equation (1) a single joint with six degrees of freedom has no effect on the mobility of the system. These joints are ignored above.

Links:



Joints:

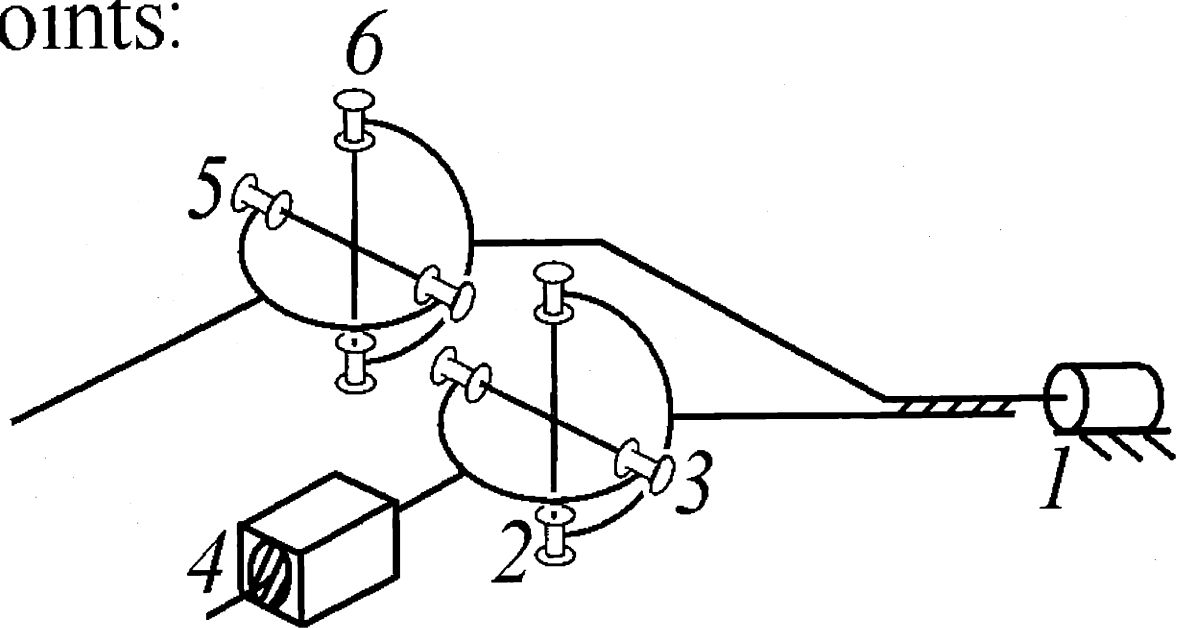


Figure 4.4 Links and Joints

arrive at the same solution. Therefore, we have found the solution requiring the least number of additional linkages and joints. It requires 2 more linkages and 3 more joints.

The simplest and most obvious combination of joints and linkages which satisfy this solution are three perpendicular revolute joints connected in series with two linkages between the slider and the distal link of the robot's universal joint (see figure 4.5a). This combination of joints and linkages is equivalent to a ball and socket joint as shown in figure 4.5b⁷ [15]. There are several other solutions which have 2 linkages and 3 joints; however, these solutions have special properties.

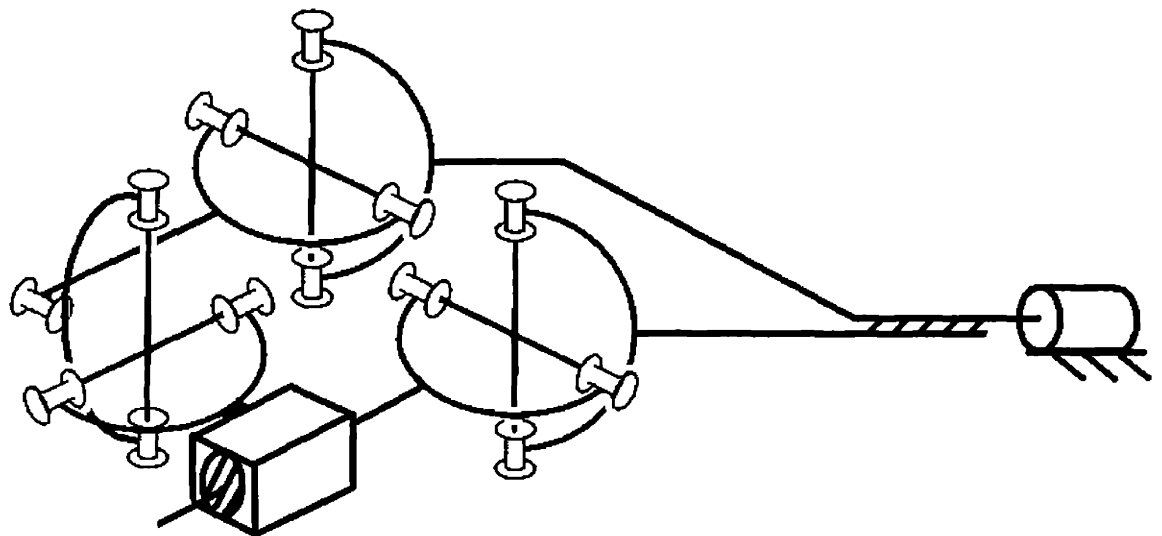


Figure 4.5a. A Gimbal Solution

⁷ Note that this is not true at the singular orientation of the gimbal. In certain configurations, two of the gimbal axes can be aligned. When these axes are aligned the last link in the chain of 3 gimbal links is not free to rotate about an arbitrary axis through the concurrency point of the axes of the gimbal. The ball joint does not have singular orientations and is free, in any orientation, to rotate about an arbitrary axis through its center point.

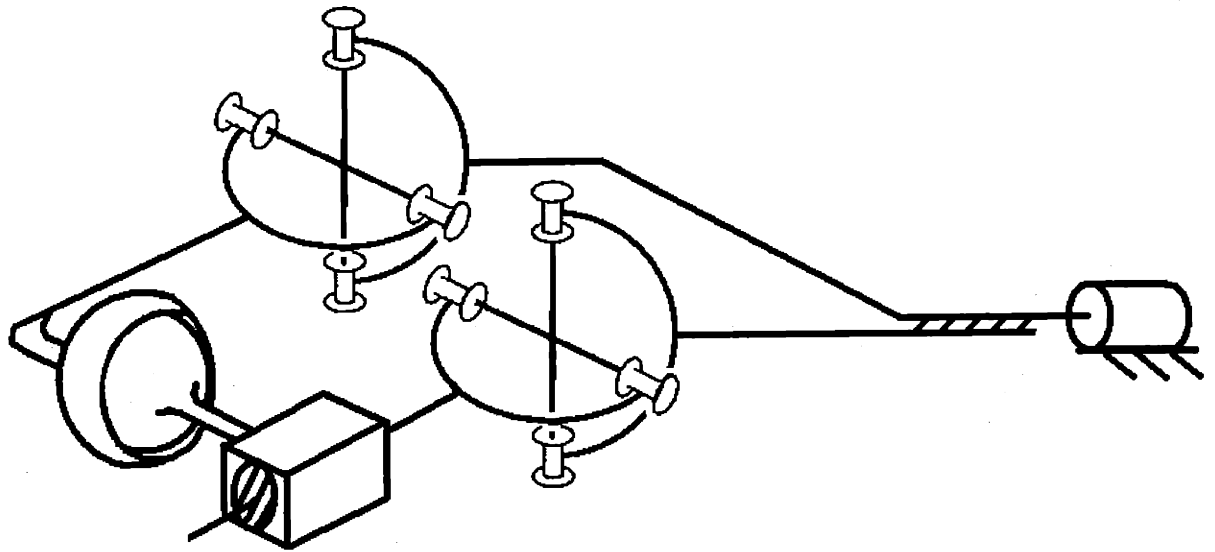


Figure 4.5b. Equivalent Ball and Socket Joint Solution

The solutions above satisfy the mobility requirement and as well allow arbitrary placement of the patient axes. Using Working Model 3D, it was shown that the location of the patient axes of abduction adduction and flexion extension can vary, within a local region about the robot axes. Figure 4.6 shows a displacement in the z direction of both the flexion extension and abduction adduction axes by $\frac{3}{4}$ of an inch. Various displacements of up to 1.5 inches in the x y and z directions (as well as other directions) were shown not to constrain the patient; with these displacements the universal joint representing the patient still had two degrees of freedom in flexion/extension and abduction/adduction. As well, combinations of these rotations were allowed.

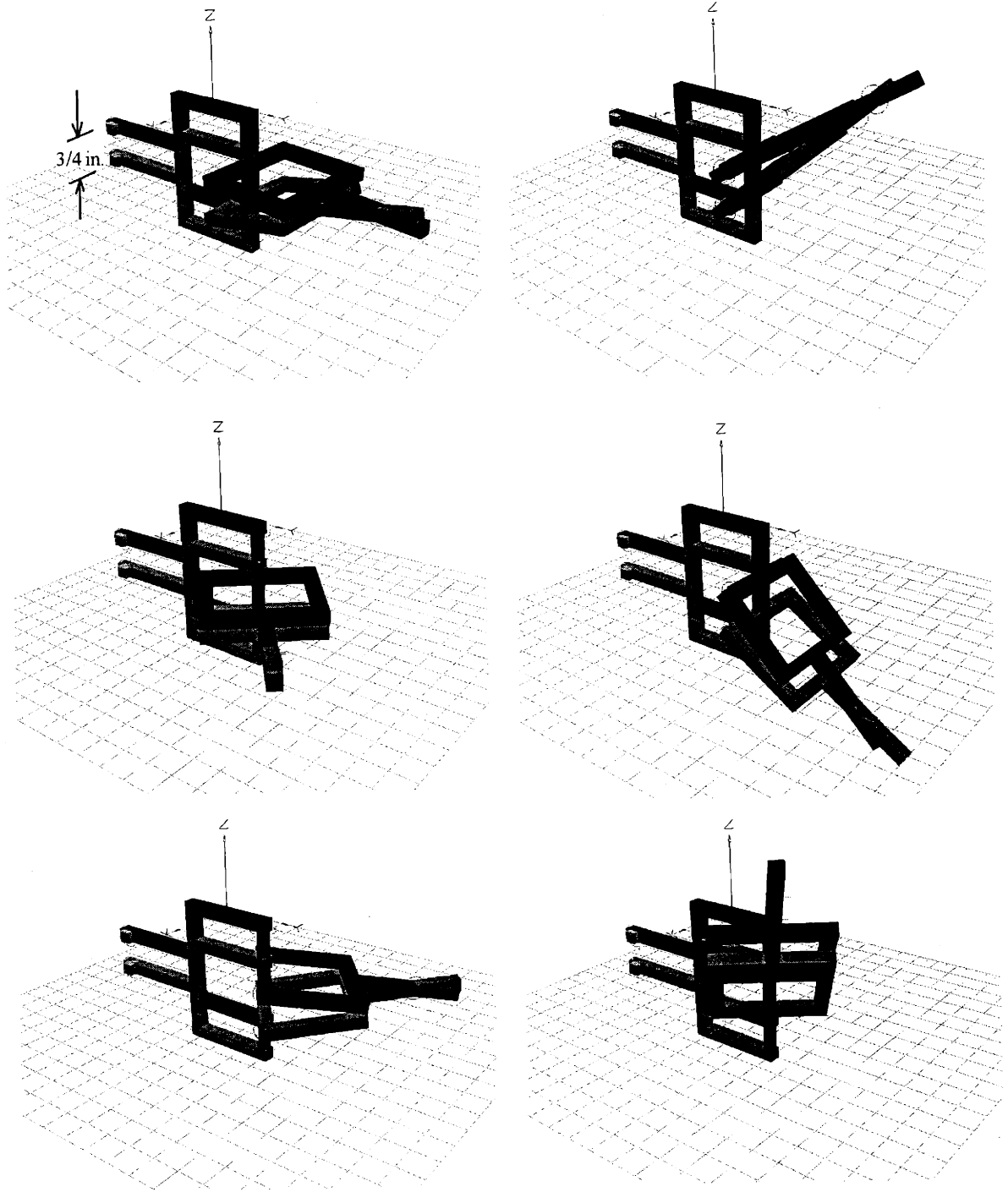


Figure 4.6 Working Model Simulation

4.3 Spherical Joint for Robot Kinematics

A spherical joint was also considered as an alternative for the robot kinematics (See figure 4.7). Note that the compliant connection between the robot and patient forearms is assumed to be the same as that in section 4.2.1. Because the mockup in figure 4.3 worked well, this connection was used for all of the kinematic options considered. Using the same method described in section 4.2.1, the relationship between the number of new links a and new joints b with the spherical joint robot kinematics is:

$$6a = 5b - 4$$

The lowest order solution to this equation gives $b=2$ and $a=1$. Figure 4.7 shows one possible solution with two added pin joints and an additional link. In this case, the robot would be required to actuate only two of the three degrees of the spherical joint. The transmission and actuator options in this case were found to be very complex.

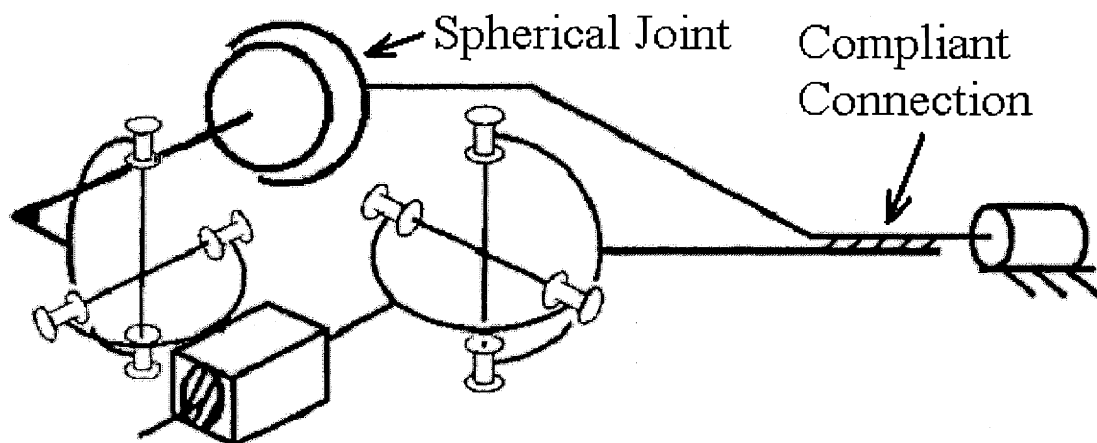


Figure 4.7 Spherical Joint for the Robot Kinematics

4.4 A Rotating Planar Mechanism

A planar mechanism with a rotating base was also considered for the robot kinematics (See figure 4.8). The planar mechanism would likely be a parallel linkage with two actuators placed at joint A. These actuators would actuate the patient in abduction/adduction. A third actuator would be placed at joint B and would rotate the patient in flexion/extension.

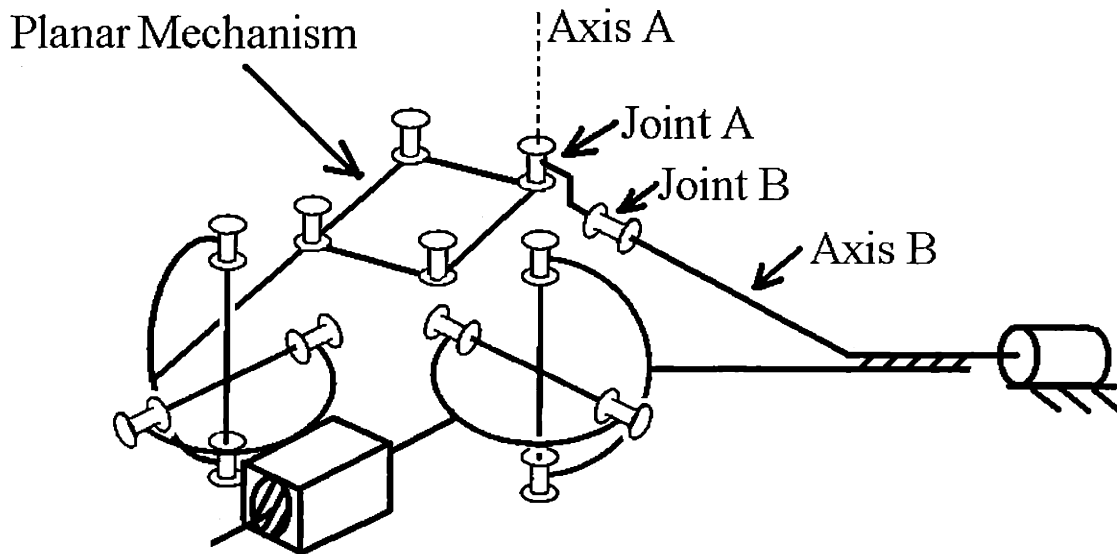


Figure 4.8 Rotating Planar Mechanism Kinematics

Using the mobility equation once again gave:

$$6a = 5b - 4$$

This equation is the same as in the previous section for spherical robot kinematics. This might be expected as the parallel planar mechanism can be simplified to a two link planar mechanism which gives a resulting serial chain of three links and three joints (the same as a gimbal). The connection between the distal end of the parallel mechanism and the

slider thus requires 1 link and 2 joints. This design is a rather complex option adding an extra actuator, two additional links, and an extra joint over the previous options.

4.5 Compliant Kinematics

Compliant kinematics were also considered for the robot kinematics. One possible configuration is shown in figure 4.9. These kinematics, it seemed, were very complex. It was quite difficult to model these kinematics and to predict how they would behave. It also was very difficult to create a transmission system which would transmit forces through these kinematics to the patient.

Compliant Kinematics

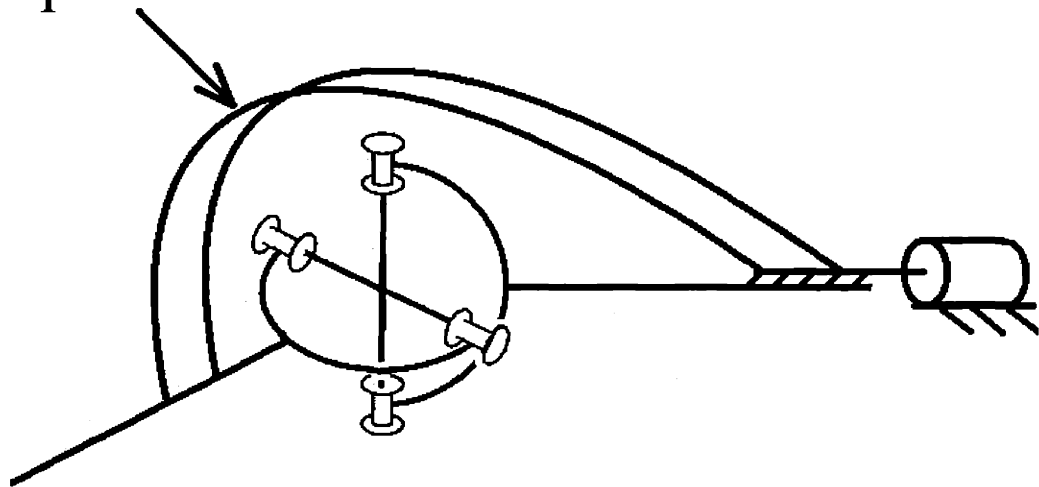


Figure 4.9 Compliant Kinematics

4.6 Mobility Conclusions

After reviewing each of the kinematic options, the universal joint kinematics were found to be the most appropriate. As will be shown in chapter 5 this design has several simple transmission and actuator options. In addition, it requires only three actuators and a minimum number of linkages. The spherical joint kinematics were mainly rejected because of the difficulty in transmitting torques to two of the three degrees of freedom of the spherical joint. The rotating planar setup was rejected because it added complexity without having additional benefits. It added an additional actuator, 2 more linkages and 1 more joint but did not appear to have any advantages over the universal joint kinematics. Finally, the compliant kinematics were rejected because they were found to be extremely difficult to model and design.

4.7 Locating the Kinematics with Respect to the Patient

So far none of the analyses have considered interference between the robot and the patient. The patient has been modeled as a universal joint without regard for the actual dimension, size and shape of the patient's hand and forearm. The actual links and joints of the robot must somehow make room for the patient. After considering a great number of options, the configuration in figure 4.10 was selected. This design offsets the robot abduction/adduction axis from the patient axes and positions the slider connected to the patient as shown. The offset of the abduction/adduction axis increases the position

dependency of the ratio of the torque input to the robot to the torque output to the patient. If each of the robot axes were perfectly aligned with the patient axes this ratio would be 1. Though it increased this position dependency, there were several reasons this offset was selected; the main reasons being that it kept the transmission system small and compact and that it allowed the actuators to be placed for easy patient access.

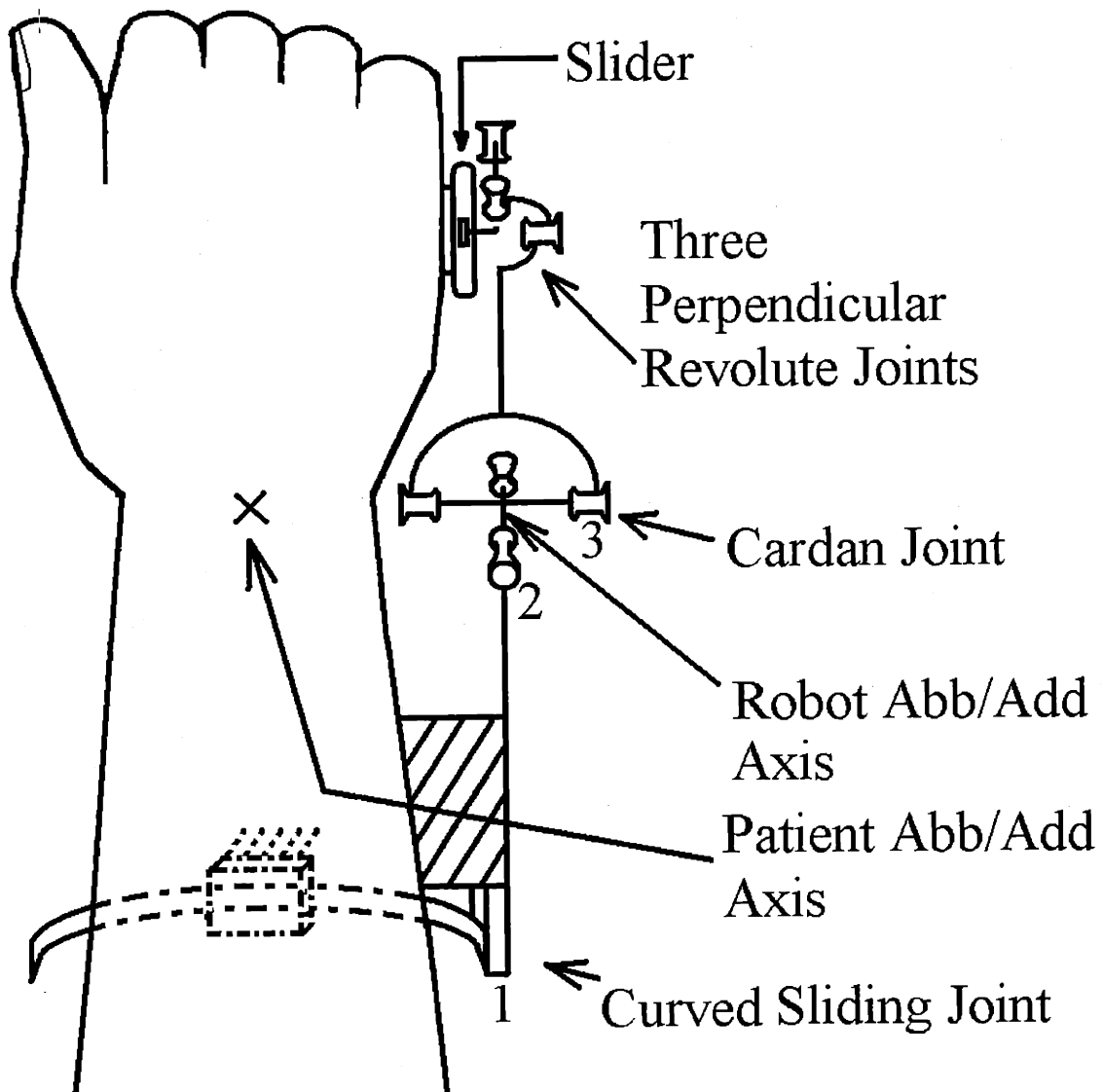


Figure 4.10 Selected Kinematic Configuration

The effects of this offset mainly increase the torque ratio position dependence in abduction/adduction. To investigate this, the system in figure 4.10 was simplified to a planar system as shown in figure 4.11. The robot's universal joint and the wrist become revolute joints and the three perpendicular revolute joints connected to the slider become a single sliding revolute joint.

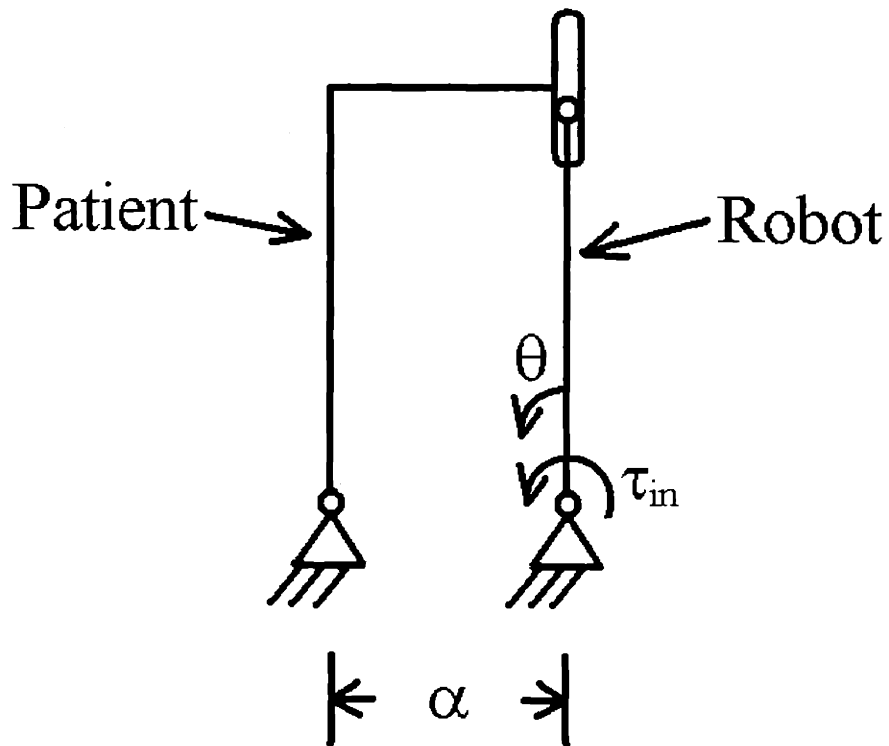


Figure 4.11 Kinematics for Abduction and Adduction Only

Assuming that the robot arm was massless and inertialess (these will be small in comparison to the patient's mass and inertia) and that the joints of the system were frictionless, a simple analysis was done to investigate the relationship between the input torque, τ_{IN} , to the robot arm and the output torque, τ_{OUT} , to the patient. This analysis

assumed the worst case scenario with the largest expected patient size (i.e $\alpha=1.5$ in) . This gave τ_{out}/τ_{in} as a function of θ as shown in figure 4.12. The position dependence shown should be acceptable considering movement in abduction/adduction is relatively small. If need be the control system can make this ratio closer to one in all positions by making the output torque a function of position.

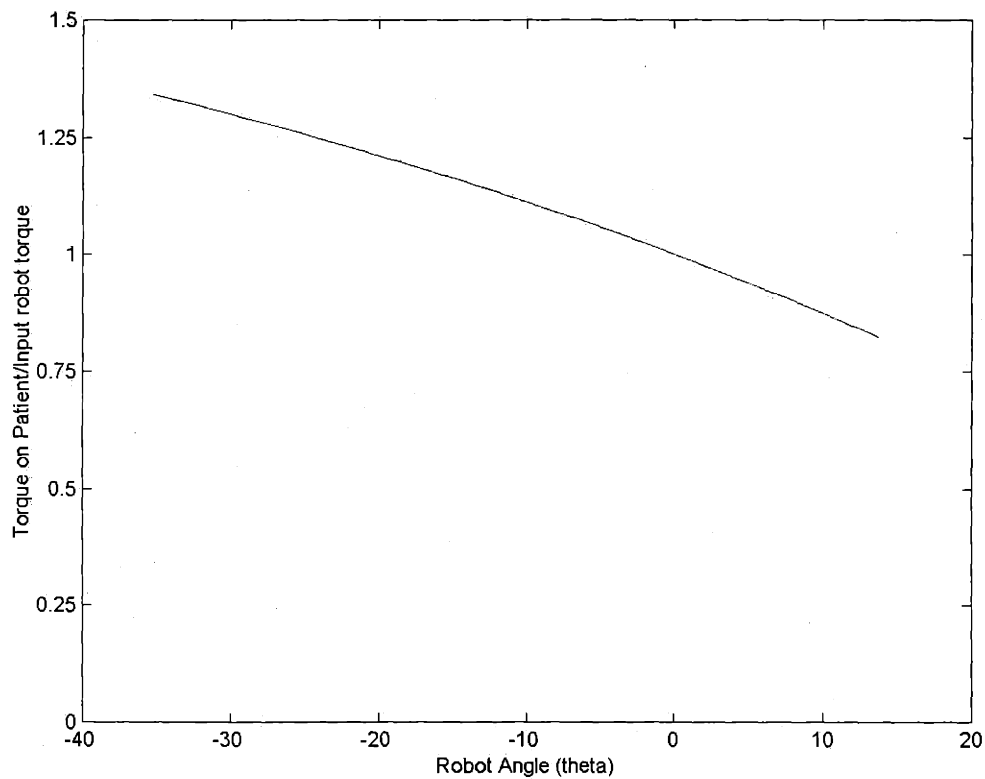


Figure 4.12 (Torque on Patient)/(Robot Input Torque) vs. Robot Angle θ

Also shown in figure 4.10 is the robot's pronation/supination axis. By using a curved slider, the axis of rotation of the robot is placed within the patient's forearm. This axis was placed toward the medial side (toward the ulna) for all expected patient sizes. As explained in section 2.2, this is the most common location for the pronation/supination axis.

4.8 A Mockup of the Kinematics

In order to check on the kinematics explained above, a mockup was built. It is shown in figures 4.13 a b c. The mockup verified that the kinematics have the correct number of degrees of freedom and do not overconstrain the patient. Also, the prismatic joint worked as expected. It insured that shear forces were not applied to the patient. The kinematics also allowed for the required misalignment of the robot and patient axes. Shifting the wrist, within reason, still allowed for smooth transfer of motion between the robot and patient and did not overconstrain the robot/patient system.

The curved slider was also tested. It verified that a compliant connection between it and the patient allowed for variability in the placement of the patient pronation/supination axes.

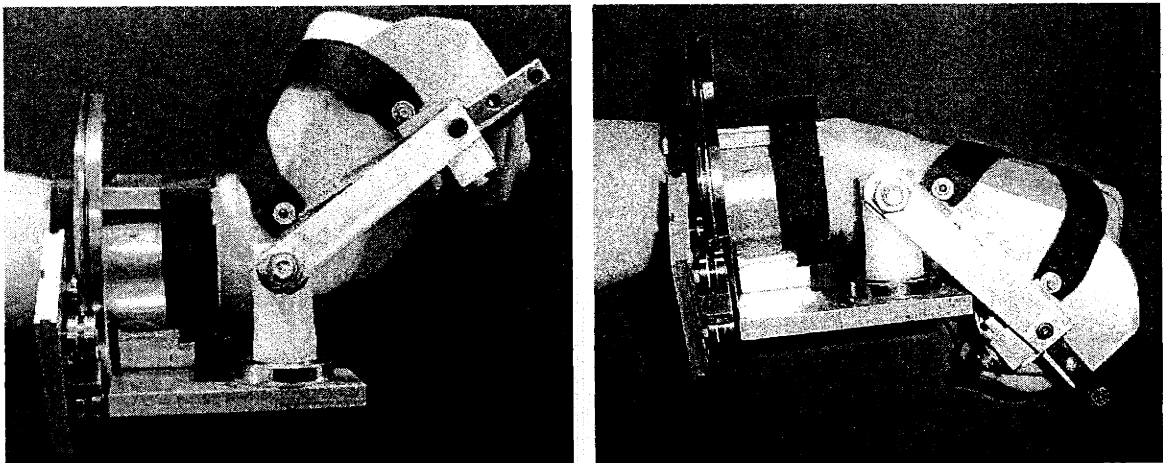


Figure 4.13a The Mockup in Flexion and Extension

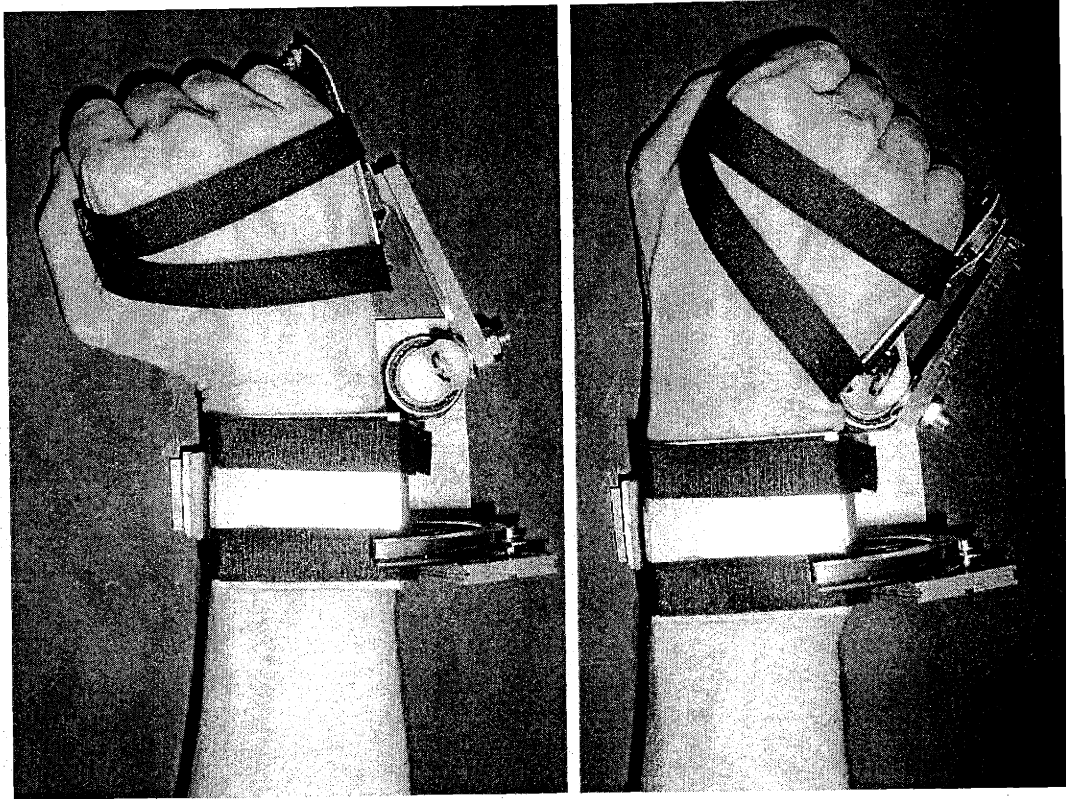


Figure 4.13b The Mockup in Abduction and Adduction

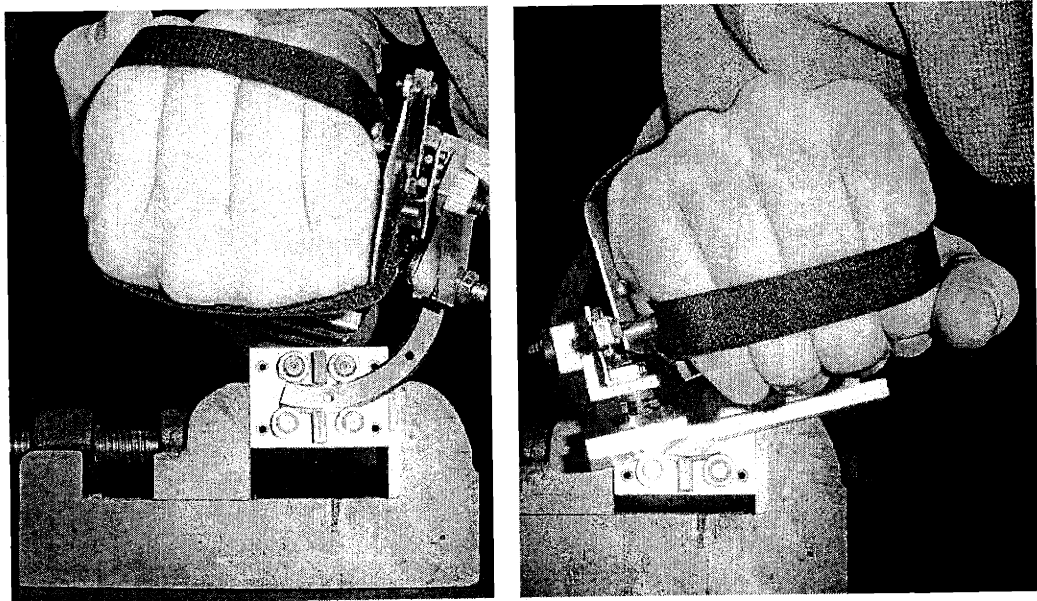


Figure 4.13c The Mockup in Pronation and Supination

Chapter 5

Actuator and Transmission Selection

With the cardan joint selected for the robot kinematics, the transmission and actuation systems were then determined. The transmission will be used to transmit, increase or reduce forces or torques from the actuators to the joints of the robot. The robot will in turn apply forces and torques to the patient.

5.1 Options for Actuator Placement and Transmission

Actuators, in the following text, are those elements which first introduce mechanical power to the system. For the most part only the more established electromechanical actuators were considered for the design. These included actuators like brushed and brushless motors, lorentz force actuators, solenoids, etc. Note that most hydraulic systems use electromagnetic actuators and fluid transmissions.

Because three uncoupled input torques are required to actuate the robot joints which correspond to flexion/extension abduction/adduction and pronation/supination a minimum of three actuators will be required. Figure 5.1 shows these actuators (actuators A,B and C) and the robot links (links 1-4) on which they might be placed.

While thinking through various actuator/transmission alternatives, three actuator placement options emerged. These options are shown in figures 5.2, 5.3 and 5.4. The first option, shown in figure 5.2, places all three actuators on the ground frame. For this option, the transmissions can have either single inputs and single outputs or multiple

inputs and multiple outputs. That is, the transmissions could connect each actuator to a single degree of freedom or several actuators could work together to actuate several degrees of freedom. One possible MIMO option is shown in figure 5.2. The second option in figure 5.3 places an actuator on the ground frame and two actuators on link 2. The transmissions in this case again can have SISOs or MIMOs. Actuators B and C can actuate joints b and c together or individually. The last option in figure 5.4 places a single actuator on links 1, 2 and 3. Actuator A will actuate joint a, actuator b will actuate joint B and actuator c will actuate joint C. In this case each transmission will have only a single input and a single output.

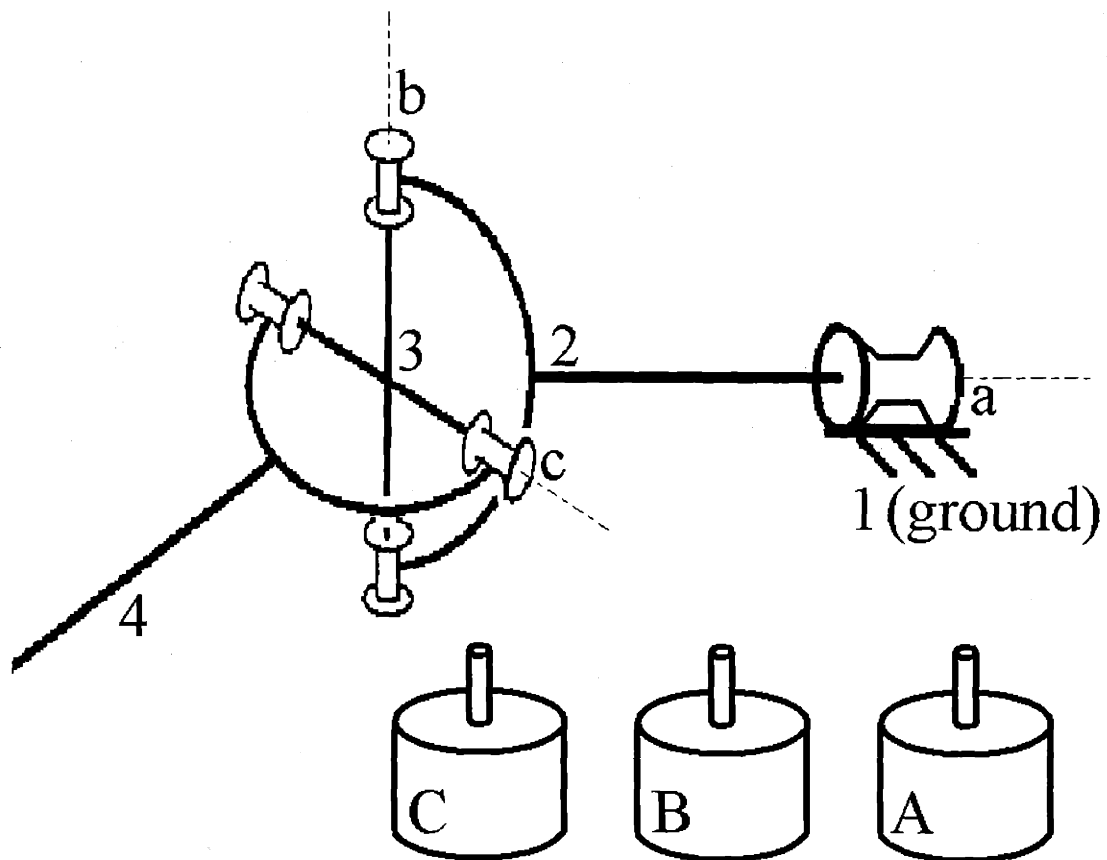


Figure 5.1 Candidate Links for Actuator Placement

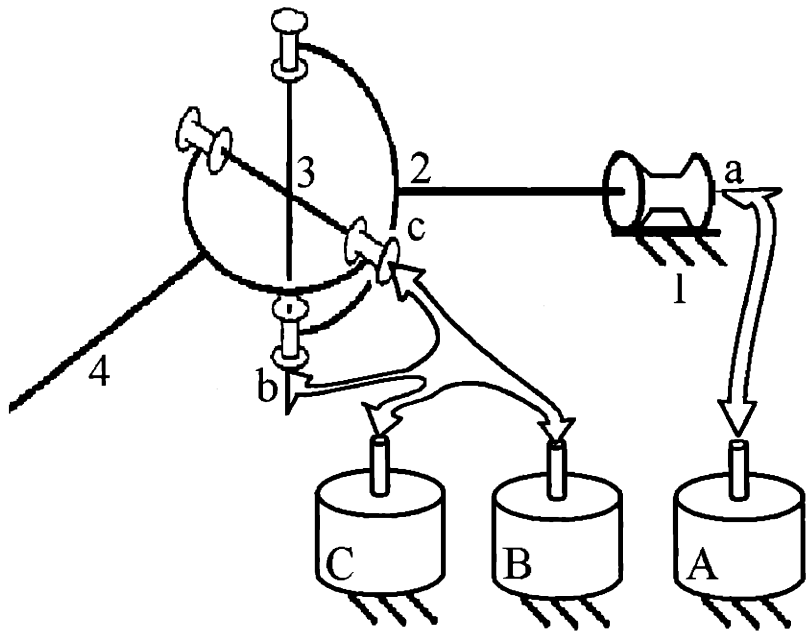
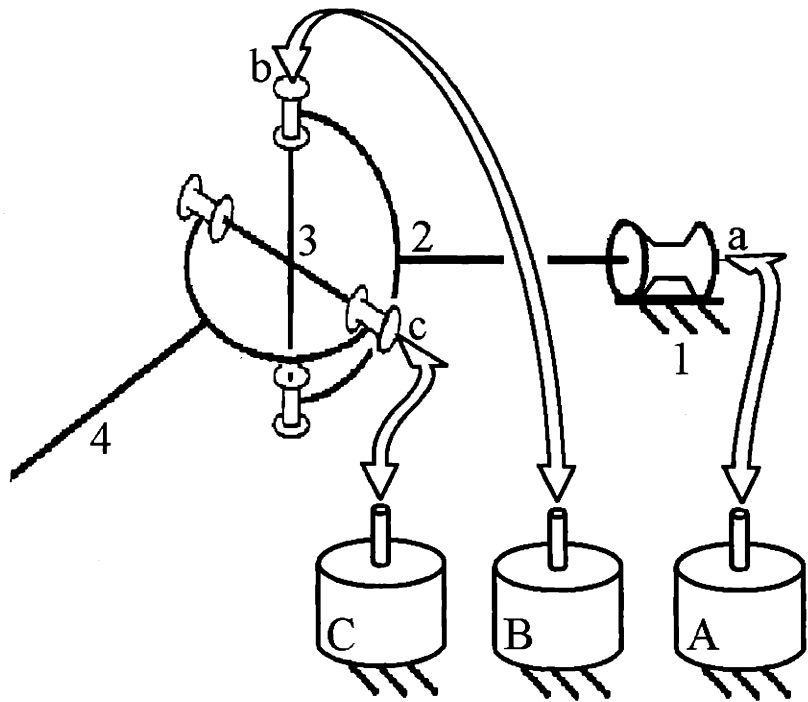


Figure 5.2 All Actuators on the Ground

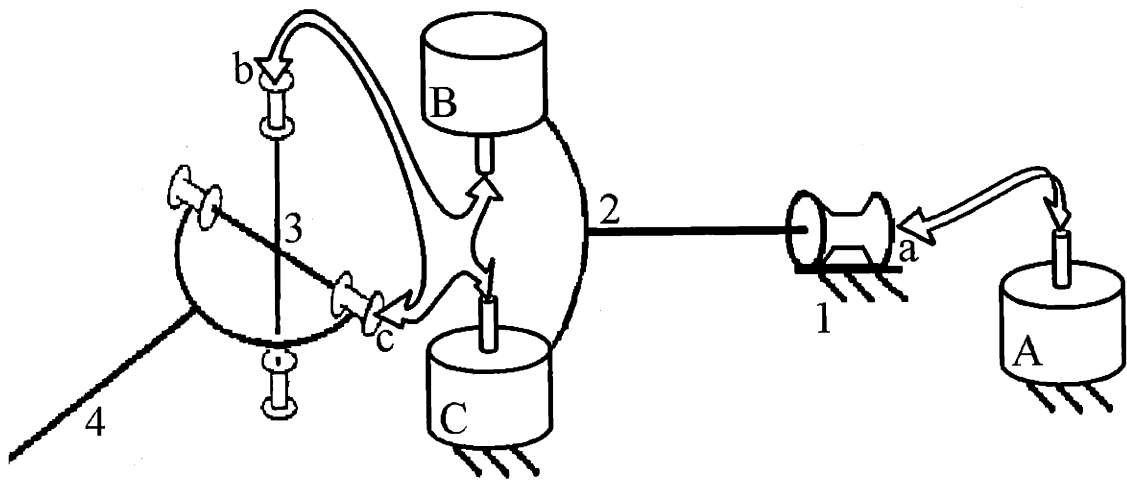
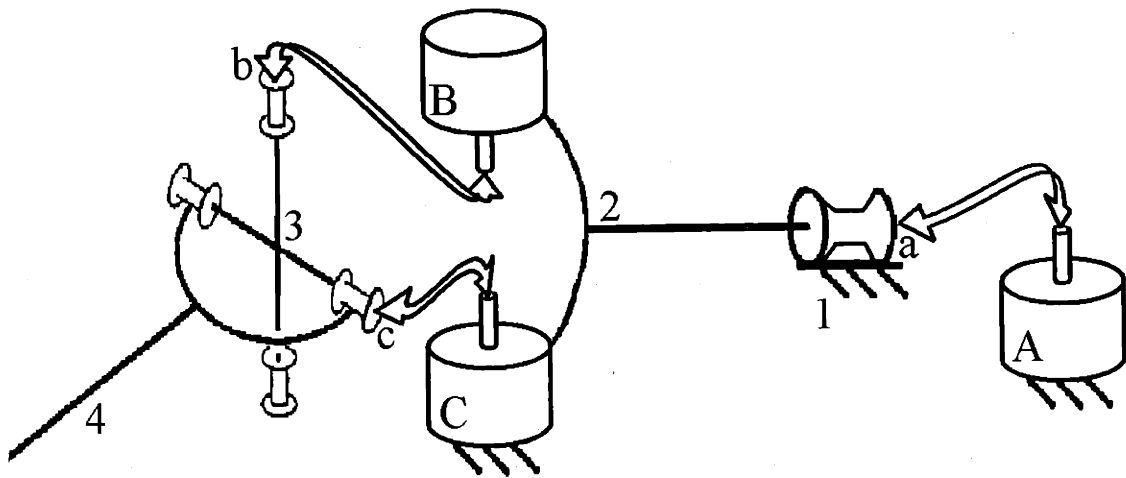


Figure 5.3 One Actuator on Ground and Two in Link 2

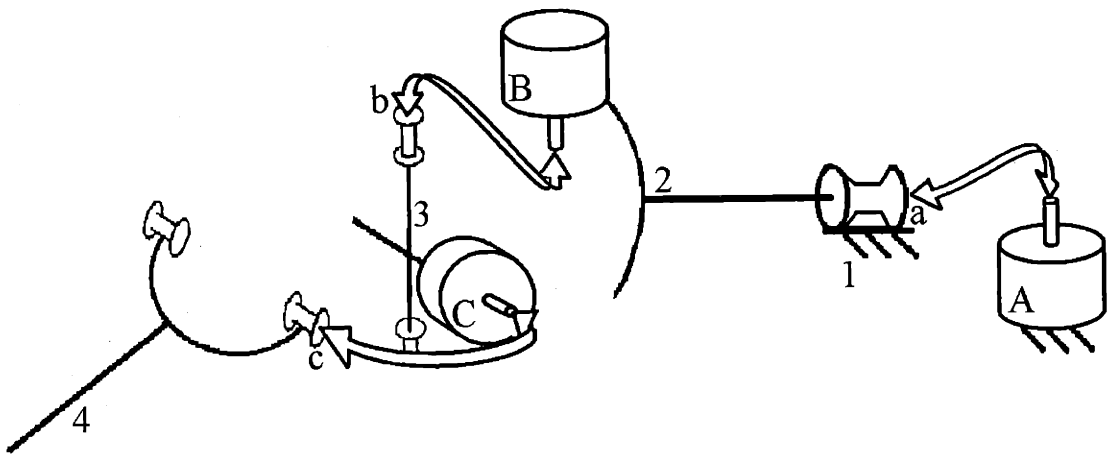


Figure 5.4 An Actuator on Links 1, 2 and 3

5.2 Transmission With All Actuators on the Ground

The main advantage of placing all actuators on the ground frame is that the inertia of the actuators need not be carried around by the patient. This configuration, however, greatly increased the complexity of the transmission system. Because the distal link of the robot (link 4 in figure 5.2) can have arbitrary orientations it is especially difficult to transmit torques to the joints which move it (joints a b and c in figure 5.2). A successful transmission system will need to transmit these torques and keep the mobility of the robot/patient mechanism at 3.

5.2.1 Hydraulic Transmission Using Flexible Lines

To transmit forces and torques to an object with arbitrary orientation it might be possible to use a hydraulic system with flexible fluid lines. The flexibility of the fluid lines would allow the transmission of forces without adding additional constraint to the system; the mobility of the robot would not change. Instead of using hydraulic fluid one could also consider using a gas as the working fluid. Modeling of such a system would be more complex, however, because of the compressibility and nonlinearities introduced by gas[9].

A feasible method for transmitting forces from ground to the joint angles is with the use of two bellows at the ends of a fluid line as shown in figure 5.5. An electromechanical actuator such as a voice coil could apply forces to the first bellows and the hydraulic fluid in the line would transmit this force to the second bellows which would apply forces to the robot.

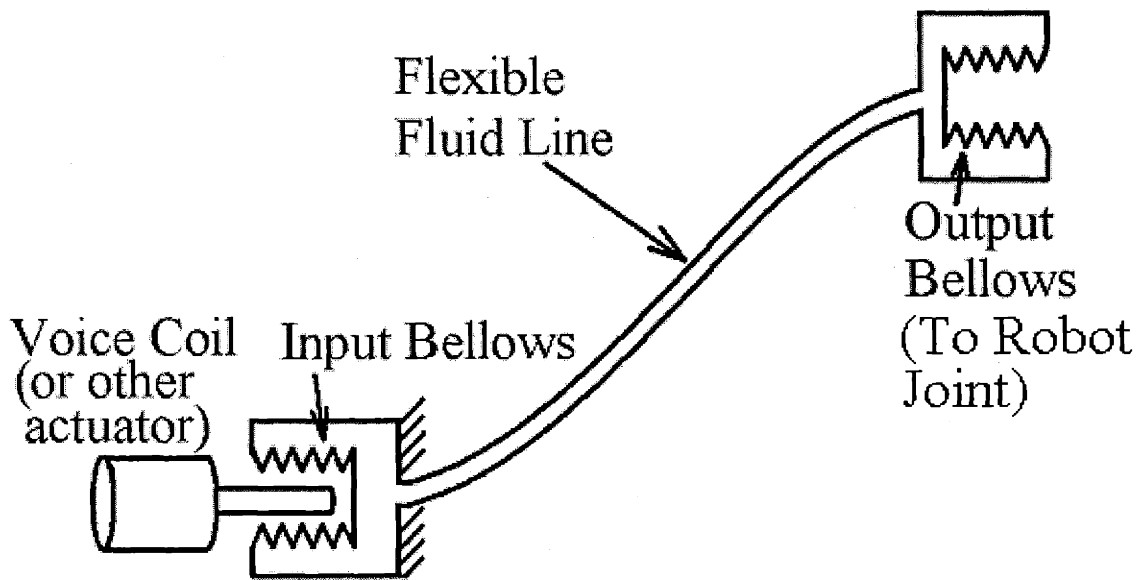


Figure 5.5 Hydraulic Transmission Using A Flexible Line and Two Bellows

A first overview of this design showed that it might be a very practical alternative; it allowed each actuator to be placed on the ground and as well the bellows and fluid lines are of relatively low cost. Unfortunately, this system will have problems with cavitation. Cavitation occurs when the pressure in the hydraulic fluid becomes lower than the vapor pressure at the given fluid temperature. This occurs when the fluid is pulled on to transmit forces from the robot to the patient or from the patient to the robot. For example, at room temperature the vapor pressure of water is approximately $3.3E-4 \text{ lb/in}^2$. Assuming that the input bellows is held stationary, and that the effective area of each bellows is say $\frac{1}{4} \text{ in}^2$, a pulling force on the output bellows of only 3.6 lb would cause cavitation in the fluid line. Assuming a mechanism changing linear motion to rotary motion is attached to

the output bellows with a moment arm of $\frac{1}{2}$ in., the user would have to apply a torque of only 1.8 in*lb or 30 oz-in to cause cavitation. This is quite small as figure 2.7 indicates.

It was thought at first that an antagonistic type bellows system as shown in figure 5.6 would solve this problem. This type of system would use two of the bellows systems in figure 5.5. Each system would create an opposing torque at the output robot joint. Rack and pinions, as shown in figure 5.6, or other means could be used to change the bellows output forces to torques.

Looking at this system a bit closer, it can be seen that this configuration will still have problems with cavitation. When there is no input power from the linear actuators, it can be seen that input torques from the patient at the robot joint will put the fluid in one line under compression and that in the other tension making it susceptible to cavitation.

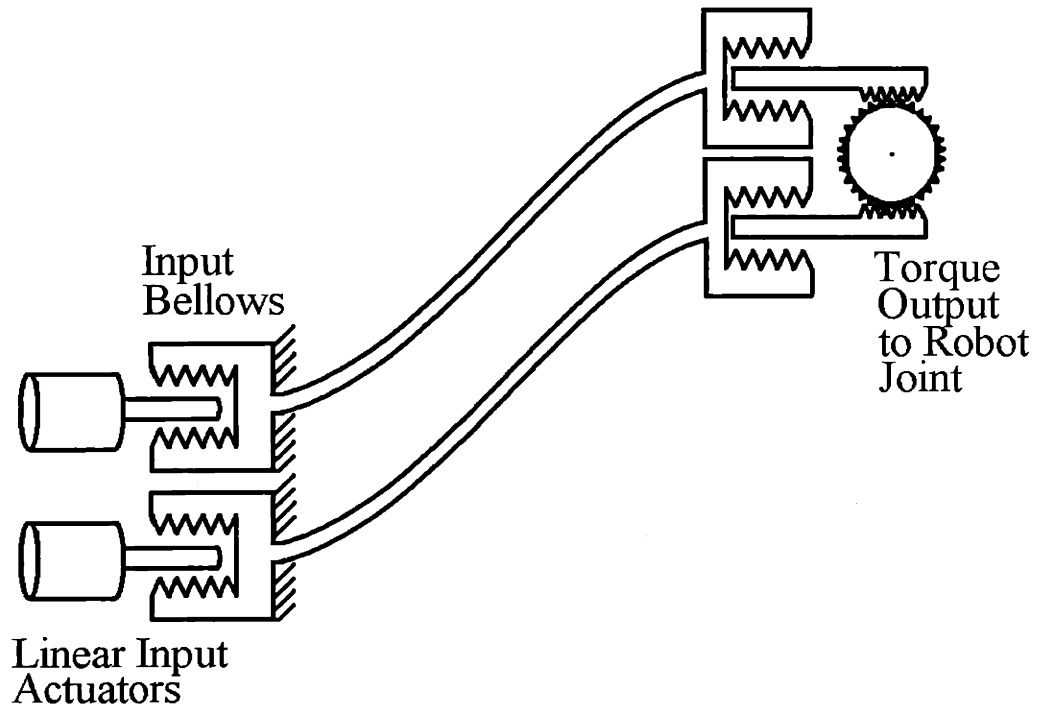


Figure 5.6 Antagonistic Bellows System

5.2.2 Arcing Sliders

Two arcing sliders as shown in figure 5.8 were also considered as transmissions allowing each actuator to be placed on the ground frame. The first arcing slider would allow actuator B to create torques about axis B and the second would allow actuator C to create torques about axis c.

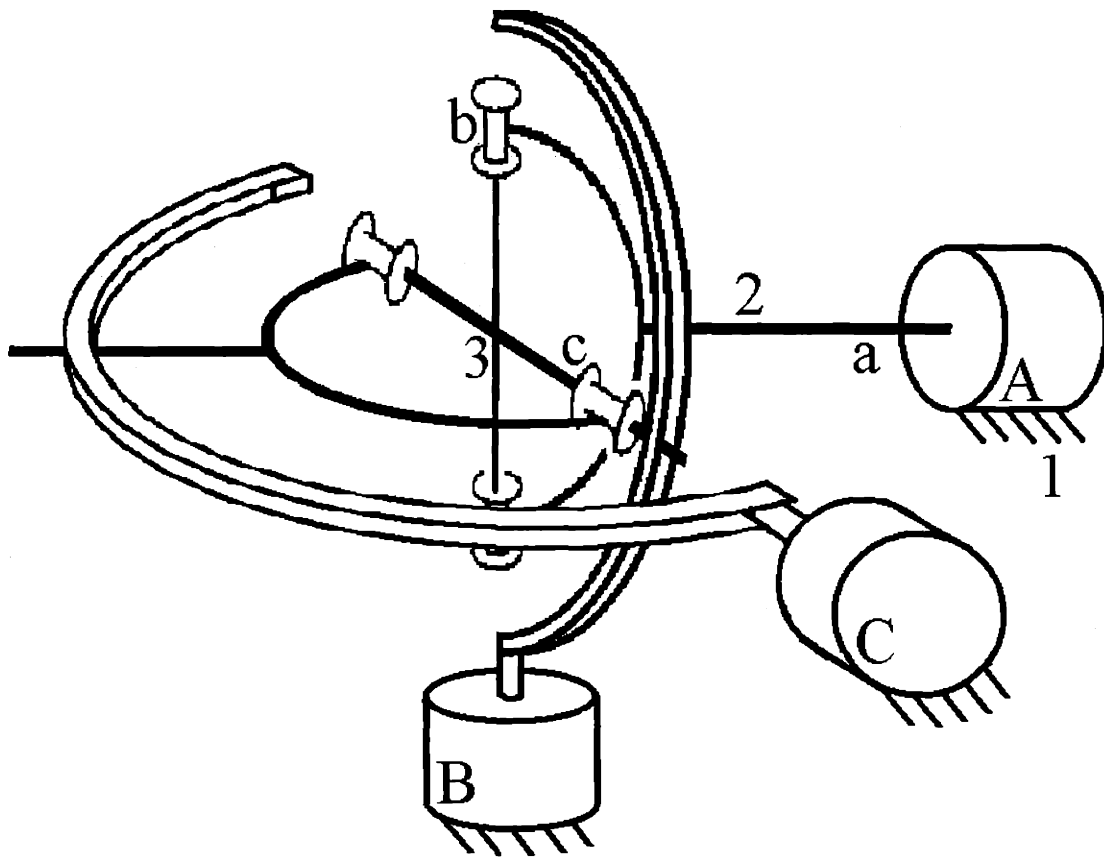


Figure 5.8 Arcing Slider Transmission

Actuator A would apply torque about axis a for pronation and supination. Note that an actual system would require links 2 and 3 to be reshaped in order that the patient wrist could be placed at the concurrency point of all the axes.

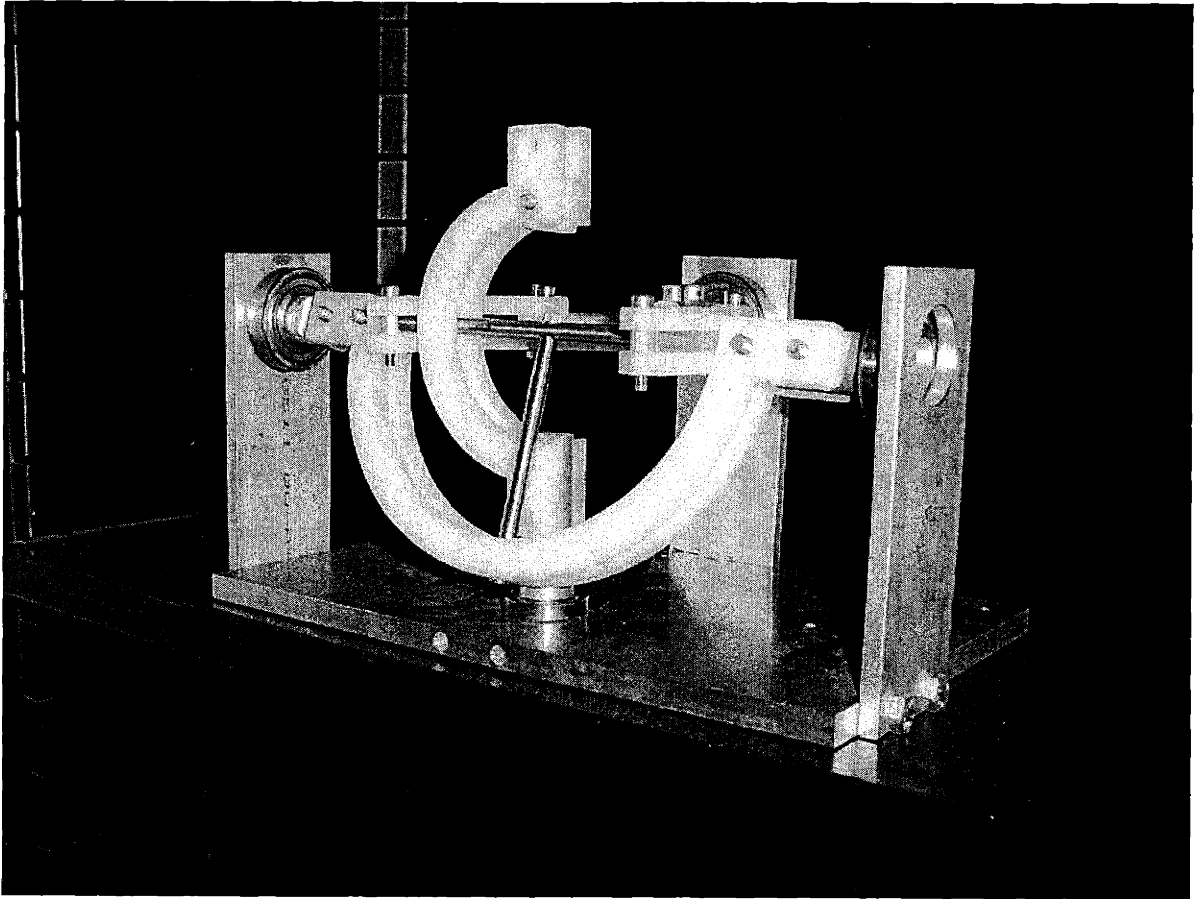


Figure 5.9 Arcing Slider Mockup

A mockup of this transmission system was also built and tested. Figure 5.9 shows the mockup.

Two issues made this design infeasible. The first issue was one of easy patient access. The arcing sliders shown above allow only a small opening (on the upper right) for patient entry. The small opening would make it difficult for an attending therapist to add and remove patients. The second problem was one of interference with the patient. When the robot was in full supination and full abduction for instance, the arcing sliders left very little room for the patient's hand. Larger sliders were the only solution to this problem and this made the system large and bulky.

5.3 Transmission with One Actuator on Ground and Two Actuators on Link Two

By placing two actuators on link 2 (see figure 5.3), the transmission options become simpler. However, placing these actuators on a moving link of the robot adds additional inertial impedance to patient movement. As shown in figure 5.3 when the patient moves in pronation and supination he will feel the reflected inertia due to the rotation of actuators B and C. This is the major drawback of this configuration and of course will depend on the mass, inertia, and placement of the given actuator. Only one transmission option was found to be feasible in this configuration and is explained in the following.

5.3.1 Differential Mechanism

The bevel gear differential mechanism is a commercially available unit often used in simple robot wrists. It consists of a central bevel gear called a spider gear and two outer bevel gears as shown in figure 5.10. The outer bevel gears are labeled A and B. In most commercial differentials all three bevel gears, the spider and gears A and B, are of the same size. Note that for simplicity the bevel gears are drawn with conical surfaces instead of teeth. These conical surfaces are assumed to roll without slip on one another.

The wrist device would make use of the differential by using it as a geared universal joint. Figure 5.10 illustrates how this will be done. On the left are the links and joints of the universal joint and on the right are the corresponding links and joints of the differential. For clarity, links 1 and 2 are left out of the differential diagram. This is okay because it is assumed for now that link 2 and thus axis b in both diagrams are fixed. The

spider gear of the differential corresponds to the distal link of the universal joint; link 4 as shown in figure 5.10. As in the universal joint, the spider gear is free to rotate about axis c. The differential's "T" shaped central shaft would serve as link 3 and would have a degree of freedom about axis b. The two additional gears, A and B, which are free to rotate on shaft 3 would then be used to drive the spider gear.

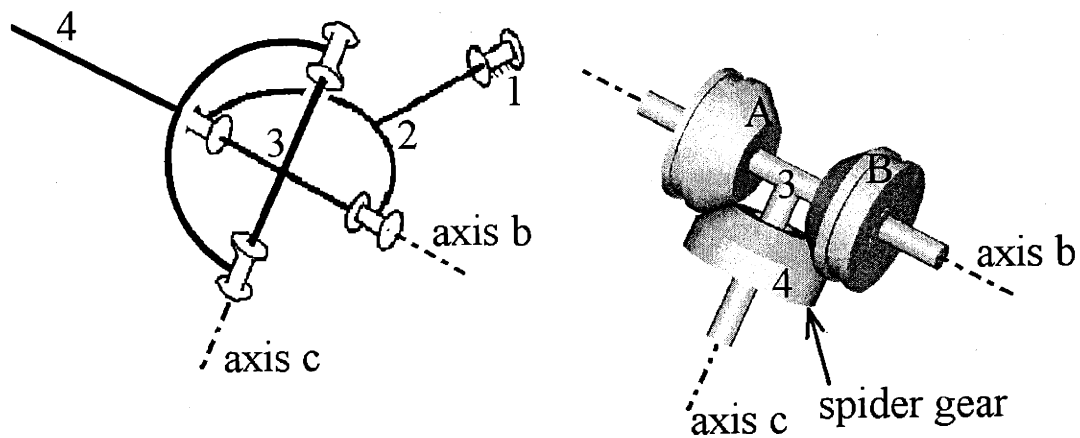
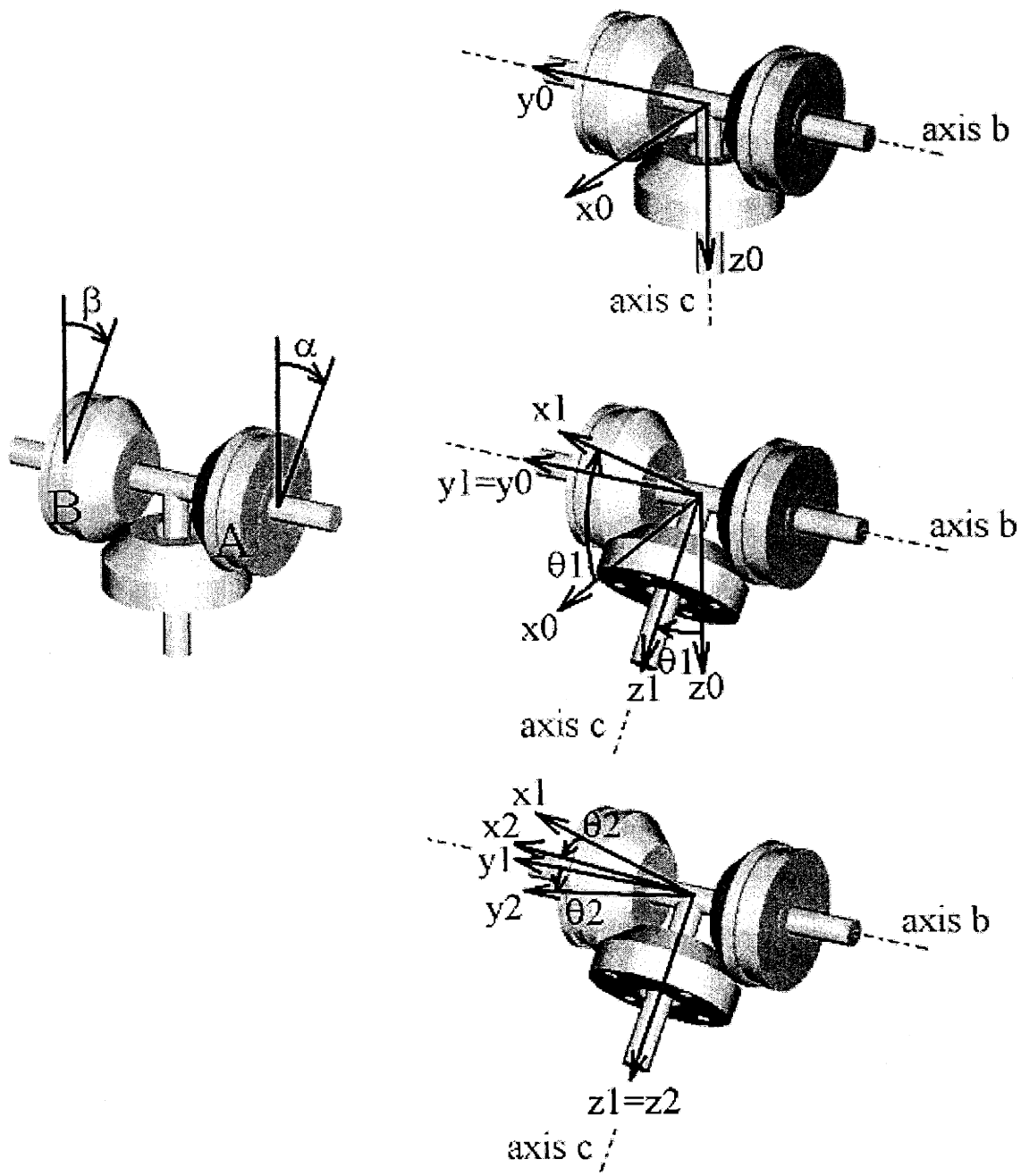


Figure 5.10 Differential as A Geared Cardan Joint

5.3.1.1 Kinematics of the Differential

Again assuming that link 2 (and thus axis b) is fixed, we can find a relationship between the input angles of gears A and B and the orientation of the spider gear. Attaching a frame to the spider gear we can describe its orientation by using angles θ_1 and θ_2 as shown in figure 5.11. These angles give the rotation of the spider gear about axes b and c respectively. α and β give the angles of gears A and B as shown. θ_1 and θ_2 are related to α and β by:

$$\theta_1 = \frac{(\alpha + \beta)}{2}, \theta_2 = \frac{(\alpha - \beta)}{2}$$



Input Angles

Output Orientation
of the Spider Gear
(Link 4)

Figure 5.11 Input Angles and Output Orientation of the Differential

To see how these equations work one can consider the case when $\alpha = \beta$ and the case when $\alpha = -\beta$. When $\alpha = \beta$, $\theta_1 = \alpha = \beta$ and $\theta_2 = 0$ and the spider gear rotates about axis b. When $\alpha = -\beta$, $\theta_2 = \alpha = -\beta$, and $\theta_1 = 0$ and the spider gear rotates about axis c. Figure 5.12 shows how these properties would allow the differential to actuate a wrist in flexion/extension and abduction/adduction. The spider gear of the differential is attached to an arm which is attached to the patient through the required additional degrees of freedom explain in section 4.2.1. Only the cases where $\alpha = \beta$ and $\alpha = -\beta$ are shown. Note that the differential would also allow for combinations of these rotations as in circumduction.

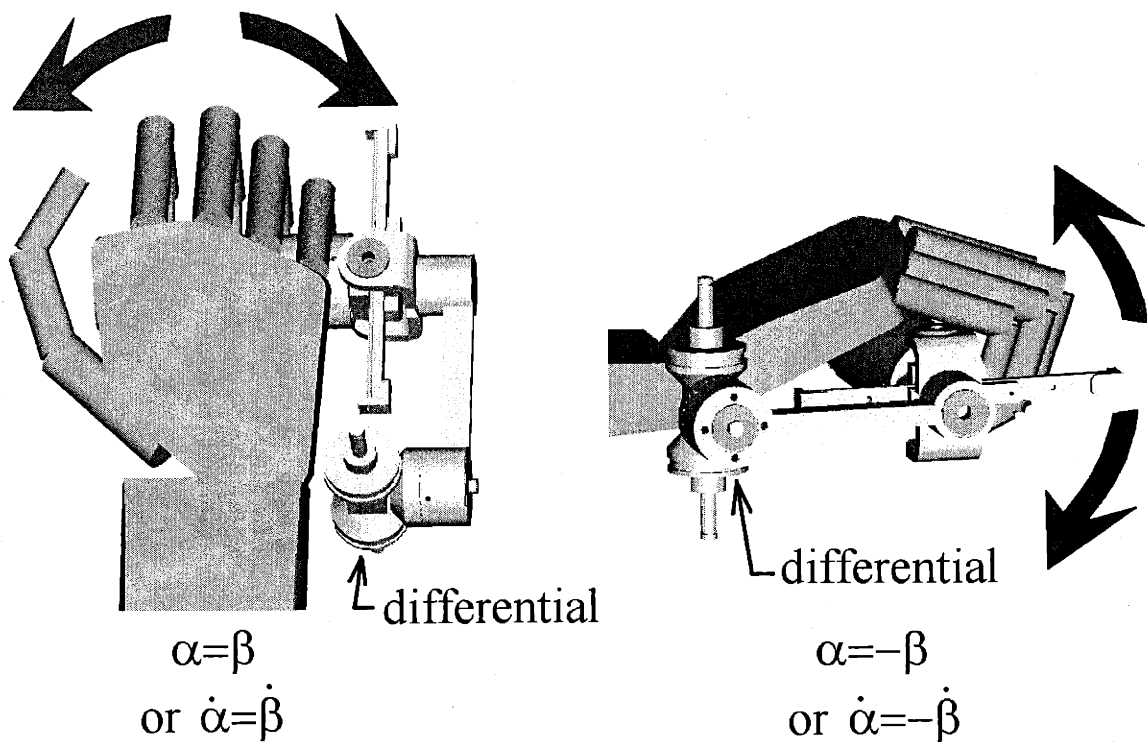


Figure 5.12 Using the Differential to actuate Abduction/Adduction and Flexion/Extension.

5.3.1.2 Torque Output

As shown in figure 5.13a, the input torques at gears A and B, τ_A and τ_B , will be transmitted to the spider gear, down an arm connected to it, and a force and a torque will be output from this arm to the remaining links which then connect to the patient. Separating the spider gear and the arm connected to it from the rest of the differential, we can see the input torque to the spider, τ_{spider} , as shown in figure 5.13b. Using a very simple analysis, it can be shown that this torque is related to τ_A and τ_B with the following relationship.

$$\tau_{spider} = (\tau_A - \tau_B)\vec{k} + (\tau_A + \tau_B)\vec{j}$$

\vec{k} and \vec{j} are as shown in figure 5.13b. Assuming the absolute value of the maximum torque input at gears A and B is τ_{max} (identical actuators would be used), it can be shown using the equation above that the range of τ_{spider} is within the diamond shown in figure 5.13b. As is shown, the maximum torque values occur along axes b and c. The maximum absolute value along axis b is $2*\tau_{max}$. This occurs, for example when $\tau_A = \tau_B = \tau_{max}$. The maximum value along axis c is again $2*\tau_{max}$. This occurs, for example, when $\tau_B = -\tau_A = -\tau_{max}$.

Because the position dependence of the torque ratio due to the misalignment of axis C with the patient axis of abduction/adduction is reasonably small (see section 4.7) τ_{spider} is a good approximation of the torque applied by the robot to the patient about their own axes of rotation .

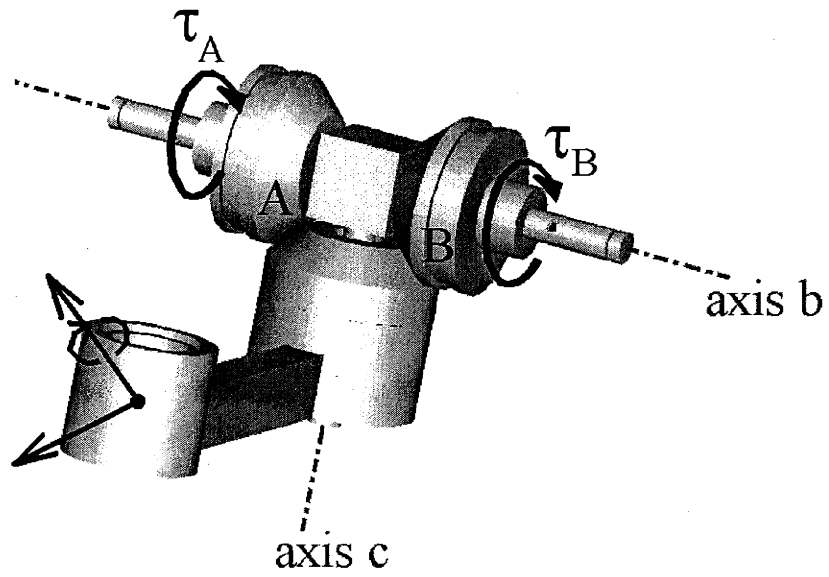


Figure 5.13a Torque Inputs to Gears A and B and Output Forces and Torques from Arm

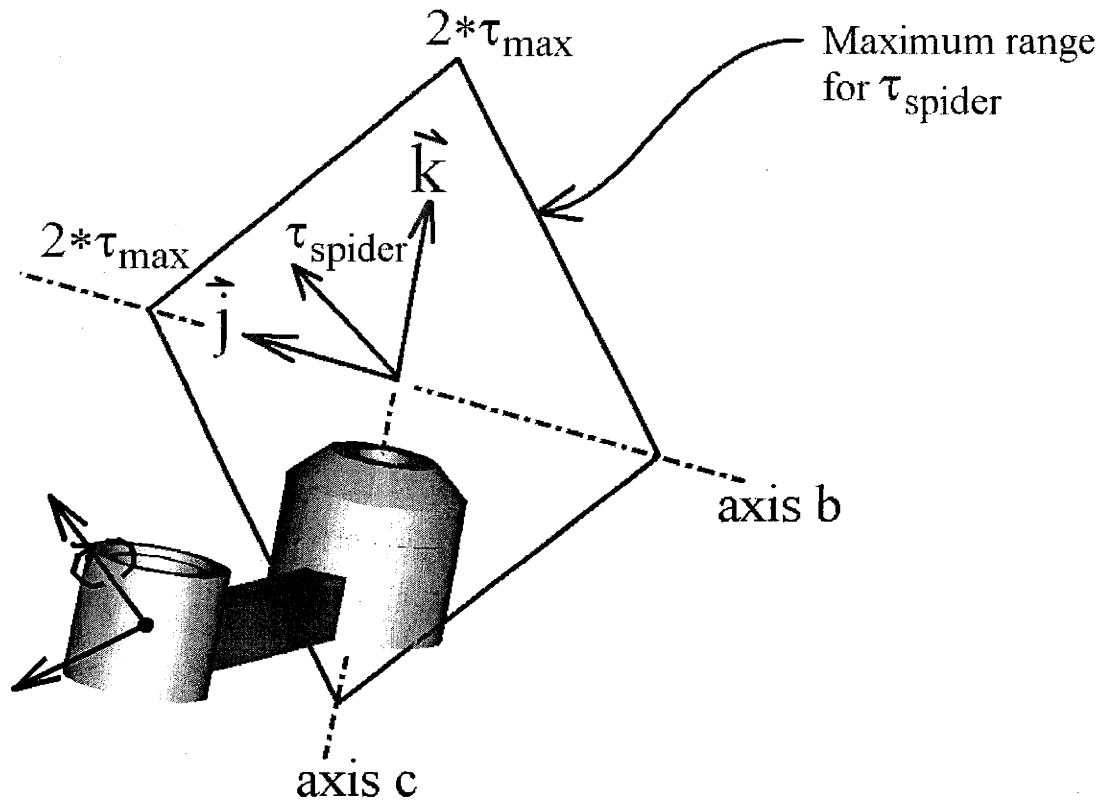


Figure 5.13b Free Body Diagram of Spider Gear and Attached Arm

5.3.2 Actuating Pronation and Supination

The above analysis explains how the differential could be used to actuate flexion and extension. The pronation/supination axis will also need to be actuated. As explained in sections 4.2.1 and 4.7 a curved slider will be used to allow link 2 to rotate about an axis through the patient's arm (see figure 4.3, 4.10). The only curved sliders offered that have an appropriate diameter are offered by Bishop Wisecarver (See section 5.7). These sliders come with an optional integral gear. Because of this, the pronation/supination axis would be driven with a simple geared transmission.

5.4 Actuators on Each Successive Link

Finally, the last actuator/transmission option places actuators on each successive link (Figure 5.14). This option is actually the simplest of the options. Assuming rotary actuators, this option would require a transmission only for reduction purposes; it would not be required to transmit torques across linkages or joints.

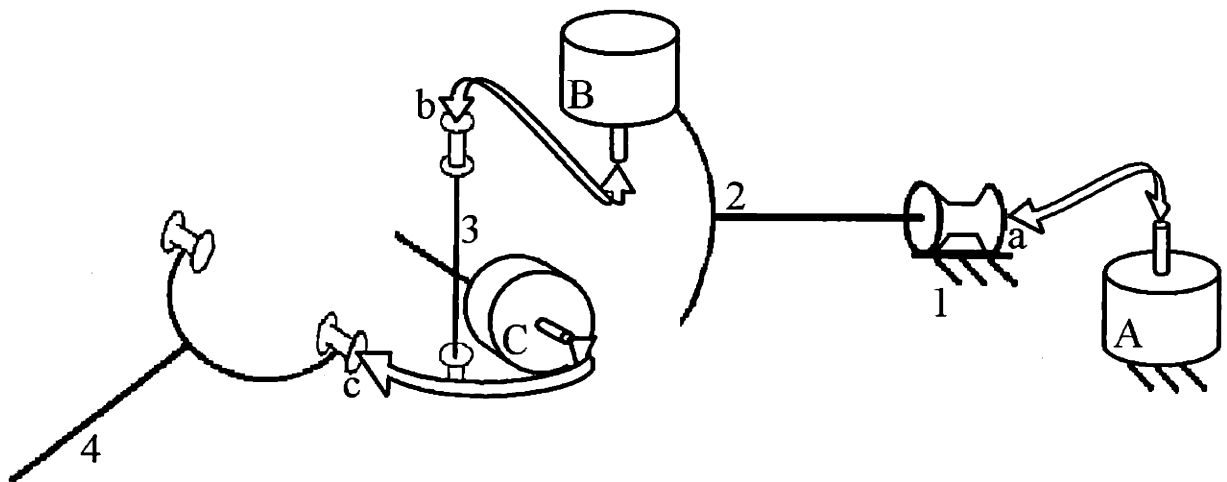


Figure 5.14 Actuators on Successive Links

However, there are several disadvantages to this type of system. First of all, because the actuators are placed on successive links, each actuator must carry the other actuators further down the series of linkages. This requires the use of larger actuators. As shown in figure 5.14 actuator B must carry actuator C. Because of this, actuator B becomes larger. The effect on actuator A is twofold; it must carry a larger B actuator and actuator C. Another possible disadvantage that this setup has is its effect on the inertia that the patient feels. When the patient moves in flexion and extension, he will feel the reflected inertia due to the moving member of actuator C. When moving in abduction/adduction, however, the patient will feel not only the reflected inertia of actuators B's moving member, but also the reflected inertia due to movement of the *entire* actuator C. Because of this, the inertia in flexion/extension and abduction/adduction will likely be quite different. As well, in pronation/supination the patient will feel the reflected inertia of actuator A's moving member and the reflected inertia of entire actuators B and C.

5.4.1 Torque Output

The actuators in this case will apply torques, τ_B and τ_C as shown in figure 5.15a. Note that reduction elements might be used in this case but are left out for simplicity. The torque output to the arm follows:

$$\tau_{out} = \tau_C \vec{j} + \tau_B \vec{k}$$

Assuming the same actuators as in section 5.3.1.2., with a maximum output torque of τ_{max} , the torque to the arm will fall within the rectangle shown in figure 5.15b. In comparison to the differential case, the resultant torque output to the arm is simpler

because its components are decoupled, however, as is shown, for the same actuators, the range of output torque, τ_{out} , is smaller.

5.5 Transmission Conclusions

Using a transmission that places each actuator on the ground frame is a very attractive alternative. If such a system were found the actuators would likely add very little inertia to each patient axis as only the inertia of their moving members would be reflected. However, both of the transmission options found for this configuration were not feasible. The first option using flexible fluid lines looked like a promising idea. It is possible that there are other configurations which do not have problems with cavitation; however, none were found. The arcing sliders idea also had potential as a transmission system, however, patient interference and large size made them infeasible.

The differential and the serial configuration were the only workable options considered. In comparing the two, the differential configuration clearly held the advantage over the serial configuration. As shown in figure 5.15b, for the same actuators, the range of output torque is up to two times larger. Another advantage not mentioned above is that the actuators can more effectively counterbalance one another in the differential configuration. This is because both actuators are placed on a single link. By placing actuators B and C symmetrically about the robot's pronation/supination axis the gravity torque produced by each actuator is canceled out. This is shown in figure 5.16. In the serial configuration this cannot be done as effectively; actuator C can shift closer to and further away from the pronation/supination axis allowing for a net gravity torque. Actuator stack up and the disproportionate inertia added in flexion/extension vs. that in

abduction/adduction also pointed to the differential as the best option. Because of these advantages, the differential was selected for the system's transmission.

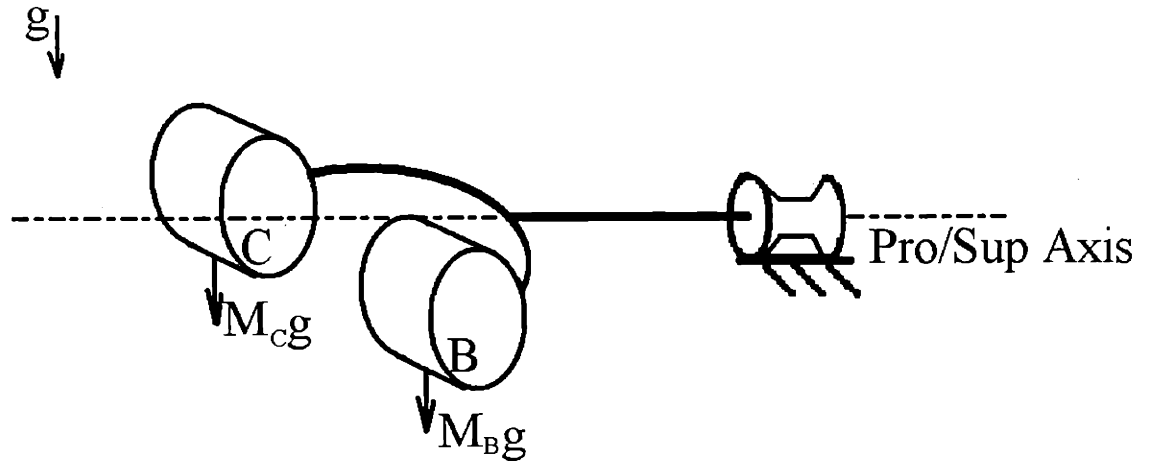


Figure 5.16 Counterbalanced Actuators

5.6 Actuator Options

With the differential selected for the system's transmission, the actuators were then selected. In a search of commercial actuators several alternatives were considered. The following were the most promising.

5.6.1 DC Servomotors

DC servomotors, for the most part, take two different forms. They can be either brushed or brushless motors. Brushed motors have windings on the rotor and permanent magnets on the stator. The rotor is the rotating member of the motor and the stator is the stationary member. Brushed motors are commutated mechanically by means of brushes which slide on a segmented slip ring. A stationary magnetic field is created by the

permanent magnets on the stator and each time the brushes move to a new segment on the slip ring the magnetic field created by the windings changes and comes out of alignment with the stator field. This creates a torque on the rotor and it turns. Brushless motors are driven in a similar way. Brushless motors have windings on the stator and permanent magnets on the rotor. A *motor driver* varies the current in the windings of the stator and creates a rotating magnetic field. The permanent magnets of the rotor follow this field. The motor driver uses Hall Effect sensors, encoder, or resolver feedback to determine the orientation of the stators rotating field.

When used in robotics, DC servomotors are run at unusually low speeds. Because of this, an effect called cogging torque can cause control problems. In fact cogging torque is the major cause of control problems at low speeds. Cogging torque is caused by the alignment of motor magnets and the lamination tooth edges about which the motor windings are wound. It is the torque you feel when a motor is rotated by hand. This torque is distinct from torque ripple which is the variation in torque *produced* as the orientation of the windings and poles changes.

There are several methods commonly used to reduce cogging torque and improve low speed performance. The most common method for reducing cogging is to slant the lamination tooth edges and thus the motor windings. The laminations then form a gradual helix and cannot align with the permanent magnets. Maximizing the number of poles and windings is also helpful.

5.6.1.1 Advantages and Disadvantages of Brushed Motors

The major advantage of brush motors is that they are simple and inexpensive to control. A power op-amp and an analog output from a servo-control algorithm are all that is need to control these motors. Another advantage of these motors is that they can be dynamically braked without any input power. The motor can act as a generator if a resistance is used to short the motor leads.

The major disadvantage of brush motors is due to their mechanical commutation. Under high torque conditions, which would be expected in this application, high current through the brushes can cause them to erode rapidly. These high currents can produce large sparks which can be harmful to other electrical devices and can produce unwanted noise. The brush friction will also add to the endpoint friction that the patient would feel.

5.6.1.2 Advantages and Disadvantages of Brushless Motors

Brushless motors have a considerable advantage over brush motors in low speed applications in that they can be operated at zero rpm and high currents indefinitely. As long as the winding temperature does not exceed its limit the motor can operate continuously. Placing the windings on the stator of the motor also has advantages. The main path of heat flow is the motor casing instead of the motor rotor.

The major disadvantage of brushless motors over brush motors is the cost of the motor and amplifier. Control complexity is also increased[11][12].

5.6.2 ServoDisc Motors

Another option considered for the wrist robot's actuators were servo disc actuators. These actuators are actually brushed motors with different winding and permanent magnet orientations. As shown in figure 5.17 the windings of this actuator are on a thin disk and the current in the windings travels radially on the disc. The magnetic field created by the permanent magnets passes axially through the disc creating a torque on it and the shaft.

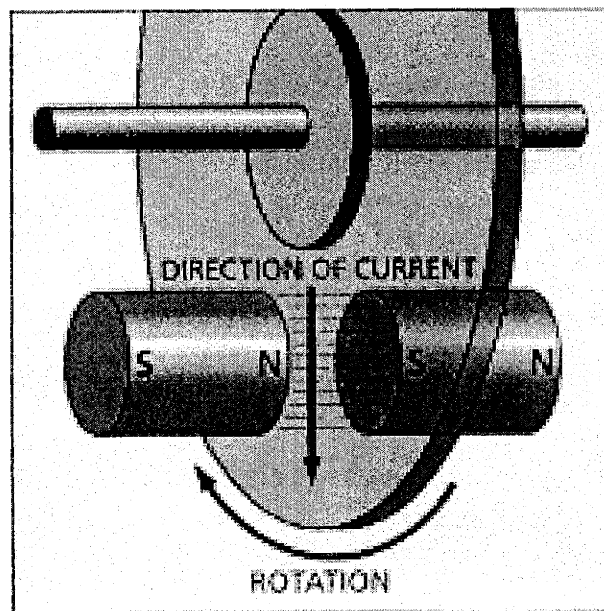


Figure 5.17 Servodisc™ Actuator (Courtesy Kollmorgen)

Servodisc motors have several advantages over conventional dc motors. Because there are no laminations, cogging torque is eliminated. Also, the electrical time constant is much smaller than that of conventional and rare earth ironcore motors. Comparisons to dc brushed motors are shown in figure 5.18 .

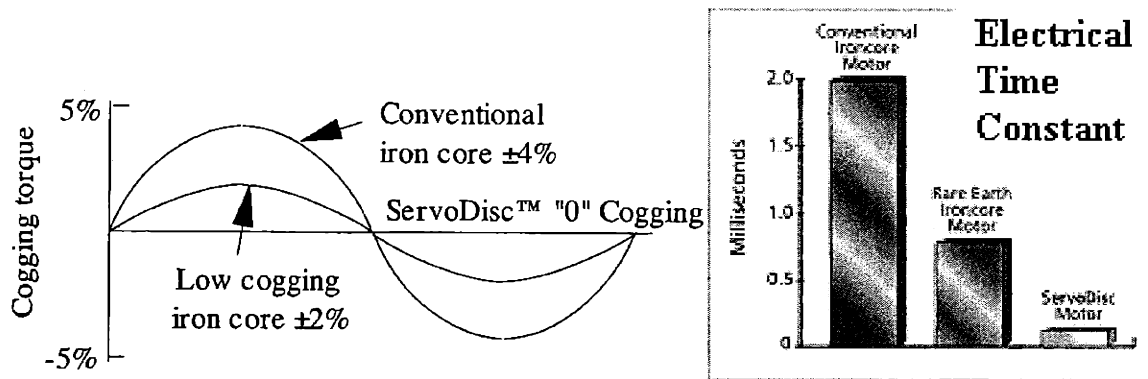


Figure 5.18 Servodisc™ Advantages (Courtesy Kollmorgen)

Servodisc motors have several attractive advantages; however, their dimensional characteristics are not compatible with the wrist robot. Because of the shape of disc the motors take a thin and flat “pancake” type shape. The motors of reasonable weight (<5 kg) have diameter of 4.72 in and a length of 1 in. Using this size motor was impractical for aesthetic and ease of patient entry reasons.

5.6.3 Ultimag Rotary Actuators

Ultimag Rotary Actuators offered by Ledex Dormeyer Products were found to be candidates for the systems actuators. These actuators operate on the principal of magnetic attraction and repulsion of opposite and like magnetic poles. As shown in figure 5.19, the actuator consists of a rotor with several permanent magnets and a stator consisting of electromagnets. There are twice as many poles on the permanent magnet armature as there are poles in the stator coil. In the de-energized state, the armature poles each share half a stator pole, causing the shaft to seek mid-stroke. When power is applied, the stator poles are polarized. This attracts half and repels the other half of the armature poles,

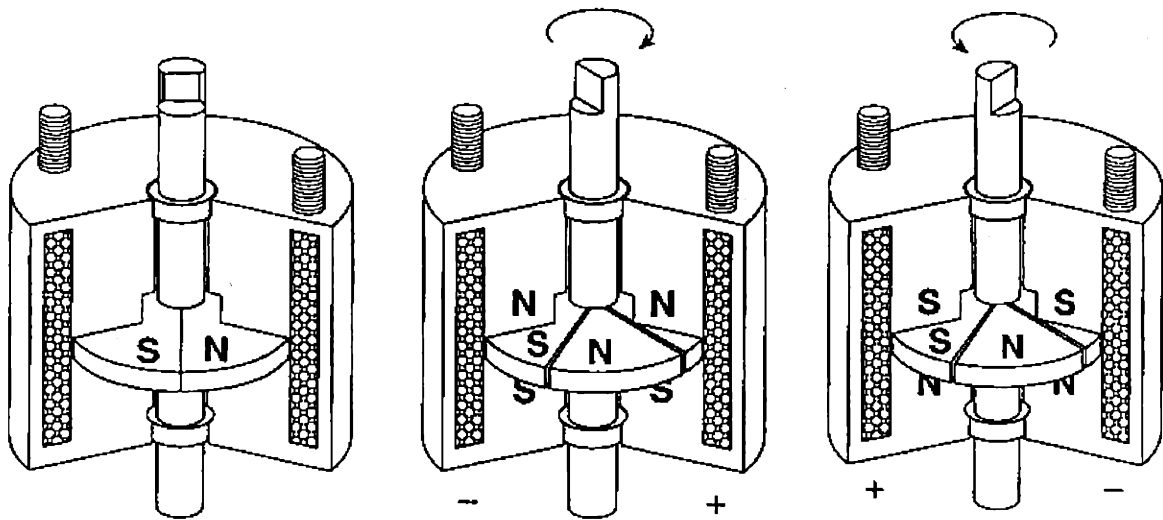


Figure 5.19 Ultimag™ Rotary Actuators (Courtesy Ledex Dormeyer)

causing the shaft to rotate. When the voltage is reversed, the stator poles are polarized with the opposite pole. Consequently, the opposite poles of the armature are attracted and repelled, thus causing rotation in the opposite direction . Figure 5.20 shows that the maximum output torque for this actuator varies as a function of position and the duty cycle of the input voltage to the actuator. As is shown, this actuator has a maximum output torque with a 10% duty cycle of about 40 oz-in. The maximum travel as is shown is 22.5° in each direction. As explained in section 3.3 the required torque in flexion/extension and abduction/adduction is 170 oz-in and that in pronation/supination is 240 oz-in. In order to meet these torque requirements the Ultimag actuators will need some sort of reduction to boost the output torque. This reduction would need to be at least a 4 or 5 to 1 reduction for abduction/adduction and flexion/extension. Unfortunately because of the limited stroke of the Ultimag actuator, the range of motion of the output

linkage with a 4:1 reduction is limited to less than 12°. The smallest range of patient motion is in abduction/adduction and must be at least 45°.

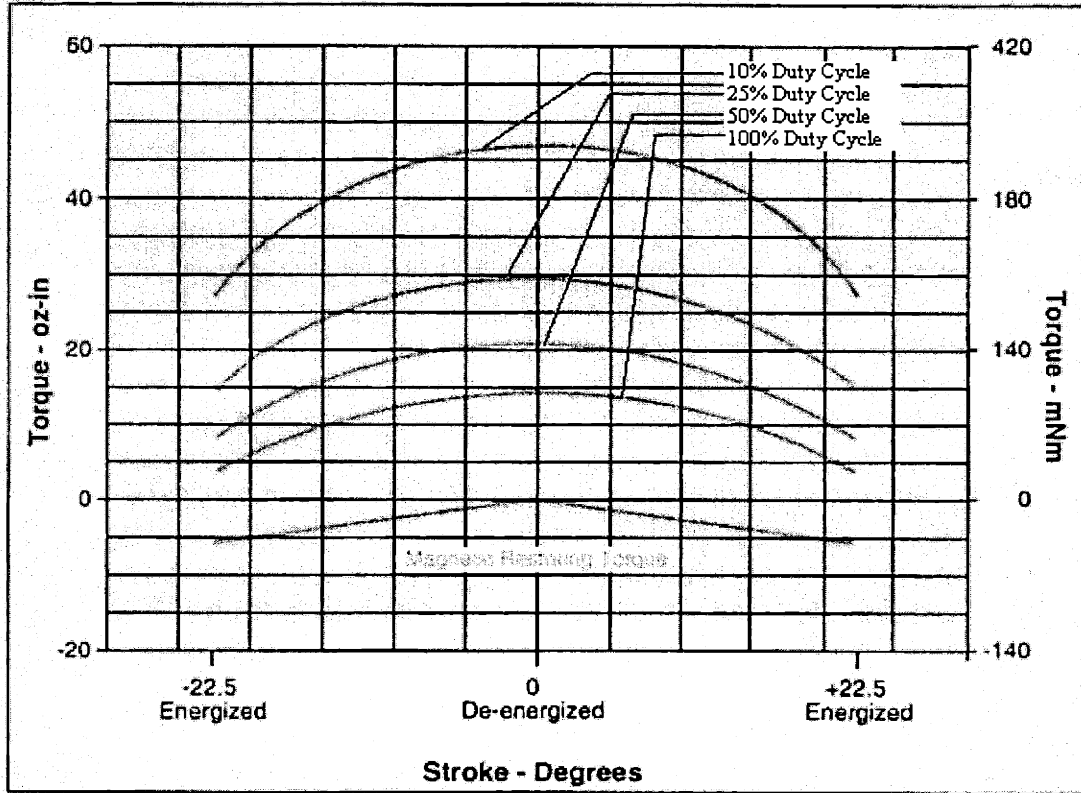


Figure 5.20 Torque vs. Position for Ultimag Actuators (Courtesy Ledex Dormeyer)

5.7 Actuator Conclusions

Considering each of the above options, the brushed and brushless motors were the only workable solutions. Of the two, the brushless motors are more appropriately run at high torques and low speeds which will be common in this application. The brushless motors also allow for better heat dissipation because the windings are on the motor stator. Because of these advantages brushless motors were selected for the wrist robot.

5.8 Actuator Selection

In order to select from the many available brushless motors, the reflected output impedances to the patient were compared for several motor brands and for individual motors. A subsequent analysis was done to ensure that the temperature of the motors were kept at an appropriate level. The motors will be in close contact with the patient and must not get hot. Because of the torque requirements of 170 oz-in in flexion/extension and abduction/adduction and 240 oz-in in pronation/supination, it is not feasible to use direct drive in this application. For example 2 of Kollmorgen's RBE 1513 motors at 900 grams a piece would be required to actuate abduction/adduction and flexion/extension. Therefore, some means of reduction is required.

The following motor brands were found to have brushless motor lines of reasonable size for the wrist robot ($< .5$ kg) . They are Parker, Pittman, and Kollmorgen brushless motors. The Parker SM160A and SM161A, the Pittman 34x1,2 and the 44x1,2,3, and the Kollmorgen 512,513,711-714 actuators were considered.

The first motors selected were the motors that actuate flexion/extension and abduction/adduction through the differential. Figure 5.21 shows the reflected inertia due to the motor shafts that the patient would feel in flexion/extension and abduction/adduction movements. Each point on the diagram represents an actuator and each of the actuators of a given brand and series (for example the Pittmann Series 44) are connected by a line. The abscissas show the reduction ratio that each motor requires in order that the maximum output torque of the differential be the required 170 oz-in. These reduction ratios were calculated by dividing the required torque of 170 oz-in by 2 times

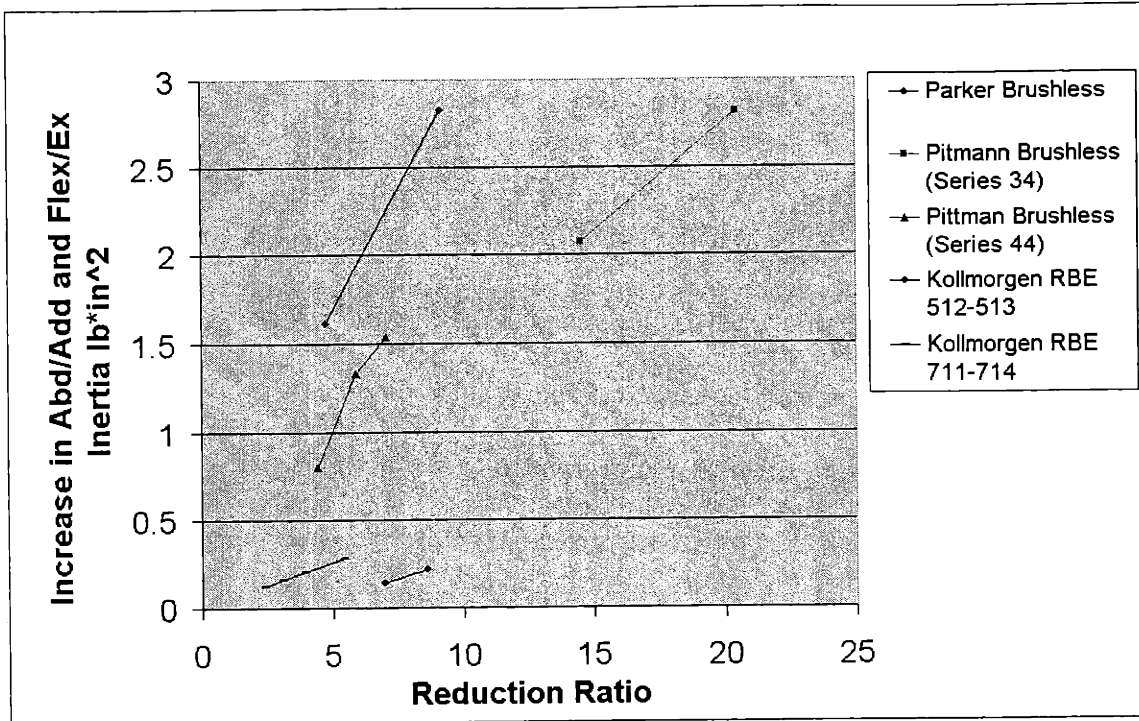


Figure 5.21 Added Inertial Impedance in Flexion/Extension and Abduction/Adduction

the maximum continuous stall torque rating of the given motor. The factor of 2 is due to the fact that in flexion/extension and abduction/adduction the torque output from the differential is the sum of the two input torques at its endgears (see section 5.3.1.2). The ordinate shows the increase in inertia in both flexion/extension and abduction/adduction. This number was found by taking $2 \cdot I_m \cdot R^2$, where I_m is the inertia of the given motor shaft, R is the reduction ratio and the factor of 2 is due to the fact that both motors will be backdriven. As is shown, the Kollmorgen series motors add by far the smallest additional inertia to each axis. However, the functional requirements allow for a 10 to 15 $\text{lb} \cdot \text{in}^2$ increase in inertia so that all of the motors with their associated reductions are reasonable.

Figure 5.22 shows the reflected static friction in both flexion/extension and abduction/adduction. The frictional values in this case were calculated with $2 \cdot F_s \cdot R$ where F_s is the static friction at the motor shaft and R is the reduction ratio. Note that the reflected frictional value varies only proportionally with the reduction ratio¹. Reflected viscous friction, which varies as the square of the reduction ratio, was found to be insignificant in comparison to the static friction at the low motor speeds expected. It was ignored. Only Kollmorgen and Parker provided static friction values for their actuators. As is shown each of the static friction values fall below the maximum 30 oz-in.

Figure 5.23 shows the increase in inertia that both of these motors would add to pronation/supination inertia. Note that when the pronation/supination motor is later selected the reflected inertia of its shaft will add additional inertia to this axis.

The smallest RBE motors (those requiring the largest reduction ratios), as figures 5.21 through 5.23 show, have the best impedance properties overall. As figure 5.21 shows, these motors and the RBE motors in general have the lowest inertial impedances due to their small shaft inertias. Though the static friction is higher than that of the Parker motors it is still well under the maximum 30 oz-in. The smaller RBE motors also add, along with the Pittman 34 series, the least amount of inertia to the pronation/supination axis. However, as shown, the RBE motors require much smaller reduction ratios. Smaller reduction ratios are desirable because they make transmissions smaller. In addition, the RBE motors have the greatest number of poles of each of the motors; having six poles instead of four. This helps to reduce cogging.

¹ For a single motor. Note again that each point in figure 5.21 and 5.22 represents a different actuator.

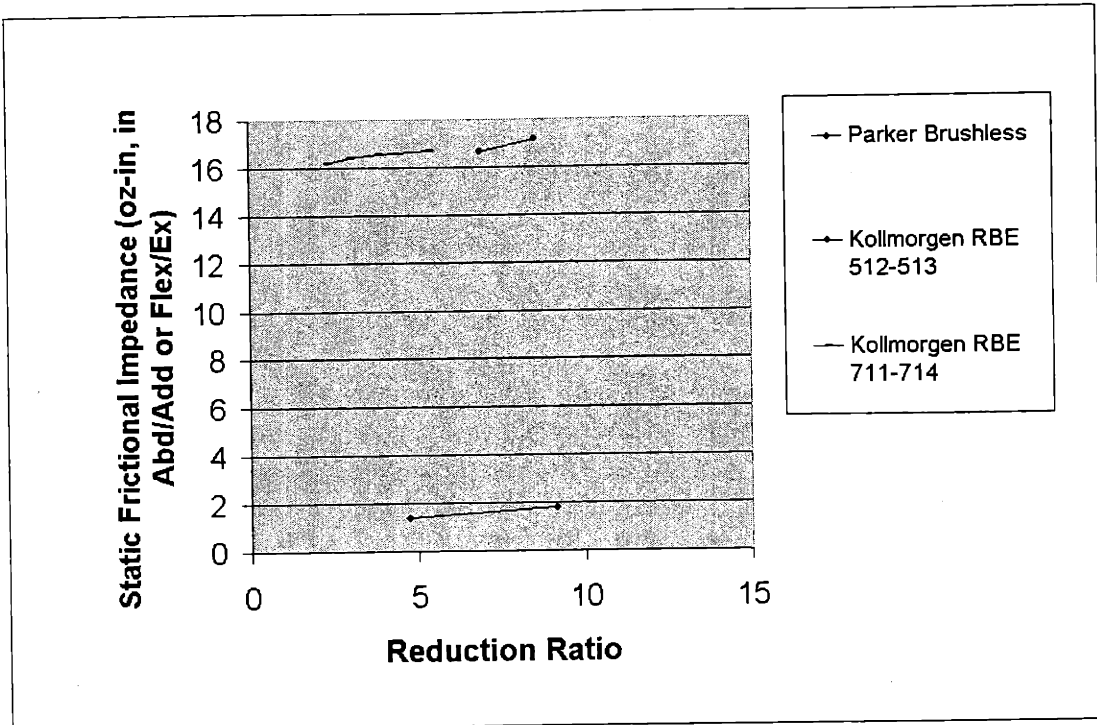


Figure 5.22 Frictional Impedance in Flexion/Extension and Abduction

Adduction

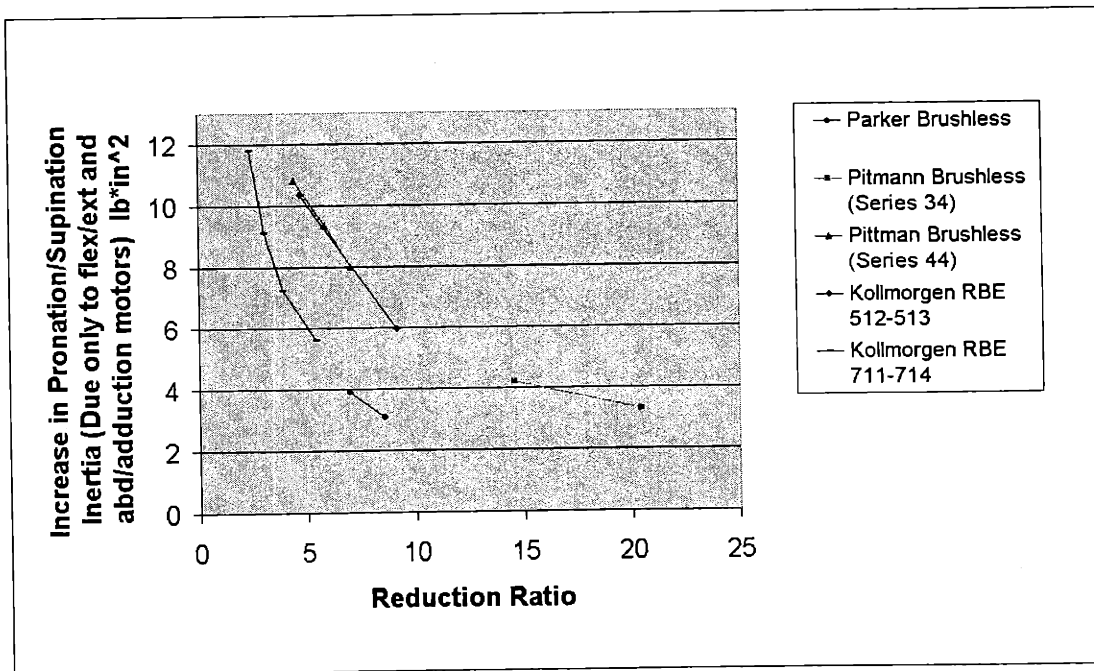


Figure 5.23 Inertia Added in Pronation/Supination Due Only to the Flexion/Extension and Abduction/Adduction Motors

With this analysis, the smallest RBE motor considered, the 512 motor, is the most appropriate motor. However, the temperature of the motor has yet to be considered. According to Kollmorgen engineers the time constant for the 512 motor to rise by 260 degrees fahrenheit when run at its maximum continuous stall torque is about 11 minutes. Because it is desired that the output from the differential be capable of continuously supporting 170 oz-in for longer periods of time, some type of compensation bringing the motor temperatures down is required. The simplest three methods for doing this are to add a heat sink, use a larger motor or increase the reduction ratio. Increasing the reduction ratio was not an option for the smallest motor as reductions over 10:1 became too large. To solve the problem the motor size was increased to a 711 motor and a heat sink was attached. A finite element analysis was used to check the steady state temperature of the motor with the attached heat sink when the motor constantly applied its maximum torque under stall conditions. It gave a steady state temperature of 120° F at the surface of the heat sink. This temperature was deemed appropriate as tissue damage occurs with contact of metal objects at temperatures over 140 degrees [2].

Finally the last motor was chosen. For consistency RBE motors were used for this axis. The static frictional impedance and the total inertial impedance for each motor/reduction ratio combination are shown in figures 5.24 and 5.25. Note that figure 5.25 is the *total* inertia that the patient would feel; due to the two downstream 711 motors and to the reflected inertia of the pronation/supination motor shaft. Unlike the other axes this axis was mainly limited by available hardware. The last axis consists of two curved slide rings which have a center of rotation within the patient's arm (See section 7.3). These slide rings come in geared and non-geared versions. For simplicity it was decided

to go with the geared version of this system instead of designing a custom gear which would then attach to a non-geared rail. The smallest version of the geared slide ring has a diameter of 93mm (3.66 in) and the next larger version has a diameter of 127mm (5 in). Looking at the anthropometric data, especially dimension C in table 2.1, the 5 in version is over 3 inches larger than the maximum expected wrist thickness of 2 in. The 3.66 in version at only 1.66 inches larger allowed for a much more compact system and therefore chosen for the wrist robot. This version of the slide has an integral spur gear with a pitch diameter of 100.8 mm and a module of 0.4². The smallest pinion gear with a module of 0.4 which can safely attach to the RBE motor shafts has a pitch diameter of 9.6mm. This gives a maximum reduction ratio of 10.5:1. This ruled out the three smallest RBE motors; the 512,513 and 711. In order to keep the system as small as possible, the 712 motor was selected from the remaining motors. The maximum continuous stall torque for the 712 motor is 21.5 oz-in. With a 10.5:1 reduction, 226 oz-in is available at the output. This was deemed to be close enough to the requirement of 240 oz-in.

² The module of a gear is its pitch diameter divided by its number of teeth. Module is used instead of pitch for metric gears. Only gears with the same module can interface properly.

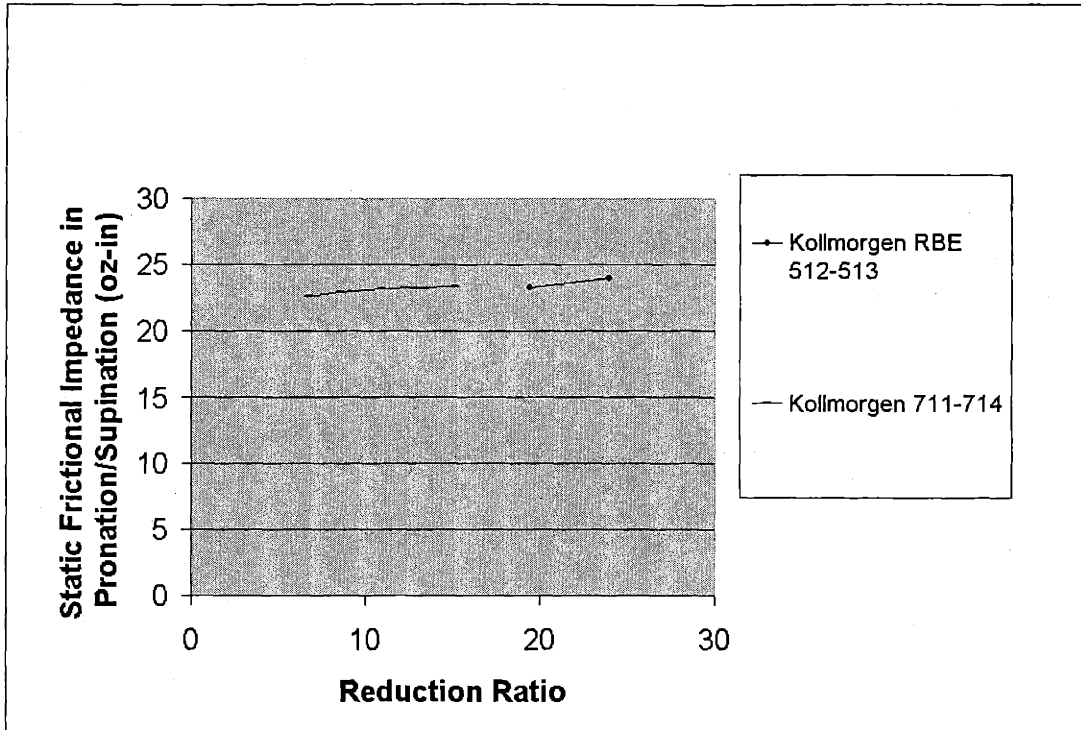


Figure 5.24 Frictional Impedance in Pronation and Supination.

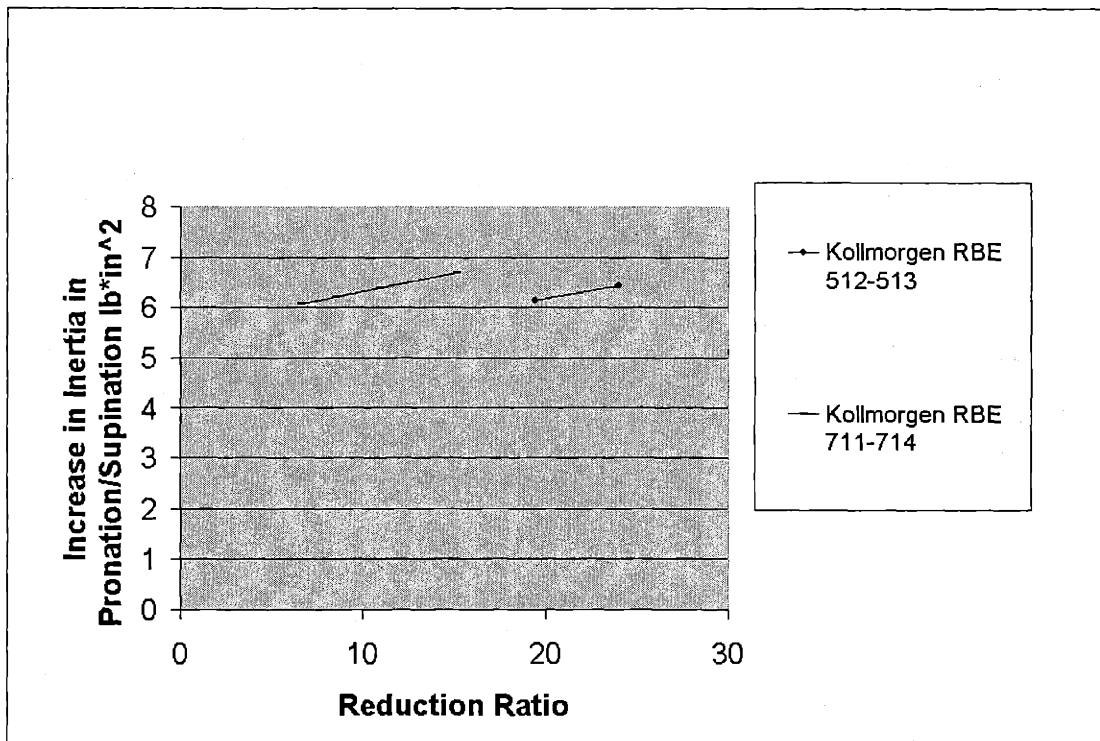


Figure 5.25 Increase in Inertial Impedance in Pronation and Supination

Chapter 6

Sensor Selection

In order to provide feedback for the control system and to gather patient data, sensors will be required. Assuming endpoint impedance of the wrist device is low, impedance control will need to sense only the orientation and angular velocity of the patient's hand. It will not be reviewed here, but it can be shown that this is possible when position and velocity are sensed at the actuator shafts. To sense position and velocity either a position and velocity sensor can be used together or a position sensor whose output is differentiated can be used. Because it is desired to keep the wrist device as small and compact as possible it was decided that only position sensors would be used. Using this method, in some cases, can introduce unwanted high frequency noise to the control system. However, simple filters can be used to suppress this noise. Manus II and Manta use position sensors with filtering for feedback and this has been shown to be quite effective for impedance control.

If the endpoint impedance is higher than expected, force sensors may be required for impedance control. However, at the present time these sensors will not be included in the design. At a later date these sensors can be added if necessary. The modularity of the

components which connect to the patient will allow new modules to be made that include force sensors.

6.1 Position Sensors

The following are the position sensors that were considered.

6.1.1 Incremental Encoders

Incremental encoders give their direction of rotation and their position by outputting two offset square wave signals as shown in figure 6.1 . Figure 6.1 shows counter clockwise rotation as square wave A leads square wave B. For clockwise rotation square wave B leads square wave A. An index signal is also output once per revolution. By counting the number of square waves from the index bit the angular position of the encoder can be determined. Using what is called interpolation the number of cycles output by the encoder for a given angle can be increased. Interpolation often gives 2, 5 or 10X the number of cycles output over the non-interpolated signal. The resolution can also be increased by using what is called quadrature decoding. Using this method, not only are the number of cycles output by the encoder counted but the edges between cycles on channels A and B are counted. This increases the resolution by four. These edges are usually referred to as counts by encoder manufacturers. Resolution is often referred to in cycles per revolution or counts per revolution.

The major advantage that incremental encoders were found to have was their size. High resolution encoders as small as $\frac{3}{4}$ of an inch in diameter and $\frac{3}{4}$ of an inch in length

were found. A disadvantage of the encoders is the need, when the encoders are turned on, to give the controller the encoder position by means of the index bit.

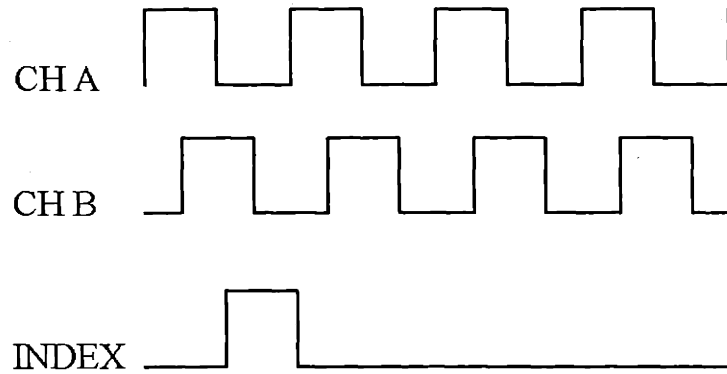


Figure 6.1 Incremental Encoder Output

6.1.2 Absolute Encoders

Absolute encoders output a digital word by means of a coded disk as shown in figure 6.2. A set of light sources shine through the disk and the light is detected by photodiodes on the opposite side. The digital word formed gives the absolute position of the encoder shaft. Because of this, when the encoder is first powered up its position is known. This provides a major advantage over incremental encoders.

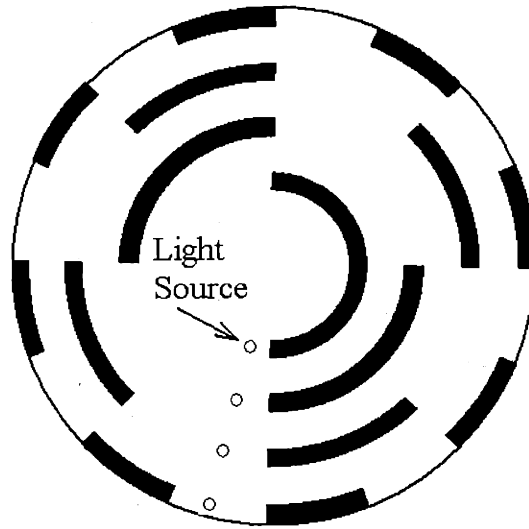


Figure 6.2 Absolute Encoder Disc.

6.1.3 Resolvers

Resolvers consist of a set of rotor and stator windings as shown in figure 6.3 . Two stator windings are offset from one another by 90° and a moving rotor winding sits between them. The rotor winding is excited by a sinusoidal voltage. The amplitude of the voltages on the stator windings vary as function of the angle of the rotor.

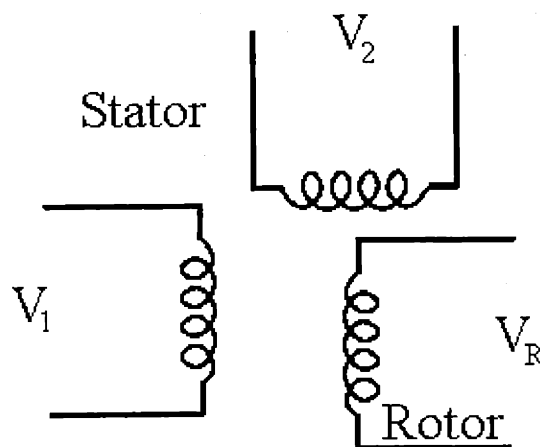


Figure 6.3 Resolver Windings

With an input voltage of $V_R = A \sin \omega t$ to the rotor, the voltages in the stator coils follow:

$$V_1 = kA \sin \omega t * \sin \theta$$

$$V_2 = kA \sin \omega t * \cos \theta$$

where k is called the coupling coefficient. In order to determine the angular position of the rotor, θ , the inverse tangent of the ratio of the stator windings is calculated.

6.2 Sensor Conclusions

The major determining factor in the selection of the type of position feedback device was size. The smallest system found was an incremental encoder from Gurley Precision instruments, the R119. It is shown in figure 6.4. This is a high resolution mini-encoder with up to 10240 cycles per revolution. The size of this device was well suited for the wrist device allowing for placement of the encoders inside of the transmission housing. Gurley encoders have also proven themselves in other robot systems in the lab.



Figure 6.4 Gurley R119 Encoders

6.3 Encoder Resolution

The servo amplifiers used to control the motors, CD Servostars, have a maximum input frequency of 3 MHz. This is the maximum number of *counts* per second that can be input to the servoamp. To be safe it was assumed that the maximum input frequency was 2MHz. With the highest interpolation supplied with the R119 encoders, 10240 cycles are output per revolution. After quadrature decoding this becomes 40960 counts per revolution. For an output of 2MHz, 2 million counts per second, the motor shaft would have to turn at 306 radians per second. Due to the 8:1 reduction ratio used in flexion/extension and abduction/adduction this would require movement of the hand at 38 rad/sec. As shown in table 2.4, the maximum angular velocity of the wrist in bending is 20 rad/sec. Therefore the highest interpolation (10X interpolation) giving 10240 cycles/rev can be used. In addition, quadrature decode can be used. This will give a very high angular resolution of .008 deg in flexion/extension and abduction/adduction. The same calculations were verified for sensing pronation/supination. For a 2 MHz output signal, the maximum allowable angular velocity of the patient in pronation/supination is 29 radians per second. As table 2.4 shows, pronation/supination angular velocity should be at most 15 radians per second. Therefore 10X interpolation and quadrature decode can also be used for this axis.

Chapter 4

Hardware Overview

The following chapter gives an overview of the hardware components of the wrist device. The major subcomponents are reviewed. At the time of writing, the components for the device are being purchased so that actual parts cannot be shown. To explain the device, screen shots from Pro/Engineer solid models will be used. Figure 7.1 shows the device completely assembled.

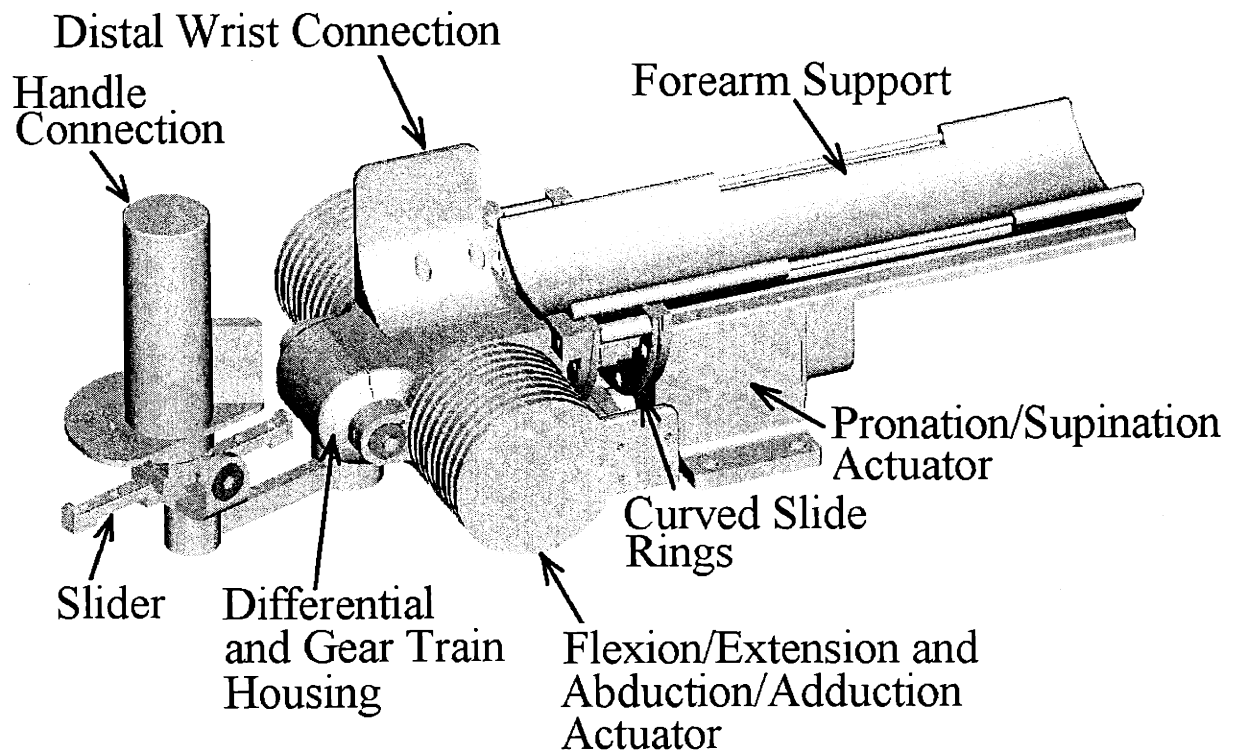


Figure 7.1 Complete Wrist Device

7.1 Connection to the Patient

The patient will be connected to the device by a series of velcro straps. Figure 7.2 shows how the patient's hand, wrist and upper forearm are to be connected. The hand will be connected to a handle by means of two straps over the back of the palm which are connected near the top of the handle and velcro to it. In addition, a single strap will also ride over the proximal or middle phalanges keeping the patient's hand tightly closed around the handle. Presently a handle will be used to connect to the patient's hand. In future versions, a connection allowing the hand to be open could be used.

Also shown on the handle is a protrusion which prevents the hand from slipping around the handle. Along with the straps, this should prevent all movement of the hand with respect to the handle.

The patient's wrist will be connected with two straps to a wrist connection piece as shown. A rigid floating square component which can be detached from the velcro straps will allow for different patient sizes. Finally the patient's forearm will be strapped to the forearm support with a velcro straps that can slide along two rails. The sliding straps will allow patients with different arm lengths and diameters to attach to the support.

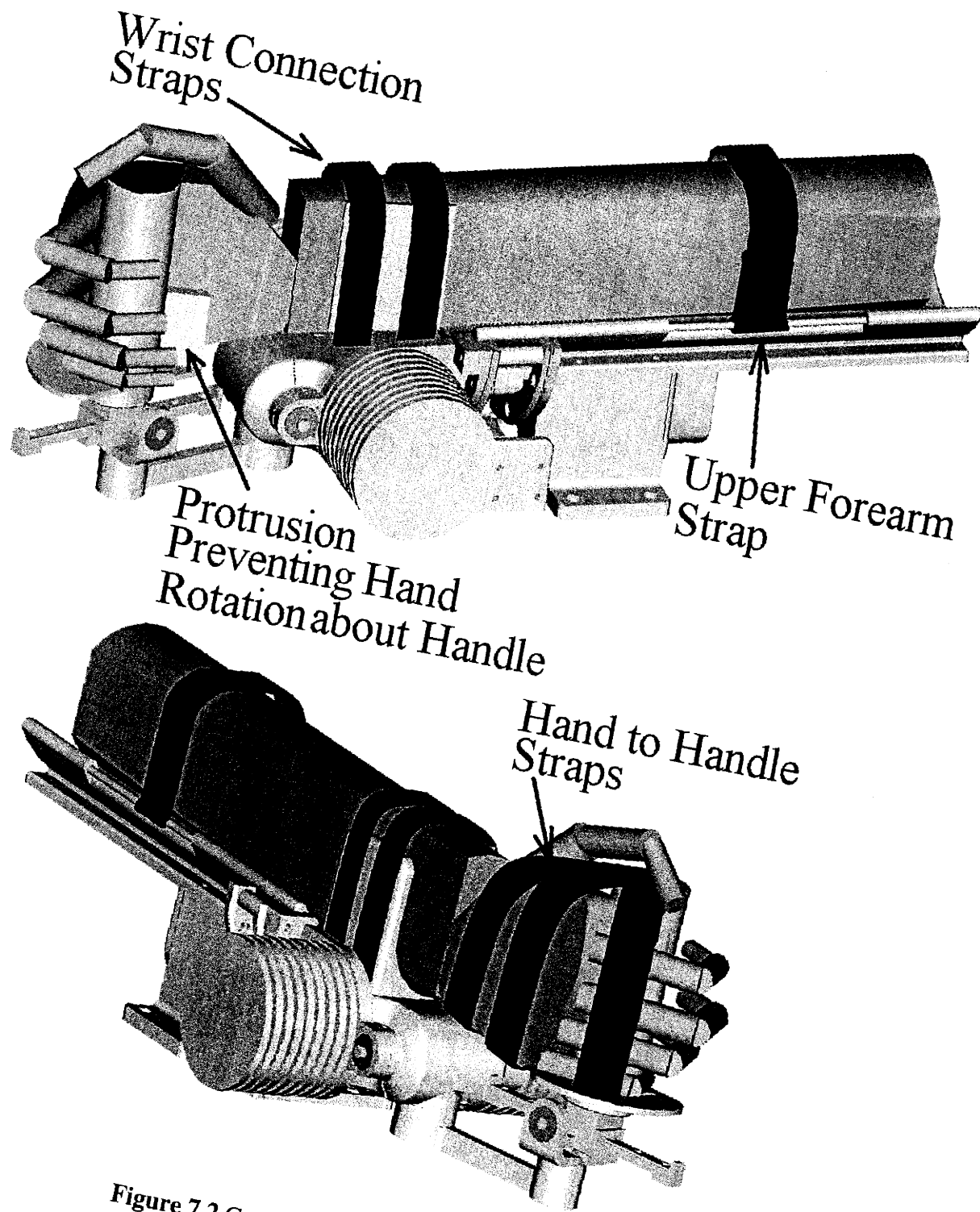


Figure 7.2 Connection to the Patient

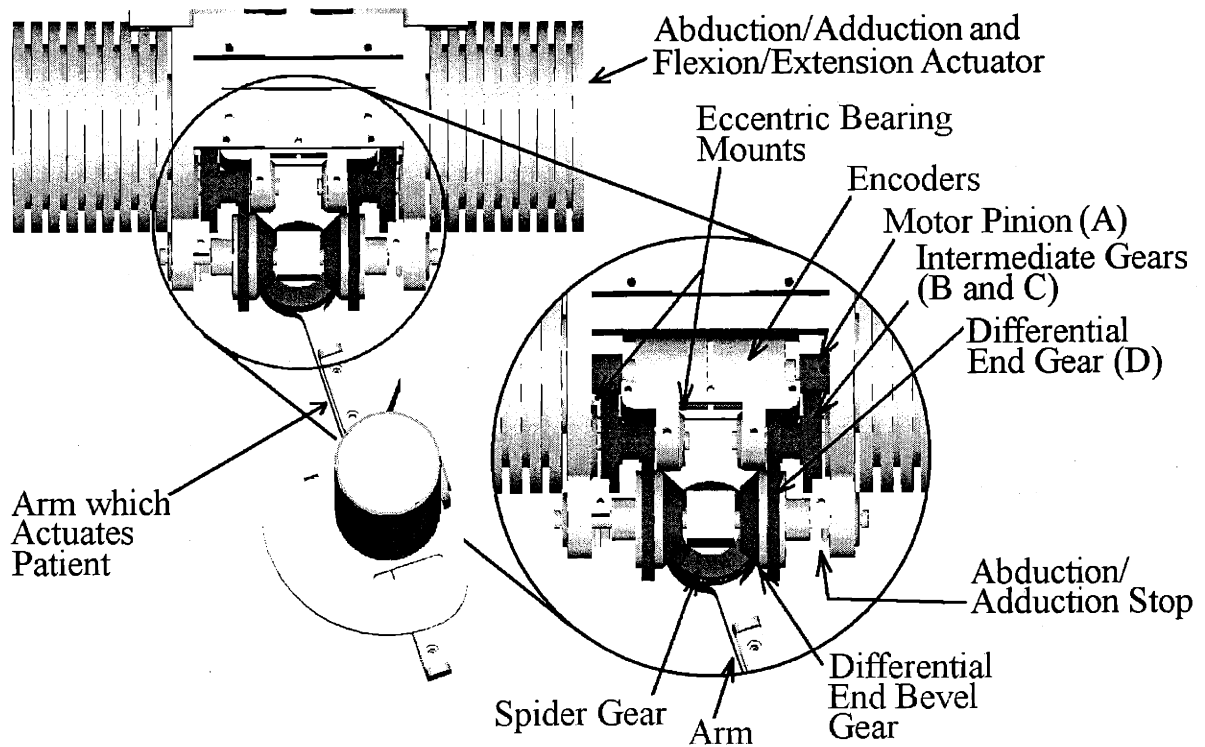


Figure 7.3 Transmission for Abduction/Adduction and Flexion/Extension

7.2 Abduction/Adduction and Flexion/Extension Transmission

Figure 7.3 shows the transmission from the abduction/adduction and flexion/extension actuators to the arm which actuates the patient. A section of the transmission housing has been removed in the close up view in order that each of the gears are visible. The gears are also darkened to distinguish them from other components. Two spur gear trains are used to transmit torque from the actuators to the differential. The spur gears are represented by their pitch cylinders which can be assumed to roll without slip on one another. The three bevel gears of the differential, the spider gear and the two

differential end bevel gears, are represented by their pitch cones. These also can be assumed to roll with out slip on one another.

The two spur gear trains in figure 7.3 each consist of four gears. These gears include the motor pinion gear (gear A), two intermediate gears which are rigidly attached and rotate together (gears B and C), and the endgear of the differential (gear D). The intermediate gears were added to keep the differential endgears and the rest of the transmission small. The total reduction in one train from the actuator pinion to the differential endgear is 8:1. The differential consists of three identical bevel gears. It is a custom differential from Sterling Engineering and is based on stock number S9550A-TS2. Table 7.1 gives the critical parameters and dimensions of each gear in the train. A few of the differential specifications are also given.

Gear	Pitch	Pitch Diameter (in.)	Teeth	Face Width (in.)	Bore (in.)
Motor Pinion (A)	72	.390	28	3/16	.2498/.2503
Intermediate Gear (Larger Gear B)	72	1.055	76	3/16	.3745/.3747
Intermediate gear (Smaller Gear C)	72	.417	30	5/32	.1877/.1880
Differential End Gear (D)	72	1.250	90	1/8	.9369/.9371
Differential Bevel Gears	64	0.82 (Ave.)	53	0.275	.3123/.3125

Table 7.1 Gear Dimensions and Parameters

To allow backlash adjustment in the spur gear trains, the bearings holding the shafts on which gears B and C lie are mounted on an eccentric mounts. These mounts allow the shaft and thus gears B and C to shift closer to and further away from the

differential endgear. According to [16] the total linear backlash measured along the pitch circle between gears of pitch 72 should be between .002 and .0055 in. The increase in center distance between two gears¹, ΔC , is related to the linear backlash , B , by:

$$\Delta C = 1.375 * B \text{ (in.)}$$

For a linear backlash of .0055 the change in center distance should be .008. The eccentric bearing mounts in the wrist device allow the shaft holding gears B and C to shift toward and away from gear D by .008 in.

To insure that the forces on the gear teeth and the forces on the shaft bearings are not too high, a static analysis was done. This analysis looked at half of the transmission system; it considered one spur gear train and one of the differential end bevel gears. In the static analysis under consideration, the gear tooth and shaft forces will be identical in the train on the opposite side of the differential. To model this part of the system, two simplifications were made. First of all, the end bevel gears of the differential were modeled with spur gears of pitch diameter equivalent to the average pitch diameter of the bevel gears. Secondly, the system was modeled as a planar system; all forces and torques were assumed to be in the same plane. Figure 7.4a shows the simplified system. As before, the gears are represented only by their pitch circles. The applied motor torque, τ_M , is shown along with F_{SE} which represents the reaction force between the spider gear and the differential end bevel gear.

¹ This is the increase over the sum of the pitch radii.

Spur Gear Representing End Bevel Gear

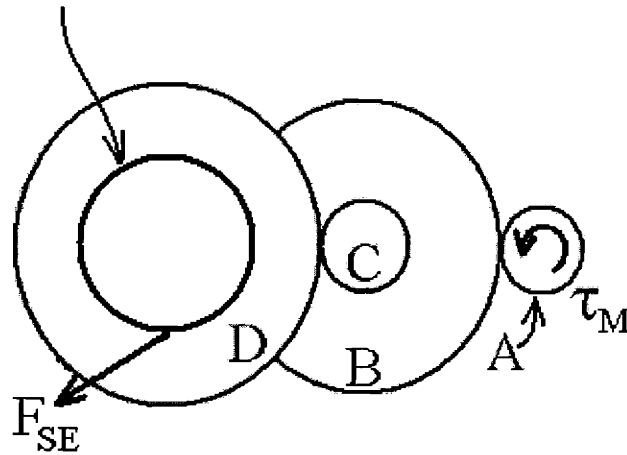


Figure 7.4a Simplified Model of Gear Train

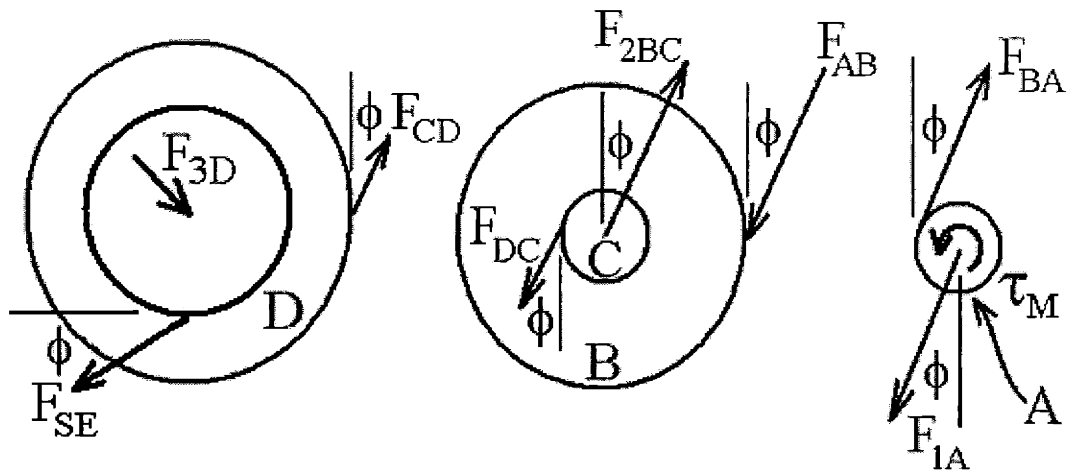


Figure 7.4b Free Body Diagram of Each Gear

Figure 7.4b shows the free body diagram of each of the gears in the train. Not shown in the figure are 3 shafts which support the gears. Shaft 1 is the motor shaft which holds pinion gear A, shaft 2 holds gears B and C and shaft 3 is the main shaft of the differential which holds the differential end bevel gear and gear D. Each shaft applies a

reaction force to the gear or gears it holds. There is also an equal and opposite reaction between each mating gear pair. The reaction forces in figure 7.4 each have two subscripts. The first subscript explains which object applies the force and the second explains which object the force is applied to. For instance, F_{1A} is the force applied by shaft 1 on gear A. The reaction forces between mating gears are applied at the contact point of the pitch circles. The forces are at an angle, ϕ , called the pressure angle, from the common tangent of the two mating pitch circles². The pressure angle for the gears in the wrist robot, and for most gears, is 20° .

In order that the torque output to the robot arm be the maximum required value of 170 oz-in (see section 3.3), the motor torque, τ_M , in figure 7.4b must be 10.6 oz-in. Note that this torque must also be applied by the motor on the opposite train. Depending on the direction of the torque on the opposite train, the robot will create torque on the patient in flexion/extension or abduction/adduction (see section 5.3.1.2). Table 7.2 gives the magnitudes of the forces in figure 7.4 when $\tau_M=10.6$ oz-in and the system is in static equilibrium.

Force	Value
$F_{1A}=F_{BA}=F_{AB}$	58 oz
F_{2BC}	205 oz
$F_{CD}=F_{DC}$	147 oz
F_{3D}	172 oz
F_{SE}	224 oz

Table 7.2 Resultant Forces on each Gear

² For each mating gear pair in figure 7.4 the common tangents are vertical lines.

To insure the loads on the spider gear were not too high, it was also modeled as a spur gear. The pitch diameter of this spur gear was set at the average pitch diameter of the spider of .82 in. The load applied to this spur gear was approximated as 224 oz-in or equivalent to F_{SE} . In the following text this load is labeled as F_{ES} .

By using what is called the Lewis equation, the maximum allowable tangential tooth load to keep the stress at the base of a given gear tooth at a safe stress level can be calculated. The Lewis equation is as follows:

$$F_{all}^T = sbY / P$$

where F_{all}^T is the allowable tangential tooth load, s is one third the ultimate tensile strength of the gear material, b is the face width of the gear, Y is a tabular number based on standard tooth geometry, and P is the diametrical pitch of the gear [17][18].

Table 7.3 shows the results of the Lewis equation applied to each of the gears in the gear train. Note that each gear in the transmission is made of 303 stainless steel. The actual tangential load calculated according to the static analysis and the allowable tooth load according to the Lewis equation are given. Note that $F_{BA}^T = F_{BA} \cos 20^\circ$.

	Actual Tooth Load (oz)	Allowable Tooth Load (oz)
F_{BA}^T	55	512
F_{AB}^T	55	640
F_{DC}^T	138	435
F_{CD}^T	138	437
F_{SE}^T	211	976
F_{ES}^T	211	976

Table 7.3 Actual and Allowable Tangential Loads

As is shown, in all cases, the allowable tooth load is at least 3 times the actual tooth load.

Note that the large face widths of the bevel gears make their allowable load much higher

than the others. It is obvious that the stress at the base of the teeth is not of critical importance if gears made of 303 stainless steel are used. As will be shown, however, the contact stresses between teeth does become a limiting factor.

In addition to checking the allowable tooth load, the allowable load to insure that pitting does not occur was also calculated. Pitting is a failure of the tooth surfaces due to high contact stress. The allowable load for pitting resistance was calculated according to an AGMA (American Gear Manufacturer's Association) pitting stress formula which is as follows:

$$F^T_{all} = \left(\frac{S_C C_L C_H}{C_P C_T C_R} \right)^2 \left(\frac{C_V F d I}{C_A C_S C_M C_F} \right)$$

This equation uses characteristics of the gear along with several analytically and experimentally determined coefficients to give an approximation of the maximum

S_C =surface fatigue strength

C_L =life factor

C_H =hardness ratio factor

C_P =elastic coefficient

C_T =temperature factor

C_R =reliability factor

C_V =dynamic factor

F =face width

d =pitch diameter of pinion

I =geometry factor

C_A =application factor

C_S =size factor

C_M =load distribution factor

C_F =surface condition factor

Table 7.4 Factors in the AGMA pitting stress equation.

allowable tangential tooth load, F_{all}^T , for pitting resistance. This equation gives a single maximum value for two teeth in contact. The coefficients in this equation are listed in table 7.4 but for brevity will not be explained. See reference [17] for more detail.

The results of the analysis using the AGMA pitting stress formula are given in table 7.5 .

	Actual Tooth Load (oz.)	Allowable Tooth Load (oz.)
F_{BA}^T	55	211
F_{AB}^T	55	211
F_{DC}^T	138	150
F_{CD}^T	138	150
F_{ES}^T	211	638
F_{SE}^T	211	638

Table 7.5 Actual and Allowable Loads for Pitting Resistance

As is shown, the actual tooth loads fall below the allowable values in each case. In the case of gears C and D, however, the values are quite close. Because of the complexity of gear C (it is a cluster gear with a hub for gear B) it was decided that it would be better to go with the stock 303 stainless steel version of the gear, instead of buying a custom hardened gear. If pitting wear does occur, gears C and D can be replaced over time or a hardened steel gear can be used.

To check that the loads on the bearings holding shafts 1 2 and 3 were not too high, the shaft loads calculated in the static analysis and given in table 7.2 were used. Table 7.6 gives the maximum expected values and the maximum allowable radial load on the bearings for a life of 1 million cycles.

	Max Expected Radial Load (oz.)	Max Allowable Radial Load (oz.)
On motor shaft	58	590
Bearings holding Shaft 2	205	1090
Bearings holding Shaft 3	172	1090

Table 7.6 Maximum Expected and Allowable Loads on Transmission Bearings

Also shown in figure 7.3 (pg. 108) are two Gurley incremental encoders. These were placed within the transmission housing to keep the system small and compact. They are attached to the motor shafts with set screws and to the transmission housing with flexible tether mounts. They are used to sense the orientation and the angular velocity of the robot arm.

The two stops that are shown in figure 7.3 prevent overrotation of the patient in abduction and adduction. These stops consist of hardened steel pins which pass through the main shaft of the differential and contact mechanical stops which prevent rotation. These stops also prevent the robot arm and handle components from contacting the other components of the robot. They limit the range of motion to 30° in adduction and 20° in abduction. Although not shown, similar stops restrict rotation in flexion and extension. They are below the differential spider gear within the robot arm piece. To prevent the robot from contact with itself, these stops limit rotation in flexion/extension to 60° in each direction. This 10° less than the flexion requirement and 5° less than the extension requirement. This was decided to be close enough to the requirement and should allow most normal wrist movements.

7.3 Pronation/Supination Transmission

The axis for pronation and supination makes use of two geared 180° slide rings from Bishop Wisecarver (part number R12-93). These are shown in figure 7.5 . Each slide ring has opposing “V” shaped edges which roll between four guide wheels with “V” shaped grooves. The lower two guide wheels are eccentric allowing adjustment in the preload of the wheels against the slide rings. The upper guide wheels are concentric and cannot be adjusted.

Two stops are also shown in figure 7.5. They limit the rotation of the wrist to 76° in pronation and 76° in supination. This is less than the requirement of 90° but still provides a large range of motion. These stops also rigidly connect the slide rings at their tips.

Each of the slide rings has an integral gear allowing it to be gear driven. To drive the slide rings there are two pinions press fit on the shaft of the pronation/supination motor. The pinion driving the front most slide ring is shown in figure 7.5. The second pinion is not in view but it drives the second slide ring. The pronation/supination motor is a custom built RBE 712 motor from Kollmorgen. The RBE motor is mounted behind the slide rings as shown and its shaft passes through the motor support mount and the guide wheel support mounts shown. To insure that the stresses on the gear teeth of the slide rings and the motor pinions were not too high, the Lewis equation was again used. To supply the maximum required torque output to the patient of 240 oz-in, the RBE motor must apply a torque 22.9 oz-in. The resultant tangential tooth load on the gear teeth and the allowable tooth load according to the Lewis equation are shown in table 7.7 .

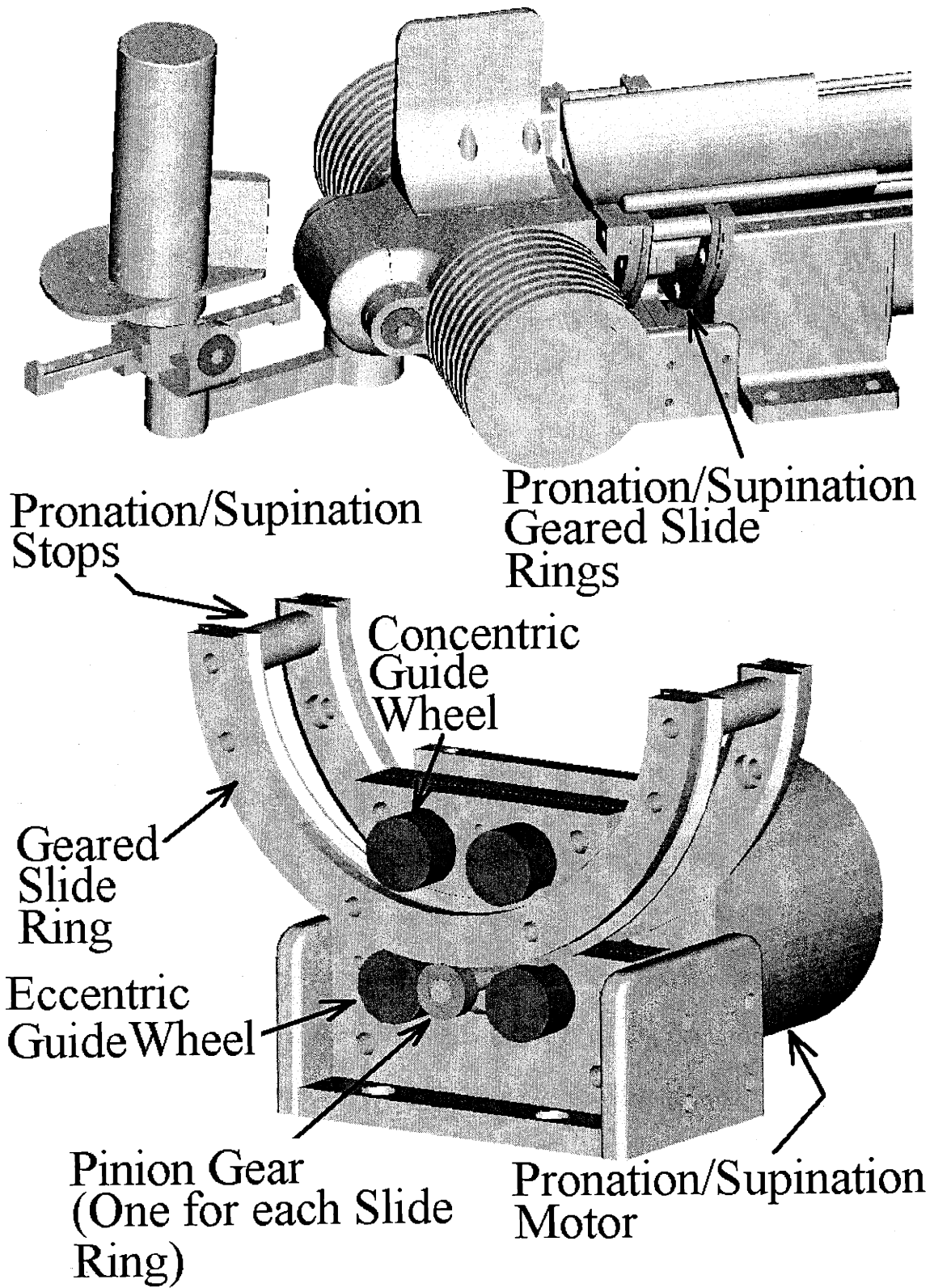


Figure 7.5 Pronation/Supination Transmission

	Actual Tangential Tooth Load (oz.)	Allowable Tangential Tooth Load (oz.)
Motor Pinion Gear	64	150
Slide Ring Gear	64	584

Table 7.7 Actual and Allowable Tangential Load

The AGMA pitting stress formula was again used to calculate the maximum tangential load for pitting resistance of the pronation/supination gears. The allowable and actual tangential tooth loads are shown in table 7.8.

	Actual Tangential Tooth Load (oz.)	Allowable Tangential Tooth Load (oz.)
Motor Pinion Gear	64	168
Slide Ring Gear	64	168

Table 7.8 Actual and Allowable Tangential Load for Pitting

To insure that the applied loads on the slide rings and their support wheels were not too high, the static analysis illustrated in figure 7.6 was done. Link A represents the rigidly connected slide rings and the transmission housing to which they attached. Forces F_1 and F_2 are the reaction forces due to the guide wheels on the slide rings. Link B represents the robot arm and the patient handle. The differential is represented by the joint between links A and B. With the differential output torque, τ_D , set at the maximum required output value of 170 oz-in, a patient force, F_P , of 58 oz at the handle will keep the robot arm and

the handle in static equilibrium. The reaction forces F_1 and F_2 can then be calculated according to:

$$F_1 = F_p \left(1 + \frac{d_2}{d_1}\right)$$

$$F_2 = F_p * \frac{d_2}{d_1}$$

These equations give $F_1=27.4$ lb and $F_2=23.8$ lb. According to the BishopWisecarver data sheet (see appendix B), the life of the slide rings at these loads will be $1.3E6$ cycles for slide ring 1 and $6.8E5$ cycles for slide ring 2. Note that slide ring 1 is the slide ring furthest from the handle to which F_1 is applied and that slide ring 2 is slide ring closer to the handle to which F_2 is applied. Assuming the patient moves at $\frac{1}{4}$ Hz through the full pronation/supination range of motion of 152° , this correspond to a life

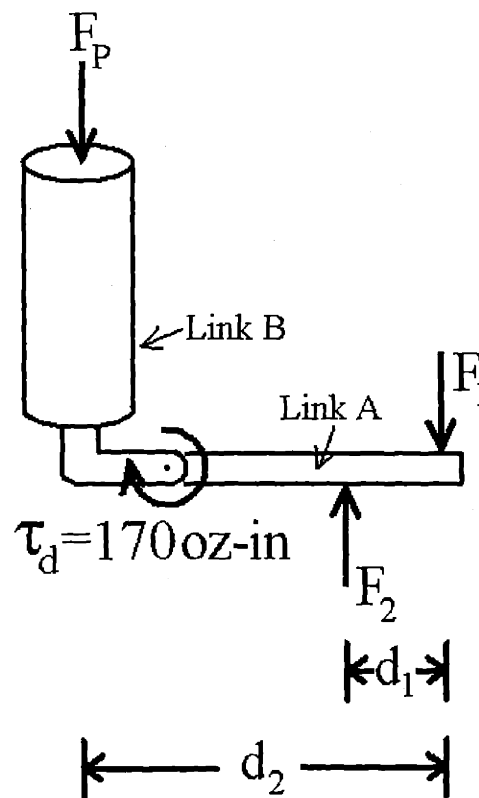


Figure 7.6 Static Analysis of Slide Rings

of 1900 hours for slide ring 1 and 950 hrs for slide ring 2.

7.4 Material Selection and Fabrication

The majority of the manufactured components will be made of aluminum. Its low cost and machinability make it a good default material for most of the components. For added strength, a few of the components will be made of 303 stainless steel. These include the stops for abduction/adduction and flexion/extension and each of the gear shafts. Two parts will be made with an aluminum casting. These include the transmission housing and the forearm support. The geometric complexity of these parts make it unreasonable to machine them with standard removal machining (see appendix C for drawings).

Chapter 8

Conclusions

In conclusion, a device capable of actuating the human wrist for therapy has been designed. The device is expected to be a very effective therapy tool as a majority of the functional requirements have been met. The kinematics of the system do not overconstrain the three degrees of freedom of patient movement. As well, the forces applied by the robot are perpendicular to the patient's skin. This will insure that the connection components do not slip off the patient. In addition, the impedance added to each patient degree of freedom fell below the allowable values. This indicates that the robot will be easy to backdrive. The connection components to the patient have been made modular allowing different types of connection components to be added to the system. At present the wrist device itself has not been made modular and cannot connect to other robots. It may be possible in the future to build extra components allowing for this. The feasibility of doing this has not been investigated and for now the device acts only as a stand alone device. The ranges of patient motion were not as large as the target values due to the interference of the robot with itself. However, the values were within 15° of the target values in all cases. The device will support the entire arm of the patient and should be easy for the therapist to use. The therapist need only place the patient in the forearm support and fasten the straps. It should also be easy to remove the patient as only

three velcro straps need be detached. Finally, the power for the design is easily attainable from a 110V AC outlet.

8.1 Present Status

Presently the robot has been completely designed. A few of the components have been purchased and others will soon be purchased. Part numbers and descriptions of off the shelf components are given in appendix A and B. Detailed drawings of the custom made and machined parts are included in appendix C.

8.2 Future Work

Soon after fabrication, the robot will need to be characterized to determine how the system actually behaves. The actuators and amplifiers will need to be characterized and the actual output robot impedance will need to be quantified.

In the future, torque sensors could be added as an integral part of the connection components. This would allow data on interaction torque to be gathered. In the case that the impedance reflected to the patient is higher than expected, these sensors could be used to implement force feedback.

If video games are again used as feedback for the patient, new games will be required for the wrist device. Because a desired wrist orientation is quite difficult to visually describe, this might be a complex task. However, it is likely that most movements with the wrist device will be only single degree of freedom rotations such as movements only in flexion/extension or only in pronation/supination. These should be easier to display.

Appendix A

Component List

Supplier/Description	Catalog Number	Quantity	Modifications	Notes
Stock Drive Products				
Precision Dowel Pins	A9X310614	2		Connection between <i>arm_2</i> and <i>slider_connection</i>
Spacers	A7X8C06031	2		"
Flanged Bearings	S9912YG1850FS2	2		"
Flanged Bearings	S9912YG1850FS2	2		Connection between <i>arm_2_shaft</i> and <i>arm_2</i> , and <i>arm_2_shaft</i> and <i>arm</i>
External Retaining Ring	A9Q29-18	1		"
Spacer	A7X8C06014	1		"
Spacer	A7X8C06016	1		"
Internal Retaining Rings	A9Q28-50	2		Connection between <i>arm</i> and <i>differential</i>
External Retaining Ring	A9Q29-18	1		"
Nonflanged Bearing	S9912YG1850PS0	1		"
Flanged Bearing	S9912YG1850FS2	1		"
Spacer	A7X8C06014	1		"
Flanged Bearings	S9912YG1850FS2	2		Connection between <i>differential</i> and <i>trans_housing</i>
Spacers	A7X8C06014	2		"
External Retaining Rings	A9Q29-18	2		"
Hardened Steel Pins	A9Q320212	2		Abb/Add Stop Pins
Gear A	S1086Z072S028	2		Gear Train
Gear B	S1268Z-072S076	2	Bore .3745/.3747 and change face width to 3/16	"
Gear C	S1F74Z-A072S030	2	Bore .1877/.1880	"
Gear D	S1269Z-072S090C	2	Bore .9369/.9371	"

Supplier/Description	Catalog Number	Quantity	Modifications	Notes
Stock Drive Products Cont.				
Pro/Sup Pinions	A1B1MY04024	2	Bore 4.00 mm, Stainless Steel	Pro/Sup Pinions
Pins for Gear C	A9Y31-0212	2		
Retaining Rings	A9Q29-18	2		For shaft_for_bc to trans_housing
Spacers	A7X8A04010	2		"
Spacers	A7X8C06010	2		"
Bearings	S9912YG1850FS2	2		"
Retaining Rings	A9Q29-18	2		For shaft_for_bc to center_axis_mount
.01 Spacers	A7X8A04010	4		"
	A7X8C06010	4		"
.02 Spacers	A7X8A04020	2		"
	A7X8C06016	2		"
Flanged Bearings	S9912YG1837FS2	2		"
NonFlanged Bearings	S9912YG1837PS2	2		"
Pins	A9Q320312	4		center_axis_mount to trans_housing
	A9Y310312	4		"
	A9Q320306	1		"
	A9Y310310	1		"
Differential	S9550A-TS2	1	See Detailed Drawings	
Forearm Support Rails	A7X104060	2		
Bischof Wisecarver				
Hepco Slide Rings	R12-93-R180	2	See Detailed Drawings	
Concentric Bearing Assembly	SJ-13-C-NS	4		
Eccentric Bearing Assembly	RSJ-13-E-NS	4		
Lubricators	LB-12-C	6		
Deltron				
Linear Slide	BSGS8-1-100	1		
Kollmorgen				
Flex/Ex and Abd/Add Motors	RBEH-00711-A02	2	See Detailed Drawings	
Pro/Sup Motor	RBEH-00712-A02	1	See Detailed Drawings	
CD Servostar ServoAmp	CE06250	3		

Supplier/Description	Catalog Number	Quantity	Modifications	Notes
Gurley				
Incremental Encoders	R119B-01024Q-5L10-A18SY-02EN	3		

Appendix B

Component Specifications

Winding Constants

There are six parameters, or winding constants, listed on the individual data page for each motor which vary according to the winding that is used in the model. The variations are governed by the number of wire turns per coil and the wire size. In some cases, values for more than one winding are listed. If none of the specified windings are suitable for a given application, additional windings are available by consulting the factory. Following is a brief description of each parameter.

Current at Continuous Torque (I_c) is the current required to obtain the nominal continuous torque from the motor with a nominal torque sensitivity K_t .

Current at Peak Torque (I_p) is the current required to obtain the nominal peak torque from the motor. At I_p , K_t will be reduced from the published K_t because K_t is reduced at torque above T_{sl} . I_p is based on the maximum current density in the winding and is available for a maximum duration of 10 seconds.

Torque Sensitivity (K_t) is the ratio of the developed torque to winding input current for the designated winding.

Back EMF Constant (K_b) is the ratio of voltage generated in the winding to the speed of the rotor. Since both K_b and K_t are determined by the same factors, K_b is directly proportional to K_t .

Motor Resistance (R_m) is the resistance measured between any two leads of the winding at 25°C.

Motor Inductance (L_m) is the winding inductance measured between any two leads of the winding. Factory tests are performed at 60 Hz with the rotor in place.

RBE(H) Motor Series

INTRODUCTION

Motor Parameters

Motor parameters are listed on the individual data page for each motor. These parameters are dependent upon the size and shape of the model, but are independent of the winding used. Following is a brief description of the motor parameters.

Maximum Continuous Output Power at 25°C Ambient (HP Rated). This is the maximum continuous power output based on a 130°C temperature rise and a standard aluminum heat sink. (Standard heat sink size is listed just above the continuous performance curves). The maximum continuous power output can be increased if additional cooling is provided.

Speed at Rated Power (N Rated) is the speed at which the maximum continuous power is output.

Maximum Mechanical Speed (N Max) is the maximum speed which will not compromise rotor integrity.

Continuous Stall Torque at 25°C Ambient (Tc) is the maximum constant torque without rotation resulting in a steady state winding temperature rise of 130°C with the standard aluminum heat sink. The size of the standard heat sink is listed above the continuous performance curve for each RBE(H) series. The continuous stall torque can be increased if additional cooling is provided.

Peak Torque (Tp) is the maximum torque available from a given size of motor and is the torque the motor will provide when peak current **Ip** is provided. Peak torque is based on the maximum current density in the winding and is available for a maximum duration of 10 seconds.

Maximum Torque for Linear Kt (Tsl) is the maximum torque for which **Kt** will be greater than 90 percent of **Kt** at low torque. As the torque increases above **Tsl**, **Kt** will drop below 90 percent of **Kt** at low torque and an incremental increase in current will yield a reduced increase in torque.

Motor Constant (Km) is the ratio of peak torque to the square root of power input at 25°C and at stall:

$$K_m = T_p / (P_p)^{.5}$$

This ratio is useful during the initial selection of a motor, because it indicates the ability of a motor to convert electrical power into torque. A common use of **Km** is to determine how much power a motor will dissipate in order to generate a certain amount of torque by using the following equation:

$$\text{Watts Dissipated} = \text{Torque}^2 / K_m^2$$

Thermal Resistance (Rth) is the ratio of winding temperature rise to average power losses continuously dissipated from the stator. Motor **Rth** values assume a standard aluminum heat sink which is specified above the continuous speed torque curve for each RBE(H) series. Customer supplied supplemental cooling can reduce the **Rth** value significantly resulting in increased continuous speed and torque operation.

Viscus Damping (Fi) is the torque loss due to rotational losses, mostly eddy current, which is proportional to speed. A lower **Fi** indicates less loss during high speed operation.

Maximum Static Friction (Tf) is the sum of the retarding torques at start-up or at stall within the motor. In a frameless brushless motor, retarding torques consist of magnetic frictional torque and cogging torque. Housed motor **TF** includes bearing and other retarding torques.

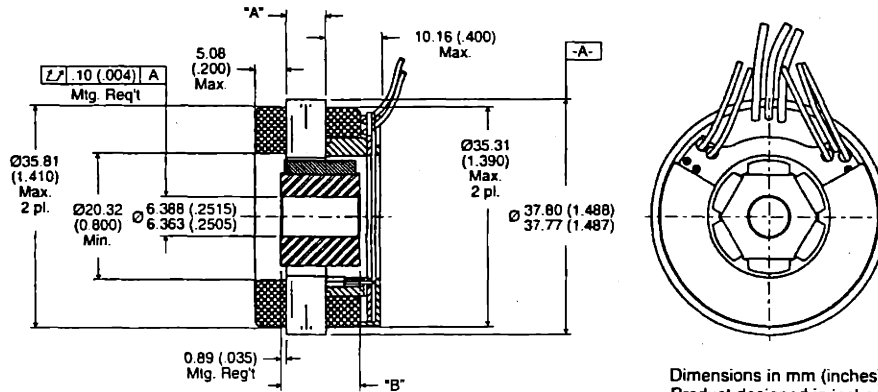
Maximum Cogging Torque (Tcog) is a torque disturbance based on the magnets in the field attraction to the teeth in the armature. Cogging torque is minimized in the motor design by strategic selection of slot / pole combinations and by skewing the laminations in the armature.

Number of Poles (P) is the number of magnetic poles in the field. The electrical cycles per revolution is equal to the number of poles to the number of poles divided by 2.

RBE(H) Motor Series

DIMENSIONS

RBE-0071X-X00



Dimensions in mm (inches).
Product designed in inches.
Metric conversions provided for reference only.

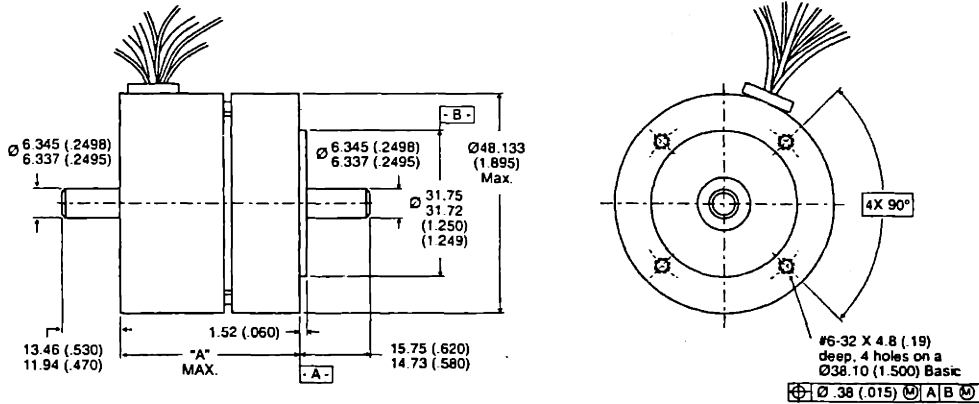
Notes:

- 1) For a C.W. rotation, as viewed from lead end, energize per excitation sequence table.
- 2) V-AB, V-BC and V-CA is back EMF of motor phases AB, BC and CA respectively, aligned with sensor output as shown for C.W. rotation only.
- 3) Mounting surface is between Ø 35.81 (1.410) and Ø 37.80 (1.488) on both sides.

MODEL NUMBER	RBE-00710	RBE-00711	RBE-00712	RBE-00713	RBE-00714
"A" Dimension	6.35 (0.250)	12.7 (0.500)	19.05 (0.750)	25.4 (1.000)	33.02 (1.300)
"B" Dimension	12.7 (0.500)	19.05 (0.750)	25.40 (1.000)	31.75 (1.250)	39.37 (1.550)

Tolerance ± .010 on "A" Dimension.

RBEH-0071X-X00



Dimensions in mm (inches).
Product designed in inches.
Metric conversions provided for reference only.

Notes:

- 1) Shaft end play: with a 6 lb reversing load, the axial displacement shall be .013-.15 (.0005-.006).
- 2) For a C.C.W. rotation, as viewed from pilot end, energize per excitation sequence table.
- 3) V-AB, V-BC and V-CA is back EMF of motor phases AB, BC and CA respectively, aligned with sensor output as shown for C.C.W. rotation only.

MODEL NUMBER	RBEH-00710	RBEH-00711	RBEH-00712	RBEH-00713	RBEH-00714
"A" Dimension	39.83 (1.568)	46.18 (1.818)	52.53 (2.068)	58.88 (2.318)	66.50 (2.618)

RBE/RBEH LEADWIRE

Motor Leads: #24 AWG Teflon coated per MIL-W-22759/11, 3 leads, 152 (6.00) min lg. ea. 1-black, 1-white, 1-red.

Sensor Leads: #26 AWG type "ET" Teflon coated per MIL-W-16878, 5 leads, 152 (6.00) min lg. ea. 1-blue, 1-brown, 1-green, 1-orange, 1-yellow.

RBE(H) Motor Series

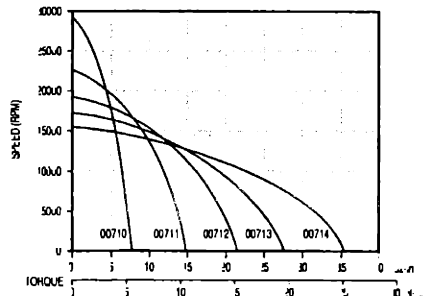
RBE(H) 00710 MOTOR SERIES PERFORMANCE DATA

Motor Parameters	Symbols	Units	00710	00711	00712	00713	00714
Max Cont. Output Power at 25°C amb.	HP Rated	HP	0.0858	0.133	0.166	0.189	0.225
	P Rated	Watts	64	99	124	141	168
Speed at Rated Power	N Rated	RPM	17700	14110	12000	10800	9750
Max Mechanical Speed	N Max	RPM	20000	20000	20000	20000	20000
Continuous Stall Torque at 25°C amb.	Tc	oz-in	8.14	15.5	21.5	27.6	35.3
		N-m	0.057	0.109	0.152	0.195	0.249
Peak Torque	Tp	oz-in	22.7	43.8	63.3	84.5	114
		N-m	0.160	0.310	0.447	0.597	0.802
Max Torque for Linear KT	Tsl	oz-in	22.7	43.8	63.3	84.5	114
		N-m	0.160	0.310	0.447	0.597	0.802
Motor Constant	Km	oz-in/√W	2.36	4.05	5.38	6.67	8.25
		N-m/√W	0.0166	0.029	0.038	0.047	0.058
Thermal Resistance*	Rth	°C/Watt	5.90	4.91	4.47	4.19	3.94
Viscous Damping	Fi	oz-in/RPM	4.40E-05	8.39E-05	1.20E-04	1.56E-04	2.00E-04
		N-m/RPM	3.11E-07	5.93E-07	8.49E-07	1.11E-06	1.41E-06
Max Static Friction	Tf	oz-in	0.90	1.54	2.12	2.70	3.40
		N-m	0.0064	0.011	0.015	0.019	0.024
Max Cogging Torque Peak to Peak	Tcog	oz-in	0.75	1.38	1.95	2.52	3.20
		N-m	0.0053	0.0097	0.0137	0.0178	0.023
Frameless Motor	Jmf	oz-in-sec ²	1.30E-04	2.00E-04	2.80E-04	3.50E-04	4.40E-04
		Kg-m ²	9.18E-07	1.41E-06	1.98E-06	2.47E-06	3.11E-06
Housed Motor	Wif	oz	2.8	4.4	5.8	7.2	8.9
		Kg	7.94E-02	1.24E-01	1.64E-01	2.04E-01	2.52E-01
Housed Motor	Jmh	oz-in-sec ²	1.30E-04	2.00E-04	2.80E-04	3.60E-04	4.50E-04
		Kg-m ²	9.18E-07	1.41E-06	1.98E-06	2.54E-06	3.18E-06
Housed Motor	Wtb	oz	7.8	9.3	11	12	14
		Kg	2.21E-01	2.65E-01	3.04E-01	3.44E-01	3.91E-01
No. of poles	P		6	6	6	6	6

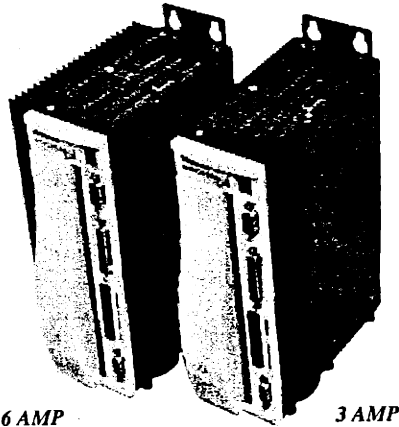
Winding Constants	Symbols	Units	A	B	C	A	B	C	A	B	C	A	B	C	A	B	C
Current at Cont. Torque	Ic	Amps	4.83	3.87	6.91	4.73	3.78	6.75	4.56	3.65	6.51	4.38	3.51	6.26	4.68	3.37	6.02
Current at Peak Torque	Ip	Amps	12.6	9.99	17.8	12.6	10.0	17.8	12.6	10.0	17.8	12.6	10.0	17.8	14.2	10.0	17.8
Torque Sensitivity	Kt	oz-in/Amp	1.87	2.34	1.31	3.60	4.50	2.52	5.19	6.49	3.63	6.92	8.65	4.85	8.26	11.5	6.43
		N-m/Amp	0.0132	0.0165	0.0092	0.0254	0.0318	0.0178	0.0367	0.0458	0.0257	0.0489	0.0611	0.0342	0.0584	0.0810	0.0454
Back EMF constant	Kb	V/KRPM	1.38	1.73	0.968	2.66	3.33	1.86	3.84	4.80	2.69	5.12	6.40	3.58	6.11	8.49	4.75
Motor Resistance	Rm	Ohms	0.629	0.991	0.311	0.790	1.24	0.390	0.933	1.47	0.461	1.08	1.70	0.533	1.00	1.97	0.618
Motor Inductance	Lm	mH	0.19	0.30	0.095	0.37	0.57	0.18	0.54	0.84	0.26	0.72	1.1	0.35	0.76	1.5	0.46

*Rth assumes a housed motor mounted to a 3.25" x 3.25" x 0.25" aluminum heatsink or equivalent

Continuous Duty Capability for 130°C Rise — RBE - 00710 Series



INTRODUCTION



Kollmorgen SERVOSTAR CD™ Amplifier

- 115 to 230 Volt Single Phase AC Input Power
- Resolver or Encoder Feedback
- Integrated Power Supply
- Fully Digital Control

The SERVOSTAR CD amplifier is a compact, fully digital amplifier designed to simplify installation and system set-up. Three control algorithms and self-tuning (to the load) functionality allows high performance operation to be achieved quickly and easily.

Since not one control algorithm is best for all machines, SERVOSTAR CD contains Pole Placement, PI, and PDFF control algorithms. SERVOSTAR CD utilizes the PC-based MOTIONLINK® for Windows™ which automatically takes you through the key steps of installation and start up.

FEATURES:

Servo Control

- Advanced patented sinewave commutation technology provides smooth, precise low-speed control and high-speed performance
- Accurate torque control due to precision balanced current loops with closed loop sensors
- Velocity loop bandwidths to 400 Hz
- Self-tuning to the load
- Patented torque angle control enhances motor performance
- Fully digital control loops
- Compact and attractive rugged metal package for space-saving, modern appearance - metal package minimizes electrical noise
- Pole Placement, PI, and PDFF control options

- Low Pass or Notch Filters for compliant & resonance machines
- Command modes: Torque (analog or serial); Velocity (analog or serial); Position (analog, serial or pulse)
- Two current ratings: 3 & 6 amp RMS/phase continuous
- 3 to 1 peak/continuous current rating
- Run time counter

Analog Command:

- 14 Bit analog conversion motion indexing
- Simple absolute & incremental thru internal profile generator

Easy Connectivity

- Built in encoder equivalent output can eliminate the need for an additional position feedback device
- RS232 or RS485 Communication
- Unique multi-drop configuration allows a PC or PLC to communicate to multiple SERVOSTAR CD amplifiers via single RS-232 connection
- SERVOSTAR CD's versatile communication capabilities make it easy to integrate machine control data directly from the factory floor to your information system
- Analog $\pm 10V$, pulse/direction, master encoder, serial port, command options

Robust Design

- Excellent protection against miswired connection on 24 Volt I/O
- ESD rugged circuit design and fully metallic enclosure
- Self-protecting intelligent power modules
- Full protection against short circuit, overvoltage, undervoltage, heatsink overtemperature, motor overtemperature, overspeed, overcurrent, and feedback loss
- UL , cUL listed, and CE
- Flash memory

Windows Start-up Environment – MOTIONLINK®

- Advanced motion "wizard" automatically walks you through set-up
- PC "Oscilloscope" for measuring real-time motion performance

Motion Indexing

- Stores up to 4 motion profiles in memory
- Start motion through serial command or digital I/O
- Homing functions

Configurable I/O

- 3 digital inputs, 1 digital output, & 1 analog output can be configured to a variety of functions to customize the SERVOSTAR CD to individual machines

SERVOSTAR CD

AMPLIFIER SPECIFICATIONS

Electrical characteristics

- Closed loop velocity bandwidth up to 400 Hz
- Motor current ripple frequency (32 kHz)
- Long term speed regulation (0.01%)
- Position loop update rate 500 μ s (2 kHz)
- Velocity loop update rate 250 μ s (4 kHz)
- Commutation update rate 62.5 μ s (16 kHz)
- Current loop update rate 62.5 μ s (16 kHz)

Fault protection

- Output phase to phase short circuit protection
- Overvoltage
- Undervoltage
- Overtemperature (motor and amplifier)
- Overspeed
- Overcurrent
- Feedback loss
- Foldback
- Supply loss
- Excessive position error

Environmental

- Operation range
 - Ambient 0 to 45°C (derated above ambient)
 - Storage -20°C to 70°C
- Humidity (non-condensing) 10% to 90%

Velocity Loop Compensation

- Vel: PI, PDFF or Pole Placement selectable algorithms
- Factory preset or field tunable
- MOTIONLINK® software provides tuning programming via RS-232 or RS-485 serial interface
- Adjustable filters

Position Loop Compensation

- PID

Inputs

- Analog command: ± 10 V
 - Resolver feedback models: 14 bit resolution provides up to 16,000 to 1 dynamic speed range
 - Encoder feedback models: 15 bit resolution provides up to 32,000 to 1 dynamic speed range
- Remote enable: 24V
- Three multi-purpose 24V inputs Configurable to: CW limit switch, CCW limit switch, gear enable, start motion, second current limit, change velocity to torque mode, home switch, search for home, move to home registration capture, active disable, control fault relay, hold position plus using two inputs, up to four stored indexes or speeds can be executed
- Pulse command: up/down, pulse/direction, pulse or quadrature encoder format into RS-485 receivers or opto isolators

Communications

- RS-232 or RS-485 serial interface 9600 or 19.2 kb

Outputs

- Fault: contact closure rated for 1 Amp, 24 Volt
- One multi-purpose 24V output configurable to: speed exceeded, current exceeded, amplifier in foldback, brake enable, motion complete, in position, zero speed detect

Operational modes

- Torque control — from analog or serial command
- Velocity control — from analog or serial command
- Pulse following / Up-Down count
- Gearing from quad encoder input
- Position control

Diagnostics

- Seven segment LED display
- Error history log
- Internal variable monitoring
- PC scope

Motor Feedback

- Resolver: sine/cosine 2V peak to peak (SERVOSTAR CD provides 4.25V peak to peak for resolver excitation)
- Encoder: 5V quadrature with or without Halls, with or without marker, up to 3 MHz before quadrature (12 MHz after quadrature)

Amplifier Ratings								
Model	Output Continuous Current Per Phase (RMS/phase)	Output Peak Current Per Phase (1/2 sec)	Rated Output Continuous Power (kW)	Internal Power Dissipation (Watts)	PWM Switching Frequency (kHz)	AC Input Line Voltage (1 phase)	Rated Input Power	Regen. Option
Cx03	3	9	1.1	37	16	115-230	1.7	ERH-26
Cx06	6	18	2.2	84	16	115-230	2.8	ERH-26

SERVOSTAR CD

RESISTIVE REGENERATION SIZING/DIMENSIONS

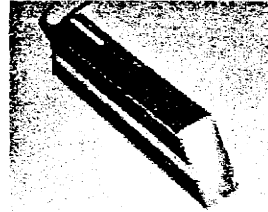
Resistive Regeneration Sizing

Shunt regeneration is required to dissipate energy that is pumped back into the DC bus during load deceleration. The amount of shunt regeneration required is a function of the sum of simultaneously decelerating loads. The loads need to be defined in terms of system inertia, maximum speed, and deceleration time. In addition, the duty cycle must be known. Application Note A-SU-001-H details a calculation method to determine proper regeneration sizing.

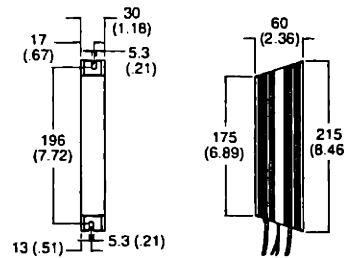
Transformer Sizing (Required only for voltage matching)

The SERVOSTAR CD can be connected to a line. Built-in soft-start circuitry protects power supply components and eliminates nuisance tripping of breakers or fuse blowing due to large in-rush currents. Transformers are only required for voltage matching purposes. In this case, the transformer should have a 115 or 230 VAC secondary depending on the operating voltage. The kVA rating of the transformer should take into account not only the servo output load requirements but also losses in the system and power factor. For single phase operated systems such as these, the transformer KVA ratings should be two times the CD amplifier output power rating.

Model	Transformer KVA rating
Cx03	2.2
Cx06	4.4



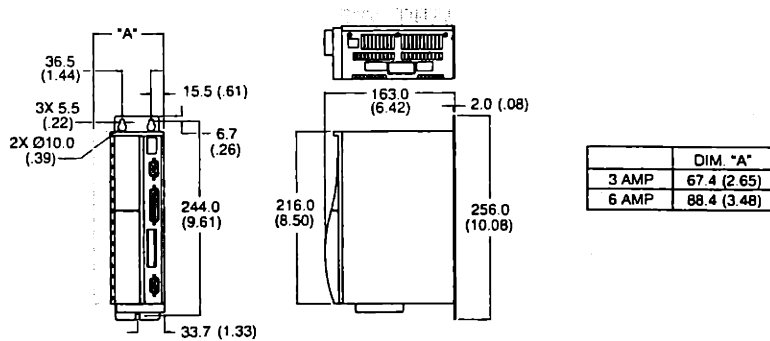
Model	Watts	Ohms
ERH-26	200	20



Resistive Regen ERH-26

SERVOSTAR CD DIMENSIONS

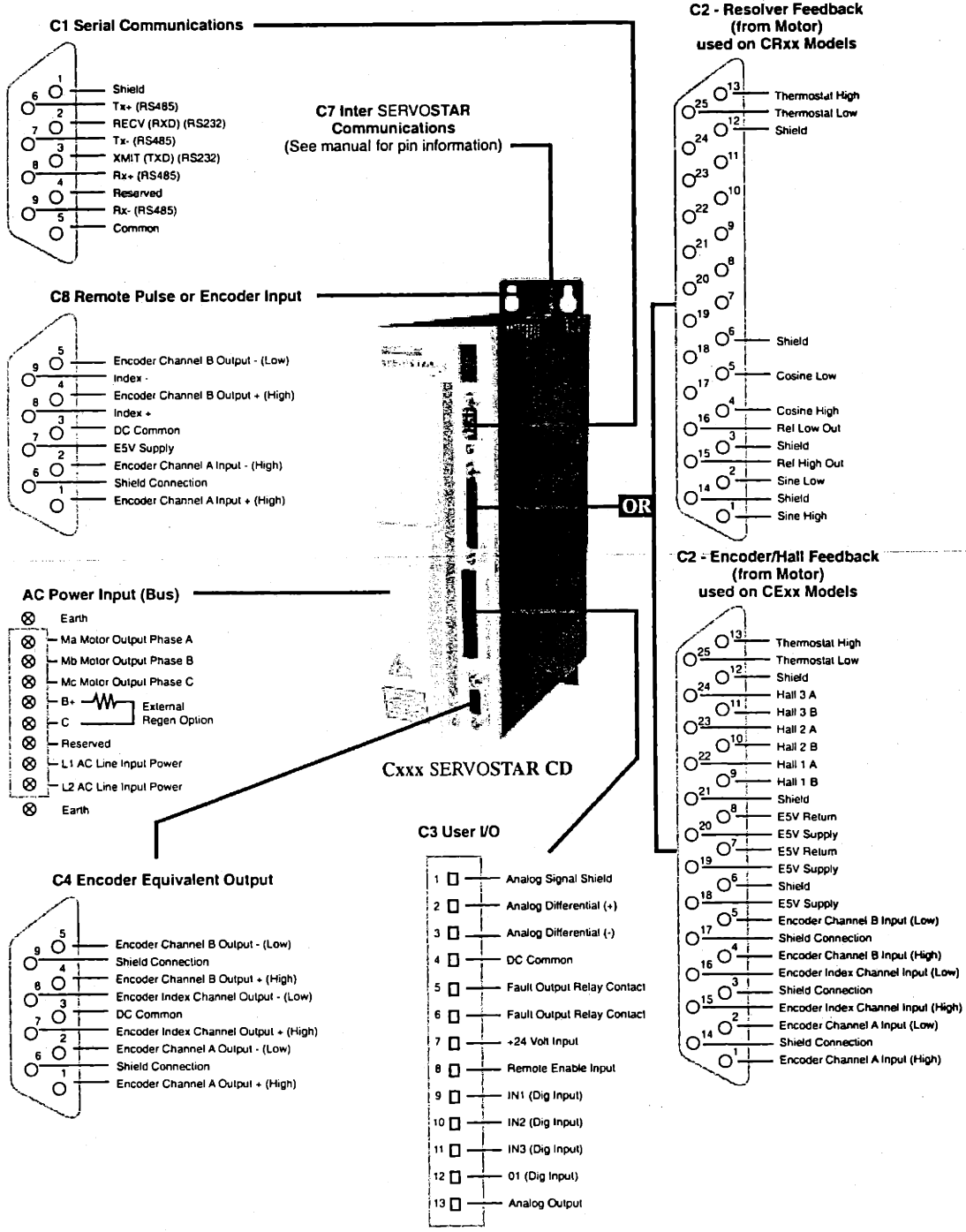
Cx03/06



Dimensions in mm (inches)

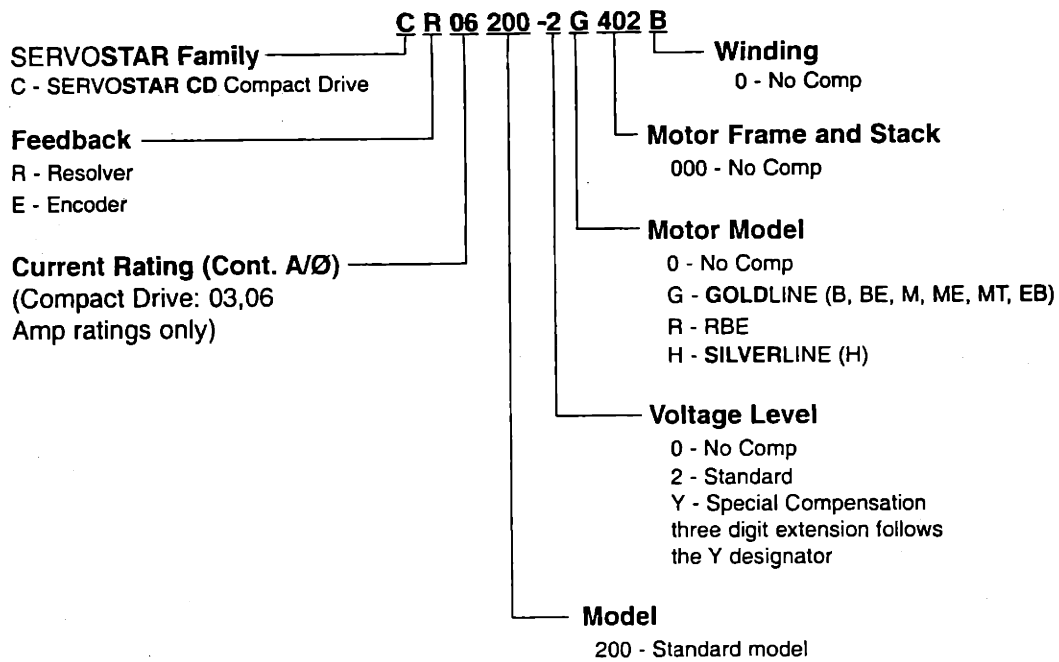
SERVOSTAR CD

CONNECTOR INFORMATION



SERVOSTAR CD

SYSTEM ORDERING INFORMATION





Gurley Precision Instruments

ISO 9001 Certified

Motion type:	Rotary
Usage Grade:	Light industrial
Output:	Incremental
Max. Resolution:	40,960 counts/rev



Model R119 Rotary Incremental Mini-Encoder

**SMALLEST HIGH
RESOLUTION ENCODER!**

The Model R119 optical incremental encoder is designed for light industrial applications that require high resolution in a very small package. It is available in both shafted and blind hollow shaft versions. The two models share these features:

- $\phi 19$ mm body
- LED illumination for long life (>100,000 hours)
- Differential photo-detectors for signal stability
- Single-board, surface-mount electronics for reliability
- RS-422 differential line driver output for noise immunity
- Zero index signal
- Monolithic integrated ASIC for internally interpolated resolutions up to 10,240 cycles/rev (40,960 counts/rev)

514 FULTON ST • TROY, NY 12181 • PHN 800-759-1844 • 518-272-6300 • FAX 518-274-0336
<http://www.gurley.com> ders@gurley.com

SPECIFICATIONS

	See Note	Model R119B or Model R119S
Maximum line count on disc		1024
Maximum cycles/rev (quad sq waves)		10,240
Max counts/rev (after quad decode)		40,960
Internal square wave interpolation		1X, 2X, 5X or 10X
Instrument error, \pm arcminutes	1, 2	4
Quadrature error, \pm electrical degrees	1, 3	24
Interpolation error, \pm quanta	1, 4	0.15
Maximum output frequency, kHz		
1X square waves		100
2X square waves		150
5X square waves		300
10X square waves		500
Starting torque, in-oz (N-m) @20°C		0.07 (4.9×10^{-4})
Running torque, in-oz (N-m) @20°C		0.04 (2.9×10^{-4})
Moment of inertia, in-oz-s ² (g-cm ²)		3.4×10^{-6} (0.24)
Maximum weight, oz (g)		0.5 (15)
Sealing		IP50
Operating temperature, °F (°C)		32 to 158 (0 to 70)
Storage temperature, °F (°C)		0 to 160 (-18 to 71)
Humidity, % rh, non-condensing		98
Shock		31 g (300 m/s ²)
Vibration		10 g (100 m/s ²)

S = Shaft version; B = Blind hollow shaft version

NOTES:

- Total Optical Encoder Error is the algebraic sum of *Instrument Error* + *Quadrature Error* + *Interpolation Error*. Typically, these error sources sum to a value less than the theoretical maximum. Error is defined at the signal transitions and therefore does not include quantization error, which is $\pm 1/2$ quantum. ("Quantum" is the final resolution of the encoder, after user's 4X quadrature decode.) Accuracy is guaranteed at 20°C.
- Instrument Error* is the sum of disc pattern errors, disc eccentricity, bearing runout and other mechanical imperfections within the encoder. This error tends to vary slowly around a revolution.
- Quadrature Error* is the combined effect of phasing and duty cycle tolerances and other variables in the basic analog signals. This error applies to data taken at all four transitions within a cycle; if data are extracted from 1X square waves on a 1X basis (i.e., at only one transition per cycle), this error can be ignored.
Error in arcminutes = (60) x (error in electrical degrees) + (disc line count)
- Interpolation Error* is present only when the resolution has been electronically increased to more than four data points per optical cycle. It is the sum of all the tolerances in the electronic interpolation circuitry.
Error in arcminutes = (21600) x (error in quanta) + (counts/rev)

As part of our continuing product improvement program, all specifications are subject to change without notice.

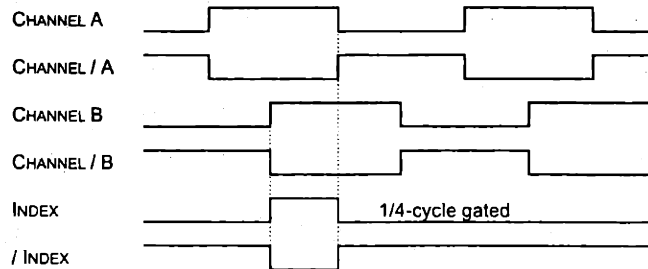
INPUT POWER

+5 VDC @100 mA max.

SQUARE WAVE OUTPUT

Quadrature square waves at 1, 2, 5 or 10 times the line count on the disc. On all channels: EIA/RS-422 balanced differential line driver, protected to survive an extended-duration short circuit across its output. May be used single-ended for TTL-compatible inputs. Index is 1/4-cycle wide, gated with the high states of channels A and B.

OUTPUT WAVEFORMS (CW rotation shown)



ELECTRICAL CONNECTIONS

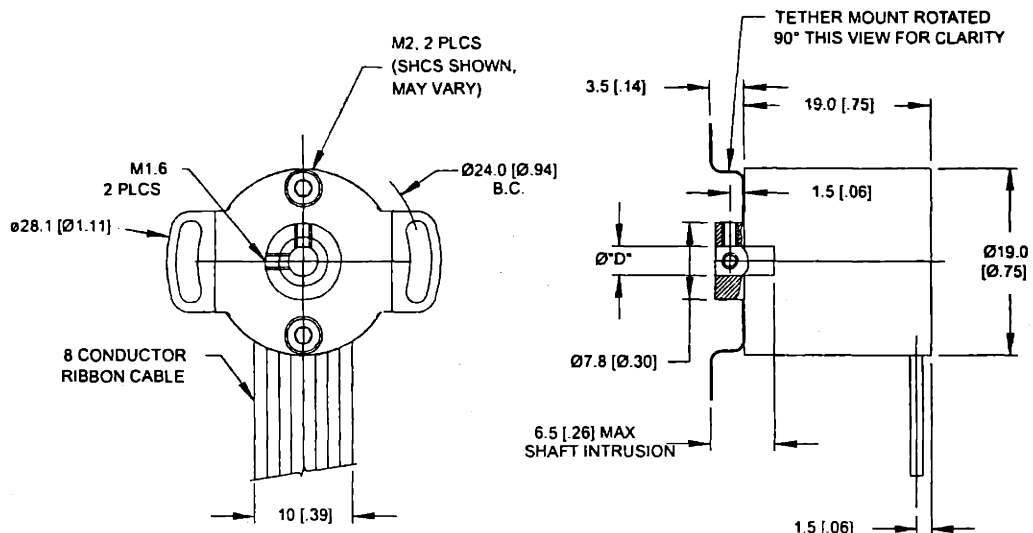
Output Functions	Wire Colors Conn. Code P	Pos. No. Conn. Code Y
A	Orange	2
/ A	Yellow	3
B	Violet	6
/ B	Gray	7
IND	Green	4
/ IND	Blue	5
+V	Red	1
COMMON	White	8

NOTE: Channel A leads Channel B for clockwise shaft rotation, viewed from the shaft end.

FLEXIBLE SHAFT COUPLING

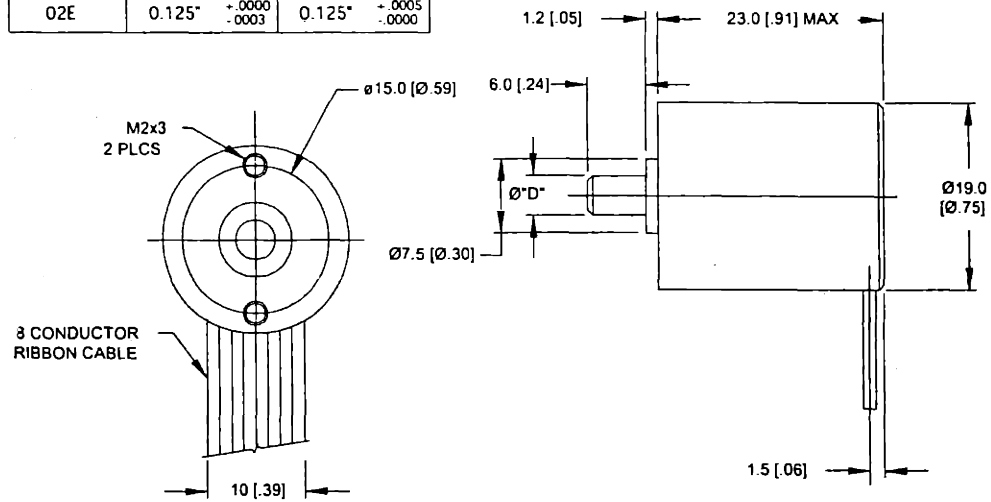
R119B Tether Mount	
Maximum parallel offset, in (mm)	0.002 (0.05)
Maximum angular misalignment, degrees	2.0
Maximum axial extension or compression, in (mm)	0.008 (0.2)

NOTE: Flexible couplings are intended to absorb normal installation misalignments and run-outs in order to prevent undue loading of the encoder bearings. To realize all the accuracy inherent in the encoder, the user should minimize misalignments as much as possible.



R119B (BASE CODE A)

"D" TABLE		
"DIA" CODE	R119S "D"	R119B "D"
04M	4mm h6	N/A
03M	3mm h6	3mm H7
02E	0.125" ^{+0.0000} / _{-0.0003}	0.125" ^{+0.0005} / _{-0.0000}



R119S (BASE CODE B)

514 FULTON ST • TROY, NY 12181 • PHN 800-759-1844 • 518-272-6300 • FAX 518-274-0336
<http://www.gurley.com> dens@gurley.com

ORDERING INFORMATION

R119 SHAFT - LINES Q - 5 L INTERP - BASE CAB S CONN - DIA SF

SHAFT

- S Shaft version
- B Blind hollow shaft

LINES - Disc line count

00360, **00500**, 00512, 00900, 01000, **01024**
Bold counts exist; others will be added.
Consult factory for other line counts

INTERP - Interpolation factor

01, 02, 05, 10

BASE

- A Use with R119B
- B Use with R119S

CAB - Cable length, inches

18 Standard

CONN - Connector

- P Pigtails (no connector)
- Y 8-pos ribbon cable socket connector
(Berg 71602-308 or equal)

DIA - Shaft diameter

- 04M 4 mm (SHAFT = S)
- 03M 3 mm (SHAFT = S or B)
- 02E 1/8" (SHAFT = S or B)

SF - Special features

- # Issued at time of order to cover special customer requirements
- N No special features

SPECIAL CAPABILITIES

For special situations, we can optimize catalog encoders to provide higher frequency response, greater accuracy, wider temperature range, reduced torque, non-standard line counts, or other modified parameters. In addition, we regularly design and manufacture custom encoders for user-specific requirements. These range from high-volume, low-cost, limited-performance commercial applications to encoders for military, aerospace and similar high-performance, high-reliability conditions. We would welcome the opportunity to help you with your encoder needs.

WARRANTY

Gurley Precision Instruments offers a limited warranty against defects in material and workmanship for a period of one year from the date of shipment.

R119 data sheet.doc
10-Jan-01

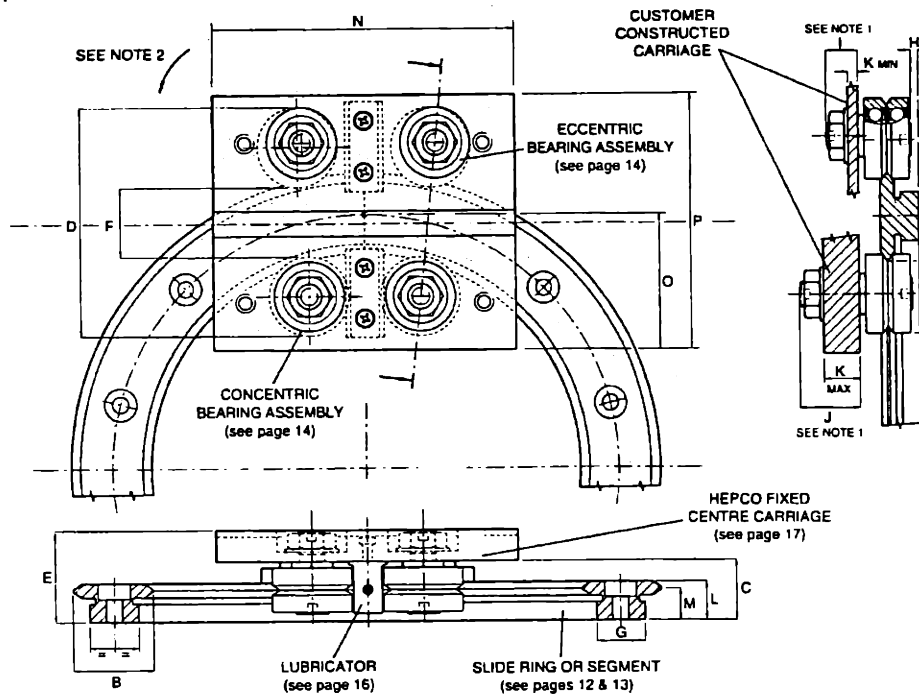
514 FULTON ST • TROY, NY 12181 • PHN 800-759-1844 • 518-272-6300 • FAX 518-274-0336
<http://www.gurley.com> der@gurley.com

HEPCO RING SLIDES AND TRACK SYSTEM

DATA & DIMENSIONS

Assembled Ring System

The Hepco Ring System may be used in either complete ring form or as segments. The carriage may be used to run on the ring track (see below) or constructed in order to embrace the complete ring (see page 11) where the bearing assemblies may be placed internally and/or externally. In all cases either the ring or the carriage may be the moving component. The specially developed Hepco 'R' series bearing assemblies have sufficient adjustment to enable complete removal of the ring slide from the carriage.



10

Slide Ring Ref. No.	A	B	C	D	E	F	G	H	I	J	K	
											Max	Min
R12-93	93	12	11.67	34.7	17.67	9.3	8.6	1.5	5.8	9.5	6	2.5
R12-127	127	12	11.67	34.7	17.67	9.3	8.6	1.5	5.8	9.5	6	2.5
R25-159	159	25	19	72.1	29	22.1	15.4	2.4	9.8	19	13	2.5
R25-255	255	25	19	71.2	29	21.2	15.4	2.4	9.8	19	13	2.5
R25-351	351	25	19	71.2	29	21.2	15.4	2.4	9.8	19	13	2.5
R44-468	468	44	24	105.9	38	37.9	26	2.7	13.8	22	14	5.5
R44-612	612	44	24	105.9	38	37.9	26	2.7	13.8	22	14	5.5
R76-799	799	76	38.5	172.8	56.5	64.7	50.5	3.8	17.8	30	20	6
R76-1033	1033	76	38.5	172.8	56.5	64.7	50.5	3.8	17.8	30	20	6

Notes:

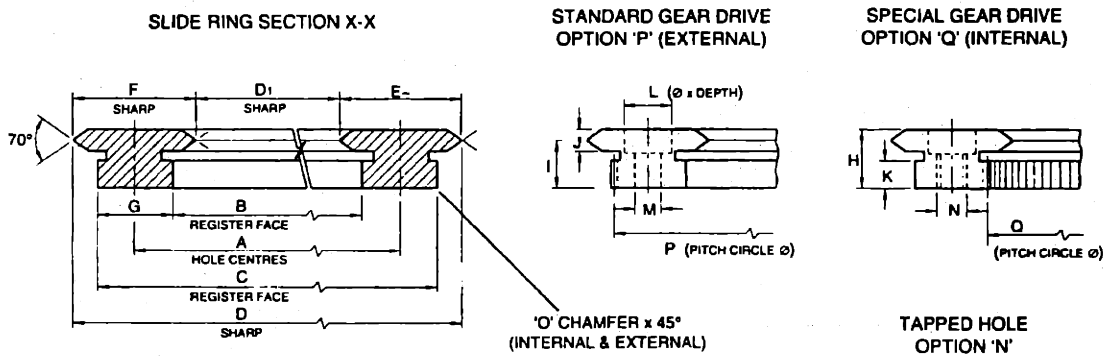
- Two lengths of stud are available for each size bearing assembly (see page 14). Choose according to your required carriage thickness.
- Offset holes in carriage for eccentric bearing assemblies necessitate adjustment rotation in direction shown.
- Standard pinions are available from most manufacturers to suit gear drive option slide rings (see page 12).
- Exact theoretical values have been given for 'Q', 'R' and 'S'. Positional accuracy of dimension 'S' will determine the axis of the ring. Positional accuracy for dimensions 'Q' and 'R' are not normally critical. Holes for bearing assemblies should be reamed to tolerance as per dimension 'R' on page 17.

HEPCO RING SLIDES AND TRACK SYSTEM

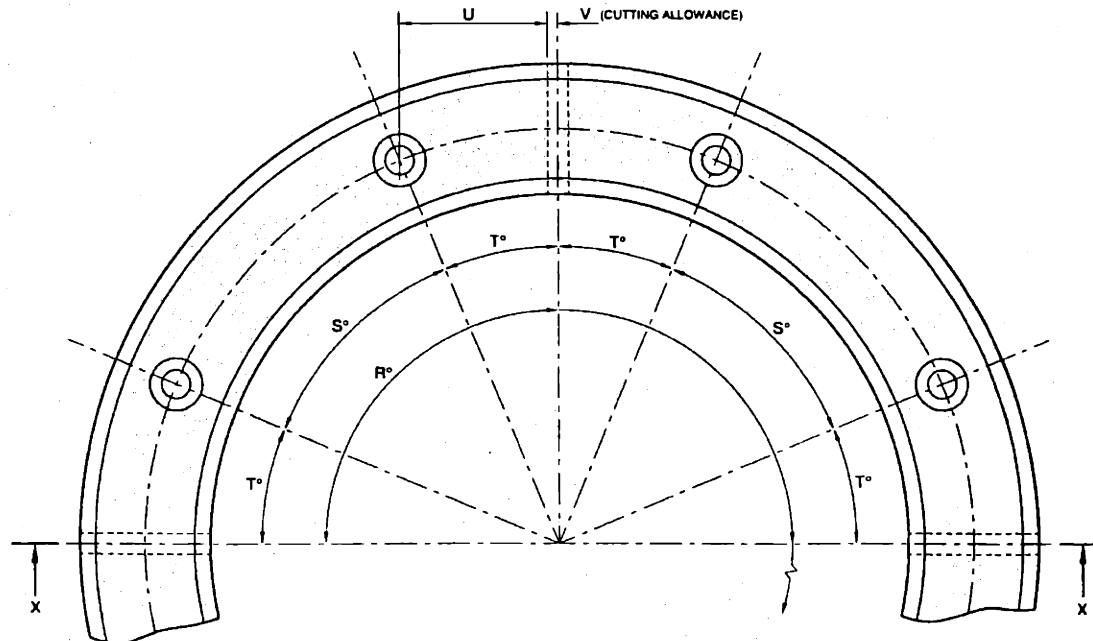
DATA & DIMENSIONS

Slide Rings & Segments

Hepco 'R' series slide rings are manufactured from high quality steel, zone hardened on the V edges and precision ground all over with datum register faces provided both internally and externally for ease of location. Gear drive options are available with teeth machined into either the internal or external register face. The number of teeth on the standard external option is divisible by 12 in order to provide maximum choice of pinion size for exact ratio requirements. Customers may also choose the tapped hole option 'N' which enables the slide ring to be bolted from below.



12



DATA & DIMENSIONS



Slide Rings & Segments

Hepco 'R' series ring segments are cut from complete 360° slide rings and held in stock in nominal 90° and 180° sections. Any length segment can be cut to customer's special order and additional holes drilled as required. Although suitable for most applications, slight out of roundness and flatness may be experienced with slide rings and segments in their free unmounted condition. This may be overcome by installing against a register and bolting to a flat surface.

Part Number	±0.2	A	B	±0.011	C	D	D ₁	E	F	G	H	±0.025	I	J	K	L	M	Socket Cap-Head Screw ISO 4762 See Note 2	N
R12-93	93	84.4	±0.011	101.6	±0.037 REF	105.37	80.63	12	12.37	8.6	7.7	6.2	3	3.5	6x3	3.7	M3*	M4x0.7	
R12-127	127	118.4	±0.011	135.2	±0.037 REF	139.37	114.63	12	12.37	8.6	7.7	6.2	3	3.5	6x3	3.7	M3*	M4x0.7	
R25-159	159	143.6	±0.013	174.4	±0.039 REF	184.74	133.26	25	25.74	15.4	12.25	10	4.5	5.75	9x6	5.5	M5	M8x1.25	
R25-255	255	239.6	±0.015	270.4	±0.041 REF	280.74	229.26	25	25.74	15.4	12.25	10	4.5	5.75	9x6	5.5	M5	M8x1.25	
R25-351	351	335.6	±0.018	366.4	±0.044 REF	376.74	325.26	25	25.74	15.4	12.25	10	4.5	5.75	9x6	5.5	M5	M8x1.25	
R44-468	468	442	±0.02	494	±0.046 REF	512.74	423.26	44	44.74	26	15.5	12.5	6	7	11x7	6.8	M6	M8x1.25	
R44-612	612	586	±0.022	638	±0.048 REF	656.74	567.26	44	44.74	26	15.5	12.5	6	7	11x7	6.8	M6	M8x1.25	
R76-799	799	748.5	±0.025	849.5	±0.051 REF	875.74	722.26	76	76.74	50.5	24	19.5	9	12	20x13	14	M12	M16x2	
R76-1033	1033	982.5	±0.028	1083.5	±0.054 REF	1109.74	956.26	76	76.74	50.5	24	19.5	9	12	20x13	14	M12	M16x2	

O	External Gear			Internal Gear			Stock Segments (See Note 1)			Number Of Holes (R=360°)		Holes Within ±0.2 Of True Position			U	V	Mass Kg (R=360°)	Part Number
	P	MOD	No. of Teeth (R=360°)	Q	MOD	No. of Teeth (R=360°)	R°	S°	T°	S°	T°							
0.2	100.8	0.4	252	85.2	0.4	213	90	180	360	8	45	22.5	16.8	1	0.16	R12-93		
0.2	134.4	0.4	336	119.2	0.4	298	90	180	360	8	45	22.5	23.3	1	0.22	R12-127		
0.5	172.8	0.8	216	145.6	0.8	182	90	180	360	8	45	22.5	29.4	1	0.77	R25-159		
0.5	268.8	0.8	336	241.6	0.8	302	90	180	360	8	45	22.5	47.8	1	1.2	R25-255		
0.5	364.8	0.8	456	337.6	0.8	422	90	180	360	12	30	15	44.4	1	1.65	R25-351		
0.5	492	1.0	492	444	1.0	444	90	180	360	12	30	15	58.6	2	5.1	R44-468		
0.5	636	1.0	636	588	1.0	588	90	180	360	16	22.5	11.25	57.7	2	6.7	R44-612		
1.0	846	1.5	564	751.5	1.5	501	90	180	360	16	22.5	11.25	75.9	2	25	R76-799		
1.0	1080	1.5	720	985.5	1.5	657	90	180	360	20	18	9	78.8	2	32	R76-1033		

13

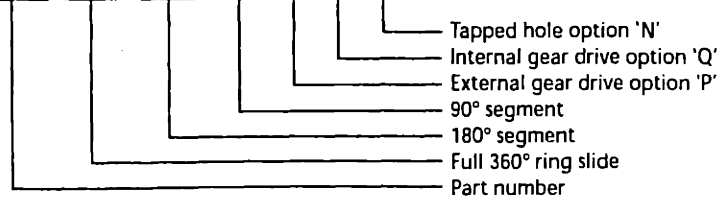
Notes:

- Standard ring segments will be slightly less than 90° and 180° because of the cutting allowance. Full 90° and 180° segments can be supplied to customer's special order.
- Socket head cap screws ISO 4762 will protrude 1mm above the surface of the R12 section slide rings. Customers requiring screws to be flush should use low head type DIN 7984, available from Hepco upon request.

Ordering Details

Example:

R25-351- (R360) - (R180) - (R90) - (P) - (Q) - (N)



HEPCO RING SLIDES AND TRACK SYSTEM

DATA & DIMENSIONS

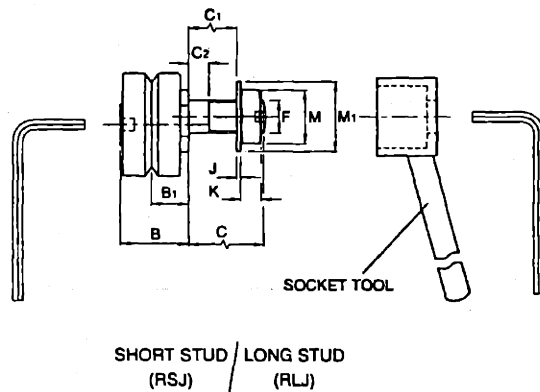
Bearing Assemblies

Two basic bearing assembly options are available, the standard economy through fixing type which requires access to the retaining nut on the opposite side of the mounting plate, and the blind hole fixing type for use where access to the opposite side is denied.

The through fixing type is available in two stud lengths to cater for most applications, the short stud version being compatible with the Hepco carriage plates. All bearing assemblies incorporate Hepco high precision ball races for durability, rigidity and friction free running. The bearings are greased for life and are supplied dust shielded as standard or neoprene sealed upon request.

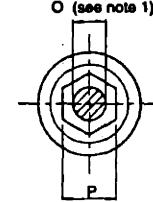
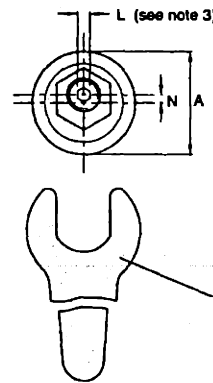
Bearing assemblies are available in concentric form to provide a datum reference and in eccentric form for ease of system adjustment.

Through Fixing Type (RSJ/RLJ)



ECCENTRIC (E)
(see note 4)

CONCENTRIC (C)
(see note 4)



14

Part Number	For Use With Ring/Slide Section (See Note 6)	A	B	±0.025 B ₁	RSJ	RLJ	RSJ	RLJ
					C	C	C ₁	C ₁
RSJ/RLJ-13-C/E / BHJ-13-C/E	R-12/TNMS-12	12.7	10.1	5.46	5.8	9.5	3	6
RSJ/RLJ-25-C/E / BHJ-25-C/E	R-25/TNS-25	25	16.6	9	9.8	19	4	13
RSJ/RLJ-34-C/E / BHJ-34-C/E	R-44/TNM-44	34	21.3	11.5	13.8	22	6	14
RSJ/RLJ-54-C/E / BHJ-54-C/E	R-76/TNL-76	54	34.7	19	17.8	30	8	20

Q	R	S	S ₁	T	T ₁	T ₂	±0.2 U	U ₁	V	W	X	Y
1.5	1.5	6.25	8	8	3.75	6.75	30	47.5	8	20	M3x0.5	5.5
3	2	7	8.5	12	5	10	50	72	14	32	M5x0.8	8.5
4	2.5	9.5	8.5	17.5	6.5	12.5	60	90.5	17	42	M6x1	10
8	3.5	14.5	14	23.5	10.5	18.5	89.5	133	25	62	M8x1.25	13

Notes:

- It is recommended that holes to suit bearing assembly mounting studs should be reamed to tolerance as per dimension 'R' on page 17.
- Thread form is metric fine. See 'F' dimension in table above.
- All RSJ/RLJ type eccentric bearing assembly fixing studs are supplied with sockets for adjustment as shown with the exception of the RSJ/RLJ-13-E.
- Nuts and washers are supplied with both concentric and eccentric RSJ/RLJ type bearing assemblies.
- 'R' Dimension is both the eccentric offset of the adjusting nut and the total adjustment available at the bearing center line for 360° rotation of the adjusting nut.
- Each size of bearing assembly has been designed for use with a specific size of ring/slide section (see table above). However, any bearing assembly may be used in conjunction with any ring/slide section larger than that for which it was designed if required by the application. Additionally, size 34 bearing assemblies may be used with size 25 ring/slide section and size 54 bearing assemblies may be used with size 44 ring/slide section.

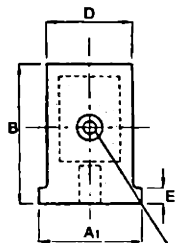
HEPCO RING SLIDES AND TRACK SYSTEM

DATA & DIMENSIONS

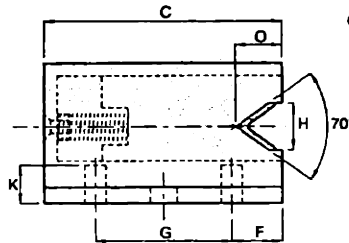
Lubricator

The Hepco Lubricator consists of an impact resistant polyacetal plastic molding, housing a spring loaded oil impregnated felt wiper and is designed to apply a constant film of oil to the working surfaces of the slide without imposing undue friction. The application of oil significantly increases the load/life of the system.

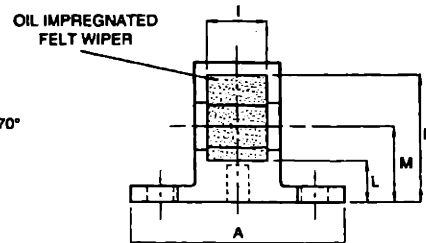
COMPACT TYPE (C)



OIL LUBRICATION POINT
(see note 2)

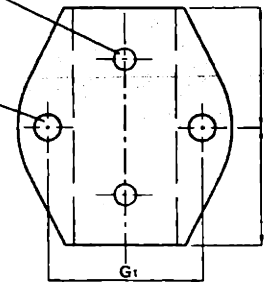


FLANGED TYPE (F)



'J' SCREW SIZE
(see note 1)

'J1' (see note 1)



16

Part Number	Use With Ring/ Segment Type	Type F	Type C	B	C	D	E
		A	A ₁				
LB-12	R/TR-12	17	7	10	13	5.2	2
LB-25	R/TR-25	25	12	16.5	28	9.9	2
LB-44	R/TR-44	34	17	20	38	15	2.4
LB-76	R/TR-76	50	25	33.5	57	22.7	4.5

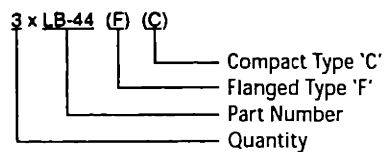
F	G	G ₁	H	I	J ØxLength	J ₁		K	L	M	N	O	Part Number
						Screw	Hole _Ø						
3	6.5	12	3.1	3	2.5x5	M2.5x0.45x6	2.7	2.5	3	5.46	9	2.2	LB-12
6	16	18	5.5	7	3x10	M3x0.5x8	3.2	4.5	5	9	15.25	5.5	LB-25
8	22	25	7	11	3x16	M4x0.7x10	4.2	5.5	6.25	11.5	18.25	8	LB-44
12	33	38	10	18	3.5x22	M5x0.8x12	5.2	9	10	19	31.5	11.5	LB-76

Notes:

- 2 x "Plastite" 45 self-tapping cross recessed pan head screws conforming generally to ISO 7049 are supplied with each lubricator for fixing via holes 'J'. Additionally, 2 x cross recessed cheese head screws -DIN 84A are supplied with flanged type lubricator for fixing via holes 'J₁'.
- Replenishment of oil should be carried out via the lubrication point provided using BP Energol GHL 68 or similar 68 viscosity EP mineral oil.

Ordering Details

Example:

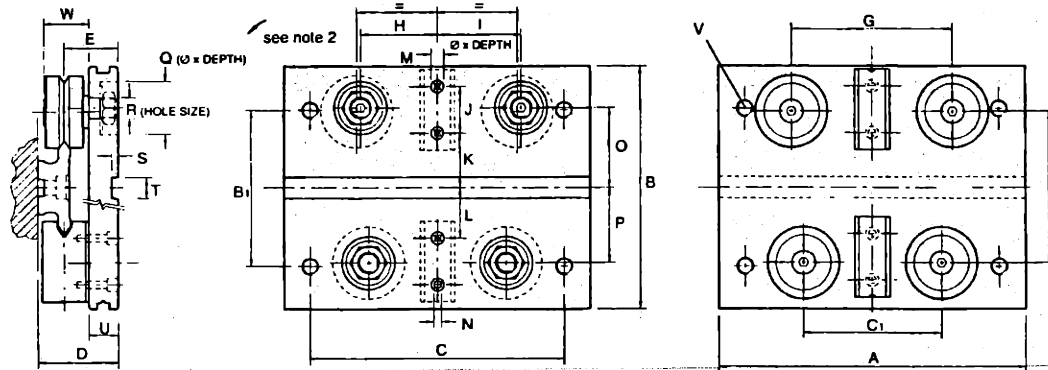


DATA & DIMENSIONS



Fixed Center Carriage

The Hepco fixed center carriage is designed for use with Hepco track systems of common bend radii without 'S' bends and also for ring slide tracks and segment tracks (see note 1). The geometry has been cleverly devised to enable the carriage to traverse from straight to curve without the necessity for each pair of bearings to independently follow the slide, thus enabling a low cost carriage to be produced. A small amount of play is experienced while the bearing assemblies traverse the joint between the straight and curve (see table on page 28) but this is not detrimental in most applications. The anodized aluminum alloy carriage plate can be manufactured to customer's special length requirements but the bearing assembly mounting hole centers must remain as specified. Each carriage is supplied fully assembled and adjusted to suit the accompanying slide if required.



Part Number	Use With Rings/Segment Type	A	B	± 0.1 B ₁	± 0.1 C	± 0.1 C ₁	$\begin{matrix} +0.13 \\ -0.05 \end{matrix}$ D	E	F	G	± 0.1 H	± 0.1 I	J
FCP-12-93	R / TR-12-93	55	40	25	45	20	17.67	11.47	22	25.56	11.86	13.70	6.5
FCP-12-127	R / TR-12-127	55	40	25	45	20	17.67	11.47	22	23.86	11.01	12.85	6.5
FCP-25-159	R-25-159	95	80	50	75	37	29	19	47.1	42.00	19.59	22.41	16
FCP-25-255	R / TR-25-255	100	80	50	80	36.5	29	19	46.1	43.88	20.53	23.35	16
FCP-25-351	R / TR-25-351	105	80	50	85	40	29	19	46.1	45.67	21.42	24.25	16
FCP-44-468	R / TR-44-468	145	115	75	120	65	38	25.5	71.9	75.96	36.21	39.75	22
FCP-44-612	R / TR-44-612	150	115	75	125	70	38	25.5	71.9	78.80	37.63	41.17	22
FCP-76-799	R / TR-76-799	190	185	100	160	90	56.5	37	118.7	104.60	49.12	55.48	33
FCP-76-1033	R / TR-76-1033	210	185	100	180	110	56.5	37	118.7	123.51	58.57	64.94	33

17

K	L	M	N ₀	± 0.1 O	± 0.1 P	Q	R ₀	$\begin{matrix} +0.1 \\ -0 \end{matrix}$ S	$\begin{matrix} +0.025 \\ -0 \end{matrix}$ T	U	V	W	Mass -g	Part Number	
9.3	7.8	4.4x2.5	2.7	11.92	11.0	11x3.5	4	$\begin{matrix} +0.008 \\ +0.018 \end{matrix}$	1.5	4	6	M4x0.7	10.1	70	FCP-12-93
8.8	7.8	4.4x2.5	2.7	11.92	11.0	11x3.5	4	$\begin{matrix} +0.008 \\ +0.018 \end{matrix}$	1.5	4	6	M4x0.7	10.1	70	FCP-12-127
17.1	10.8	5.4x3.2	3.2	25.50	23.0	22x6.9	8	$\begin{matrix} +0.010 \\ +0.022 \end{matrix}$	2	8	10	M6x1.0	16.6	400	FCP-25-159
15.9	14	5.4x3.2	3.2	24.55	23.0	22x6.9	8	$\begin{matrix} +0.010 \\ +0.022 \end{matrix}$	2	8	10	M6x1.0	16.6	410	FCP-25-255
15.6	14	5.4x3.2	3.2	24.55	23.0	22x6.9	8	$\begin{matrix} +0.010 \\ +0.022 \end{matrix}$	2	8	10	M6x1.0	16.6	420	FCP-25-351
25.8	23	5.4x2.1	3.2	37.93	35.75	25x8.5	10	$\begin{matrix} +0.010 \\ +0.022 \end{matrix}$	3	10	14	M8x1.25	21.3	1000	FCP-44-468
25.5	23	5.4x2.1	3.2	37.93	35.75	25x8.5	10	$\begin{matrix} +0.010 \\ +0.022 \end{matrix}$	3	10	14	M8x1.25	21.3	1000	FCP-44-612
43	40	6.5x2.7	3.8	62.67	59.25	32x11.5	14	$\begin{matrix} +0.015 \\ +0.027 \end{matrix}$	4	10	18	M10x1.5	34.7	3300	FCP-76-799
43	40	6.5x2.7	3.8	62.67	59.25	32x11.5	14	$\begin{matrix} +0.015 \\ +0.027 \end{matrix}$	4	10	18	M10x1.5	34.7	3400	FCP-76-1033

Notes:

1. Fixed center carriage FCP-25-159 cannot be used with a track system.
2. Offset holes in carriage for eccentric bearing assemblies necessitate adjustment rotation in the direction shown.

Ordering Details

Simply specify the quantity and part number required.

Example:

6 x FCP-44-612

HEPCO RING SLIDES AND TRACK SYSTEM

LOAD/LIFE CALCULATIONS

Load Capacity and Life Expectancy

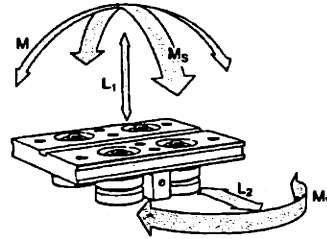
The load capacity and life expectancy of Hepco ring, segment and track systems will be determined by several factors. These are the size of the ring and the size and number of bearing assemblies used, the presence of lubrication, the magnitude and direction of loads, the speed of operation (see note 2, page 25) and the length of the path traversed (see note 3, page 25).

It is usual to run systems with less than the maximum load to prolong the life, which can be calculated using the data and formulae in this section. For calculation purposes, Hepco ring slide and track systems fall into two categories, those in which a carriage runs on a ring segment or track, and those in which a ring rotates captivated by a number of bearing assemblies (or a similar arrangement where the ring is stationary and the bearing assemblies and load rotate).

Wherever possible, Hepco ring and track systems should be lubricated using the Hepco lubricators (see page 16). Such lubrication will greatly increase the load capacity and extend the life of the system (see tables on pages 24 & 25 and nomograms on pages 25 & 26).

Systems with Carriages on Rings, Segments and Tracks

When calculating the life, the loading on the system should be resolved into the direct load components L_1 and L_2 and the moment load components M , M_v and M_s (see adjacent diagram and refer also to note 2).



24

Carriage	Maximum Lubricated Load Capacity					Maximum Unlubricated Load Capacity				
	Direct Loads (N)		Moment Loads (Nm)			Direct Loads (N)		Moment Loads (Nm)		
	L_1	L_2	M	M_v	M_s	L_1	L_2	M	M_v	M_s
FCP-12-93	120	120	1.25	1.25	0.6	80	80	0.8	0.8	0.4
FCP-12-127	120	120	1.2	1.2	0.6	80	80	0.8	0.8	0.4
BCP-12	120	120	1.7*	1.7*	0.6	80	80	1.2*	1.2*	0.4
FCP-25-159	800	800	16	16	9	300	300	6	6	3.5
FCP-25-255	800	800	15	15	9	300	300	6	6	3.5
FCP-25-351	800	800	17	17	9	300	300	7	7	3.5
BCP-25	800	800	27*	27*	9	300	300	10*	10*	3.5
FCP-44-468	1600	1600	57	57	35	600	600	22	22	14
FCP-44-612	1600	1600	65	65	35	600	600	24	24	14
BCP-44	1600	1600	75*	75*	35	600	600	28*	28*	14
FCP-76-799	3800	3800	165	165	140	1400	1400	62	62	55
FCP-76-1033	3800	3800	210	210	140	1400	1400	81	81	55
BCP-76	3800	3800	220*	220*	140	1400	1400	86*	86*	55

*See Note 1

To calculate the life of a system using a standard carriage, first obtain the load factor L_f by entering the values for L_1 , L_2 , M , M_v and M_s in respect of the proposed duty into equation [1] below, together with the maximum load capacities from the table above.

$$[1] \quad L_f = \frac{M}{M_{(max)}} + \frac{M_v}{M_{v(max)}} + \frac{M_s}{M_{s(max)}} + \frac{L_1}{L_{1(max)}} + \frac{L_2}{L_{2(max)}}$$

The life for the system can be read from the nomogram on page 25 (for lubricated systems) or on page 26 (for systems running dry) by taking the life figure on the lower scale opposite the calculated value for L_f on the upper scale (see examples, pages 26 & 27).

Notes:

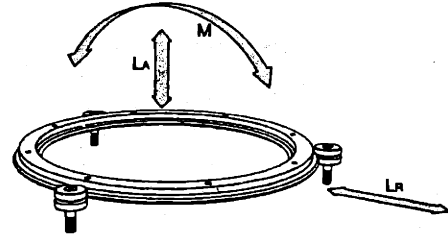
1. If using a bogie type carriage which differs from the standard length, then M and M_v moment load capacities will increase pro rata with the increase in the distance between the bogie swivel centers (see dimension 'F' on page 23).
2. When calculating L_2 and M_s , the centrifugal force must be included, which acts radially outwards from the center of mass (COM) of the moving object. Its magnitude is $F = DV^2/R$ where V is the velocity of the COM in m/s, R is the distance of the COM from the ring axis in m and D is the mass in kg. F is in N (newtons).

LOAD/LIFE CALCULATIONS



Systems with Rings Rotating Within Enclosing Bearing Assemblies

In those duties having a complete ring which rotates in a number of encircling bearing assemblies, it is usual to equally space the bearing assemblies around the ring (see note 1). When calculating the life, the loading on the system should be resolved into the direct load components L_A and L_R and the moment load component M (see adjacent diagram and refer also to note 2 on page 24).



Bearing Assembly Size	Used With Ring Part Number	Number of Bearing Assemblies Equally Spaced	Maximum Lubricated Load Capacity			Maximum Unlubricated Load Capacity		
			L_A (N)	L_R (N)	M (Nm)	L_A (N)	L_R (N)	M (Nm)
RSJ/BHJ-13	R12-93 R12-127	3	90	52	$18x\varnothing c^*$	60	34	$13x\varnothing c^*$
		4	113	60	$22.5x\varnothing c^*$	75	40	$16x\varnothing c^*$
		Each Additional 1	23	15	$4.5x\varnothing c^*$	5	3	$1.2x\varnothing c^*$
RSJ/BHJ-25	R25-159 R25-255 R25-351	3	600	350	$150x\varnothing c^*$	230	125	$55x\varnothing c^*$
		4	750	400	$187x\varnothing c^*$	285	150	$69x\varnothing c^*$
		Each Additional 1	150	100	$37x\varnothing c^*$	18	12	$5x\varnothing c^*$
RSJ/BHJ-34	R44-468 R44-612	3	1200	700	$300x\varnothing c^*$	460	255	$110x\varnothing c^*$
		4	1500	800	$375x\varnothing c^*$	575	300	$138x\varnothing c^*$
		Each Additional 1	300	200	$75x\varnothing c^*$	38	24	$27x\varnothing c^*$
RSJ/BHJ-54	R76-799 R76-1033	3	2850	1650	$750x\varnothing c^*$	1050	600	$260x\varnothing c^*$
		4	3600	1900	$875x\varnothing c^*$	1300	700	$325x\varnothing c^*$
		Each Additional 1	700	470	$175x\varnothing c^*$	75	50	$18x\varnothing c^*$

*See Note 4

*See Note 4

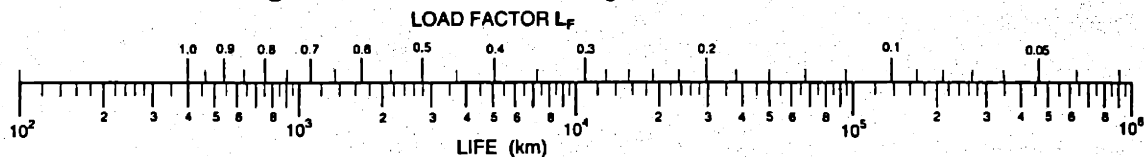
25

To calculate the life of this type of system, first obtain a value for the load factor L_f by entering the values for L_A , L_R , and M in respect of the proposed duty, into equation 2 below, together with the maximum load capacities from the table above.

$$[2] \quad L_f = \frac{M}{M_{(max)}} + \frac{L_A}{L_{A(max)}} + \frac{L_R}{L_{R(max)}} \quad \text{See note 2 on page 24}$$

The life for the system can be read from the nomogram below (for lubricated systems) or on page 26 (for systems running dry) by taking the life figure on the lower scale opposite the appropriate value for L_f on the upper scale (see example, page 26).

Load/Life Nomogram for Lubricated Systems



Notes:

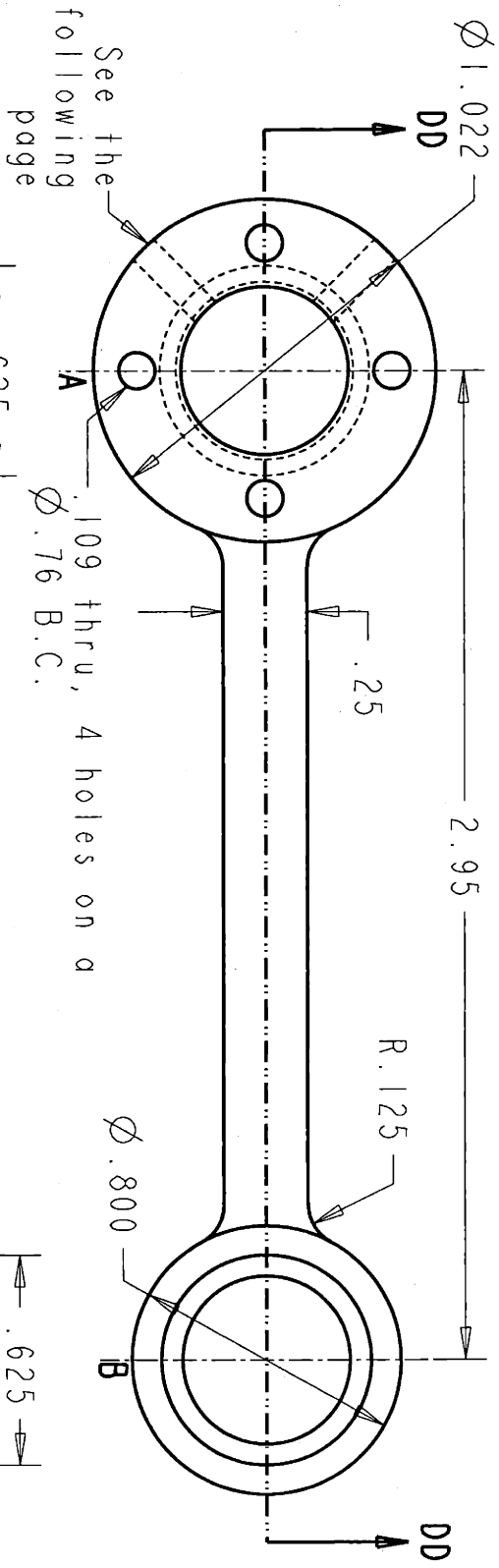
- In certain applications in which the bearing assemblies rotate with the load, and this has large L_R or M components, it may be beneficial to space the bearing assemblies unequally around the ring. Consult Hepco for details.
- SPEED OF OPERATION.** Hepco ring, segment and track systems are rated for speeds of 1m/s without lubrication or 1.5m/s when lubricated. Greater speeds may be tolerated at reduced loads. Consult Hepco for details.
- SHORT STROKE OPERATION.** The life of Hepco ring, segment and track systems will be reduced when the length of the path traversed in each cycle is very short. For path lengths below 0.2m, the life will reduce pro-rata with the path length, e.g., a system with a 0.08m stroke will have its life reduced by a factor of $0.08m \div 0.2 = 0.4$ compared to that calculated from the appropriate nomogram.
- $\varnothing c$ is the contact diameter, i.e. the diameter of the circle which passes through the points of contact between bearing assemblies and the ring. This will be equal to the P.C.D. of the ring $\pm 9, 20, 37$ & 64 mm for the 12, 25, 44 & 76 sections respectively (depending on whether the bearing assemblies are running on the outside or inside of the ring).

Appendix C

Detailed Drawings

2

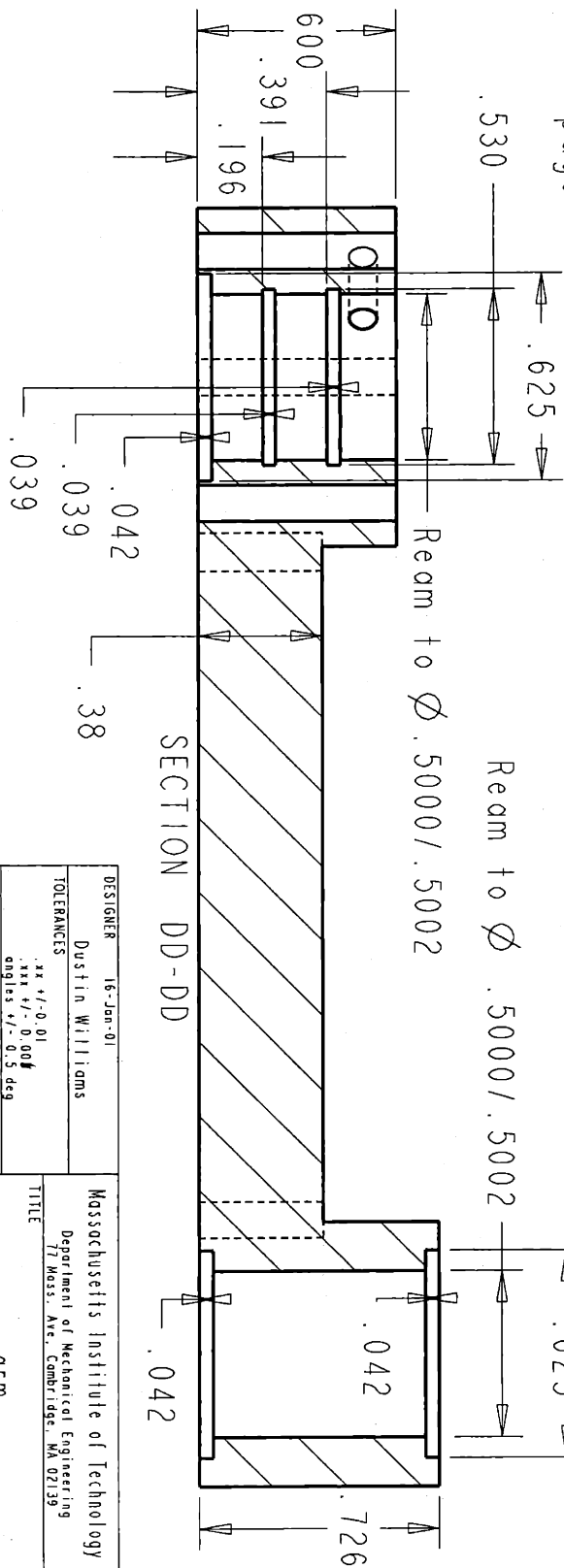
For Educational Use Only



A

B

For Educational Use Only



SECTION DD-DD

DESIGNER	16-Jan-01 Dustin Williams	Massachusetts Institute of Technology Department of Mechanical Engineering 77 Mass. Ave. Cambridge, MA 02139
TOLERANCES	.xx +/- 0.01 .xxx +/- 0.0004 angles +/- 0.5 deg	
MATERIAL	aluminum	Q1M
INTERPRET PER ANST		Prof/ Drawing file
114.5		ARM
ALL DIMENSIONS IN INCHES UNLESS SPECIFIED OTHERWISE		
SIZE A	SCALE 1:980	SHEET 1 OF 2

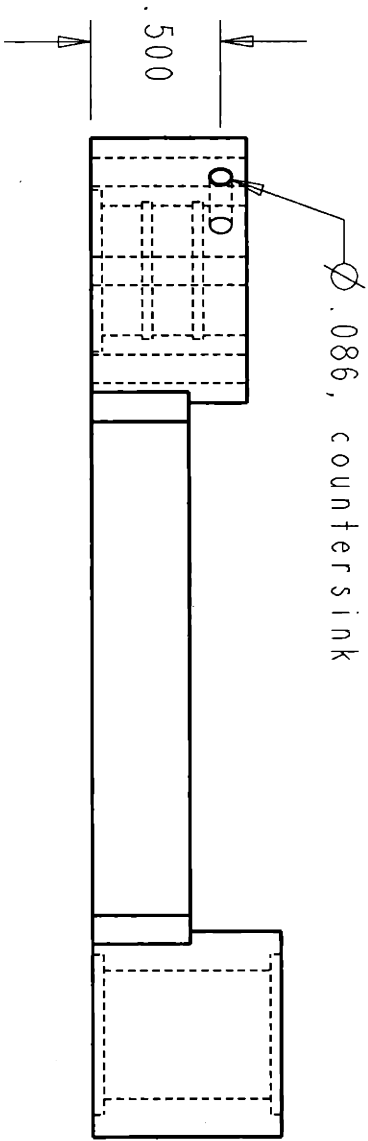
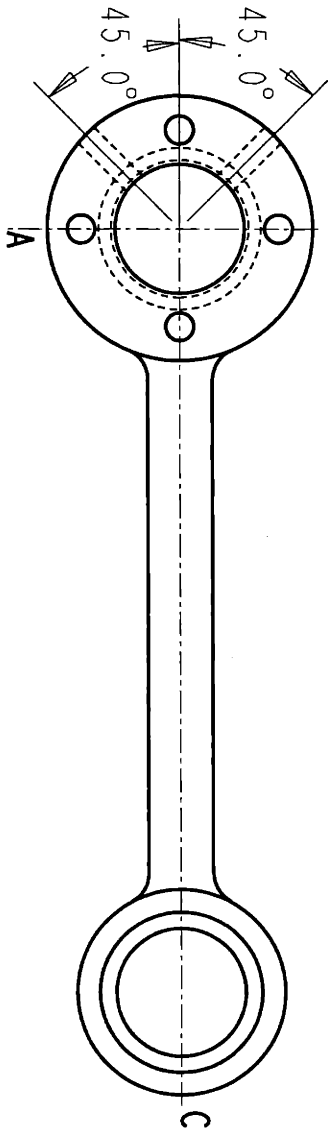
2

For Educational Use Only

1

For Educational Use Only

For Educational Use Only



Ø .086, countersink

A

B

For Educational Use Only

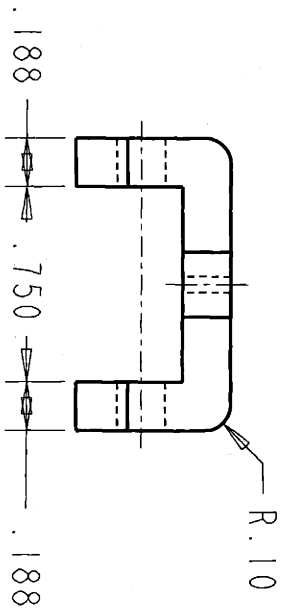
For Educational Use Only

DESIGNER	11-Jan-01	Massachusetts Institute of Technology Department of Mechanical Engineering 77 Mass. Ave., Cambridge, MA 02139
DESIGNER	8DESIGNER	
TOLERANCES	.xx +/- 0.01 .xxx +/- 0.001 angles +/- 0.5 deg	TITLE
MATERIAL	AMATERIAL	Prof/E Drawing Title
INTERPRET PER AMSI V14.5		ARM
ALL DIMENSIONS IN INCHES UNLESS SPECIFIED OTHERWISE		SIZE A
		SCALE 1:500
		SHEET 2 OF 2

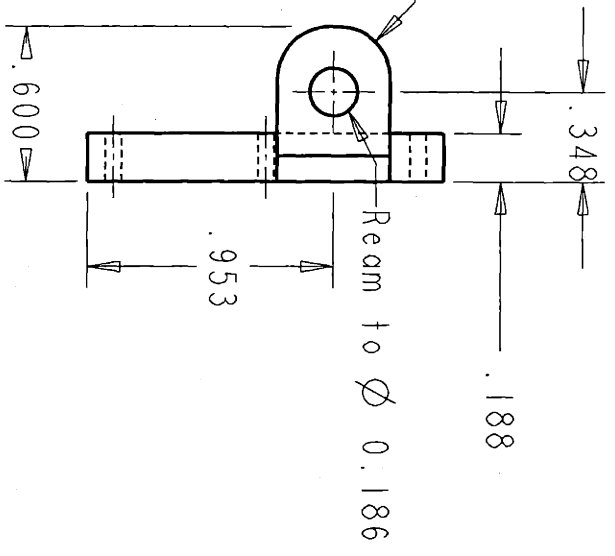
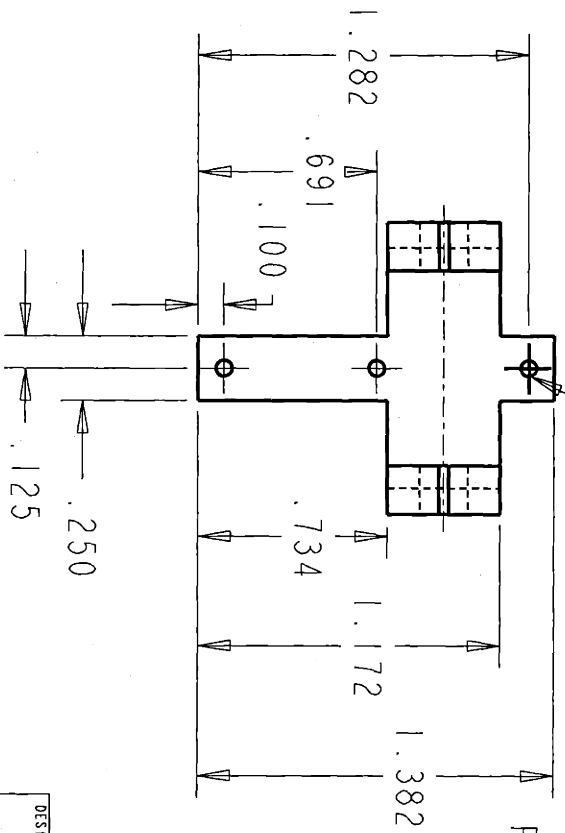
For Educational Use Only

B

B

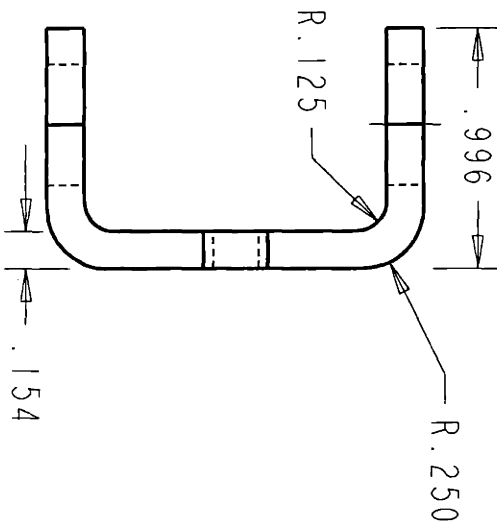
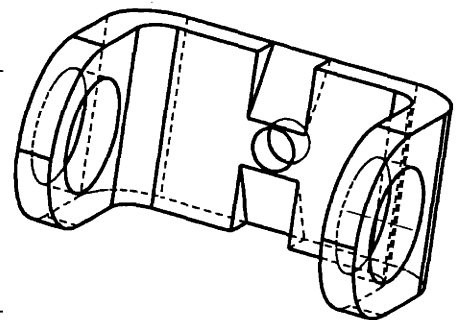
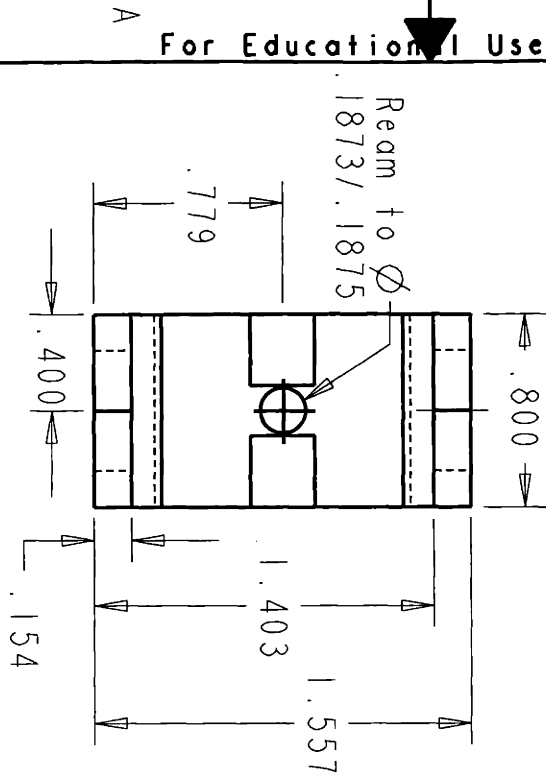
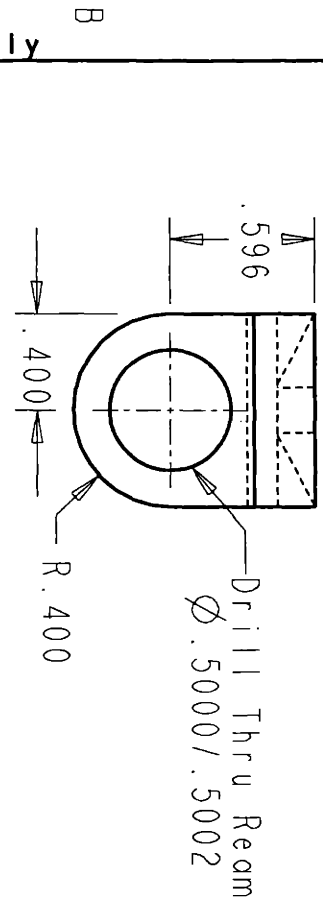


A

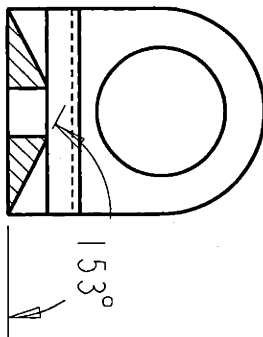
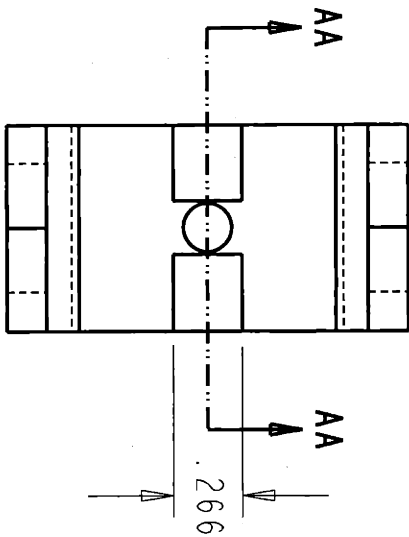


B

DESIGNER Dustin Williams 16-Jan-01	TITLE slider_connection
TOLERANCES xx +/- 0.01 xxx +/- 0.008 angles +/- 0.5 deg	
MATERIAL aluminum	PROJECT DRAWING FILE SLIDER_CONNECTION
INTERPRET PER ANSI Y14.5	
ALL DIMENSIONS IN INCHES UNLESS SPECIFIED OTHERWISE	
MASSACHUSETTS INSTITUTE OF TECHNOLOGY Department of Mechanical Engineering 77 Mass. Ave., Cambridge, MA 02139	SCALE 1:500
SIZE A	SHEET 1 OF 1



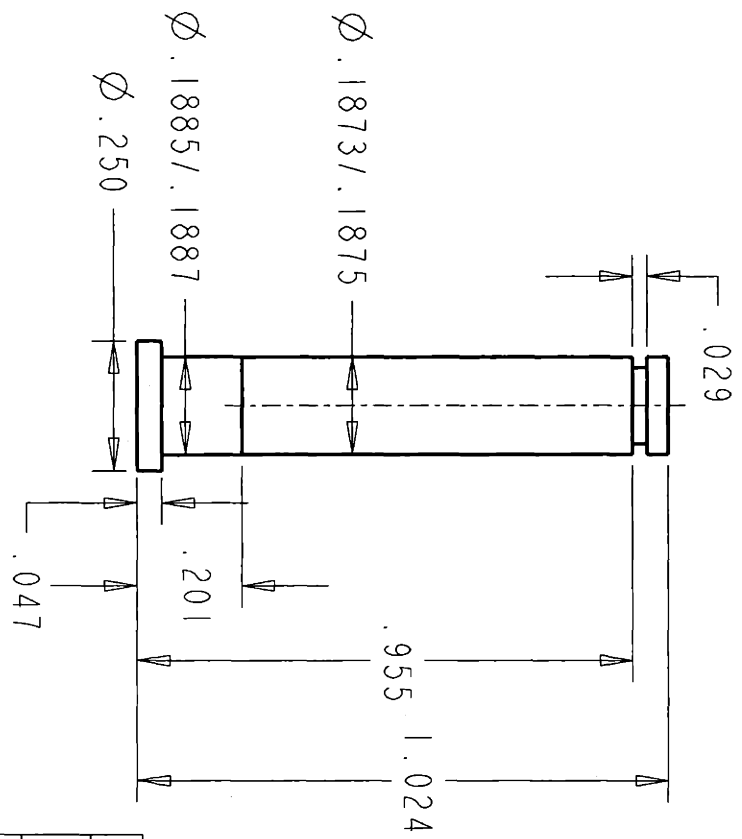
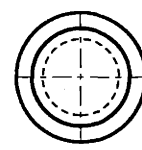
DESIGNER Dustin Williams 16-Jan-01	Massachusetts Institute of Technology Department of Mechanical Engineering 77 Mass. Ave., Cambridge, MA 02139
TOLERANCES .xx +/- 0.01 .xxx +/- 0.008 angles +/- 0.5 deg	TITLE Q1M_2
MATERIAL aluminum	Prof/ Drawing File ARM_2
INTERPRET PER ANSI Y14.5	SIZE A
ALL DIMENSIONS IN INCHES UNLESS SPECIFIED OTHERWISE	SCALE 1.400
	SHEET 1 OF 2



SECTION AA-AA

For Educational Use Only

DESIGNER	16-Jan-01	Massachusetts Institute of Technology Department of Mechanical Engineering 77 Mass. Ave. Cambridge, MA 02139
DESIGNER		
TOLERANCES	.25 ±.0001 .25 ±.0008 angles ±.003 deg	TITLE
MATERIAL	304 STAINLESS STEEL	ARM_2
INTERPRET PER ANSI 114.5		Prof. Drawing file ARM_2
ALL DIMENSIONS IN INCHES UNLESS SPECIFIED OTHERWISE		SIZE A SCALE 1:500 SHEET 2 OF 2

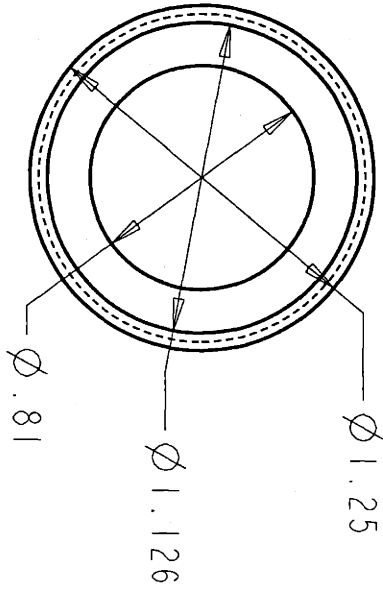
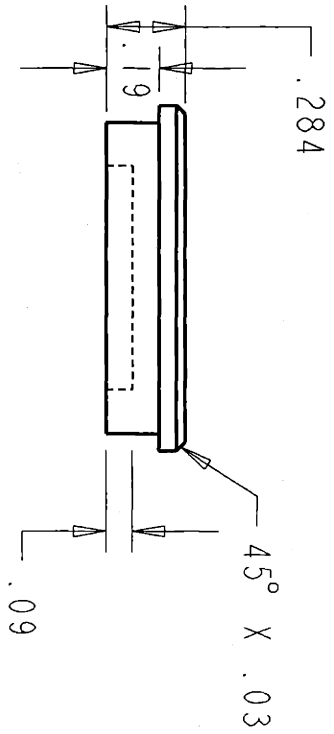


For Educational Use Only

DESIGNER Dustin Williams 16-Jan-01	Massachusetts Institute of Technology Department of Mechanical Engineering 77 Mass. Ave., Cambridge, MA 02139
TOLERANCES xxx +/- 0.008 angles +/- 0.5 deg	TITLE arm2 shaft
MATERIAL 303 stainless steel	Prof Drawing File
INTERPRET PER ANSI Y14.5	ARM2_SHAFT
ALL DIMENSIONS IN INCHES UNLESS SPECIFIED OTHERWISE	SIZE A
	SCALE 3:000
	SHEET 1 OF 1

For Educational Use Only

For Educational Use Only



2

For Educational Use Only

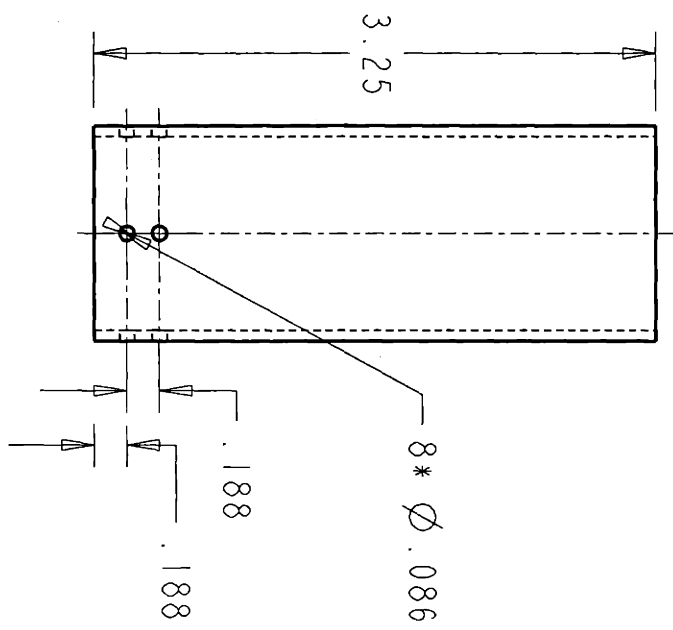
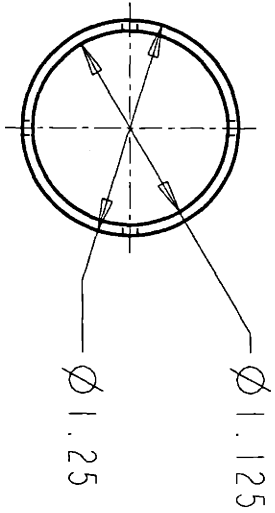
2

For Educational Use Only

DESIGNER Dustin Williams 07-Jan-01	TITLE handle-plug-top Project Drawing File	MASSACHUSETTS INSTITUTE OF TECHNOLOGY Department of Mechanical Engineering 77 Mass. Ave., Cambridge, MA 02139
TOLERANCES xx +/- 0.01 xxx +/- 0.004 angles +/- 0.5 deg		
MATERIAL aluminum	PROF/DRAWING FILE	SIZE A
INTERPRET PER ANSI Y14.5	HANDLE_PLUG_TOP	SCALE 1:600
ALL DIMENSIONS IN INCHES UNLESS SPECIFIED OTHERWISE		SHEET 1 OF 1

For Educational Use Only

For Educational Use Only





2

For Educational Use Only

2

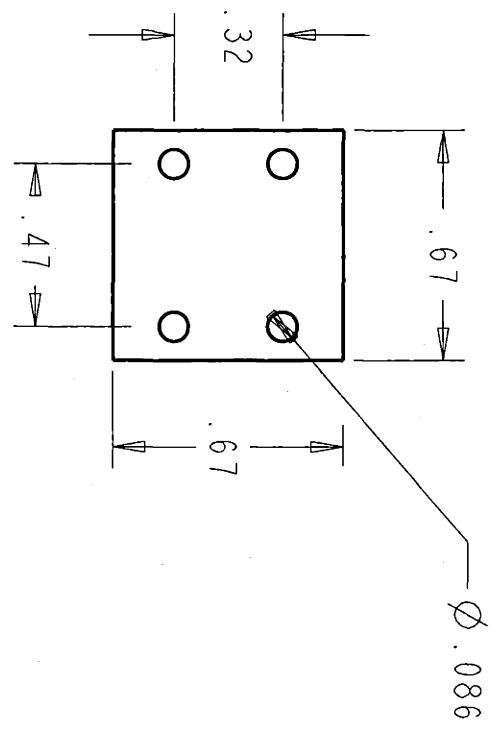
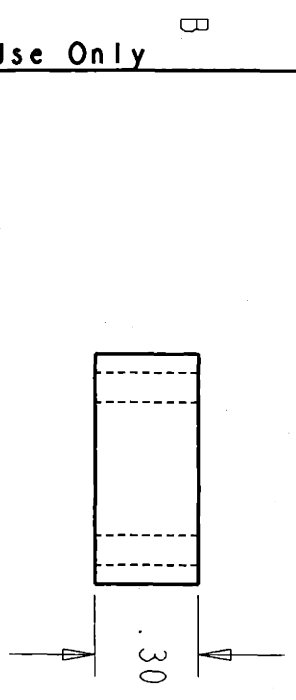
For Educational Use Only

DESIGNER	07-Jan-01 Dustin Williams	Massachusetts Institute of Technology Department of Mechanical Engineering 77 Mass. Ave. Cambridge, MA 02139
TOLERANCES	.xx +/-0.01 .xxx +/-0.000 angles +/- 0.5 deg	
MATERIAL	aluminum	TITLE handle
INTERPRET PER ANSI 114.5	 	
ALL DIMENSIONS IN INCHES UNLESS SPECIFIED OTHERWISE		PROJECT DRAWING FILE HANDLE
SIZE A	SCALE 1:000	SHEET 1 OF 1

For Educational Use Only

2

For Educational Use Only



For Educational Use Only

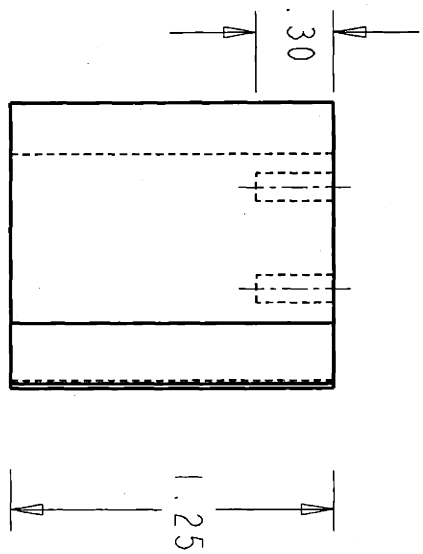
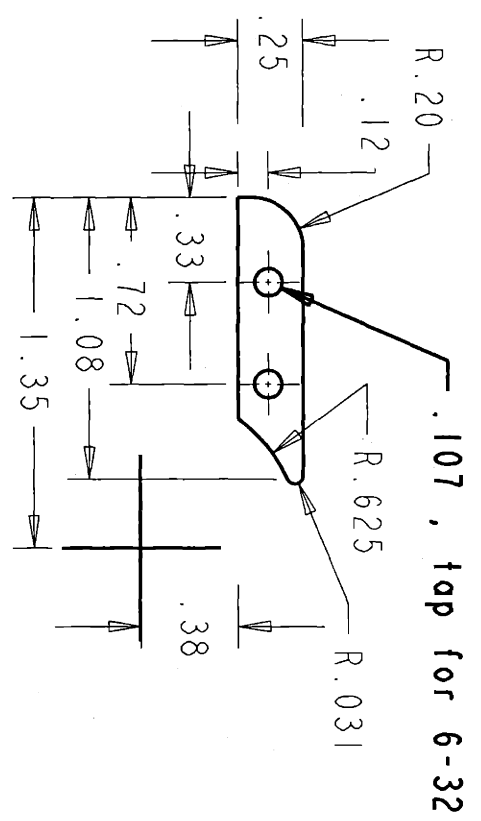
2

For Educational Use Only

DESIGNER 16-Jan-01 Dustin Williams	Massachusetts Institute of Technology Department of Mechanical Engineering 77 Mass. Ave. Cambridge, MA 02139
TOLERANCES .xx +/- 0.01 .xxx +/- 0.004 angles +/- 0.5 deg	TITLE handle_spacer
MATERIAL aluminum	Prof/E Drawing File HANDLE_SPACER
INTERPRET PER ANSI Y14.5	SIZE A
ALL DIMENSIONS IN INCHES UNLESS SPECIFIED OTHERWISE	SCALE 2.000
	SHEET 1 OF 1

For Educational Use Only

For Educational Use Only



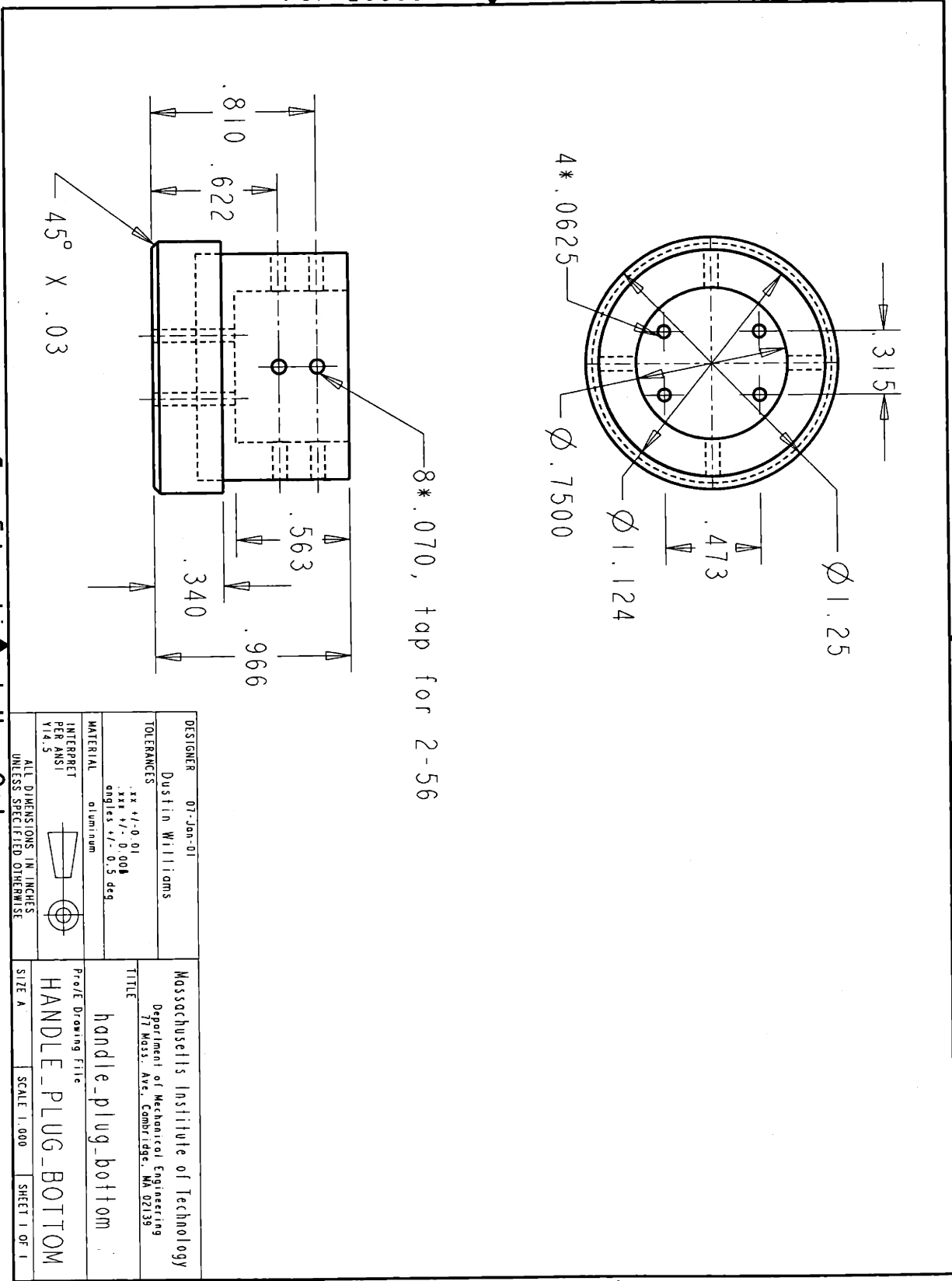
2 For Educational Use Only

2 For Educational Use Only

DESIGNER	01-Jan-01 Justin Williams	Massachusetts Institute of Technology Department of Mechanical Engineering 77 Mass. Ave., Cambridge, MA 02139
TOLERANCES	.xx +/- 0.01 .xxx +/- 0.008 angles +/- 0.5 deg	TITLE handle_anti_rotate
MATERIAL	aluminum	PROF Drawing Title HANDLE_ANTI_ROTATE
INTERPRET PER ANSI Y14.5		SIZE A
ALL DIMENSIONS IN INCHES UNLESS SPECIFIED OTHERWISE		SCALE 1.500
		SHEET 1 OF 1

For Educational Use Only

For Educational Use Only



2

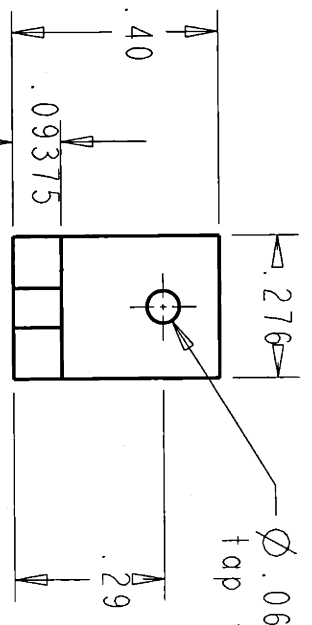
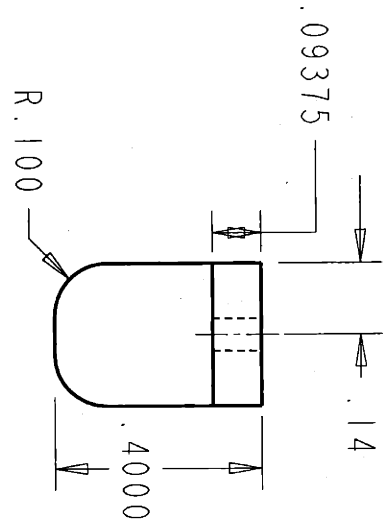
For Educational Use Only

2



For Educational Use Only

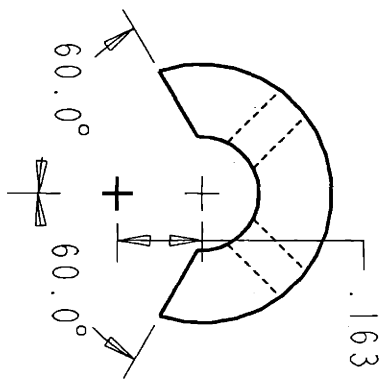
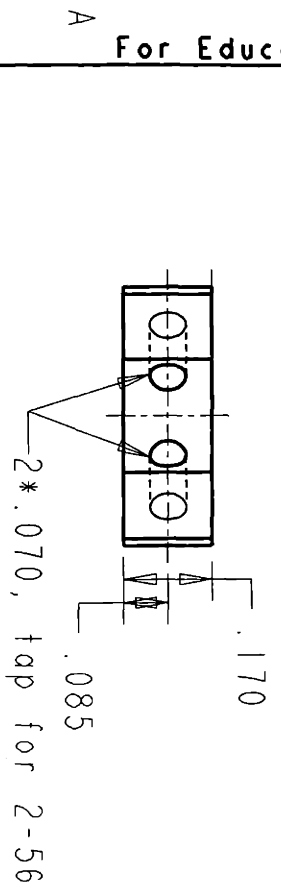
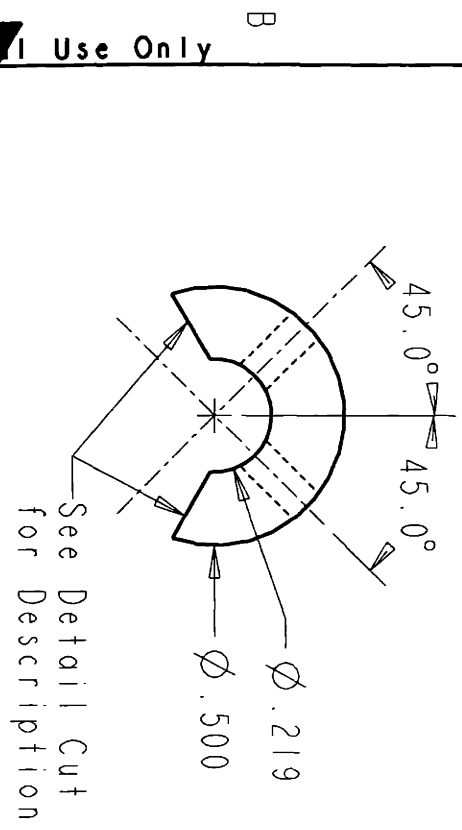
DESIGNER Dustin Williams 07-Jan-01	TITLE handle-plug-bottom Project Drawing File
TOLERANCES xx +/- 0.01 xxx +/- 0.000 angles +/- 0.5 deg	
MATERIAL aluminum	PROJECT INFORMATION PROJECT NAME PROJECT NUMBER PROJECT DATE
INTERPRET PER ANSI Y14.5	
ALL DIMENSIONS IN INCHES UNLESS SPECIFIED OTHERWISE	
SIZE A	SCALE 1:000
SHEET 1 OF 1	

For Educational Use Only



Note: Make two pieces

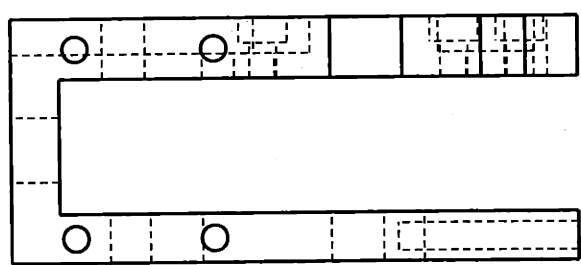
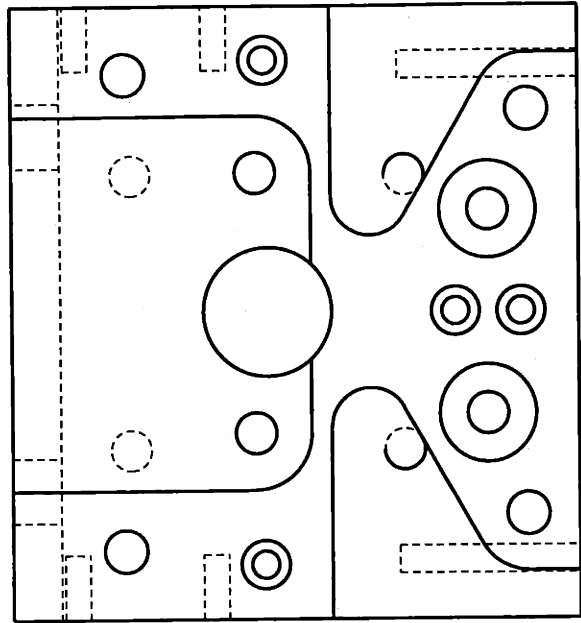
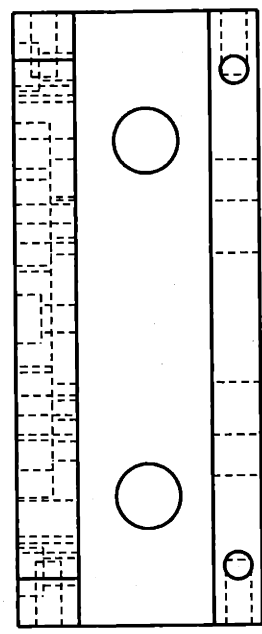
DESIGNER	09-Jan-01 Dustin Williams	Massachusetts Institute of Technology Department of Mechanical Engineering 77 Mass. Ave. Cambridge, MA 02139
TOLERANCES	xx +/-0.01 xxx +/-0.004 angles +/-0.5 deg	TITLE slider_stops
MATERIAL	aluminum	Prof/Drawing File SLIDER_STOPS
INTERPRET PER ANSI	 	SIZE A
ALL DIMENSIONS IN INCHES UNLESS SPECIFIED OTHERWISE		SCALE 3:000
		SHEET 1 OF 1



Detail Cut
 With a 3/8 in. cutter
 starting at .163
 from the center
 move off and to the left
 and to the right at 60°
 as shown.

DESIGNER Dustin Williams	05-Feb-01	Massachusetts Institute of Technology Department of Mechanical Engineering 77 Mass. Ave., Cambridge, MA 02139
TOLERANCES xx +/- 0.01 xxx +/- 0.004 angles +/- 0.5 deg		TITLE flexex_stops
MATERIAL 303 Stainless Steel		Pro/E Drawing File FLEXEX_STOPS
INTERPRET PER ANSI Y14.5		SIZE A
ALL DIMENSIONS IN INCHES UNLESS SPECIFIED OTHERWISE		SCALE 0.111
		SHEET 1 OF 1

For Educational Use Only



2

For Educational Use Only

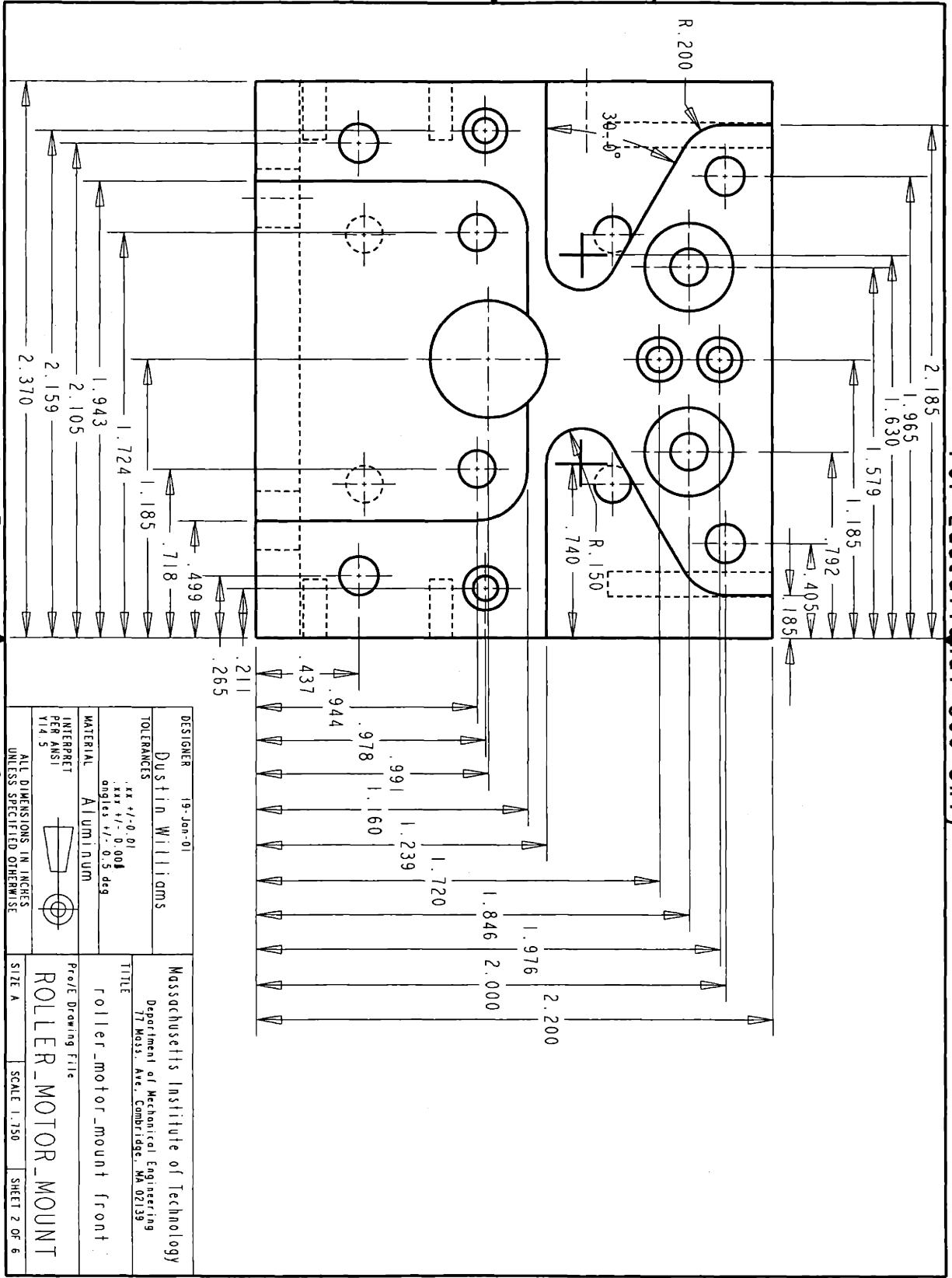
2

For Educational Use Only

DESIGNER	19-Jan-01	Massachusetts Institute of Technology Department of Mechanical Engineering 77 Mass. Ave., Cambridge, MA 02139
Dustin Williams		
TOLERANCES	.xx +/- 0.01 .xxx +/- 0.004 angles +/- 0.5 deg	TITLE
MATERIAL	Aluminum	roller_motor_mount
INTERPRET PER ANSI Y14.5		Prof/Drawing File ROLLER_MOTOR_MOUNT
ALL DIMENSIONS IN INCHES UNLESS SPECIFIED OTHERWISE		SIZE A SCALE 1:500 SHEET 1 OF 6

For Educational Use Only

A **For Educational Use Only** B



2

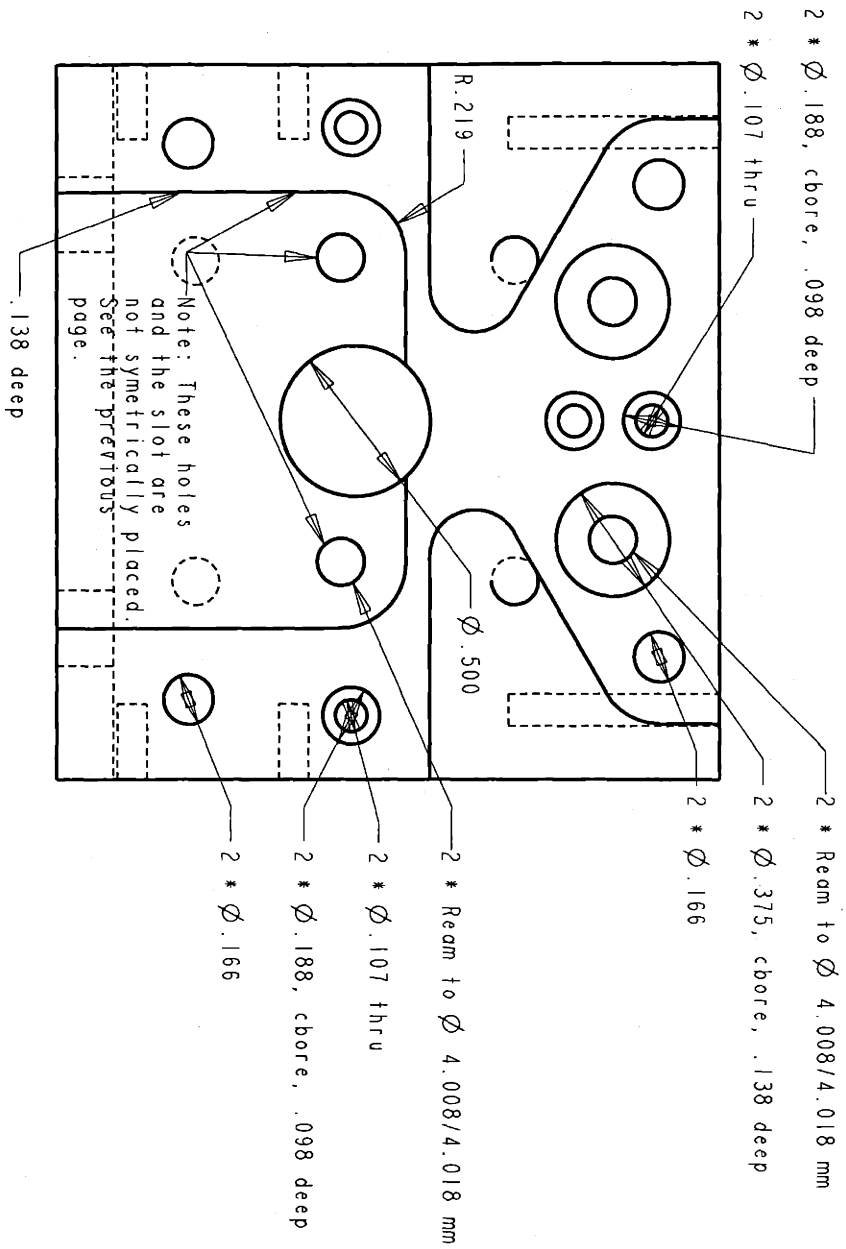
For Educational Use Only

DESIGNER	19-Jan-01
DUSTIN WILLIAMS	
TOLERANCES	xx +/- 0.01 xxx +/- 0.004 angles +/- 0.5 deg
MATERIAL	ALUMINUM
INTERPRET PER ANSI Y14.5	

DESIGNER	19-Jan-01
DUSTIN WILLIAMS	
TOLERANCES	xx +/- 0.01 xxx +/- 0.004 angles +/- 0.5 deg
MATERIAL	ALUMINUM
INTERPRET PER ANSI Y14.5	

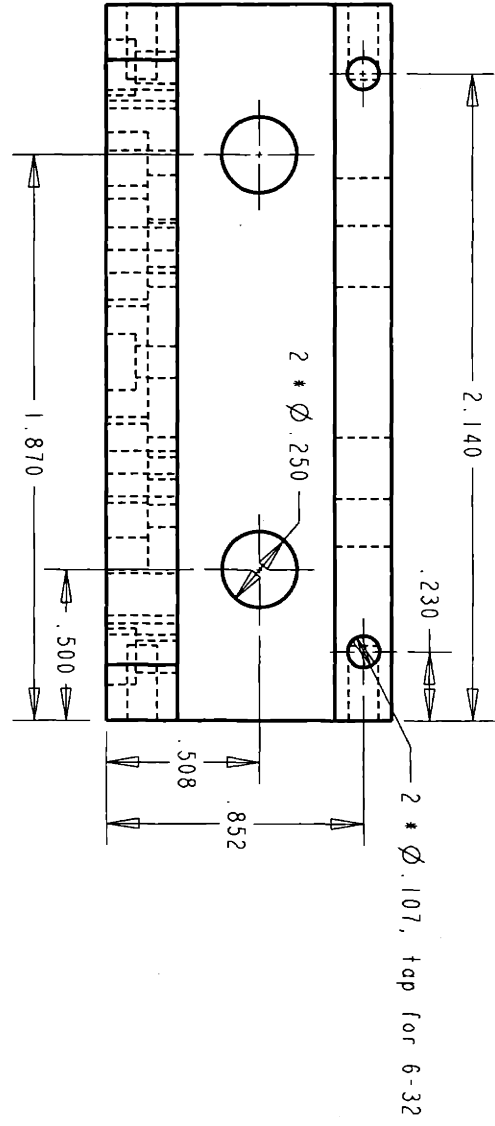
DESIGNER	19-Jan-01
DUSTIN WILLIAMS	
TOLERANCES	xx +/- 0.01 xxx +/- 0.004 angles +/- 0.5 deg
MATERIAL	ALUMINUM
INTERPRET PER ANSI Y14.5	

For Educational Use Only B



DESIGNER Dustin Williams	19-Jan-01	Massachusetts Institute of Technology Department of Mechanical Engineering 77 Mass. Ave., Cambridge, MA 02139
TOLERANCES xx +/- 0.01 xxx +/- 0.008 angles +/- 0.5 deg		TITLE roller_motor_mount front holes
MATERIAL ALUMINUM		PROJECT DRAWING FILE ROLLER_MOTOR_MOUNT
INTERPRET PER ANSI V14.5		SIZE A
ALL DIMENSIONS IN INCHES UNLESS SPECIFIED OTHERWISE		SCALE 1:120
		SHEET 3 OF 6

A ▼ B
For Educational Use Only



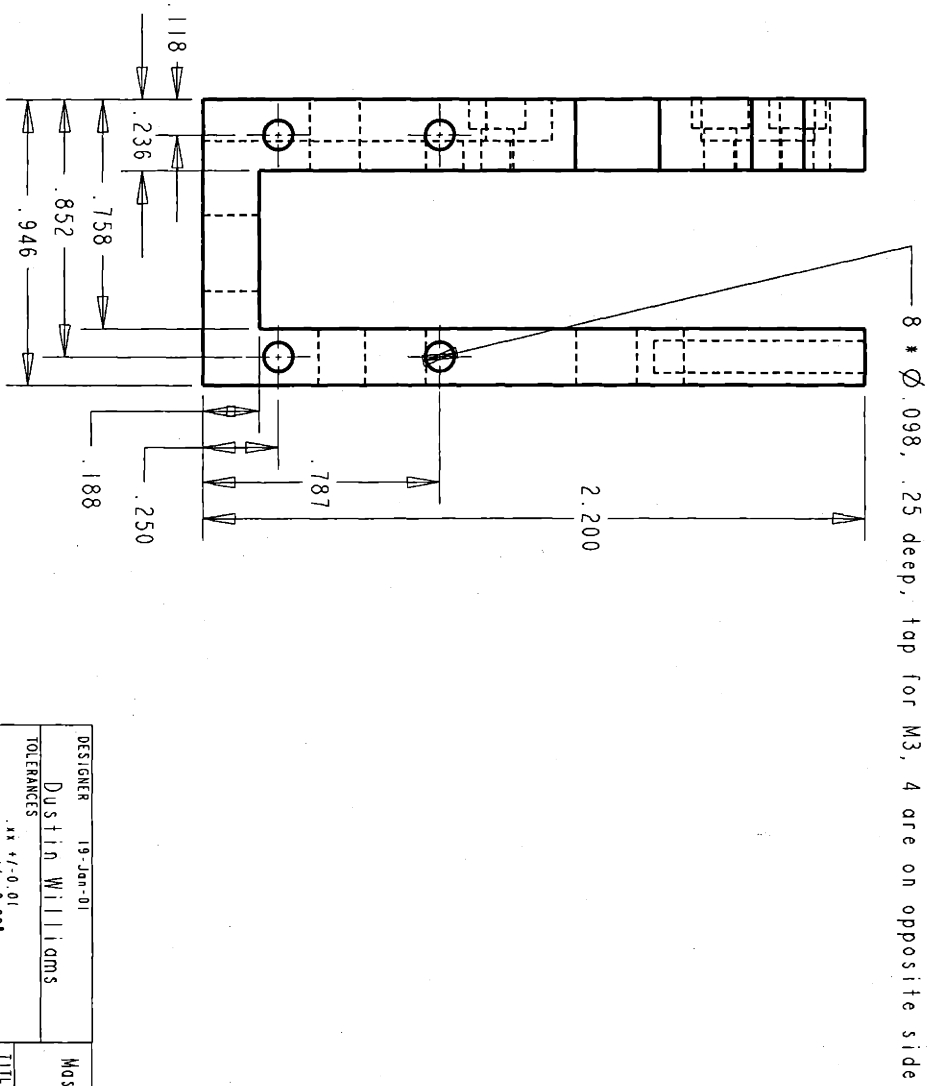
2
For Educational Use Only ▼

DESIGNER Dustin Williams 19-Jan-01	Massachusetts Institute of Technology Department of Mechanical Engineering 77 Mass. Ave. Cambridge, MA 02139
TOLERANCES xx +/- 0.01 xxx +/- 0.004 angles +/- 0.5 deg	TITLE roller_motor_mount_top
MATERIAL ALUMINIUM	Proj: Drawing File
INTERPRET PER ANSI Y14.5	ROLLER_MOTOR_MOUNT
ALL DIMENSIONS IN INCHES UNLESS SPECIFIED OTHERWISE	SIZE A
	SCALE 1:150
	SHEET 4 OF 6

2
For Educational Use Only ▼

B
For Educational Use Only

For Educational Use Only



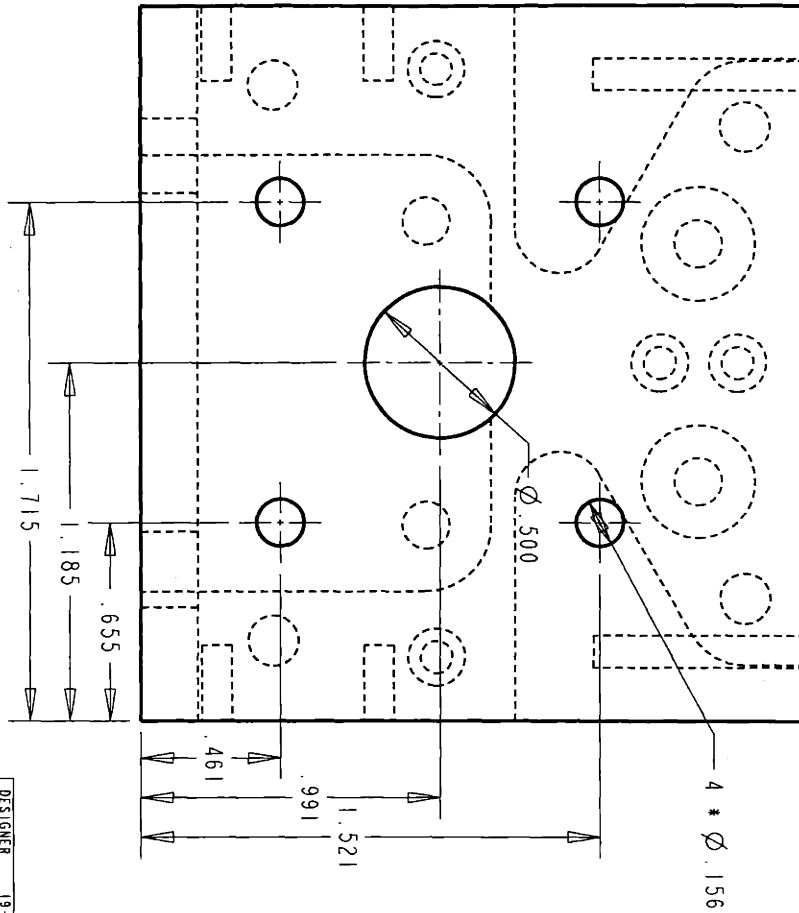
For Educational Use Only

For Educational Use Only

DESIGNER	19-Jan-01	Massachusetts Institute of Technology
	Dustin Williams	Department of Mechanical Engineering
TOLERANCES	xx +/- 0.01 xxx +/- 0.004 angles +/- 0.5 deg	77 Mass. Ave, Cambridge, MA 02139
MATERIAL	ALUMINIUM	roller_motor_mount_right
INTERPRET PER ANSI Y14.5		Pro/E Drawing File
ALL DIMENSIONS IN INCHES UNLESS SPECIFIED OTHERWISE		ROLLER_MOTOR_MOUNT
SIZE A	SCALE 1:150	SHEET 5 OF 6

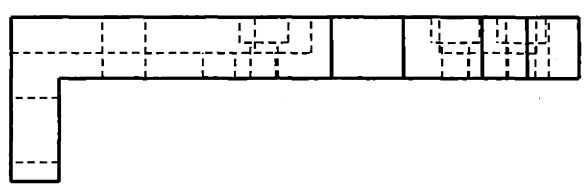
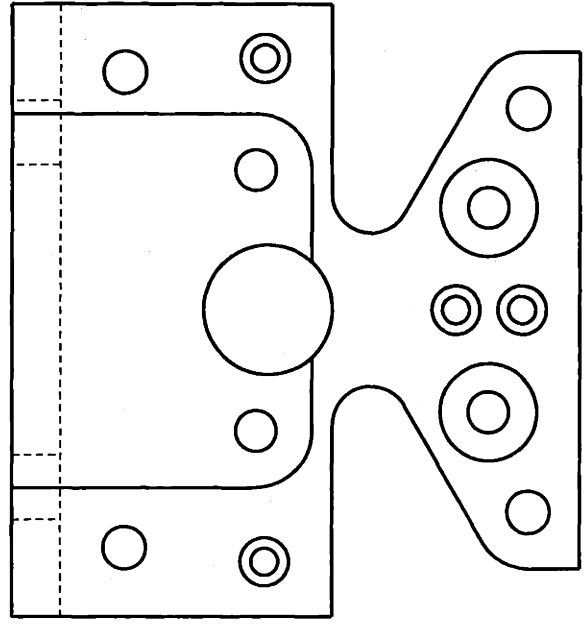
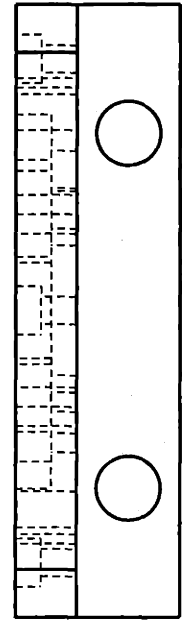
For Educational Use Only

Note: Rear View



DESIGNER	19-Jan-01 Dustin Williams	Massachusetts Institute of Technology Department of Mechanical Engineering 77 Mass. Ave. Cambridge, MA 02139
TOLERANCES	.xx +/- 0.01 .xxx +/- 0.008 angles +/- 0.5 deg	TITLE roller_motor_mount_rear
MATERIAL	Aluminum	Pro/E Drawing File
INTERPRET PER ANSI Y14.5		ROLLER_MOTOR_MOUNT
ALL DIMENSIONS IN INCHES UNLESS SPECIFIED OTHERWISE		SIZE A
		SCALE 1.750
		SHEET 6 OF 6

For Educational Use Only



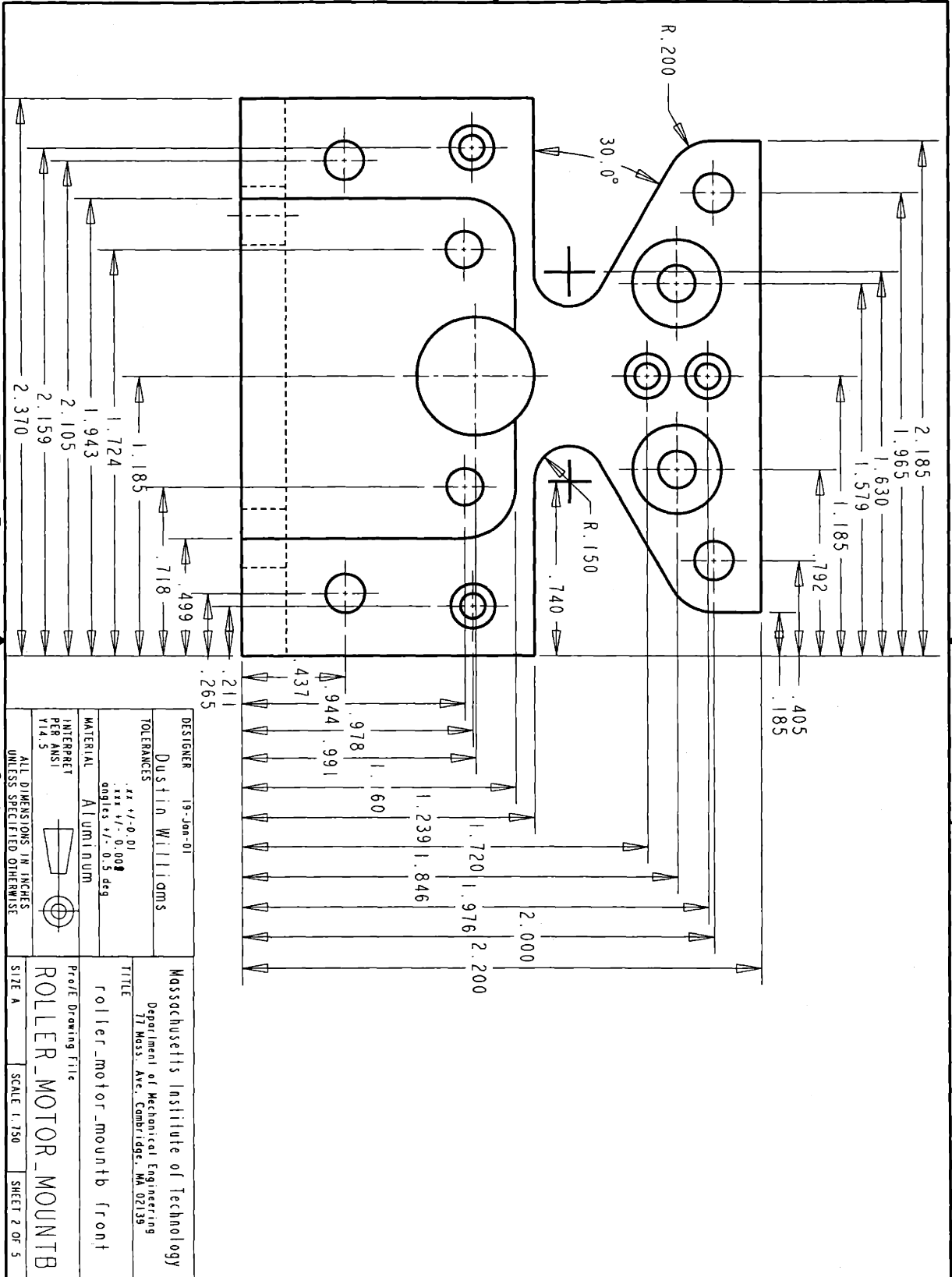
For Educational Use Only

For Educational Use Only

DESIGNER Dustin Williams 19-Jan-01	TITLE roller_motor_mountb
TOLERANCES .xx +/- 0.01 .xxx +/- 0.001 angles +/- 0.5 deg	
MATERIAL ALUMINUM	Pro/E Drawing file ROLLER_MOTOR_MOUNTB
INTERPRET PER ANSI Y14.5	
ALL DIMENSIONS IN INCHES UNLESS SPECIFIED OTHERWISE	
SIZE A	SCALE 1.500
SHEET 1 OF 5	

For Educational Use Only

For Educational Use Only

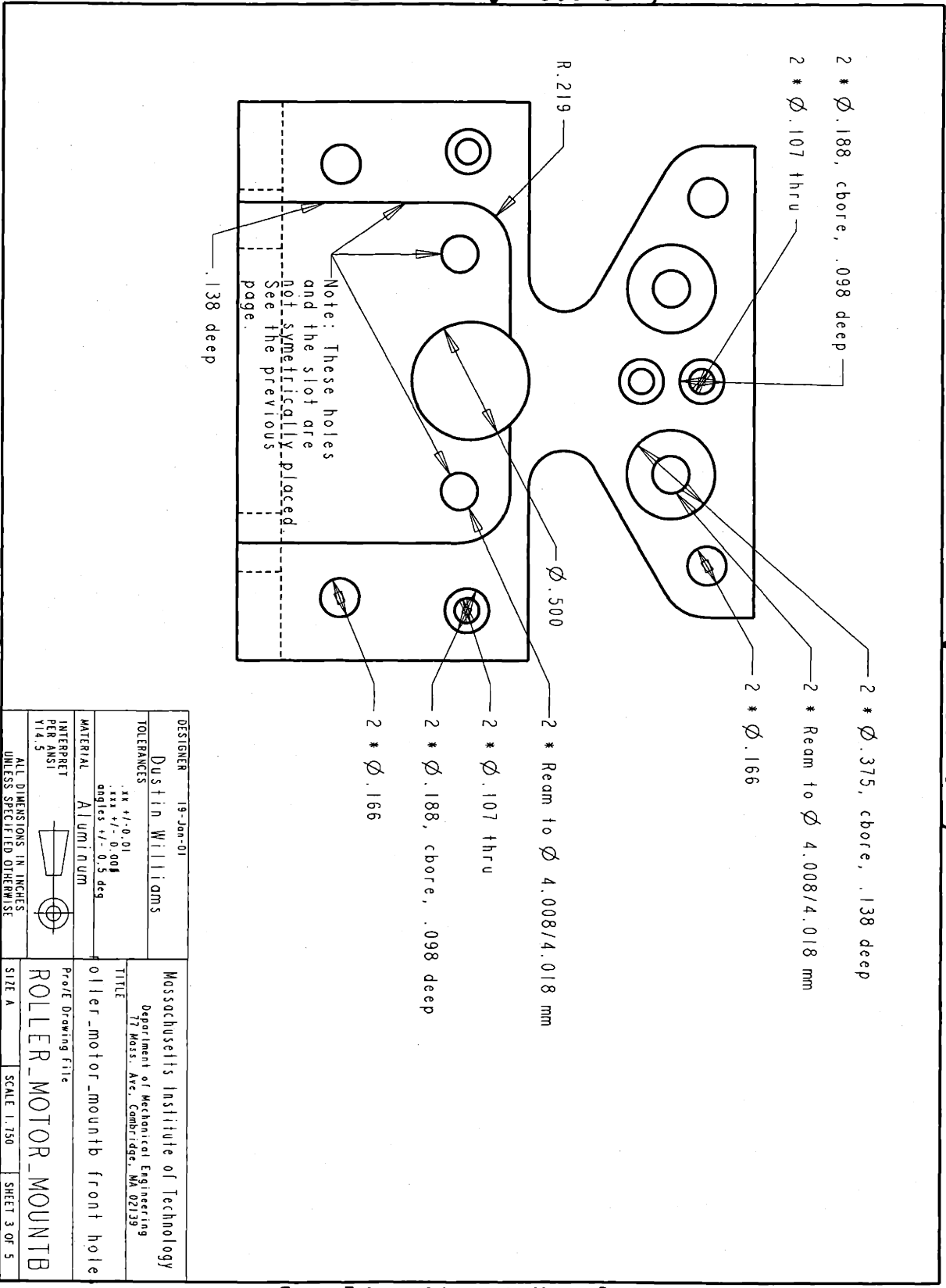


2

For Educational Use Only

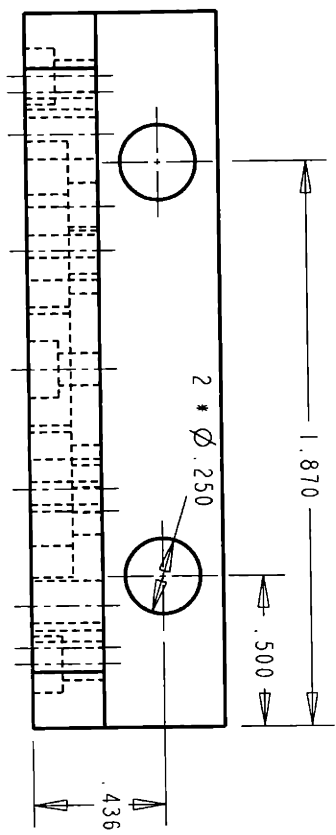
DESIGNER	19-Jan-01	Massachusetts Institute of Technology Department of Mechanical Engineering 77 Mass. Ave. Cambridge, MA 02139
Dustin Williams		
TOLERANCES	xxx +/- 0.01 xxx +/- 0.008 angles +/- 0.5 deg	TITLE roller_motor_mountb front
MATERIAL	ALUMINUM	
INTERPRET PER ANSI Y14.5		PROFILE Drawing file ROLLER_MOTOR_MOUNTB
ALL DIMENSIONS IN INCHES UNLESS SPECIFIED OTHERWISE		
SIZE	A	SCALE 1:150
		SHEET 2 OF 5

For Educational Use Only



DESIGNER	19-Jan-01 Dustin Williams	Massachusetts Institute of Technology Department of Mechanical Engineering 77 Mass. Ave. Cambridge, MA 02139
TOLERANCES	.xx +/- .01 .xxx +/- .0008 angles +/- .5 deg	TITLE roller_motor_mountb front hole
MATERIAL	Aluminum	Pro/E Drawing file
INTERPRET PER ANSI Y14.5		ROLLER_MOTOR_MOUNTB
ALL DIMENSIONS IN INCHES UNLESS SPECIFIED OTHERWISE		SIZE A
		SCALE 1:150
		SHEET 3 OF 5

A ▼ For Educational Use Only B



2

For Educational Use Only

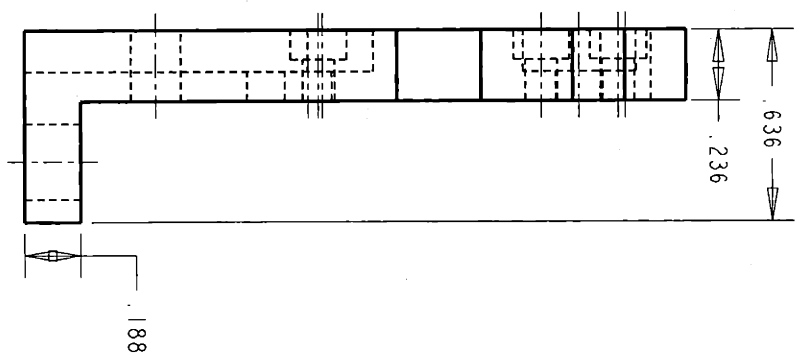
2

For Educational Use Only

DESIGNER	19-Jan-01 Dustin Williams	TITLE	Massachusetts Institute of Technology Department of Mechanical Engineering 77 Mass. Ave., Cambridge, MA 02139
TOLERANCES	xx +/- 0.01 xxx +/- 0.004 angles +/- 0.5 deg	roller_motor_mountb_top	
MATERIAL	ALUMINUM	PROJE Drawing file	
INTERPRET PER ANSI Y14.5		ROLLER_MOTOR_MOUNTB	
ALL DIMENSIONS IN INCHES UNLESS SPECIFIED OTHERWISE		SIZE A	SCALE 1:150 SHEET 4 OF 5

For Educational Use Only B

For Educational Use Only



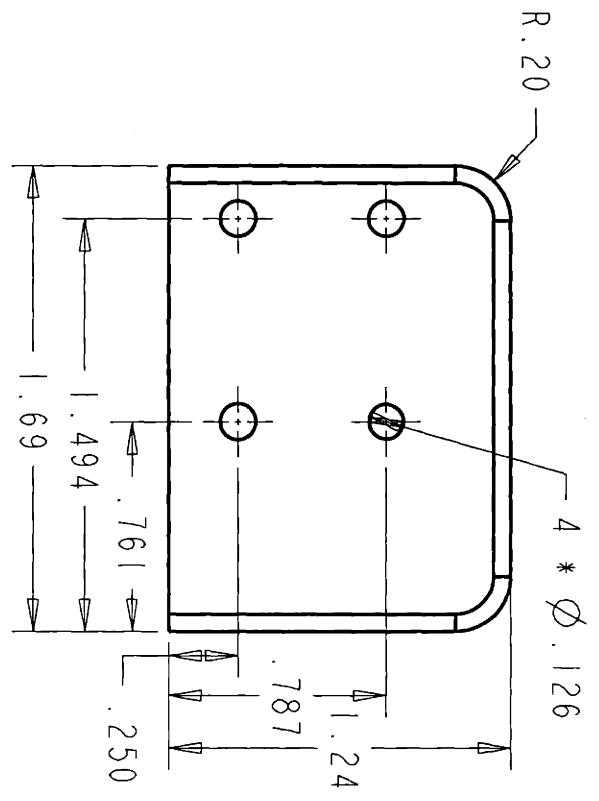
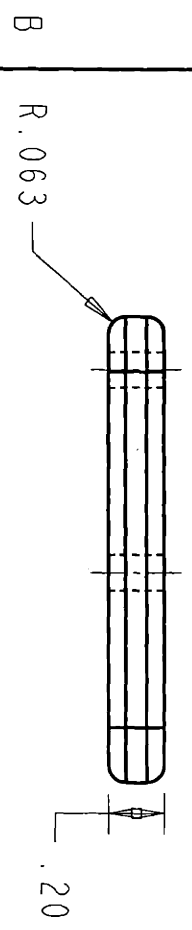
DESIGNER	19-Jan-01	Dustin Williams
TOLERANCES	xx \pm 0.01	
	xxx \pm 0.004	
	angles \pm 0.5 deg	
MATERIAL	ALUMINUM	
INTERPRET PER ANSI Y14.5		
ALL DIMENSIONS IN INCHES UNLESS SPECIFIED OTHERWISE		
DESIGNER	19-Jan-01	Dustin Williams
TITLE	roller_motor_mountb right	
PROJECT	roller_motor_mountb right	
PROJ. DRAWING FILE	ROLLER_MOTOR_MOUNTB	
SIZE	A	
SCALE	1.750	
SHEET	5 OF 5	

For Educational Use Only

For Educational Use Only

For Educational Use Only

2 For Educational Use Only



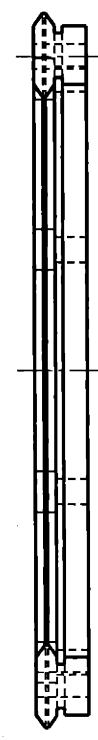
Note: Make 2 pieces

DESIGNER Dustin Williams 20-Jan-01	TITLE roller_motor_mount_cover
TOLERANCES xx +/- 0.01 xxx +/- 0.004 angles +/- 0.5 deg	PROJECT roller_motor_mount_cover
MATERIAL Aluminum	PROJ Drawing File
INTERPRET PER ANSI V14.5	ROLLER_MOTOR_MOUNT_COVER
ALL DIMENSIONS IN INCHES UNLESS SPECIFIED OTHERWISE	
SIZE A	SCALE 1.600 SHEET 1 OF 1

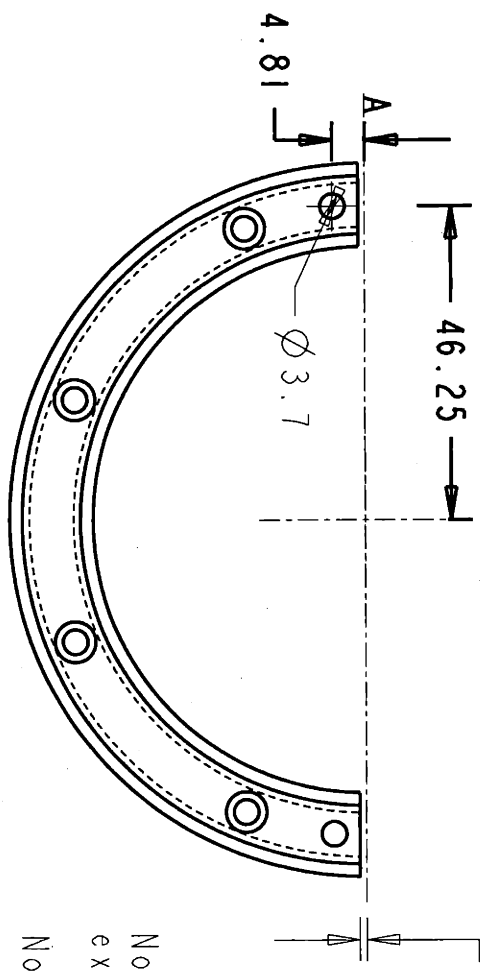
2 For Educational Use Only

For Educational Use Only

B



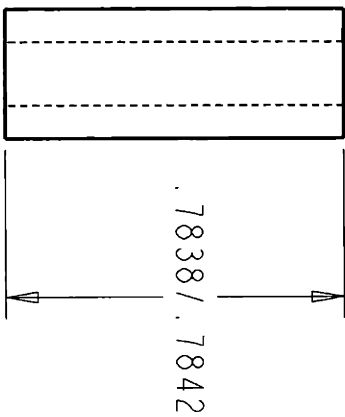
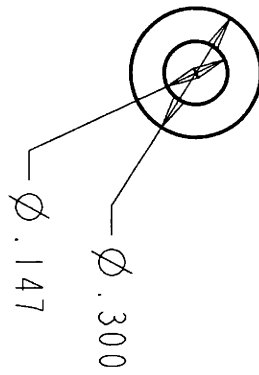
A



1 mm Cutting Allowance

Note: Same as R12-93 R180 P
 except for two added holes
 Note: Make Two Pieces

DESIGNER	03-Jan-01	TITLE	Massachusetts Institute of Technology Department of Mechanical Engineering 77 Mass. Ave. Cambridge, MA 02139
TOLERANCES	.xx +/- 0.01 .xxx +/- 0.001 angles +/- 0.5 deg		
MATERIAL		PROJ. DRAWING FILE	BWC_rail_metric
INTERPRET PER ANSI Y14.5		SCALE	0.1:1
ALL DIMENSIONS IN INCHES UNLESS SPECIFIED OTHERWISE		SIZE	A
		SHEET	1 OF 1

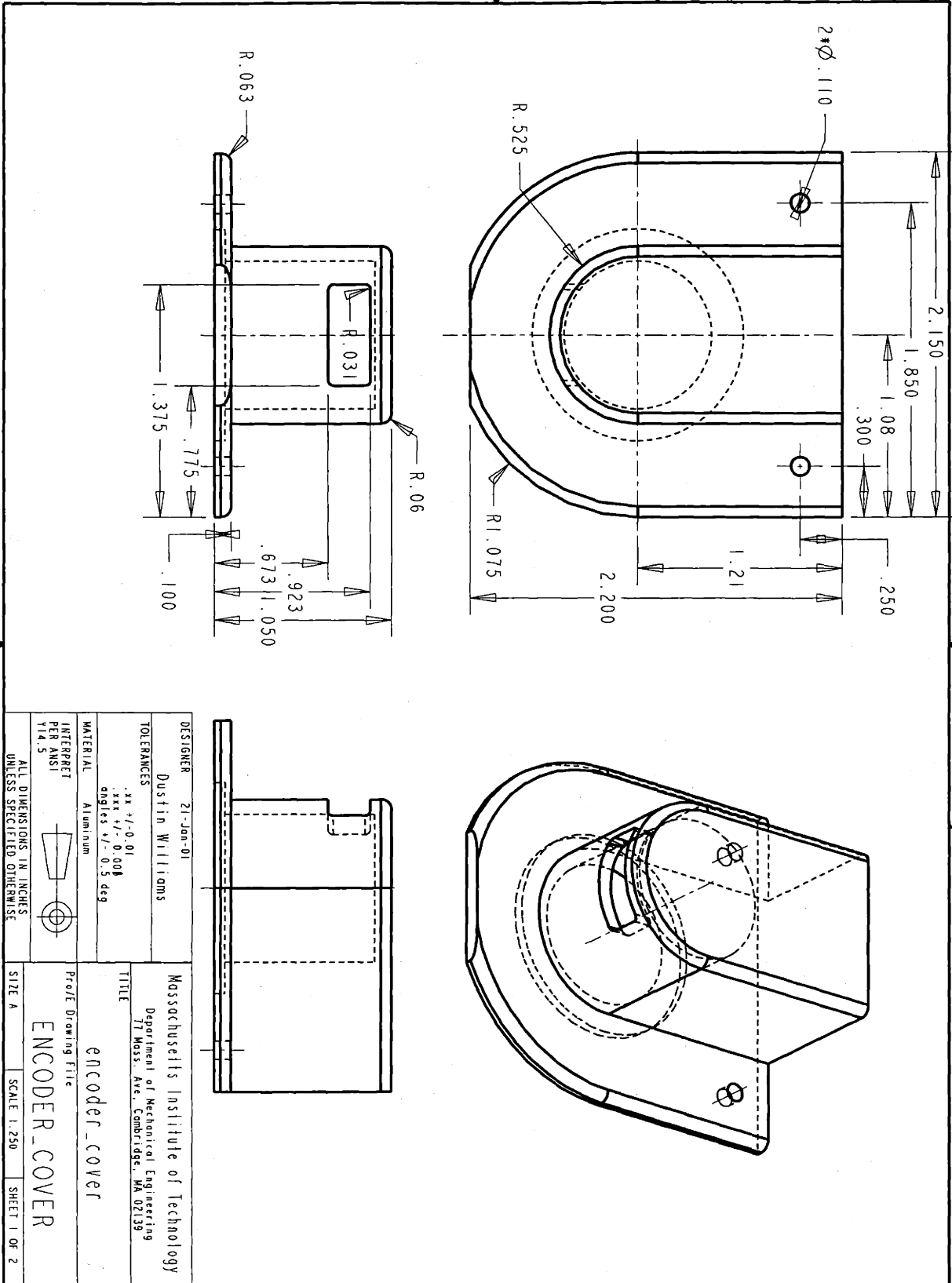


Note: Make 4 pieces

DESIGNER Dustin Williams	19-Jan-01	TITLE bwc_rail_connect	PROJECT Prof/E Drawing File
TOLERANCES xx +/- 0.01 xxx +/- 0.008 angles +/- 0.5 deg			
MATERIAL 303 stainless steel		SIZE A	SCALE 2:500
INTERPRET PER ANSI Y14.5			

ALL DIMENSIONS IN INCHES
UNLESS SPECIFIED OTHERWISE

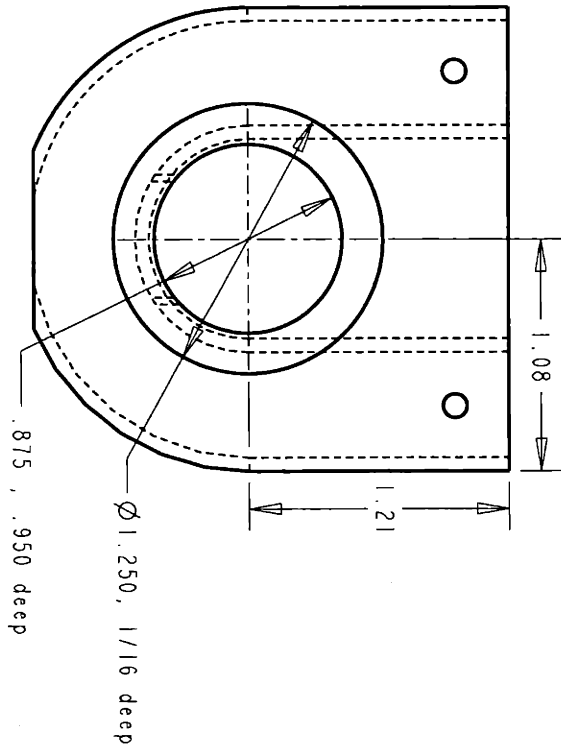
For Educational Use Only



For Educational Use Only

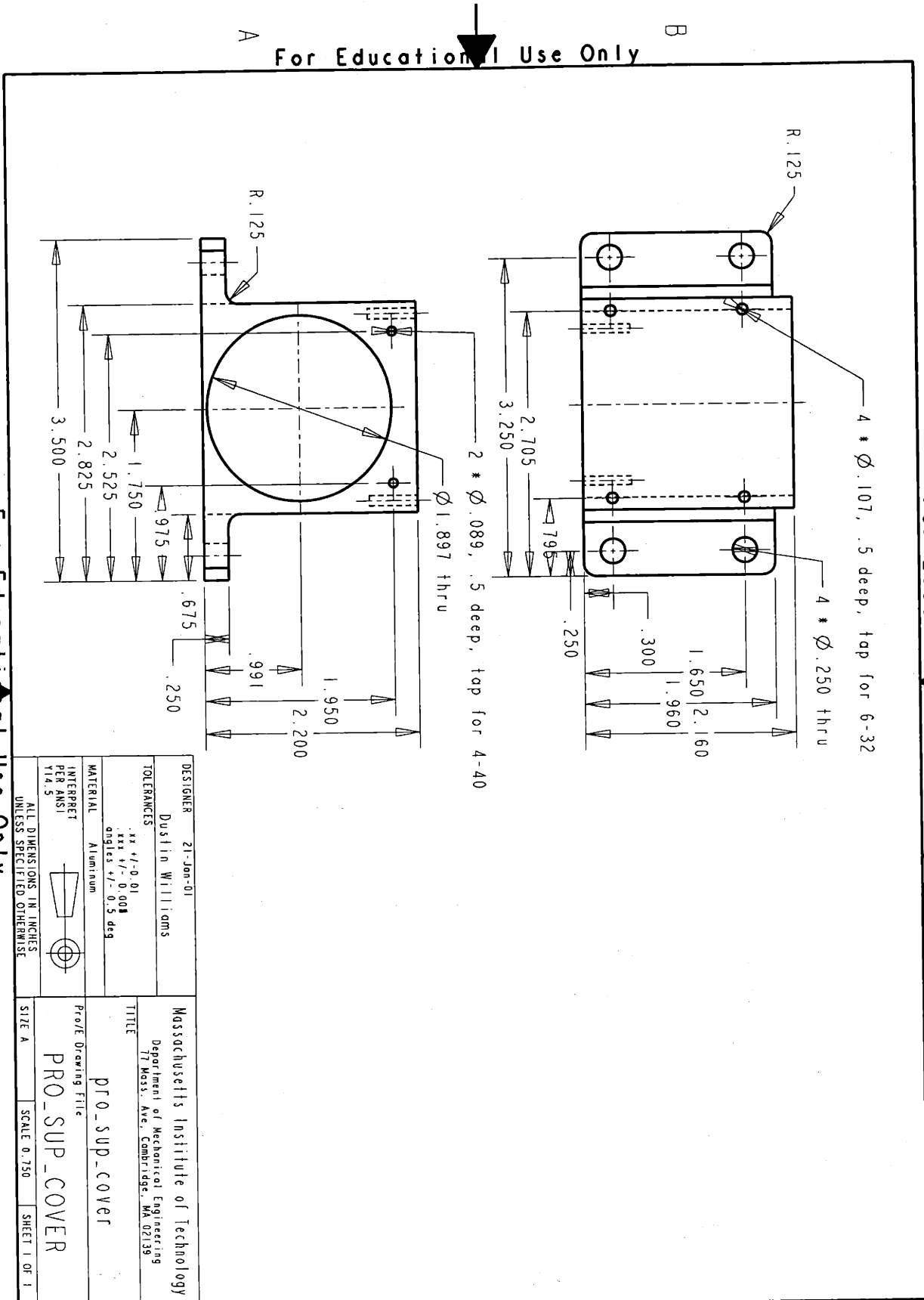
Reverse Detail

For Educational Use Only



DESIGNER	31-Jan-01	Massachusetts Institute of Technology	
TOLERANCES	Dustin Williams	Department of Mechanical Engineering 77 Mass. Ave., Cambridge, MA 02139	
INTERPRET PER ANSI Y14.5	xx +/- 0.01 xxx +/- 0.008 angles +/- 0.5 deg	TITLE	encoder _ cover
MATERIAL	ALUMINUM	Pre/E Drawing file	ENCODER_COVER
ALL DIMENSIONS IN INCHES UNLESS SPECIFIED OTHERWISE		SIZE A	SCALE 1.250
			SHEET 2 OF 2

For Educational Use Only



For Educational Use Only

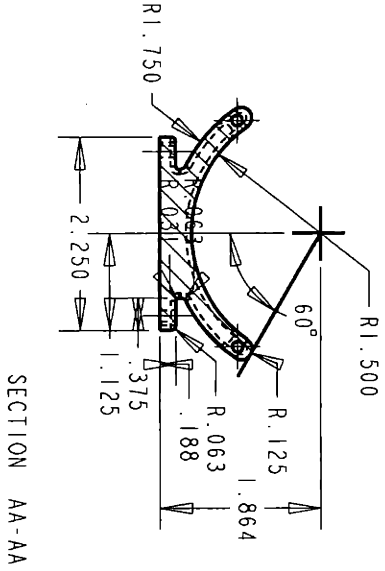
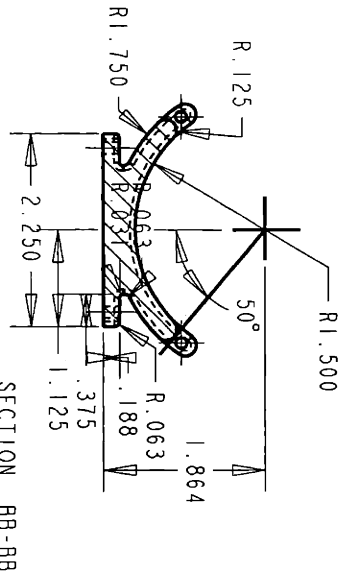
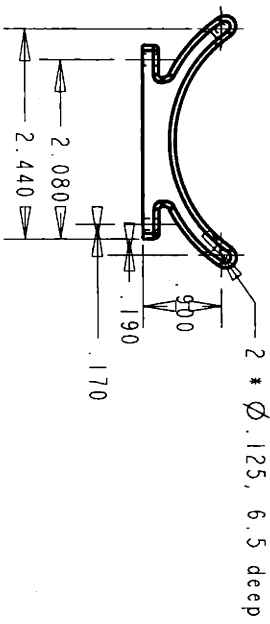
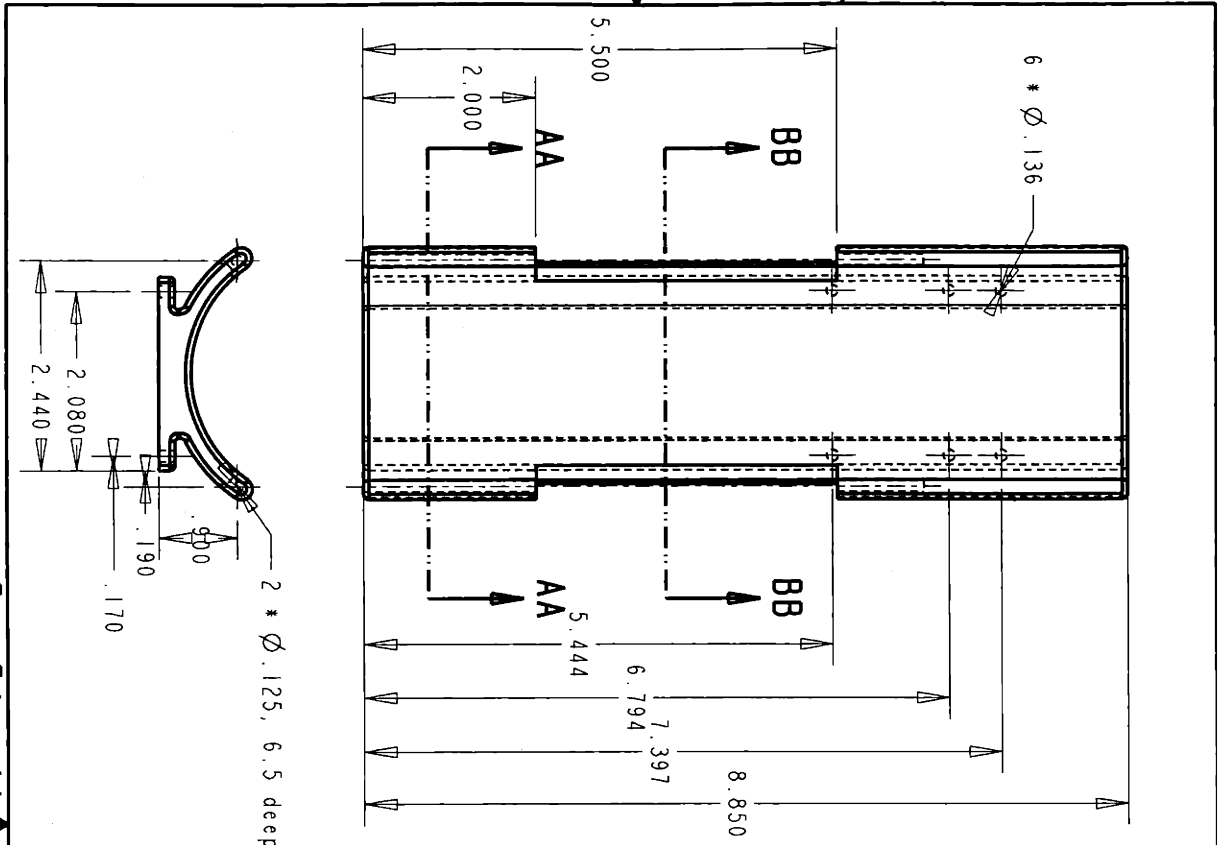
B

DESIGNER	21-Jan-01	Dustin Williams
TOLERANCES	.xx \pm .0.01	.xxx \pm .0.008
	angles \pm .0.5 deg	
MATERIAL	Aluminum	
INTERPRET PER ANSI 114.5		
ALL DIMENSIONS IN INCHES UNLESS SPECIFIED OTHERWISE		
DESIGNER	21-Jan-01	Dustin Williams
TITLE	PRO_SUP_COVER	
MATERIAL	Aluminum	
INTERPRET PER ANSI 114.5		
ALL DIMENSIONS IN INCHES UNLESS SPECIFIED OTHERWISE		
DESIGNER	21-Jan-01	Dustin Williams
TITLE	PRO_SUP_COVER	
MATERIAL	Aluminum	
INTERPRET PER ANSI 114.5		
ALL DIMENSIONS IN INCHES UNLESS SPECIFIED OTHERWISE		
DESIGNER	21-Jan-01	Dustin Williams
TITLE	PRO_SUP_COVER	
MATERIAL	Aluminum	
INTERPRET PER ANSI 114.5		
ALL DIMENSIONS IN INCHES UNLESS SPECIFIED OTHERWISE		
DESIGNER	21-Jan-01	Dustin Williams
TITLE	PRO_SUP_COVER	
MATERIAL	Aluminum	
INTERPRET PER ANSI 114.5		
ALL DIMENSIONS IN INCHES UNLESS SPECIFIED OTHERWISE		
DESIGNER	21-Jan-01	Dustin Williams
TITLE	PRO_SUP_COVER	
MATERIAL	Aluminum	
INTERPRET PER ANSI 114.5		
ALL DIMENSIONS IN INCHES UNLESS SPECIFIED OTHERWISE		

For Educational Use Only

B

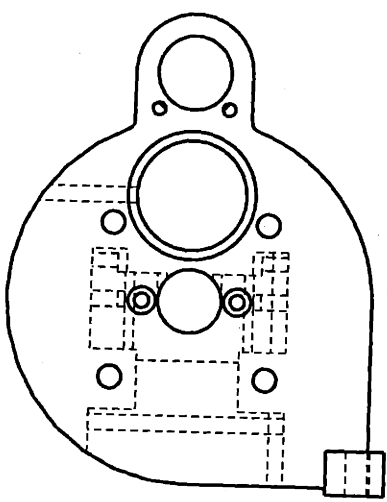
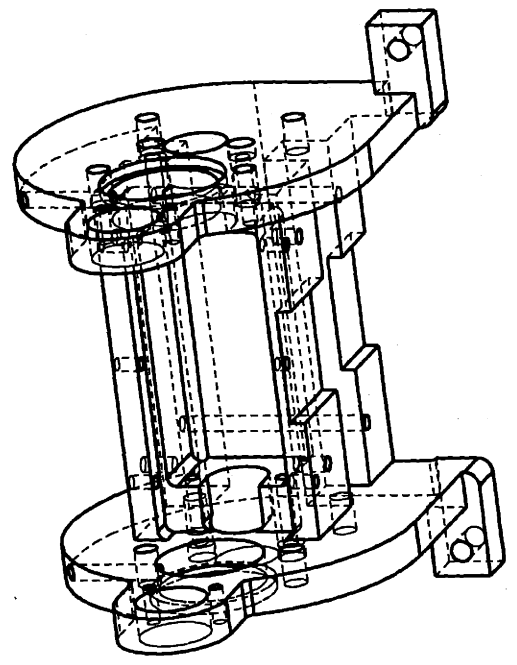
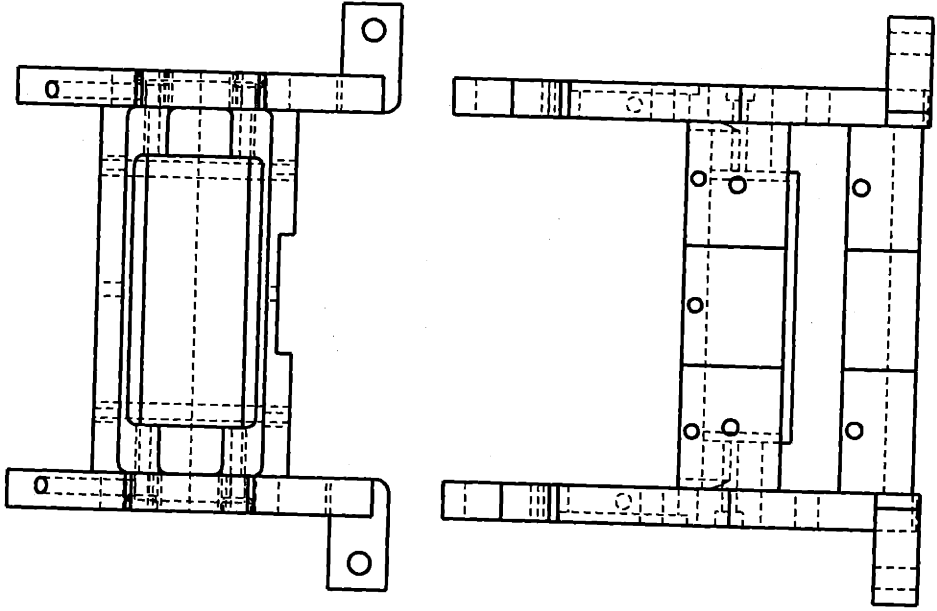
For Educational Use Only



DESIGNER 21-Jan-01 Dustin Williams	Massachusetts Institute of Technology Department of Mechanical Engineering 77 Mass. Ave., Cambridge, MA 02139
TOLERANCES xx +/- 0.01 xxx +/- 0.004 angles +/- 0.5 deg	TITLE Forearm support
MATERIAL	Project Drawing File
INTERPRET PER ANSI Y14.5	FOREARM_SUPPORT
ALL DIMENSIONS IN INCHES UNLESS SPECIFIED OTHERWISE	SCALE 0.111
	SHEET 1 OF 1

For Educational Use Only

For Educational Use Only

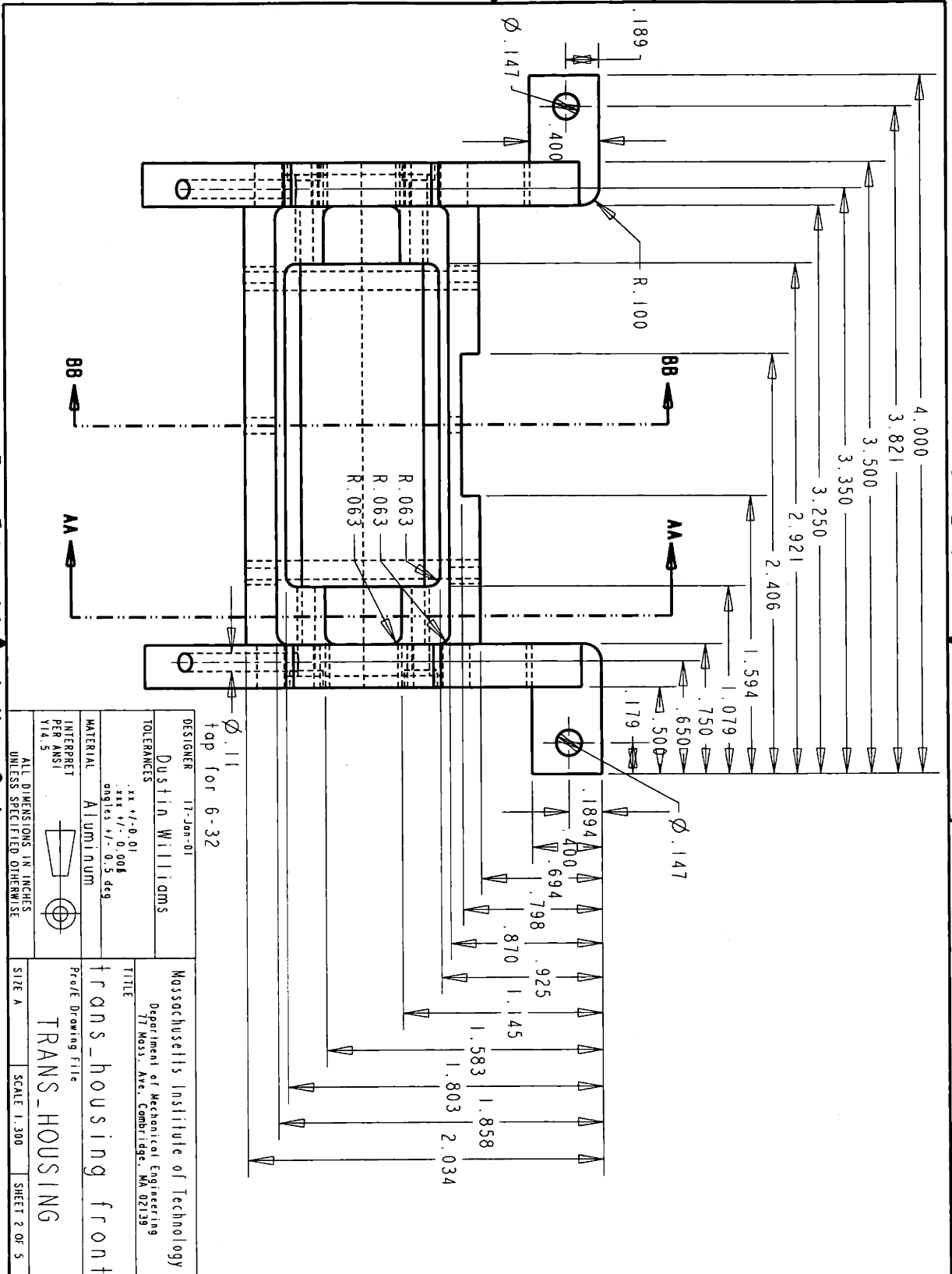


DESIGNER	17-Jan-01	Massachusetts Institute of Technology	SIZE A	SCALE 0.850	SHEET 1 OF 5
DESIGNER	Dustin Williams	Department of Mechanical Engineering	TITLE		
TOLERANCES	xx +/- 0.01 xxx +/- 0.004 angles +/- 0.5 deg	77 Mass. Ave., Cambridge, MA 02139	TRANS_HOUSING		
MATERIAL	ALUMINUM		PROJECT DRAWING TITLE		
INTERPRET PER ANSI Y14.5			PROJECT DRAWING TITLE		
ALL DIMENSIONS IN INCHES UNLESS SPECIFIED OTHERWISE					

For Educational Use Only

For Educational Use Only

For Educational Use Only

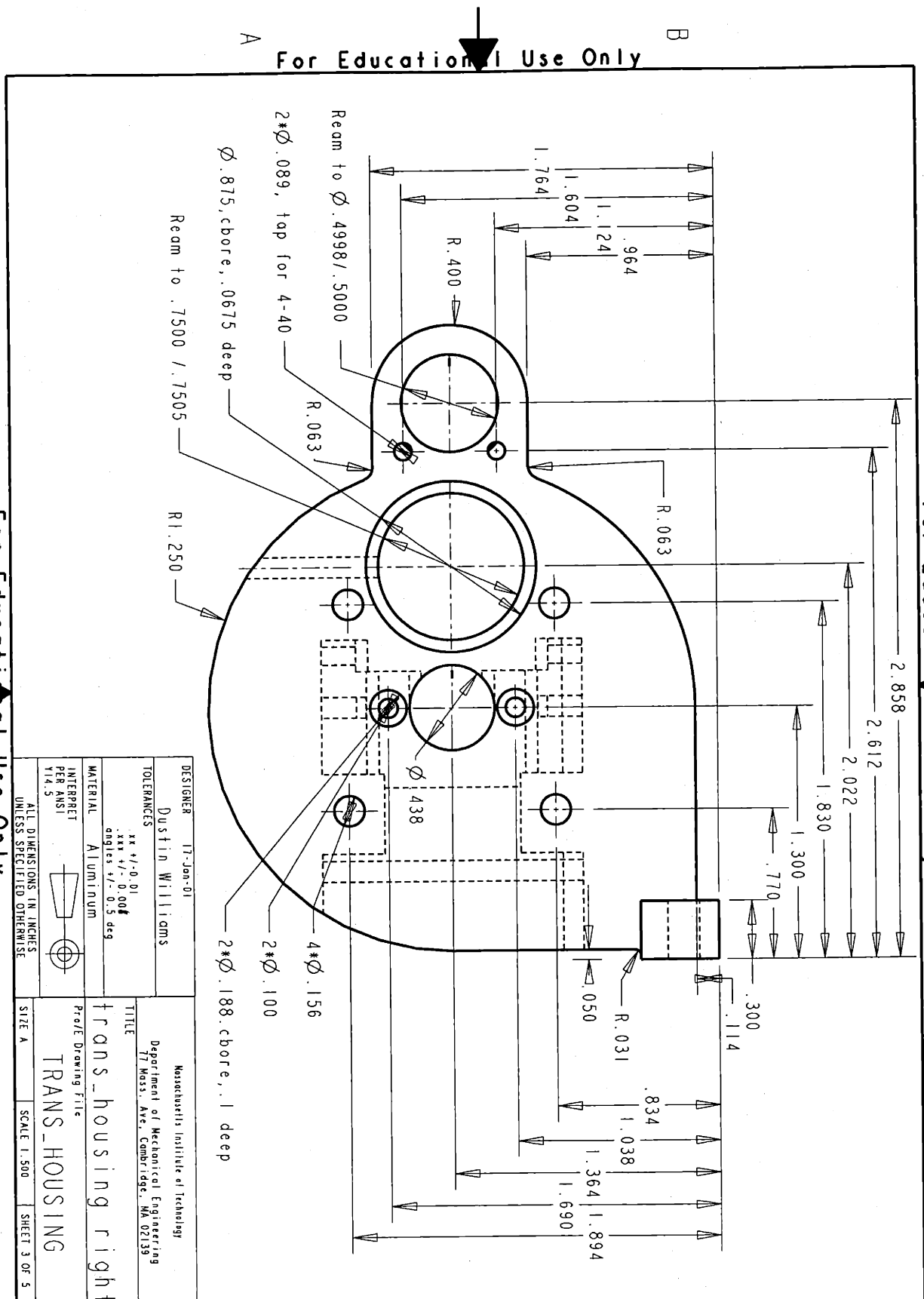


For Educational Use Only

For Educational Use Only



DESIGNER	17-Jan-01	Masachusetts Institute of Technology
DRAWN	Dustin Williams	Department of Mechanical Engineering
TOLERANCES	.xx +/- 0.01 .xxx +/- 0.008 angles +/- 0.5 deg	77 Mass. Ave. Cambridge, MA 02139
MATERIAL	ALUMINIUM	
INTERPRET PER ANSI Y14.5		
ALL DIMENSIONS IN INCHES UNLESS SPECIFIED OTHERWISE		
SIZE A	SCALE 1.300	SHEET 2 OF 5

For Educational Use Only



For Educational Use Only

For Educational Use Only

DESIGNER	17-Jan-01 Justin Williams	TITLE Massachusetts Institute of Technology Department of Mechanical Engineering 77 Mass. Ave. Cambridge, MA 02139
TOLERANCES	xx +/- 0.01 .xxx +/- 0.004 angles +/- 0.5 deg	
MATERIAL	Aluminum	TRANSHOUSING right TRANSHOUSING
INTERPRET PER ANSI Y14.5	 	
ALL DIMENSIONS IN INCHES UNLESS SPECIFIED OTHERWISE		Prof/ Drawing File
SIZE A	SCALE 1:500	SHEET 3 OF 5

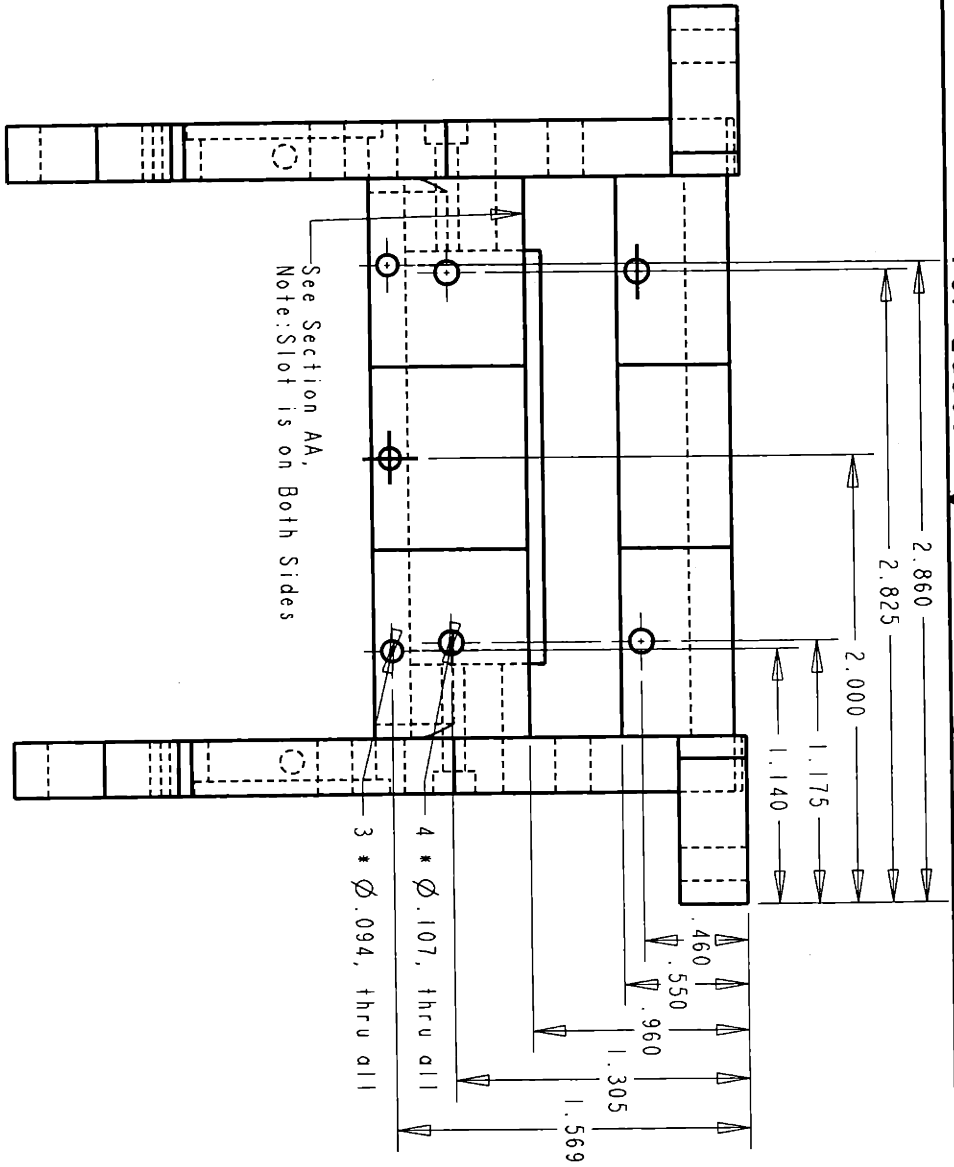
A

For Educational Use Only

B

2

For Educational Use Only



See Section AA,
Note: Slot is on Both Sides

DESIGNER Dustin Williams 17-Jan-01	Massachusetts Institute of Technology Department of Mechanical Engineering 77 Mass. Ave., Cambridge, MA 02139
TOLERANCES xx +/- 0.01 xxx +/- 0.005 angles +/- 0.5 deg	TITLE trans_housing top
MATERIAL ALUMINUM	Project Drawing File TRANS_HOUSING
INTERPRET PER ANSI Y14.5	SIZE A
ALL DIMENSIONS IN INCHES UNLESS SPECIFIED OTHERWISE	SCALE 1.300
	SHEET 4 OF 5

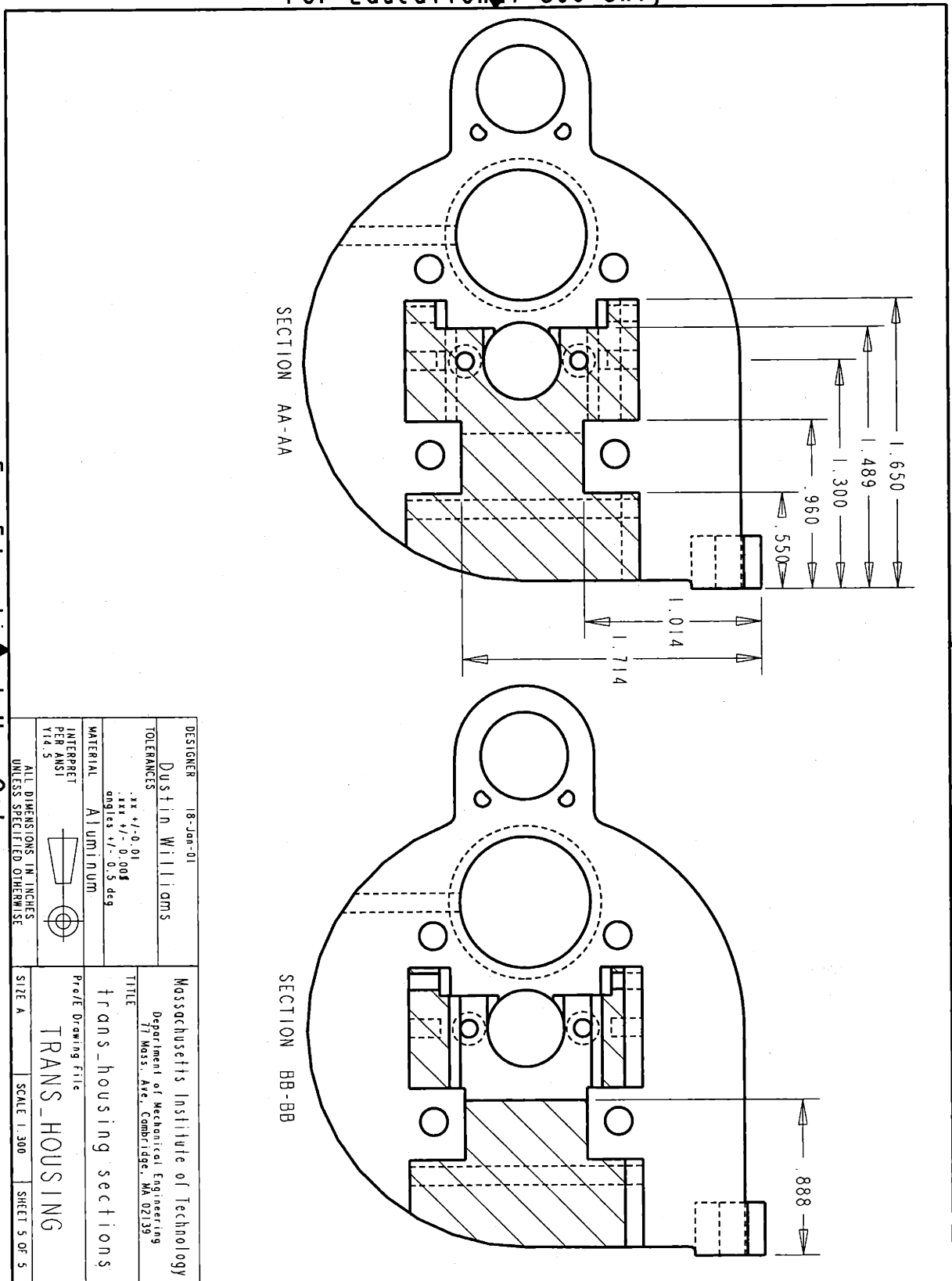
For Educational Use Only

2

For Educational Use Only

B

A ▼ B
 For Educational Use Only



2

For Educational Use Only

2

For Educational Use Only

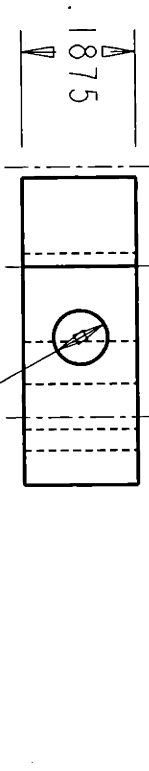
DESIGNER	18-Jan-01	Dustin Williams
TOLERANCES	.xx +/- 0.01 .xxx +/- 0.004 angles +/- 0.5 deg	
MATERIAL	ALUMINUM	
INTERPRET PER ANSI		
ALL DIMENSIONS IN INCHES UNLESS SPECIFIED OTHERWISE		
TITLE	Trans-housing sections	
PROJECT	Prac/E Drawing file	
SIZE	A	
SCALE	1:300	
SHEET	5 OF 5	

For Educational Use Only B

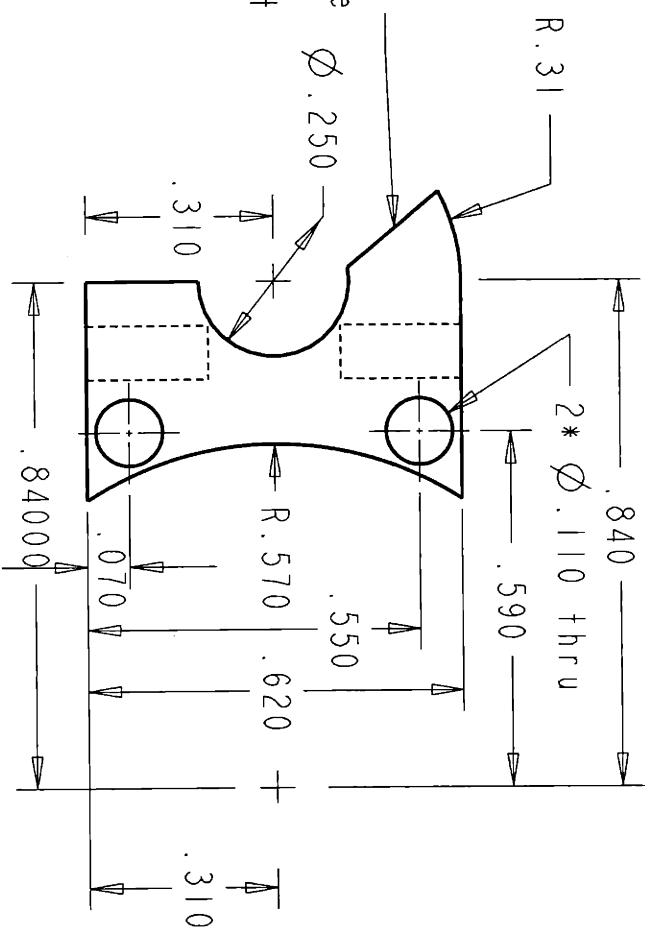
For Educational Use Only

2

For Educational Use Only



$\phi .089$, .200 deep, tap for 4-40
same on bottom side



See the following page for description of cut

Note: Make Two Pieces

DESIGNER	17-Jan-01 Dustin Williams	Massachusetts Institute of Technology Department of Mechanical Engineering 77 Mass. Ave., Cambridge, MA 02139
TOLERANCES	.xx +/- 0.01 .xxx +/- 0.004 angles +/- 0.5 deg	TITLE abd_add_stop
MATERIAL	303 stainless steel	Profile Drawing File ABD_ADD_STOP
INTERPRET PER ANSI Y14.5		SIZE A
ALL DIMENSIONS IN INCHES UNLESS SPECIFIED OTHERWISE		SCALE 3.500
		SHEET 1 OF 2

For Educational Use Only

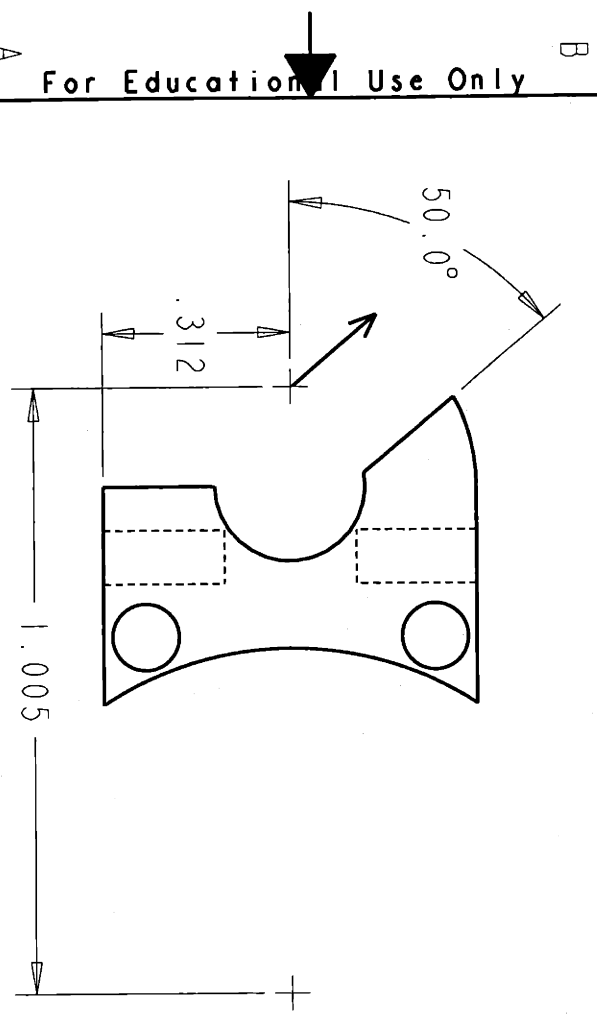
2



For Educational Use Only

2

For Educational Use Only

Using a 3/8 in cutter starting at the location shown move up and to the left at 50°



DESIGNER	17-Jan-01	Massachusetts Institute of Technology Department of Mechanical Engineering 77 Mass. Ave. Cambridge, MA 02139
Dustin Williams		
TOLERANCES	xx +/- 0.01 xxx +/- 0.008 angles +/- 0.5 deg	TITLE
MATERIAL	303 Stainless Steel	abd_add_stop
INTERPRET PER ANSI Y14.5	 	Pro/E Drawing File
ALL DIMENSIONS IN INCHES UNLESS SPECIFIED OTHERWISE		ABD_ADD_STOP
SIZE A	SCALE 3.500	SHEET 2 OF 2

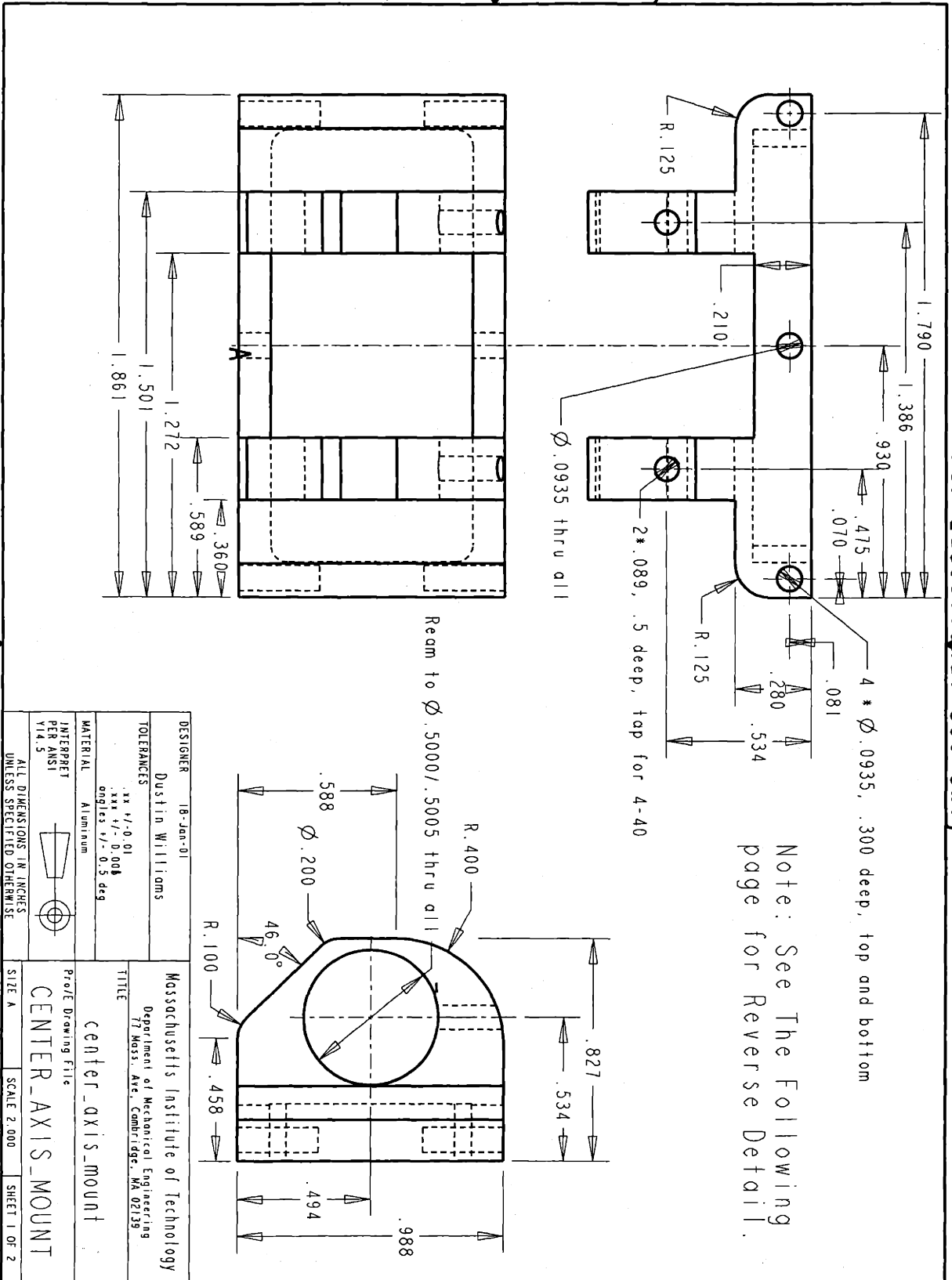
2

For Educational Use Only

1

For Educational Use Only

For Educational Use Only



For Educational Use Only

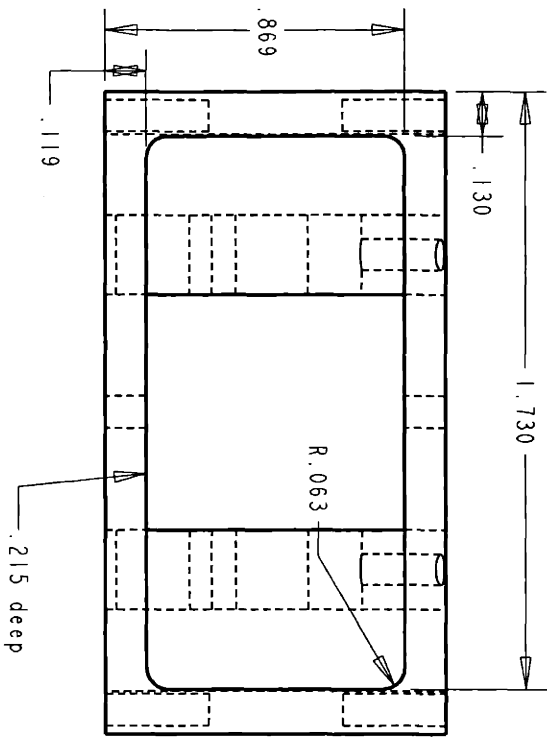
2

For Educational Use Only

2

For Educational Use Only

A For Educational Use Only B

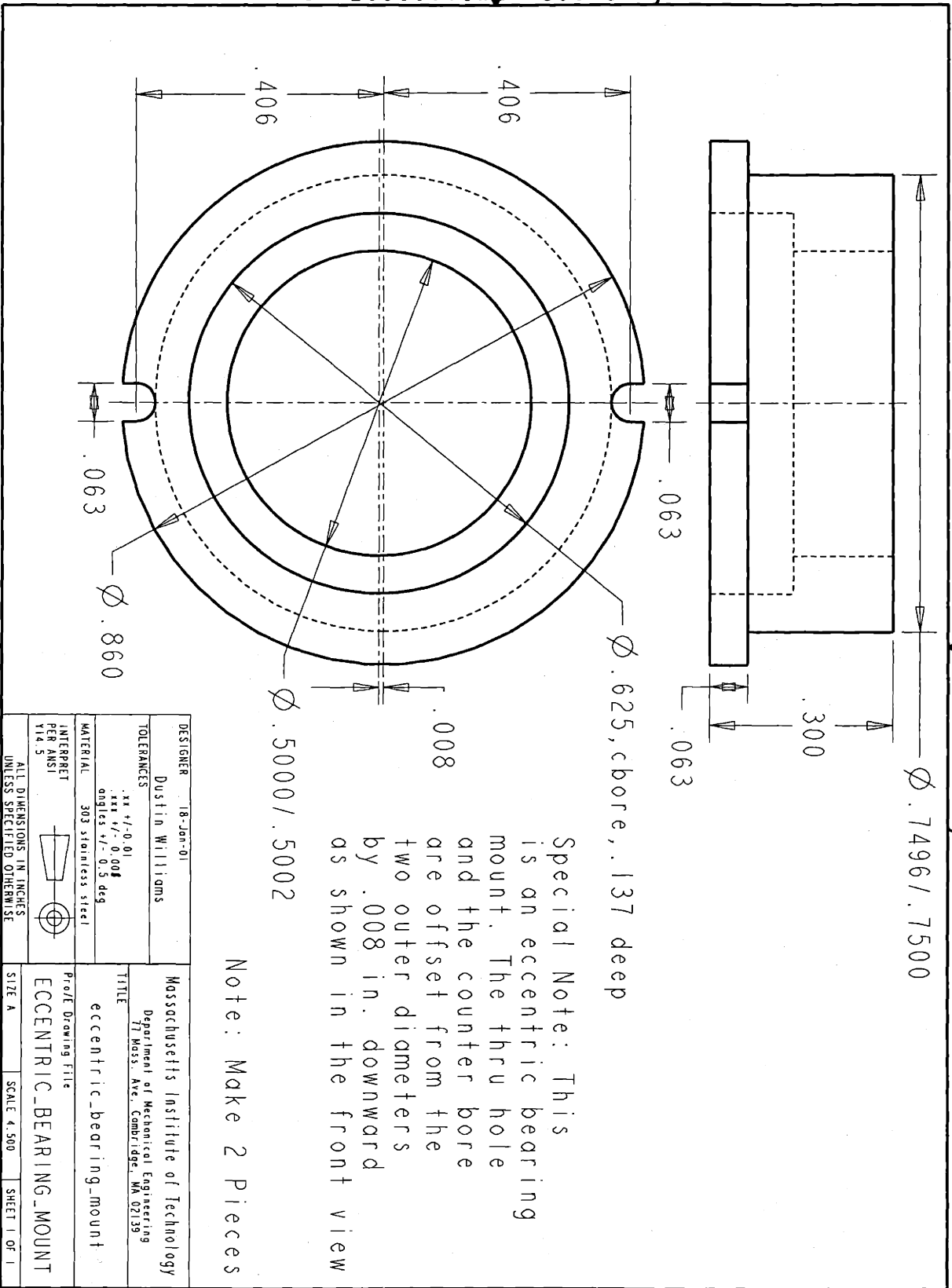


Reverse Detail

DESIGNER	19-Jan-01	DESIGNER	19-Jan-01
TOLERANCES	.xx +/- .0.01 .xxx +/- .0.008 ANGLES +/- .0.5 deg	TITLE	center_axis_mount reverse
MATERIAL	AMATERIAL	PROJECT	center_axis_mount reverse
INTERPRET PER ANSI Y14.5		PROJECT FILE	center_axis_mount reverse
ALL DIMENSIONS IN INCHES UNLESS SPECIFIED OTHERWISE		SCALE	2:000
		SHEET	2 OF 2

For Educational Use Only B

For Educational Use Only



2

For Educational Use Only

2

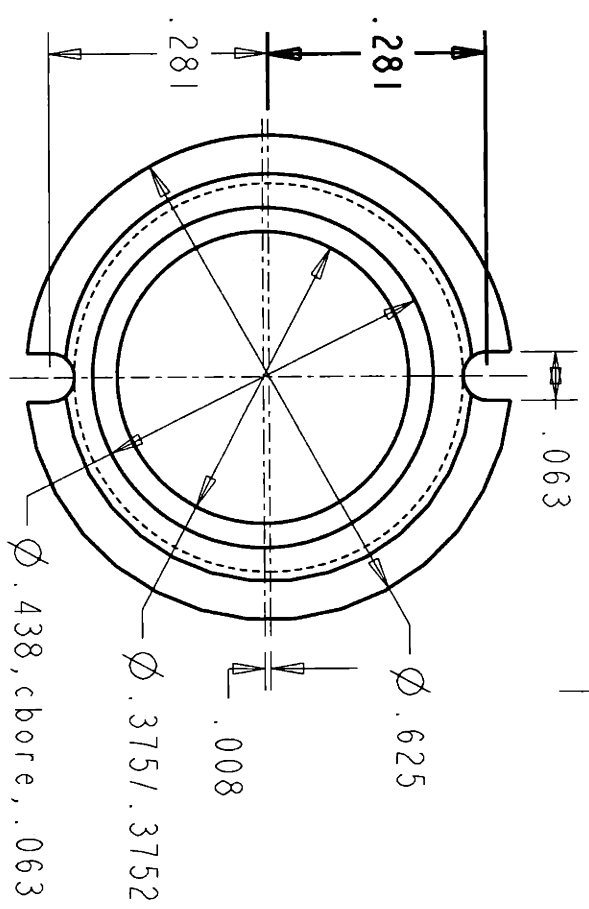
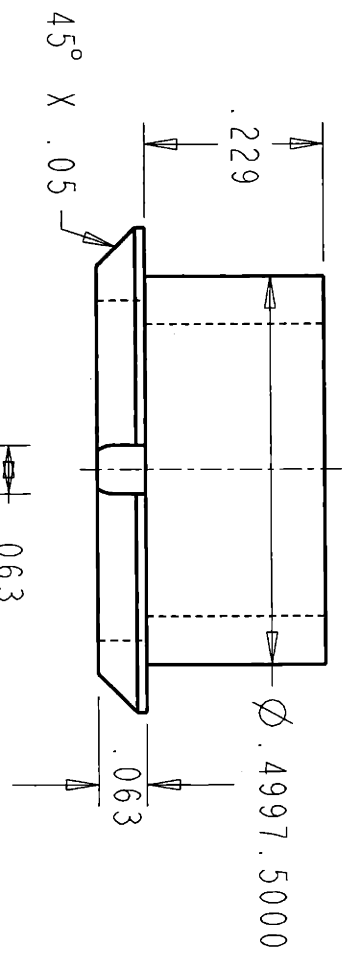
For Educational Use Only

1

For Educational Use Only

Special Note: This is an eccentric bearing mount. The thru hole and the counter bore are offset from the two outer diameters by $.008$ in. downward as shown in the front view

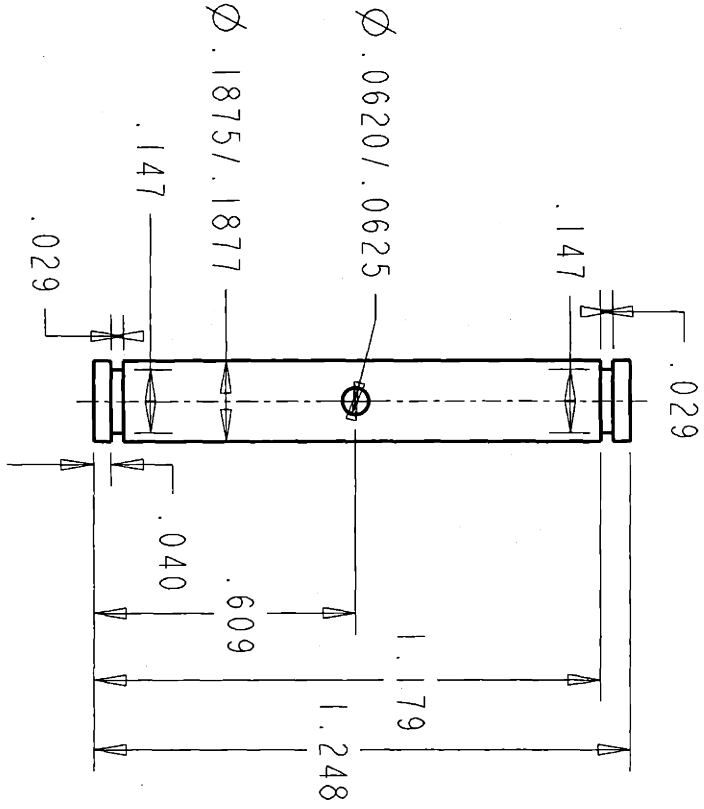
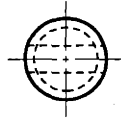
Note: Make 2 Pieces



Special Note: This is an eccentric bearing mount. The thru hole and the counter bore are offset from the two outer diameters by .008 in. downward as shown in the front view

Note: Make two pieces

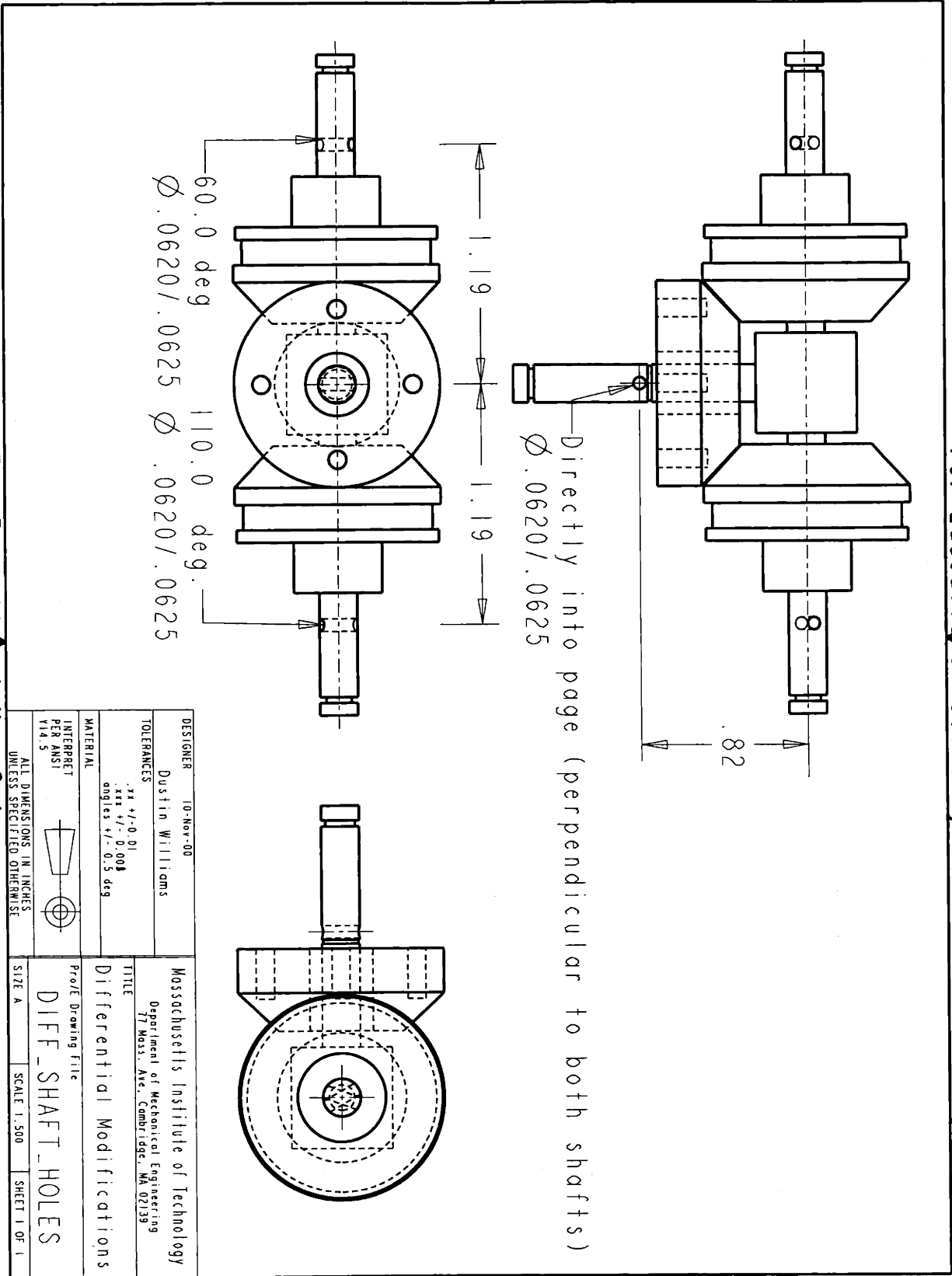
DESIGNER Dustin Williams	18-Jan-01	Massachusetts Institute of Technology Department of Mechanical Engineering 77 Mass. Ave. Cambridge, MA 02139	
TOLERANCES .xx +/- 0.01 .xxx +/- 0.005 angles +/- 0.5 deg		TITLE eccentric_bearing_mount2	
MATERIAL 303 Stainless Steel		Pro/E Drawing File ECCENTRIC_BEARING_MOUNT2	
INTERPRET PER ANSI Y14.5		SIZE A	SCALE 4.500 SHEET 1 OF 1
ALL DIMENSIONS IN INCHES UNLESS SPECIFIED OTHERWISE			



Note: Make 2 pieces

DESIGNER	18-Jan-01 Dustin Williams	Masachusetts Institute of Technology Department of Mechanical Engineering 77 Mass. Ave., Cambridge, MA 02139
TOLERANCES	.xx +/- 0.01 .xxx +/- 0.008 angles +/- 0.5 deg	TITLE shaft_for_bc
MATERIAL	303 stainless steel	Pro/E Drawing Title SHAFT_FOR_BC
INTERPRET PER ANSI Y14.5		SIZE A
ALL DIMENSIONS IN INCHES UNLESS SPECIFIED OTHERWISE		SCALE 2.500
		SHEET 1 OF 1

For Educational Use Only



2

For Educational Use Only

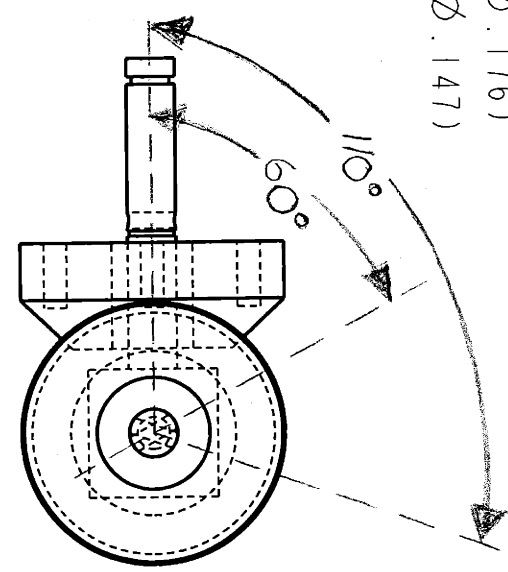
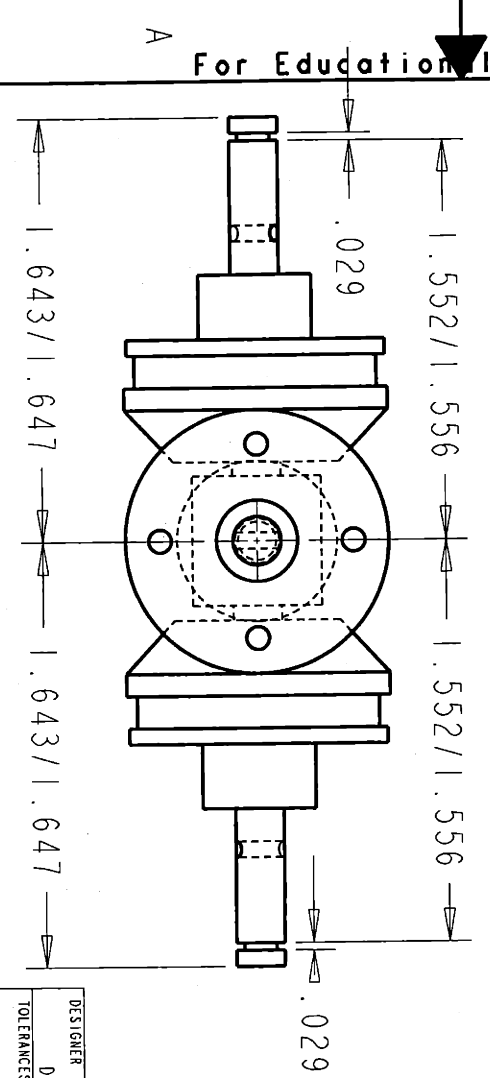
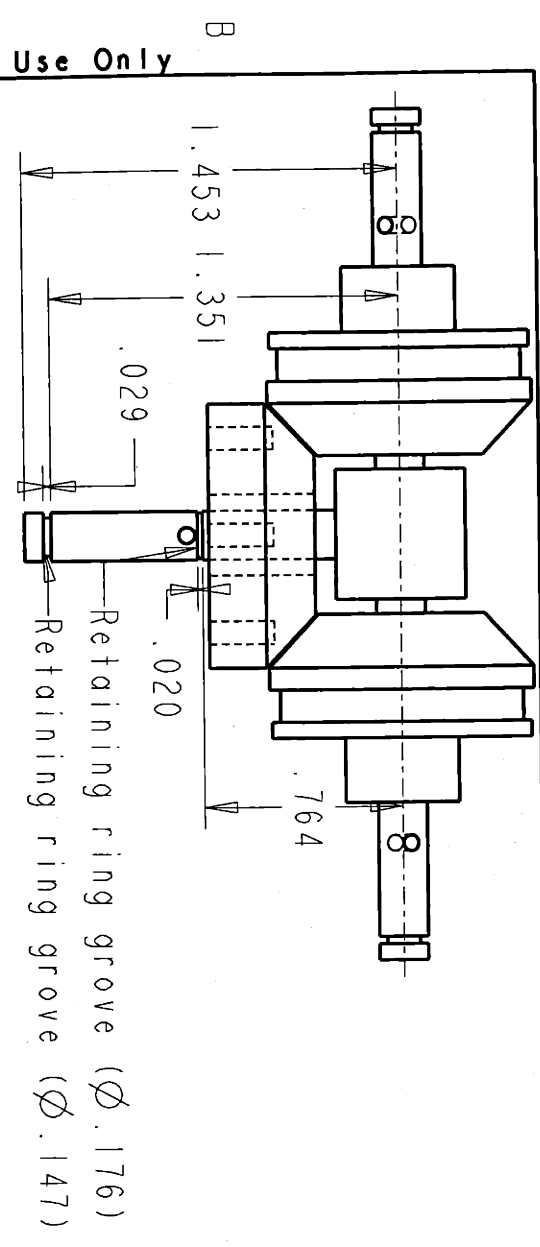
2

For Educational Use Only

DESIGNER	10-Nov-00 Dustin Williams	MATERIAL	INTERPRET PER ANSI Y14.5	ALL DIMENSIONS IN INCHES UNLESS SPECIFIED OTHERWISE
TOLERANCES	xx +/- 0.01 xxx +/- 0.004 angles +/- 0.5 deg	TITLE	DIFF_SHAFT_HOLES	SIZE A
Massachusetts Institute of Technology Department of Mechanical Engineering 77 Mass. Ave. Cambridge, MA 02139		DIFFERENTIAL MODIFICATIONS		
Profile Drawing File		SCALE 1:500		
SHEET 1 OF 1		SHEET 1 OF 1		

For Educational Use Only

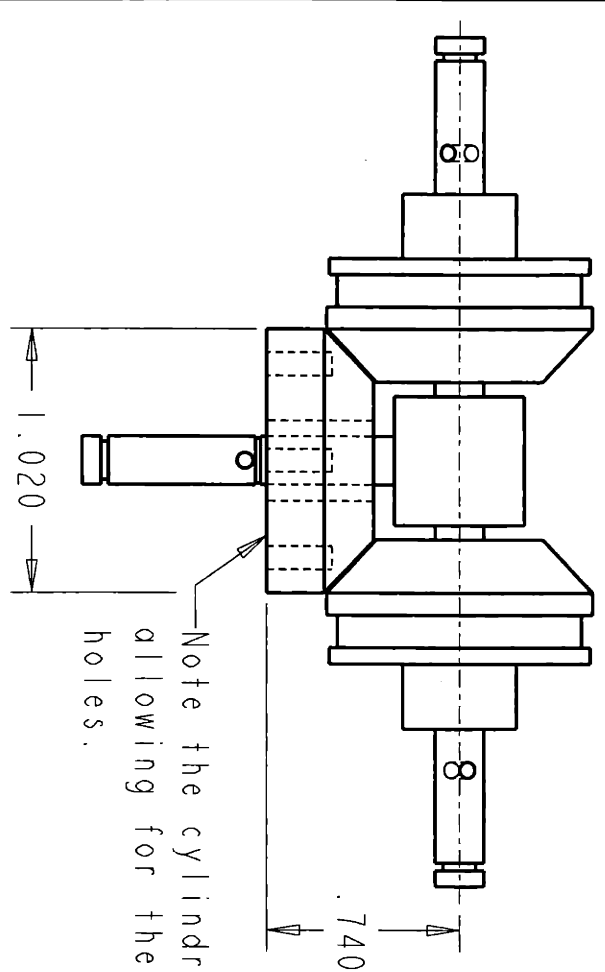
For Educational Use Only



For Educational Use Only

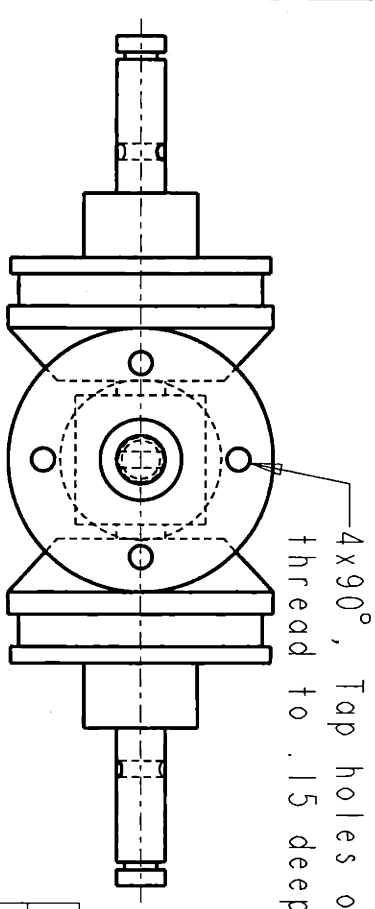
DESIGNER	10-Nov-00	Massachusetts Institute of Technology Department of Mechanical Engineering 77 Mass. Ave., Cambridge, MA 02139
DESIGNER	Dustin Williams	
TOLERANCES	.xx +/- 0.01 .xxx +/- 0.004 angles +/- 0.5 deg	TITLE Differential Modifications
MATERIAL		
INTERPRET PER ANSI Y14.5		DIFFERENTIAL
ALL DIMENSIONS IN INCHES UNLESS SPECIFIED OTHERWISE		
SIZE A	SCALE 1:500	SHEET 1 OF 1

For Educational Use Only



Note the cylindrical shape of the spider gear allowing for the placement of the 4 tapped holes.

For Educational Use Only

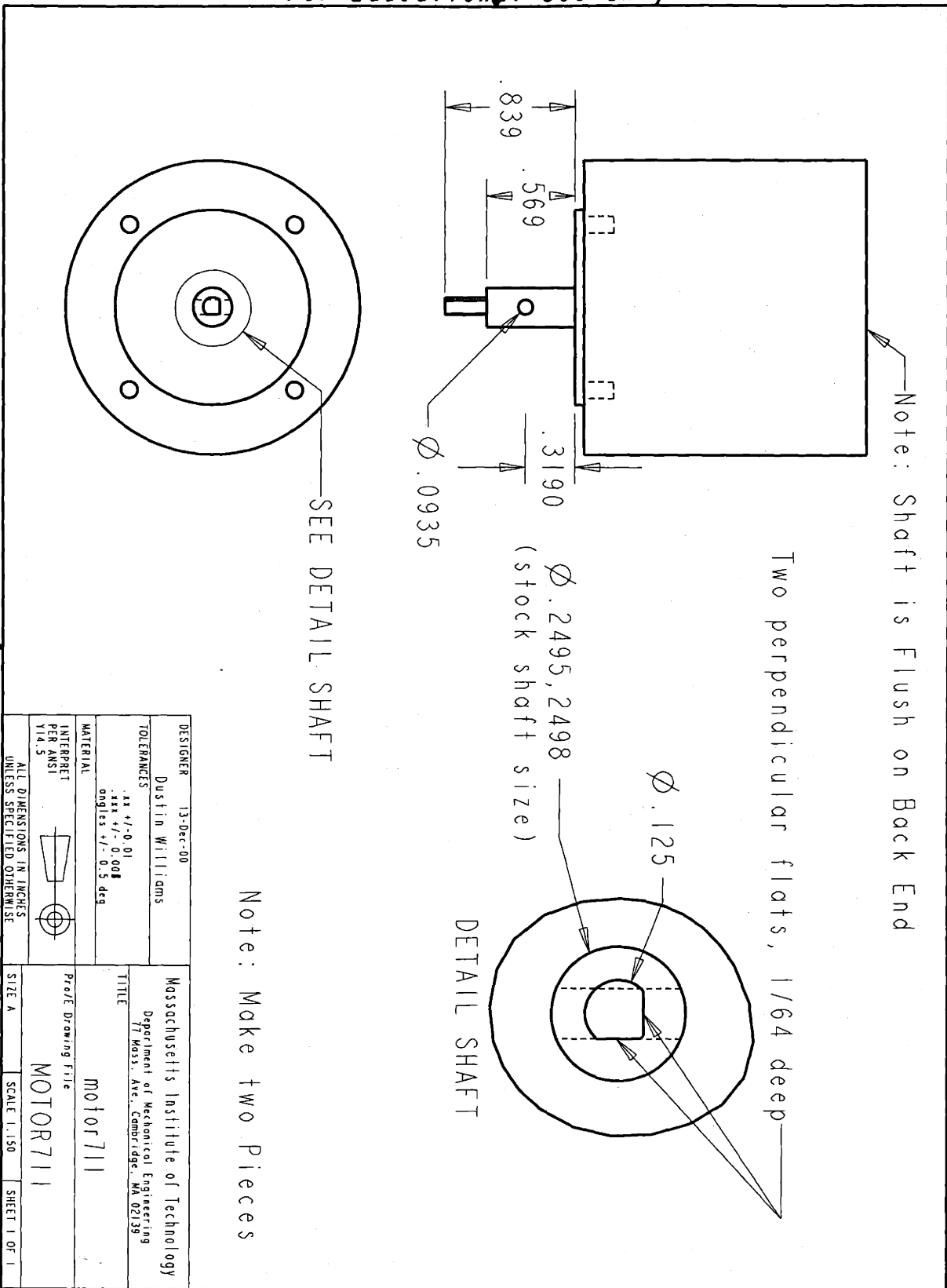


4x90°, Tap holes on Basic \varnothing 0.760, #4-40, .23 deep thread to .15 deep

DESIGNER	10-Nov-00	Massachusetts Institute of Technology Department of Mechanical Engineering 71 Mass. Ave. Cambridge, MA 02139
DRAWN	Dustin Williams	
TOLERANCES	.xx +/- 0.01 .xxx +/- 0.005 angles +/- 0.5 deg	TITLE
MATERIAL		Differential Modifications
INTERPRET PER ANSI Y14.5		Pro/E Drawing File
ALL DIMENSIONS IN INCHES UNLESS SPECIFIED OTHERWISE		SPIDER_GEAR_DETAIL
SIZE A	SCALE 1:500	SHEET 1 OF 1

For Educational Use Only

For Educational Use Only



2 For Educational Use Only

SEE DETAIL SHAFT

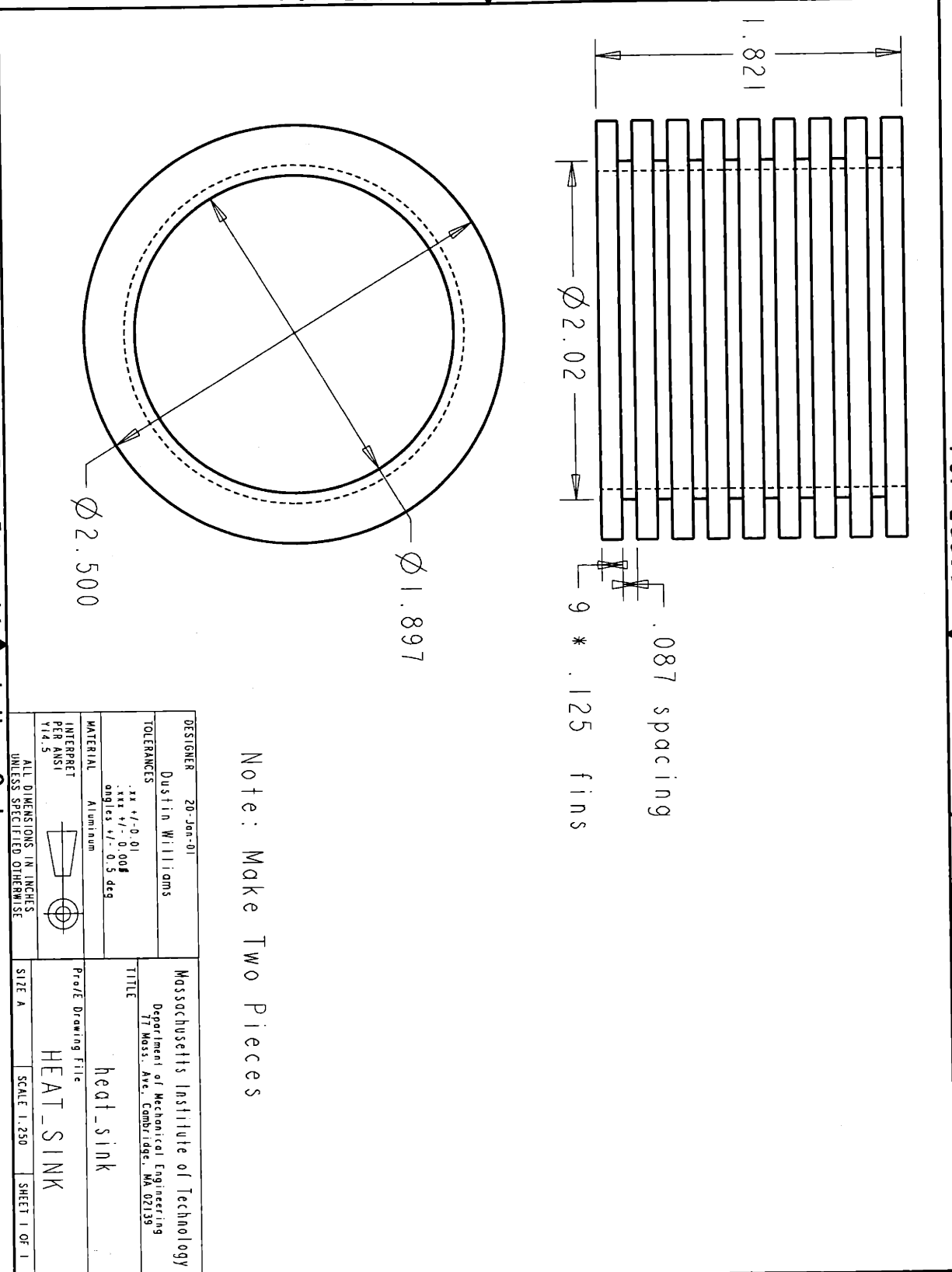
Note: Make two Pieces

DESIGNER	13-Dec-00	Massachusetts Institute of Technology
	Dustin Williams	Department of Mechanical Engineering
TOLERANCES	.xx +/- 0.01	77 Mass. Ave. Cambridge, MA 02139
	.xxx +/- 0.001	
	angles +/- 0.5 deg	
MATERIAL		motor 711
INTERPRET PER ANSI Y14.5		Motor 711
ALL DIMENSIONS IN INCHES UNLESS SPECIFIED OTHERWISE		
SIZE A	SCALE 1:150	SHEET 1 OF 1



2 For Educational Use Only

For Educational Use Only

For Educational Use Only



Note: Make Two Pieces

DESIGNER Dustin Williams	20-Jan-01	Massachusetts Institute of Technology Department of Mechanical Engineering 77 Mass. Ave., Cambridge, MA 02139
TOLERANCES xx +/- 0.01 xxx +/- 0.008 angles +/- 0.5 deg		
MATERIAL Aluminum		TITLE heat_sink Pro/E Drawing File
INTERPRET PER ANSI Y14.5		
ALL DIMENSIONS IN INCHES UNLESS SPECIFIED OTHERWISE		HEAT_SINK SIZE A SCALE 1:250 SHEET 1 OF 1

For Educational Use Only

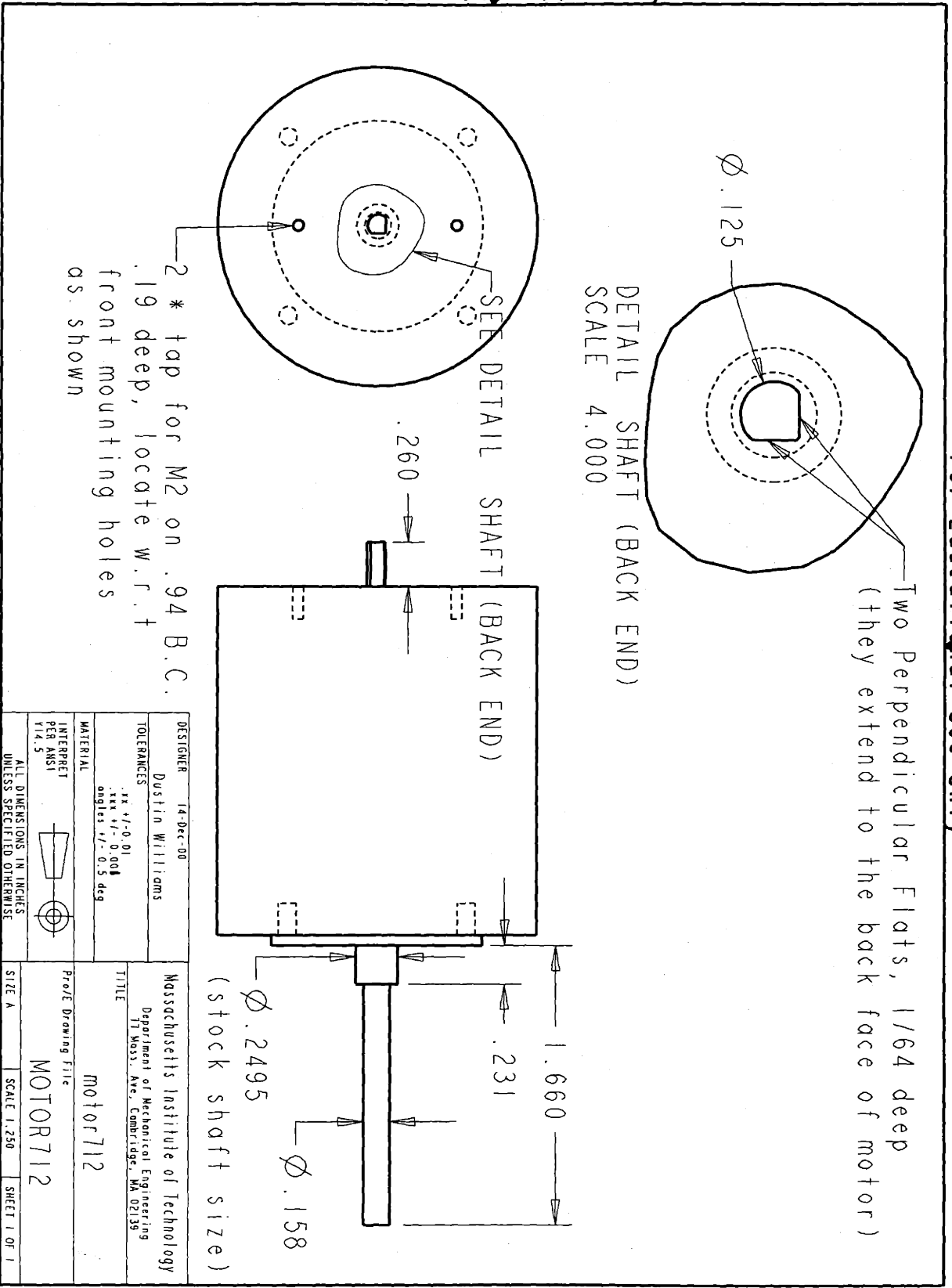
For Educational Use Only

2

2

For Educational Use Only

For Educational Use Only



2 For Educational Use Only

2 For Educational Use Only

For Educational Use Only

Bibliography

- [1] The National Stroke Association, *The Effects of Stroke*, www.stroke.org
- [2] Tilley, Alvin R., *The Measure of Man and Woman: Human Factors in Design*, The Whitney Library of Design, NY, 1993
- [3] Webb Associates, *Anthropometric Source Book Volume I: Anthropometry for Designers*, Scientific and Technical Information Office, Yellow Springs, Ohio, 1978
- [4] Palastanga Nigel, *Anatomy and Human Movement: Structure and Function 2nd Edition*, Butterworth Heinemann, Jordan Hill, Oxford, Britain
- [5] Charnnarong Jain, *The Design of an Intelligent Machine for Upper-Limb Physical Therapy*, MIT SM Thesis, 1988
- [6] Ryu J., *Wrist Joint Motion*, Springer-Verlag, NY, 1991
- [7] McConville John T., *Anthropometric Relationships of Body and Body Segment Moments of Inertia*, National Technical Information Service, Yellow Springs, Ohio, 1980
- [8] Prelle C., "An Electropneumatic Actuator for a Compliant Robot", *Proceedings of the Eighth Bath International Fluid Power Workshop*, (1995)
- [9] Rosenberg R., *Introduction to Physical System Modeling*, Mcgraw-Hill Publishing Company, NY, 1983
- [10] Trombly Catherine A., *Occupational Therapy for Physical Dysfunction*, Williams and Wilkins, Baltimore, 1995
- [11] Slocum, Alex H., *Precision Machine Design*, Society of Manufacturing Engineers, Dearborn, Michigan
- [12] Asada H., *Direct Drive Robots*, MIT Press, Cambridge, MA
- [13] Riven Eugene I., *Mechanical Design of Robots*, Mcgraw-Hill Inc., NY
- [14] Susan E. Fasoli, personal communication.
- [15] Waldron Kenneth J., *Kinematics Dynamics and Design of Machinery*, John Wiley and Sons, NY
- [16] Oberg Erik., *Machinery's Handbook*, Industrial Press Inc., NY

[17] Shigley Joseph E., *Mechanical Engineering Design Fifth Edition*, McGraw-Hill, NY

[18] Stock Drive Products, *Handbook of Gears*, New Hyde Park, NY